MULTIPLE ROLES OF FLAVONOIDS IN PLANT-RHIZOBIA SYMBIOSES AND PLANT-PATHOGEN INTERACTIONS

Samira Hassan

January 2015

Australian National University

A thesis submitted for the degree of Doctor of Philosophy of

The Australian National University

DECLARATION

This thesis contains my original work and has not been submitted for any other award. The specific contributions by others are referred to in the Acknowledgements.

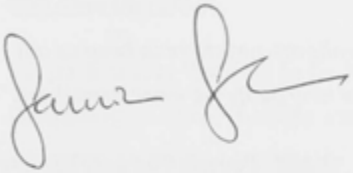

Samira Hassan

"The brick walls are there for a reason. The brick walls are not there to keep us out. The brick walls are there to give us a chance to show how badly we want something."

Randy Pausch, The Last Lecture

ACKNOWLEDGEMENTS

First and foremost, I would like to thank my supervisor Dr Ulrike Mathesius for her continual support during my PhD candidature. I would like to also extend my gratitude towards my advisors Dr Peter Solomon and Dr Adrienne Hardham for their valuable insights. I am grateful for the ANU Postgraduate Scholarship and Australian Government's Research Training Scheme for their financial support to complete this work.

I'm particularly thankful to Dr Anton Wasson who initially worked on the roles of flavonoids in plant-rhizobia symbioses as part of his thesis. The constructs for silencing *chalcone synthase* in the vector pHellsgate8 was generated by Anton Wasson and Dr Flavia Pellerone. Ulrike Mathesius and Anton Wasson collected the plant material for transcriptome analysis using microarrays. I contributed with data analysis and inference. The Nod factor overexpressing rhizobia strain E65 was kindly provided by Dr Sharon Long and Dr Melanie Barnett. Thanks to Dr. Naresh Verma for brainstorming ideas on how best to integrate GFP into the E65 strain.

I am also thankful to fellow PhD student; Jason Ng for optimizing a method for IAA quantification using LC MS/MS. Dr Thy Thruong of the RSB Mass Spectrometry Facility also assisted me in running mass spectrometry and provided excellent support even on weekends. I am indebted to Professor Lloyd Sumner of the Noble Foundation, USA for training me in the fundamental concepts of mass spectrometry. My thanks also extend to his colleagues Drs David Huhman, Dongsik Yang, Bonnie Watson, Zhentian Lee and Mohamed Bedair for demonstrating the methods for quantification of plant metabolites including flavonoids so that I could set up similar protocols at the ANU.

I thank Dr Rao Uppalapati for useful insights into plant-fungal interactions and mapping data for exploratory transcriptome analysis. I was also assisted by Dr Stephen Ohms (Biomolecular Research Facility, JCSMR, ANU) who was generous with his time and expertise in teaching me Partek Genomics Suite for microarray data analysis.

The staffs at the Research School of Biology have provided excellent support services to allow me to complete my research. I am particularly thankful to Stephanie McCaffery for helping me optimise plant-growth rooms during the stress of building moves. Sharon Seltabanis showed tremendous patience when autoclaving my constant influx of plant-growth media. And Roseanne Holm who was never tired of assisting me in chasing up product suppliers.

Finally, I am grateful to have wonderful friends and family whose company and unconditional support has always encouraged me. I am indebted to my friends – Chooi, Debora and Nicole for parafilming hundreds of Petri dishes for me when I couldn't do it anymore. Thank you Chooi for being my soul-sister and always cheering me to do better. Thanks to Giulia Russo who showed me culturing techniques for mycorrhizae, which I hope to use in future. Thank you Jason for your infinite wisdom that even Socrates would envy and Giel for engaging F1 and cricket analysis. Thanks to Patchy for being an awesome travelling mate. And finally, thanks to my other PhD buddies Richa, Shubhanshi, Vinson, Sabrina and Esther, I will forever miss the great times we shared.

ABSTRACT

Flavonoids are secreted by plant roots to activate and attract nitrogen-fixing bacteria known as rhizobia. Rhizobia perceive flavonoids and reciprocate with secretion of Nod factors required to initiate nodule organogenesis. In this thesis I have explored the roles flavonoids play in the roots during early nodulation of *Medicago truncatula*. To achieve this goal, I silenced or overexpressed genes encoding key enzymes in the flavonoid biosynthesis pathway in hairy root cultures. I used RNA interference as a mechanism to silence multiple copies of the genes *chalcone synthase, flavonol synthase, isoflavone synthase, dihydroflavonol-4-reducase* and *flavone synthase II.* I also used a 35S promoter to overexpress the genes *chalcone synthase, flavonol synthase, isoflavone synthase* and *dihydroflavonol-4-reducase*, although only *isoflavone synthase* overexpression showed quantifiable increase in the targeted metabolites using LC-MS/MS.

Flavonoids have been described to affect the spatio-temporal balance of the plant hormone auxin through the inhibition of polar auxin transport and its breakdown. Using constitutive Nod factor overexpressing rhizobia to inoculate flavonoid-silenced (*CHS*i) roots, I have demonstrated that flavonoids regulate nodule organogenesis in part through the control of auxin synthesis in the root, by regulating gene expression of *YUCCA1*, a central enzyme in auxin biosynthesis. In contrast, flavonoids did not alter the expression of genes encoding PIN and LAX auxin efflux and influx transporters, even though these flavonoids were required for the inhibition of acropetal auxin transport by rhizobia. The inhibition of polar auxin transport was regulated most strongly by root flavonols and isoflavonoids, however, only flavonols were found to be important for nodule formation. The synthetic auxin transport inhibitor, TIBA, failed to complement *CHS*i roots, suggested that flavonoids play additional roles in nodule organogenesis apart from controlling auxin transport.

To explore further functions for flavonoids in nodulation, I studied the transcriptomic changes 6 and 24 hours post inoculation of *CHS*i roots with constitutive Nod factor expressing rhizobia. Inoculated *CHS*i roots over-

accumulated many defense related genes compared to control roots, but failed to express structural enzymes that could be involved in infection thread formation. These roots also differentially expressed genes encoding proteins involved in the synthesis and response factors of hormones gibberelins, ethylene, cytokinin and auxin. GFP-labelled, constitutively Nod factor expressing rhizobia were shown to form infection threads in control but not *CHS*i roots, suggesting that flavonoids are involved in infection of rhizobia. *CHS*i roots also did not trigger reactive oxygen species accumulation, suggested to be required for cross-linking of glycoproteins in the matrix of infection threads.

Flavonoids have previously also been demonstrated to be important as plant-defense compounds. Using the transgenic hairy roots with altered flavonoid metabolite profile, I suggest a link between auxin-mediated plant-defense and the presence of flavonoids in the roots. This was investigated by challenging roots with the pathogens *Rhizoctonia solani* (AG8) and *Aphanomyces euteiches*. One mechanism by which roots show tolerance to pathogens is through secondary root formation to outgrow and evade pathogens. Roots showing reduced expression of *flavonol synthase* showed a reduction in the ability to form secondary roots and showed increased susceptibility to the fungal and oomycete pathogens. Conversely, isoflavonoids are precursors to a number of protective phytoalexins. Increasing the expression of *isoflavone synthase* led to an increase in tolerance to the root pathogens. This could have important implications in increasing productivity of agricultural crops exposed to environmental stresses.

TABLE OF CONTENTS

List of Figures

List of Tables

List of Abbreviations

Ae – Aphanomyces euteiches
ANOVA – Analysis of Variance
ATI – Auxin transport inhibitor/inhibition
BMM – Bergersen's modified medium
CHS – Chalcone synthase
DFR – Dihydroflavonol-4-reductase
dpi – Days post inoculation
dsRNA - double stranded RNA
E65 – *Sinorhizobium meliloti A2102* overexpressing *nodD3*
EV – Empty vector
FLS – Flavonol synthase
FSII – Flavone synthase II
GFP – Green fluorescent protein
GUS - β- glucuronidase
hpi – Hours post inoculation
HR – Hypersensitive response
IAA – Indole-3-acetic acid
IFS – Isoflavone synthase
IT – Infection thread
LC MS/MS – Liquid chromatography tandem mass spectrometry
LOD – Limit of detection
LOQ – Limit of quantitation
NF – Nod factor
NPA - 1-N-naphthylphthalamic acid
Ox – Overexpression
PAT – Polar Auxin Transport
PCR – Polymerase chain reaction
QC – Quiescent Centre
qRT-PCR – Quantitative Real-time PCR
RAM – Root Apical Meristem
RNAi – RNA interference
ROS – Reactive oxygen species
Rs – Rhizoctonia solani
siRNA – Short interfering RNA
Sm – Sinorhizobium meliloti
Sm^R – Streptomycin resistance
Sp^R – Spectinomycin resistance
TIBA - 2,3,5-triiodobenzoic acid

Chapter 1. The role of flavonoids in root-rhizosphere signaling – opportunities and challenges for improving plant-microbe interactions

The chapter presented here has been published in Journal of Experimental Botany in 2012. Two updates of the same chapter have been published as book chapters.

HASSAN, S. & MATHESIUS, U. 2012. The role of flavonoids in root-rhizosphere signalling: opportunities and challenges for improving plant-microbe interactions. Journal of Experimental Botany, 63, 3429-44.

HASSAN, S. & MATHESIUS, U. 2013. Roles of Flavonoids in Symbiotic Root–Rhizosphere Interactions. In: BRUIJN, F. J. D. (ed.) Molecular Microbial Ecology of the Rhizosphere. John Wiley & Sons, Inc. doi:10.1002/9781118297674.ch51

HASSAN, S. & MATHESIUS, U. in press. Flavonoids play multiple roles in symbiotic root-rhizosphere interaction. In: BRUIJN, F. J. D. (ed.) Biological Nitrogen Fixation. Wiley/Blackwell.

Summary

The flavonoid pathway produces a diverse array of plant compounds with functions in UV protection, as antioxidants, pigments, auxin transport regulators, defence compounds against pathogens and during signalling in symbiosis. This chapter highlights some of the known function of flavonoids in the rhizosphere, in particular for the interaction of roots with microorganisms. Depending on their structure, flavonoids have been shown to stimulate or inhibit rhizobial *nod* gene expression, cause chemo-attraction of rhizobia towards the root, inhibit root pathogens, stimulate mycorrhizal spore germination and hyphal branching, mediate allelopathic interactions between plants, affect quorum sensing and chelate soil nutrients. Therefore, the manipulation of the flavonoid pathway to specifically synthesize certain products has been suggested as an avenue to improve root-rhizosphere interactions. I also discuss possible strategies to alter

flavonoid exudation to the rhizosphere. Possible challenges in that endeavour include limited knowledge of the mechanisms that regulate flavonoid transport and exudation, unforseen effects of altering parts of the flavonoid synthesis pathway on fluxes elsewhere in the pathway, spatial heterogeneity of flavonoid exudation along the root as well as alteration of flavonoid products by microorganisms in the soil. In addition, the overlapping functions of many flavonoids as stimulators of functions in one organism and inhibitor of another suggests caution in attempts to manipulate flavonoid rhizosphere signals.

1.1 Introduction

The flavonoid pathway is one of the best-studied biosynthetic pathways of specialized metabolites. Flavonoids are phenylpropanoid metabolites, most of which are synthesized from p-coumaroyl-CoA and malonyl-CoA and share their precursors with the biosynthetic pathway for lignin biosynthesis (Stafford, 1990). However, some rare flavonoids are synthesized from CoA esters of substrates like cinnamic acid or dihydro-coumaric acid, e.g. (Friederich et al., 1999). To date, more than 10,000 flavonoids have been identified in plants and their synthesis appears to be ubiquitous in plants (Ferrer et al., 2008). Their diversity stems from the generation of a number of basal flavonoid structures that include flavones, flavonols, flavan-3-ols, flavanones, isoflavonoids, isoflavans and pterocarpans (Figure 1.1). The flavonoid skeleton can be modified by glycosylation, malonylation, methylation, hydroxylation, acylation, prenylation or polymerisation, leading to the diversity of end products (Winkel-Shirley, 2001). These substitutions have important effects on flavonoid function, solubility, mobility and degradation.

The synthesis of flavonoids is in general well understood and the majority of enzymes have been identified, often from multiple species, e.g., (Winkel-Shirley, 2001, Dixon and Steele, 1999, Du et al., 2010). Flavonoid synthesis starts on enzyme complexes located on the cytosolic side of the endoplasmic reticulum (Jorgensen et al., 2005). Some of the enzyme complexes localize to the tonoplast where they might channel flavonoid intermediates for subsequent glycosylation reaction and storage in the vacuole (Winkel, 2004, Aoki et al., 2000). Flavonoid synthesis and accumulation is often very specific for certain cell types. For example, along the length of a root, flavonoids are often accumulated at the root tip and in root cap cells (Figure 1.2a). Specific flavonoid end products are also localized to specific cell types (Figure 1.2b) where they could have functions in regulating development (Mathesius, 2001, Mathesius et al., 1998a). Within the cell, flavonoids also show specificity for their location. Flavonoids have been localized to the nucleus, the vacuole, the cell wall, cell membranes and the cytoplasm (Figure 1.2b, c, d) (Naoumkina and Dixon, 2008, Saslowsky et al., 2005, Hutzler et

al., 1998, Erlejman et al., 2004). Flavonoid localisation and synthesis in different cell types and in response to environmental stimuli can be regulated by a number of transcription factors, in particular of the MYB and bHLH families (Koes et al., 2005, Quattrocchio et al., 2006). In many cases, the regulation of cell specificity is unknown.

Flavonoids can also be transported within and between cells and tissues. Within the cell, flavonoids are likely to move via vesicle-mediated transport or through membrane bound transporters of the ABC (ATP Binding Cassette) or MATE (Multidrug And Toxic Extrusion compound) families (Zhao and Dixon, 2009). Flavonoids transport into vacuoles can be achieved by conjugation of glutathione with flavonoids in the cytoplasm, followed by ATP-driven transport via glutathione-S-transferase pumps (Marrs et al., 1995, Goodman et al., 2004, Mueller et al., 2000). Long distance transport of flavonoids is less well understood but has been demonstrated in *Arabidopsis*, where application of flavonoids to the root or the shoot led to their transport towards distal tissues (Buer et al., 2007). Application of transporter inhibitors showed that the long distance transport is likely to be mediated by members of the ABC transporter families and is also altered by glutathione, which is likely to act as a transport vehicle for flavonoids after binding. To date, the exact mechanisms of flavonoid transport out of cellular organelles and out of the cell, as well as long distance transport remain poorly understood.

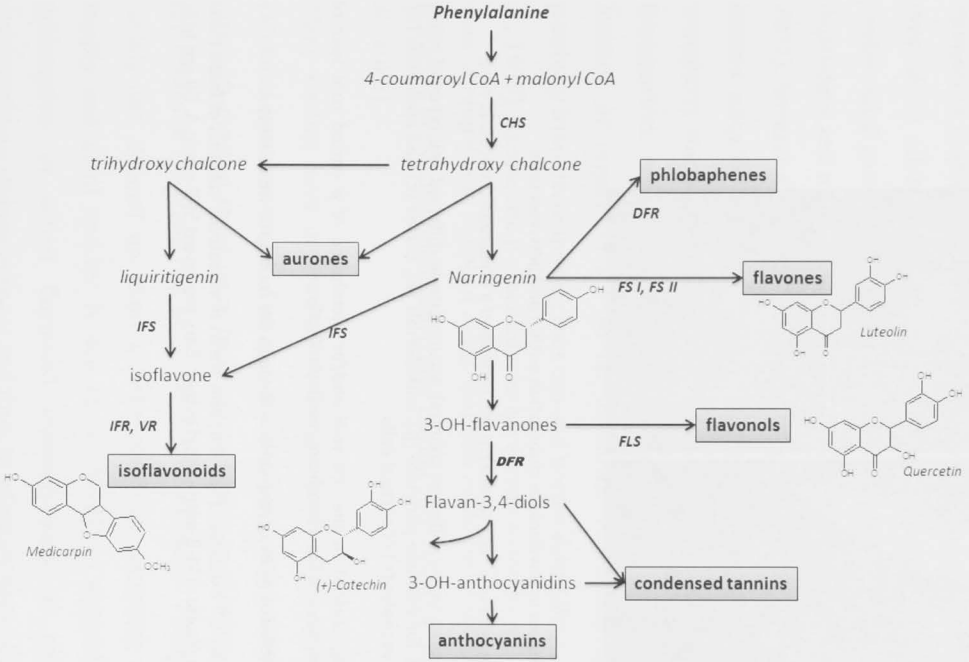

Figure 1.1 – Major branches of the flavonoid biosynthesis pathway. Some of the critical enzymes are highlighted in bold and are abbreviated as follows - CHS, Chalcone synthase; DFR, Dihydroflavonol 4-reductase ; FS I/II, Flavone synthase I/II; FLS, Flavonol synthase; IFS, Isoflavone synthase; IFR, Isoflavone reductase; LCR, Leucoanthocyanidin reductase; VR, Vesitone reductase. Examples of a few structures of compounds discussed in the text are provided. Major classes of end products are emphasized in grey boxes

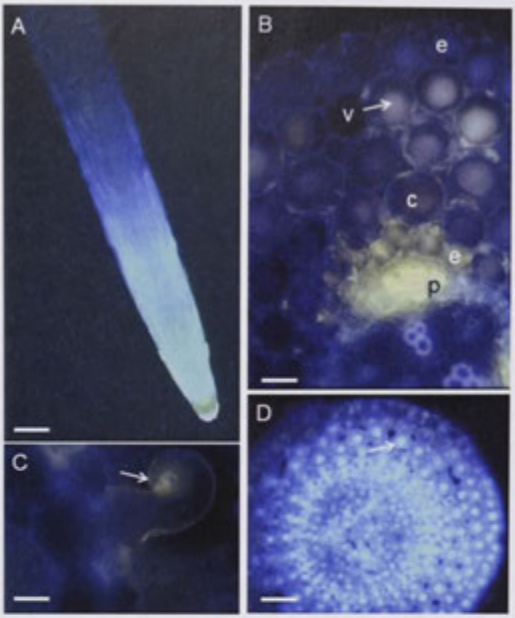

Figure 1.2– Spatial differences in flavonoid accumulation within and between cells.

A: Flavonoid accumulation (yellow fluorescence) at the root tip of a Medicago truncatula root.

B: Specific flavonoids (fluorescing in different colours) accumulate in different cell types of white clover (Trifolium repens), for example pericycle (p), endodermis (e), cortex (c) and epidermis (e). Flavonoids are located in vacuoles (v) of cortical cells.

C: Flavonoids (fluorescing orange) in the cell wall and/or membrane of a curled root hair of Medicago truncatula in response to Sinorhizobium meliloti infection.

D: Nuclear localisation of flavonoids in a cross section through the root tip of white clover.

All photos were taken under UV excitation (365 nm) and are from vibratome sections of fresh roots stained with 0.5% diphenylboric acid-2-aminoethyl esther. Bars represent 500 µm in A, 50 µm in B, 25 µm in C and 75 µm in D.

1.2 *Flavonoids in the rhizosphere*

Flavonoids are not only found within the plant but constitute a large part of root exudates (Cesco et al., 2010). Flavonoid exudation into the rhizosphere is not well understood although some progress has been made towards the identification of transporters. Flavonoids are likely to be actively exuded from roots, often in response to elicitors (Schmidt et al., 1994, Armero et al., 2001). ABC transporter mutants of *Arabidopsis* were shown to have altered root exudate profiles, although they likely affect multiple compounds (Badri et al., 2008). Exudation of the isoflavonoid genistein from soybean root plasma membrane vesicles was ATP-dependent and most likely catalysed by an ABC-type transporter (Sugiyama et al., 2007). Several phenylpropanoid exudates were affected in the ABC transporter mutant *abcg30*, although it was not shown whether this transporter directly transports the altered phenolics (Badri et al., 2009). Altogether, most of the transporters responsible for flavonoid exudation into the rhizosphere, their location or regulation are so far unknown. Flavonoids can also be released passively from decomposing root cap and border cells (Shaw et al., 2006, Hawes et al., 1998). Apoplastic β-glucosidases have been found to release isoflavones from their conjugates in soybean roots, and this could be an important mechanism for releasing active flavonoid aglycones during root-microbe interactions (Suzuki et al., 2006).

Many studies have determined types and concentrations of flavonoids in root exudates (summarized in Cesco et al., 2010, see also León-Barrios et al., 1993), although most of these were from plants grown in solution. Both aglycones and glycosides of flavonoid can be found in root exudates. Their concentrations vary widely and depend on plant growth condition, sampling techniques, nutrient supply and plant species (Cesco et al., 2010). In general there is only little information of actual flavonoid concentrations in soil and how these concentrations change in space and time. In addition, there are large differences in exudation of flavonoids along the root, with larger amounts being reported to be exuded from the root tip (Graham, 1991, Hawes et al., 1998; see also Figure 1.2a). During cluster root formation in lupins, isoflavonoid exudation, together with

citrate release, is spatially and temporally regulated to coincide with maturation of the cluster roots (Weisskopf et al., 2006, Tomasi et al., 2008). Solid phase root zone extraction with the use of micro-tubes that can be placed along the root could be used in future studies to determine spatial and temporal changes in flavonoid exudation along roots grown in soil (Mohney et al., 2009, Weidenhamer et al., 2009)

Once in the rhizosphere, the fate of flavonoids depends on various conditions in the soil. Flavonoids can be absorbed to the cell wall and to soil particles with cationic binding sites, thus becoming unavailable (Shaw and Hooker, 2008). Depending on their modifications, flavonoid solubility and mobility in the soil varies. While glycosylation improves their solubility in water, it is likely that flavonoid glycosides are quickly deglycosylated by microorganisms and plant exoenzymes, leaving the more hydrophobic aglycone (Hartwig and Phillips, 1991). Flavonoid persistence in the soil varies and can be less than 72 h, depending on the structure (Shaw and Hooker, 2008). Persistence in non-sterile soil can be much shorter than in sterile soil, suggesting degradation by microorganisms. Some bacteria metabolize flavonoids as a carbon source, while others specifically modify flavonoids. For example, rhizobia can modify *nod* gene inducing flavonoids by partial breakdown to produce flavonoids more or less active as *nod* gene inducers (Rao and Cooper, 1995).

Flavonoids also alter the soil by acting as antioxidants and metal chelators. Chelation and reduction of metals can alter nutrient concentration in the soil, and this might have importance especially for the availability of phosphorus and iron. For example, an isoflavonoid identified in *Medicago sativa* (alfalfa) root exudates was able to dissolve ferric phosphate, thus making both phosphate and iron available to the plant (Masaoka et al., 1993). Flavonoids, including genistein, quercetin and kaempferol can also alter iron availability by reducing Fe(III) to Fe(II) and by chelating iron otherwise unavailable in iron oxides (Cesco et al., 2010).

Flavonoids can be synthesized and released specifically in response to abiotic and biotic signals in the rhizosphere (Dixon and Paiva, 1995). For example, flavonoid

synthesis is affected by phosphorus (Juszczuk et al., 2004) and nitrogen supply (Coronado et al., 1995) in the soil. Flavonoids are specifically induced by symbionts and pathogens (see below) and also respond to purified signaling molecules of these organisms. Recently, a study demonstrated that silencing of soybean isoflavonoids led to significant changes in the diversity of the bacterial communities in the rhizosphere (White et al., 2014). The following sections highlight some examples for the diverse function of flavonoids in the rhizosphere along with some of the opportunities for using flavonoids are regulators of rhizosphere functions (Figure 1.3).

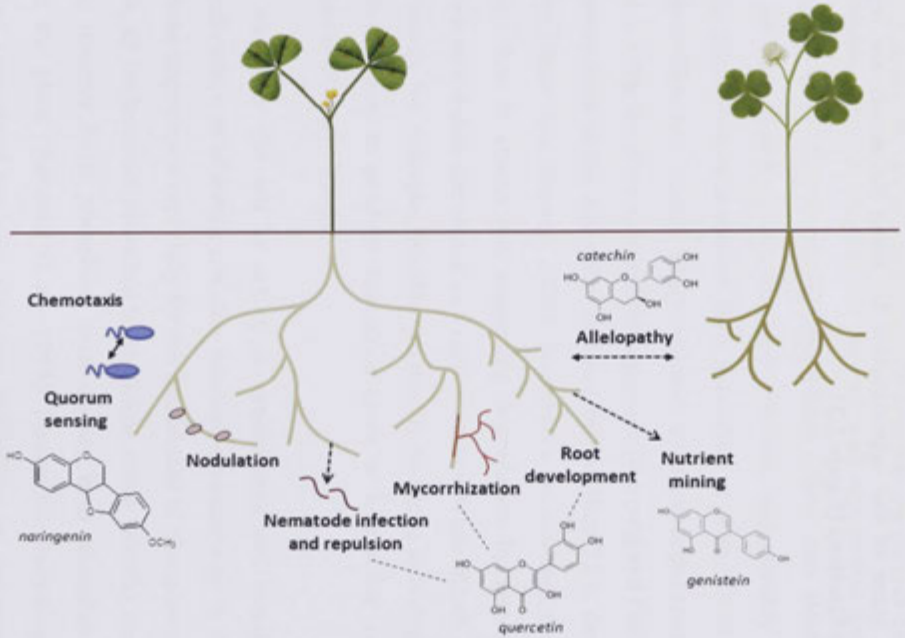

Figure 1.3 – Schematic overview of flavonoid functions in the rhizosphere. Flavonoid functions in the rhizosphere range from *nod* gene inducers and chemo-attractants in rhizobia, stimulators of mycorrhizal spore germination and hyphal branching, possible quorum sensing regulators in bacteria, repellents for parasitic nematodes, nutrient mining and as allelochemicals in plant-plant interactions. They can also affect root development. Examples of biologically active flavonoids mediating the different interactions are shown.

1.3 Multiple roles for flavonoids in nodulation

Most legumes have the ability to form root nodules that house symbiotic nitrogen fixing bacteria or rhizobia. In addition, members of several families of non-legumes, so-called actinorhizal plants, form symbioses with nitrogen-fixing actinomycetes, in particular *Frankia* species. The rhizobia fix atmospheric nitrogen into a form that the plant can use to fulfill its nitrogen requirement while the plant provides the bacteria with a source of carbon. Nodules are root organelles that are developed through signal exchange between the plant roots and the bacteria. In this symbiosis, flavonoids act as chemoattractants, inducers of nodulation (*nod*) and other genes, determinants of host specificity, developmental regulators and regulators of phytoalexin resistance in rhizobia (Cooper, 2004).

One well-studied role of root-exuded flavonoids is their action as regulators of *nod* genes in rhizobia. A number of *nod* gene products are necessary to synthesize species-specific Nod factors, lipochitin oligosaccharides required for nodule formation in the host (Spaink, 1995). The *nod* gene transcription is regulated by NodD, a transcription factor of the LysR family of transcriptional regulators. Binding of an appropriate flavonoid to NodD is thought to enhance the access of RNA polymerase and improve transcriptional ability of the *nod* genes at the site in the promoter where NodD is localized (Li et al., 2008, Peck et al., 2006). The perception of flavonoids by rhizobia is also linked to elevation in concentrations of intracellular calcium in rhizobia that subsequently induces NodD proteins for Nod factor expression (Moscatiello et al., 2010). The first flavonoids to be discovered to act as *nod* gene inducers were luteolin, isolated from *M. sativa* and 7,4' dihydroxyflavone from *Trifolium repens* (white clover) (Peters et al., 1986, Redmond et al., 1986). Since then many other flavonoids have been discovered to have *nod* gene inducing roles (summarized by Cooper, 2004). Most of these flavonoids are active as *nod* gene inducers at nano- to low micromolar concentrations. It has been suggested that a mixture of flavonoids is more effective in inducing *nod* genes as opposed to a single compound (Bolanos-Vasquez and Warner, 1997, Begum et al., 2001). The specific exudation of flavonoid (mixtures) from legume hosts together with the specific perception of flavonoids by NodD

proteins of different rhizobia is partially responsible for the host specificity of the symbiosis.

Interestingly, some flavonoids also show *nod* gene repressing activity for certain rhizobia. For example, the isoflavonoids medicarpin and coumestrol have been shown to negatively control Nod factor production in *Sinorhizobium meliloti* (Zuanazzi et al., 1998). The *nod* gene activators and repressors together are thought to maintain an optimal level of Nod factor production and prevent elicitation of defense responses by the plant (Savouré et al., 1997, Zuanazzi et al., 1998).

Flavonoid exudation from the root changes during the symbiosis. Altered flavonoid exudates have been found in rhizobia-inoculated roots of several legumes. This alteration in flavonoid profiles could fine-tune Nod factor synthesis during different stages of symbiosis (Dakora et al., 1993, Schmidt et al., 1994). Altered flavonoid exudate profiles could also be the result of flavonoid metabolism by rhizobia themselves, causing changes in the activity of flavonoids as *nod* gene inducers or repressors (Rao and Cooper, 1995).

Some flavones and flavonones that induce *nod* genes, such as luteolin and apigenin, have also been shown to evoke a strong chemoattractant response from the rhizobia, with different flavonoids attracting different *Rhizobium* species (Aguilar et al., 1988, Dharmatilake and Bauer, 1992). These responses occur at flavonoid concentrations of 10^{-6} to as little as 10^{-10} M, a much lower minimum concentration that reported for flavonoid activity as *nod* gene inducers.

In actinorhizal symbioses, flavonoids might also play a role in host specificity and selection of rhizobia, even though no canonical *nod* genes have been found in *Frankia* (Normand et al., 2007). Flavonoids were found to accumulate inside actinorhizal nodules (Laplaze et al., 1999). Flavonoids from seeds of actinorhizal plants were shown to enhance or inhibit symbiosis, although the flavonoids were not identified in this study (Benoit and Berry, 1997). Flavonoids extracted from fruits of the host *Myrica gale* had positive effects on growth and nitrogen fixation in compatible, but negative effects in incompatible *Frankia* strains (Popovici et al.,

2010), suggesting that flavonoids could play a role in selection of compatible rhizobia by the host. This is similar to the situation in legumes, where it has been shown that the phytoalexin medicarpin produced by clover and medic species inhibits the growth of incompatible but not that of compatible strains (Pankhurst and Biggs, 1980). This effects might be due to the fact that certain (iso)flavonoids can induce resistance to phytoalexins in rhizobia at micromolar concentrations (Parniske et al., 1991), thus enabling host plants to simultaneously exude phytoalexins to inhibit pathogens while still allowing rhizobial infection.

Flavonoids have also been shown to regulate a number of other *Rhizobium* genes, including those for exopolysaccharide synthesis, which is important for regulating defense responses in the host. For example, genistein at 1 μM concentration altered exopolysaccharide concentration and composition in *Rhizobium fredii* cultures (Dunn et al., 1992). In addition, type III secretion systems, which play a role in nodulation in some rhizobia, as well as the production of exported proteins, can be induced by flavonoid exudates (Krishnan et al., 2003). Proteome analysis also found a number of other proteins in response to host flavonoids, many of which await characterization (Guerreiro et al., 1997)

Nod factors are important in inducing the initial response of root cortical cell division and root hair curling. Certain flavonoids act as negative regulators of auxin transport and could thus cause accumulation of auxin at the nodule initiation site to stimulate cell division and nodule organogenesis (Mathesius et al., 1998b, Wasson et al., 2006, Boot et al., 1999). Exactly how flavonoids redirect auxin transport during nodule initiation is not known, but the perception of Nod factors by the plant is thought to induce endogenous flavonoids that could locally inhibit auxin transport (Mathesius et al., 1998a). In *M. truncatula*, silencing of different branches of the flavonoid pathway showed that flavonols like kaempferol are the most likely candidates for auxin transport inhibitors (Zhang et al., 2009). Whether auxin transport regulation occurs during nodulation of legumes forming determinate nodules, e.g. soybean, is still unclear, but it is likely that other flavonoids, possibly isoflavonoids, are involved (Subramanian et al., 2006).

Changes in auxin accumulation could also be due to auxin breakdown by peroxidases, which can be modulated by flavonoids. The isoflavonoid formononetin, which accumulates in the nodule primordia of white clover, accelerated auxin breakdown. In contrast, a derivative of 7,4'-dihydroxyflavone (DHF) and free DHF, which accumulate in the vacuoles of the cortical cells that later form the nodule primordia, were shown to inhibit auxin breakdown (Mathesius, 2001). The local changes in auxin may be critical in regulating cell divisions during nodule development.

One of the opportunities in nodulation research could be the expression of appropriate flavonoid synthesis pathways in non-legumes in future efforts to extend nodulation beyond legumes. In addition, altered branches of the flavonoid pathway could be engineered to extend legume host ranges to non-specific rhizobia. This is demonstrated in Chapter 2 where I have engineered *M. truncatula* roots to express silencing or overexpression constructs targeting known genes encoding flavonoid biosynthesis enzymes. I have further investigated if auxin accumulation and response in flavonoid-silenced roots are altered in response to rhizobia inoculation (Chapter 3).

1.4 Effects of flavonoids on quorum sensing-regulated behaviours

Many behaviours of rhizosphere bacteria are coordinated by cell-to-cell signals called quorum-sensing signals (Fuqua et al., 2001). Quorum sensing signals are synthesized by most bacteria and the so-far best-studied signals belong to the class of acyl homoserine lactones (AHLs), which are used by many gram-negative bacteria. Quorum sensing signals diffuse into and out of bacterial cells and can bind to receptors inside the bacteria once their concentration exceeds a certain threshold (Fuqua et al., 1994). This activates the expression of hundreds of bacterial genes, many of which are important in plant-microbe interactions, including genes responsible for biofilm formation, nitrogen fixation, synthesis of degradative enzymes, exopolysaccharides and toxins, as well as motility and conjugation (von Bodman et al., 2003, Gonzalez and Marketon, 2003).

In the past years, a number of molecules have been identified that interfere with quorum sensing, including halogenated furanones produced by red algae (Manefield et al., 1999). A number of land plants have been shown to synthesize quorum-sensing mimics, which can both inhibit and stimulate AHL-dependent genes in various reporter strains, although most of these compounds remain unidentified (Teplitski et al., 2000, Gao et al., 2003). The first mimic signal identified from plants was lumichrome, a riboflavine derivative (Rajamani et al., 2008). Another potential AHL mimic is the phenolic compound p-coumaric acid, a lignin precursor that can be exuded by roots into the soil (Bodini et al., 2009). P-coumaric acid can also be produced by breaking down flavonoids from root exudates (Rao and Cooper, 1995). In addition, p-coumaric acid can form p-coumaroyl-homoserine lactone, a distinct quorum-sensing signal used by some bacteria (Schaefer et al., 2008). Thus, p-coumaroyl-HSL could have two functions, to sense the presence of a host plant and to control density-dependent bacterial behaviors. A flavonoid identified from the medicinal tree *Combretum albiflorum*, catechin, which also occurs in many other plant species, also showed activity as a quorum-sensing mimic, although at rather high concentrations of between 0.125 and 4 mM (Vandeputte et al., 2010). Catechin can also be present in the rhizosphere of plants, for example as an exudate of spotted knapweed, where it acts as a potent allelochemical (Weir et al., 2003). Another flavonoid with inhibitory effects on quorum sensing regulated reporters is naringenin, which was shown to inhibit quorum sensing in *E. coli* and *Vibryo fischeri* at concentrations of 20 -360 μM (Vikram et al., 2010) as well as in *P. aeruginosa* at 4 mM concentration (Vandeputte et al. 2011). Naringenin is exuded by some legume roots and also acts as a *nod* gene inducer in rhizobia (Novak et al., 2002). Therefore, it would be interesting to test the effect of naringenin on quorum sensing-regulated genes in rhizobia.

Interestingly, the flavonoid pathway is activated in legumes by exposure to quorum sensing signals from rhizobia, and it has also been shown that bacterial AHLs (at 50 μM concentrations) can stimulate production of AHL mimics by *M. truncatula* (Mathesius et al., 2003). These results strongly suggest a link between AHL perception by plants, activation of the flavonoid pathway and possible

feedback on bacteria by production of possible AHL mimics. However, effective concentrations of potential flavonoid mimics in the rhizosphere will have to be established. A recent study found that *nod* gene inducing flavonoids increased AHL synthesis in three species of rhizobia at low micromolar concentrations, concomitant with enhanced expression of AHL synthesis genes (Perez-Montano et al., 2011). This suggests coordination between *nod* gene induction and quorum sensing, possibly to enhance symbiotic behaviours of rhizobia. If flavonoids indeed act as quorum sensing mimics and activators in plant-associated bacteria at relevant concentrations this could be explored as an avenue to alter the ability of bacteria to colonize and infect host plants.

1.5 Mycorrhizal symbioses

Mycorrhizal fungi are important symbionts of the majority of land plants that contribute primarily to plant phosphorus nutrition. Mycorrhizal symbioses are stimulated under phosphorus deficiency in the soil. Mycorrhizal fungi germinate from spores and form hyphae in the soil which branch in response to root exudates, which attract the hyphae to a host root. Hyphae then penetrate the host root tissue and form ecto- or endomycorrhizal invasion structures (Harrison, 2005). Some of the host exudates that stimulate spore germination, hyphal branching in the soil and root colonization, often in a symbionts-specific manner, have been identified as flavonoids (Steinkellner et al., 2007, Siqueira et al., 1991, Scervino et al., 2007, Scervino et al., 2005, Kikuchi et al., 2007). Most of these studies reported active flavonoid concentrations of between 0.5 and 20 μM. Not surprisingly, some of the flavonoids enhancing mycorrhizal infection are induced under phosphorus stress (Akiyama et al., 2002). The isoflavonoid coumestrol has been identified as a particularly active stimulator of hyphal growth (Morandi et al., 1984) and an *M. truncatula* mutant hyper-accumulating coumestrol was also found to be hyperinfected by its mycorrhizal symbiont (Morandi et al., 2009).

Flavonoids are also likely to play a role during fungal invasion and arbuscule formation inside the root. Infection of roots with vesicular arbuscular mycorrhizal fungi was shown to induce the flavonoid pathway in a number of host species, in particular in infected cells (Harrison and Dixon, 1994).

Flavonoid accumulation starts before the onset of infection and was shown to vary with different stages of infection and in response to different symbionts (Harrison and Dixon, 1993, Larose et al., 2002). One of the roles of flavonoids inside the root could be to regulate defense reactions, and it has been hypothesized that mycorrhizal invasion triggers a temporary defense response in the root that involves induction of flavonoid phytoalexins (Harrison and Dixon, 1993). However, compared to the induction of phytoalexins in response to pathogens, mycorrhizal induction of these flavonoids is relatively low (Morandi, 1996). Flavonoids may also be responsible for an autoregulation of mycorrhization at later stages of the symbiosis (Larose et al., 2002). Split-root studies have demonstrated that formononetin and its glycoside are down-regulated systemically by either rhizobia or mycorrhizae, concomitant with autoregulation of both symbioses, and that their external application restored the symbioses (Catford et al., 2006).

Interestingly, pyranoisoflavones produced by white lupin, which is not a host for mycorrhizal fungi, inhibited hyphal branching of mycorrhizal fungi, suggesting that flavonoids could play both stimulating and inhibitory roles on fungal symbionts in the soil (Akiyama et al., 2010). However, inhibitory activity of flavonoids on hyphal branching was also reported from host plants (Tsai and Phillips, 1991), and therefore, it is likely that host and non-host plants can modulate the establishment of symbiosis by altering the profile of flavonoid exudates. While flavonoids clearly appear to enhance mycorrhization through stimulation of spore germination, hyphal branching and host infection, their presence in the host is not essential for the symbiosis. Experiments in flavonoid-deficient carrot and maize plants have shown that mycorrhizal infection was not abolished (Becard et al., 1995).

Mycorrhial fungi can also protect plants from pathogens (Whipps, 2004) and enhance symbiosis with rhizobia. One possibility is that the flavonoids induced by mycorrhizal fungi also stimulate Nod factor synthesis. For example, daidzein is induced by mycorrhizal fungi in soybean (Morandi et al., 1984), where it also acts as a *nod* gene inducer for *Bradyrhizobium japonicum* (Kosslak et al., 1987). On the

other hand, coumestrol is induced by mycorrhizal symbionts in *M. truncatula* (Harrison and Dixon, 1994), where it could act as a *nod* gene inhibitor in *S. meliloti* (Zuanazzi et al., 1998). It is possible that combinations of flavonoids, rather than single compounds, need to be tested in more detail for their combined effects on multiple symbionts. The tripartite symbiosis between soybean and its mycorrhizal and rhizobial symbionts was shown to enhance nodulation compared to inoculation of plants only with rhizobia. In the co-inoculated plants, flavonoid profiles changed specifically in response to both symbionts, although interestingly, flavonoid accumulation was largely inhibited by the symbionts, including the flavonoids with activities as *nod* gene and hyphal branching inducers (Antunes et al., 2006). Therefore, enhanced symbiosis in tri-partite interactions might be due to enhanced nutrient uptake rather than, or in addition to, stimulation of flavonoids.

The protection of the host plant from pathogens by mycorrhizal fungi has also been partially attributed to the enhanced synthesis of flavonoid (phytoalexins) in response to the mycorrhizal symbiont (Morandi, 1996), although data are still scarce and the protective effect could have multiple causes (Borowicz, 2001). While some studies have shown increased phenolic content of roots co-inoculated with mycorrhizal fungi and pathogens (Cordier et al., 1998, Dehne and Schonbeck, 1979), others found decreased phytoalexin accumulation in co-inoculated plants compared to plants only inoculated with mycorrhizal symbionts (Carlsen et al., 2008).

1.6 Flavonoids are involved in defence against root pathogens

Flavonoids and other phenolics have been found to inhibit a range of root pathogens and pests ranging from bacteria to fungi and insects (Makoi and Ndakidemi, 2007). This has been attributed to their role as antimicrobial toxins (Cushnie and Lamb, 2011) and anti- or pro-oxidants (Jia et al., 2010). Their role within the plant as antioxidants is suspected to be protective, although clear evidence is lacking (Hernández et al., 2009). Some of the major gaps in knowledge pertain to fact that because of their highly oxidative nature, the transport and storage of flavonoids is tightly regulated. Hence, the mechanism in which these

compounds may become available to prevent oxidative stress in case of a pathogen attack is unknown.

The challenge from a pathogen can lead to *de novo* synthesis of flavonoid phytoalexins that exhibit antifungal and antibacterial activities. These molecules can also be stored in an inactive form to function as broad-spectrum phytoanticipins to mount a quick defense against future attacks (Lattanzio et al., 2006).

Isoflavonoids represent a major class of phytoalexins in legumes. Using a promoter:GUS fusion, it was shown that the expression of isoflavone synthase (Figure 1.1) was elevated when elicited with salicylic acid and cyst nematodes (Subramanian et al., 2004) suggesting their direct involvement in plant defense. Derivatives of isoflavonoids called pterocarpans such as medicarpin, pisatin and maackiain are known to have antimicrobial properties (Naoumkina et al., 2010). Maackiain also inhibited the oomycete *Pythium graminicola* at a concentration of 20 μg/L (Jimenez-Gonzalez et al., 2008). Medicarpin from alfalfa and pea protects the plants from the pathogenic fungus *Rhizoctonia solani* (Pueppke and Vanetten, 1974, Kapulnik et al., 2001) possibly by having inhibitory activities on the elongation of fungal germ tube and mycelial growth (Blount et al., 1992, Higgins, 1978). There is also genetic evidence that pisatin from pea contributes to resistance against the fungus *Nectria haematococca* (VanEtten and Wu, 2004), as a knockdown of enzymes responsible for pisatin biosynthesis reduced its concentration from 28 μg/g dry weight by one third and increased the susceptibility of pea roots towards the fungal infection.

The mechanism of resistance against fungal infection through pterocarpanoid phytoalexins is suspected to be through a hypersensitive response (HR) mediated cell death (Heath, 2000). The cell death through this pathway incorporates an initial oxidative burst with an influx of Ca^{2+}, followed by alkalinisation of the apoplast through K^+/H^+ exchange leading to the depolarisation of the membrane and an extended period of oxidative state. Isoflavonoids are thought to be oxidized during this process leading to generation of toxic free radicals that may cause cell

death. Alternatively, it is also suggested that some pterocarpans target the membrane ATPase and mitochondrial electron transport for degradation, leading to cell death (Graham et al., 2007).

It is also interesting to note that in some plant-microbe interactions the pterocarpans may not accumulate within the roots but be secreted instead. When chickpea seedlings were challenged by the endogenous elicitor glutathione, an increase in pterocarpan biosynthesis was observed (Armero et al., 2001). It was also shown that these compounds were released by the roots to the surrounding, possibly to cause damage to the pathogens before they can infect the roots.

Flavonols also contribute to resistance against pathogens. One of the most widely distributed flavonol, quercetin has strong antimicrobial properties. Quercetin binds to GyrB subunit of *Escherichia coli* DNA gyrase and inhibits the ATPase activity. However, the promotion of DNA cleavage was induced only at concentrations above 80 μM (Naoumkina et al., 2010, Plaper et al., 2003). Quercetin also inhibited the growth of the fungus *Neurospora crassa* (Parvez et al., 2004). The plant carnation (*Dianthus caryophyllus*) mounts a defense against *Fusarium* attacks through increasing the concentration of the fungitoxic flavonol triglycoside of kaemferide at concentrations as low as 50 nM (Curir et al., 2005).

Global gene expression studies have also shown that elevation of flavonoid synthesis occurs when *M. truncatula* plants were challenged by *Phymatotrichopsis omnivora*, cause of cotton root rot disease (Uppalapati et al., 2009). In order to successfully colonize the plant, virulent strains of pathogens such as *P. omnivore, N. haematococca* and *R. solani* have 'learned' to evade many of these flavonoids (Denny and Vanetten, 1981, Denny and Vanetten, 1982, Padmavati et al., 1997, Pedras and Ahiahonu, 2005).

An appealing opportunity to enhance plant protection would be to engineer plants with increased, or inducible expression of effective flavonoid phytoalexins and phytoanticipins, however, it might be necessary for the plant to synthesize a range of active antimicrobial flavonoids to avoid emergence of resistance by pathogens. Using the constructs generated in this study, I have investigated if overexpression

of isoflavone synthase led to increased tolerance against root pathogens such as *R. solani* and *Aphanomyces euteiches*. In future, it would be imperative to test whether ectopic expression of these flavonoids would cause any harm to beneficial rhizosphere organisms.

1.7 Flavonoids in nematode interactions

Plant parasitic nematodes, including root knot, cyst and root lesion nematodes, constitute some of the major root pathogens. Many of these pathogens exhibit a wide host range, often of thousands of plant species. Sedentary endoparasitic nematodes cause the formation of feeding structures that are characterized by multiple cell divisions and endoreduplication in root tissues, leading to the formation of galls or cyst (Goverse et al., 2000, Gheysen and Mitchum, 2011). Invasion of roots with root knot and cyst nematodes induces the flavonoid pathway in infection structures (Jones et al., 2007, Hutangura et al., 1999), and it has been hypothesized that the flavonoids could act as regulators of auxin transport and accumulation during gall formation (Hutangura et al., 1999, Grunewald et al., 2009). In *M. truncatula* plants deficient in flavonoids, gall formation still occurred, although galls were smaller and showed less cell divisions (Wasson et al., 2009). In flavonoid-deficient *Arabidopsis* and tobacco mutants, reproduction of several species of nematodes was not affected (Wuyts et al., 2006a, Jones et al., 2007). However, flavonoids did have an effect on nematode behaviour, for example certain flavonoids acted as repellents for specific nematode species and inhibited their motility and hatching at mM concentrations (Wuyts et al., 2006b). Therefore, while flavonoids do not seem to be essential for feeding site development in the host plant, flavonoids exuded into the rhizosphere could alter nematode attraction to the roots. This could be exploited for designing nematode trap plants that could be intercropped to reduce the infection of crop roots.

1.8 Flavonoids can cause allelopathy

Allelopathy, the inhibition of plant growth and germination by other plants, plays an important role in parasitic and invading plants and can have far-reaching

ecological consequences. In some cases, flavonoids have been implicated as allelochemicals in the rhizosphere. The parasitic weed *Striga* constitutes one of the major problems in African agriculture with yield losses up to 100% in large parts of sub Saharan Africa, thus inhibiting its germination would be an important achievement (Gressel et al., 2004). In a search for intercropping plants, the forage legume *Desmodium uncinatum* was found to significantly inhibit post-germination and attachment of *Striga*, and this inhibition was mimicked by several (iso)flavonoids identified from its root exudates (Khan et al., 2010, Hooper et al., 2010). In addition, at least one of the isoflavones stimulated germination, which could be used to cause 'suicidal' germination of the weed. Therefore, the use of *Desmodium* as a 'push-pull' intercrop plant has been a cheap and successful strategy for smallholder farmers to control *Striga* infestations (Hooper et al., 2009, Khan et al., 2006).

The success of some invasive weeds has also been attributed to flavonoid allelochemicals. For example, spotted knapweed (*Centaurea maculosa*), which has been invading large parts of North America, exudes (-)-catechin, which can induce reactive oxygen species in susceptible species that lead to cell death and demise of the root system (Bais et al., 2003). A racemic mixture of catechin can also have detrimental effects on legume nodulation at high (~3 mM) concentrations (Alford et al., 2009). (-)-catechin has also been suggested to inhibit germination and growth of native species, but it has been questioned whether soil concentrations of (-)-catechin would be high enough to be effective (Blair et al., 2005, Duke et al., 2009).

1.9 Flavonoid metabolic flux engineering

The biosynthesis of flavonoids involves several branches of pathways to which multiple strategies could be applied to alter the metabolic flux. The production of secondary metabolites requires the plant to invest its energy and therefore, the pathways are tightly regulated. The initial committed step for flavonoid biosynthesis is catalyzed by chalcone synthase (CHS). Silencing of *CHS* transcripts has been demonstrated to cause dramatic decrease in flavonoid accumulation within the plant (Wasson et al., 2006, Zhang et al., 2009).

Many strategies can be adopted for engineering the flux of metabolites through the biosynthesis pathways. Some of these include –

1 – Changes in enzyme specificity through changes in the active site configuration. By studying the crystal structure of the enzymes' active sites, novel methods to manipulate it may be developed to affect substrate specificity. Jez et al. (2002) demonstrated that the substrate specificity could be altered by inducing single point mutations at the active site of CHS.

2 – Since flavonoid biosynthesis is an energy consuming process, the plants utilize control points for each branch. Knockouts or knockdowns of these critical enzymes would direct the flux into alternative branches. Some of the enzymes that may be directed with this strategy include isoflavone synthase, flavone synthase II and vestitone reductase. Zhang et al. (2009) confirmed that knockdown of isoflavone synthase and flavone synthase led to the generation of roots deficient in isoflavonoids and flavones, respectively. The authors were then able to demonstrate that plants can nodulate even in the absence of isoflavonoids that are thought to play an essential role in the process.

3 – Transporters. Flavonoids are synthesized in the cytoplasm but often have to be transported for exudation into the rhizosphere or storage. Similar to enzymes, the expression of transporters would also have an impact in the direction of the flux. This was recently demonstrated when a MATE type transporter was knocked down to generate proanthocyanidin-rich plants (Zhao et al., 2011, Zhao and Dixon, 2009).

4 – Modification enzymes. Transport, activity and storage of flavonoids often require modifications of their structure. Changes in abundance or activity of enzymes responsible for these modification may increase or decrease generation of the end product. An example of such an enzyme is O-methyl transferase (OMT) that is responsible for 4'-O-methylation and 3'-O'-methylation of isoflavonoids in the generation of phytoalexins. Silencing of OMTs in pea affects the flux in the biosynthetic pathway leading to the reduction in the phytoalexin pisatin (Liu et al., 2006). A similar strategy may be applied to other modification enzymes although

it may be challenging to find enzymes that are not catalytically promiscuous and allowing control of a single pathway.

5 – Transcription factors. Altered expression of transcription factors regulating different parts of the flavonoid pathway could be an approach to altering activity of more than one enzyme. Members of the MYB, bHLH and WD40 transcription factors play an important role in regulating the flavonoid pathway (Koes et al., 2005, Du et al., 2010). For example, it has been shown that ectopic expression of MYB transcription factors can significantly increase anthocyanin synthesis in tomato (Butelli et al., 2008). In soybean, isoflavonid synthesis was increased by a combination of ectopic expression of maize transcription factors and inhibition of the competing anthocyanin pathway (Yu et al., 2003).

1.10 Challenges in manipulating the flavonoid pathway

While it appears opportunistic to modify the flavonoid pathway in order to manipulate root-rhizosphere interactions, the many interactions between plants, flavonoids and microorganisms demand a cautionary approach. First, while most studies on the function of flavonoids have been done under laboratory conditions, their demonstration in real rhizosphere conditions remains to be carried out to determine how effective some of the flavonoids functions remain under conditions of breakdown, adsorption, metabolism and altered solubility in the soil. Second, there are likely to be unforseen effects of flavonoids on non-target organisms. Whereas certain flavonoids could enhance nodulation or mycorrhization of host plants, they could also indirectly affect bacterial quorum sensing, plant-plant interactions and soil biochemistry. For example, catechin could inhibit quorum sensing in host related soil bacteria, while it may also suppress plant growth as a potent allelopathic signal. Similarly naringenin, which induced *nod* gene expression in several rhizobia, could have an effect on quorum sensing regulation in non-target bacteria. Exudation of isoflavonoids from soybean can stimulate attraction of its symbionts *Bradyrhizobium japonicum* as well as the devastating pathogen *Phytophthora sojae* (Morris et al., 1998). In addition, metabolism of flavonoids by rhizosphere bacteria could alter their activity and availability in the soil and could affect other bacteria (Shaw et al., 2006). Third, altering

concentrations or forms of flavonoids inside the plant tissue is likely to have effects on plant development, which could be either beneficial or detrimental for the plant host. Flavonoids, via their effect on auxin transport (Brown et al., 2001) have been shown to alter cell morphology, root growth, gravitropism, and light responses (Buer and Djordjevic, 2009, Buer and Muday, 2004, Ringli et al., 2008).

Flavonoid exudation is also likely have effects on microbial community structure in the soil because it could increase species that use flavonoids as a carbon source while inhibiting the growth of others as phytoalexins (Walker et al., 2003, Rao and Cooper, 1994). Increased phenolics exudation in the Arabidopsis *abcg30* mutant was shown to have wide ranging effects on bacterial and fungal community structure, although this mutation also affected other exudates (Badri et al., 2009).

Alteration of flavonoid synthesis is feasible and has been demonstrated in many studies in various plants, and both overexpression and inhibition of the flavonoid pathway using RNA interference have been successful (Wang et al., 2011). In some cases, the transfer of single gene encoding flavonoid enzymes might be sufficient to have an effect. For example, transfer of stilbene synthase from grapevine to tobacco resulted in increased resistance to *Botrytis cinerea* (Hain et al., 1993). Altering glycosylation or targeting vacuolar transporters are other options that would allow the release of stored flavonoids from the vacuole for subsequent export (Weisshaar and Jenkins, 1998, Zhao et al., 2011b). One aspect of the manipulation of flavonoid synthesis or glycosylation is that it would be most efficient if it was targeted in the appropriate tissues (Figure 1.2), for example the root epidermis for subsequent exudation. This would require the use of epidermal-specific promoters, which are currently not available for most crop plants.

An important drawback in the manipulation of specific branches of the flavonoid biosynthesis pathway could be that it alters fluxes through other branches of the flavonoid pathway or related pathways (Wang et al., 2011, Liu et al., 2002). This has been cited as one reason why sufficient flavonoid accumulation for large scale production in engineered plants has not been successfully achieved (Fowler and Koffas, 2009). For example, mutants that show changes in the flavonoid pathway

have been shown to have altered lignin biosynthesis, and *vice versa*, as both pathways share the same precursors. In the *cra* (*compact root architecture*) mutant of *M. truncatula*, alterations in the flavonoid pathway are accompanied by altered lignin biosynthesis with effects on root growth (Laffont et al., 2010). Similarly, silencing of lignin synthesis in transgenic Arabidopsis plants resulted in increased flavonoid accumulation and this increase was hypothesized to reduce plant growth (Besseau et al., 2007). However, this was refuted in a more recent study that showed that a double mutant defective in p-coumaroyl shikimate 3'-hydroxylase (showing reduced lignin biosynthesis) and chalcone synthase (unable to synthesize flavonoids) showed similar growth to the single p-coumaroyl shikimate 3'-hydroxylase mutant (Li et al., 2010).

The challenge of manipulating the flavonoid pathway in order to affect rhizosphere biology will involve more detailed information on the regulation of flavonoid transport and exudation than we currently have. While some flavonoid transporters are known, to our knowledge none have definitively been demonstrated to be specific for exudation of flavonoids into the rhizosphere. Increased exudation of specific flavonoids into the rhizosphere would involve (1) alteration of specific branches of the flavonoid pathway to overexpress, newly express or inhibit synthesis or to alter glycosylation, (2) up-regulation of flavonoid exudation, and (3) coupling of altered expression to rhizosphere signals that would specifically induce the desired pathways. The latter would require detailed knowledge of promoters and transcription factors that are specific for flavonoid induction by the correct trigger (Grotewold, 2008). Since flavonoid storage is compartmentalized within the cell and between different cell types (Figure 1.2), altering flavonoid synthesis without control of their final destination could result in storage of flavonoids in the vacuole without release or release from the wrong region of the root where the target micro-organisms are not found. For example, rhizobia only infect roots close to the root tip so flavonoid exudation would be most effective in that region.

As an alternative to genetic manipulation of the flavonoid pathway, it will be useful to exploit the huge diversity of flavonoids synthesized in different plant

species (Dakora, 1995). As described above, the selection of intercropping plants producing *Striga*-inhibiting flavonoid exudates is one example that has shown success in making actual improvements to crop yields for farmers in sub-Saharan Africa.

1.11 Aims of this study

This chapter has described the wide range of roles flavonoids are known or speculated to play in plant-microbe interactions. Therefore, the central aim of this thesis is to engineer the flavonoid biosynthesis pathway in the model legume *Medicago truncatula* and conduct a systematic genetic study to identify the class of flavonoids associated with these roles. The motivation for this study is driven by the ability of legumes to form both symbiotic and pathogenic relationships with microorganisms therefore, elucidating overlaps in these two associations.

Specifically, the four subsequent chapters presented deal with the following questions as they appear in this thesis –

In Chapter 2, I have investigated and demonstrated if targeting of genes encoding flavonoid biosynthesis enzymes for silencing or overexpression led to significant changes in accumulation of flavonoid metabolites. I have used RNAi induced genes silencing mechanisms to silence multiple copies of these genes or used a Cauliflower mosaic virus promoter (35s) to drive overexpression of these genes. The methods were subsequently used to generate transgenic roots with altered flavonoid profiles for analysis as outlined in Chapters 3-5. For all comparisons, an empty vector expression hairy root control was used. Therefore, the study could be independent of any externally induced changes, such as phytohormones produced by the microbes as both control and flavonoid synthesis altered roots were treated in a similar manner.

In Chapter 3, I have done a functional analysis of the changes in auxin accumulation, synthesis and response due to altered root-flavonoid profiles. Could a specific flavonoid group be responsible for the accumulation and response of the plant hormone auxin? I also addressed the question if the function of flavonoid as

an inhibitor of polar auxin transport could be replaced with synthetic auxin-transport inhibitors to restore nodulation in flavonoid-deficient roots.

In Chapter 4, I explored additional roles of flavonoids in the root-rhizobia interactions. If polar auxin transport inhibition was insufficient to induce nodulation in the flavonoid-silenced roots, what other additional gene expression changes were induced by flavonoids in these roots? Could the antioxidant and prooxidant behaviour of flavonoids have roles in infection thread formation for successful rhizobia colonization?

In Chapter 5, I investigated the behaviour of the transgenic roots with altered flavonoid-profiles in their interaction with root-pathogens *Rhizoctonia solani* and *Aphanomyces euteiches*. Could silencing or overexpression of specific branches of flavonoid biosynthesis lead to changes in the roots' tolerance towards these pathogens? Could interactions with pathogens lead to an accumulation of specific flavonoids in *M. truncatula* hairy roots as a defence mechanism?

Finally in Chapter 6, I assimilate the results obtained from all the studies and discuss a model for the flavonoid-induced changes in root-microbe interactions. I also discuss future experiments that would support the findings presented in this thesis.

Chapter 2. Generation of RNAi and overexpression constructs for inducing flavonoid metabolic changes

Summary

The aim of this chapter was to establish the methods used to generate the RNAi and overexpression constructs for inducing flavonoid metabolic changes in *M. truncatula* roots. Here I have described the targeted genes of the flavonoid biosynthesis enzymes and the methods used to clone them into *Agrobacterium rhizogenes* which induces hairy roots in *M. truncatula roots.* Subsequently, the methods used to determine the expression of genes at the transcript level are presented. The confirmation of flavonoid metabolite changes have been done through metabolite analysis using LC-MS/MS.

It was found that multiple copies of flavonoid biosynthesis enzymes exist in *M. truncatula*. Targeting multiple copies of these genes was possible through RNA interference; however, overexpression of a single copy of the enzyme was not as successful in increasing the flavonoid content of the respective targeted pathways. It is hypothesised that this could be due to a) the metabolic enzyme being present very high up in the pathway where it does not act as a rate limiting step, or b) the selected copy of the gene encoding the flavonoid synthesis enzyme not being expressed actively in hairy roots.

2.1 Introduction

Flavonoids are synthesized in legume plants through a network of pathways. The major branches of the flavonoid biosynthesis pathway include flavonols, isoflavonoids, flavones and anthocyanins. In this chapter, the aim was to create transgenic hairy roots of the model legume *Medicago truncatula* expressing RNA silencing complexes against these major branches or overexpression constructs to amplify synthesis of flavonoid end products.

Engineering the flavonoid biosynthesis pathway in M. truncatula roots

Flavonoids in legumes are synthesised from a common precursor – phenylalanine. As shown in Chapter 1, Figure 1.1, the first committed step of this pathway is catalysed by the enzyme chalcone synthase. Silencing of this enzyme has been shown to knock down all flavonoid metabolites in *M. truncatula* roots (Wasson et al., 2006, Zhang et al., 2009). This post-transcriptional gene silencing was mediated through the mechanism of RNA interference (RNAi) (Figure 2.1). The RNAi was induced through experimentally introducing an inverted repeat of the transgene that encoded the conserved sequence region found in multiple copies of the genes coding for the chalcone synthase enzyme. The mechanism of RNAi relies on the recognition of double stranded RNA (dsRNA) by the Dicer enzyme complex which degrades it into 21 nucleotide mRNAs called short interfering RNAs or siRNAs. These mRNAs get incorporated in to a nuclease-containing complex called RNAi silencing complex or RISC. Any mRNA that binds to the siRNA on the RISC gets degraded and its translation is inhibited (Waterhouse and Helliwell, 2003). This principle has been used to study plant genomes through selectively targeting genes for post-transcriptional gene silencing (Waterhouse et al., 1998). Therefore, the same principle was used to silence the mRNA encoding flavonoid synthesis enzymes downstream of chalcone synthase.

The flavonoid metabolic pathway could also be manipulated by overexpressing the same synthesis enzymes that were targeted for silencing earlier. Using a constitutive promoter, it is possible to express a functional copy of a gene at higher levels in a plant tissue. This has allowed researchers to identify phenotypes that were not induced by knocking down a gene (Bouché and Bouchez, 2001).

Overexpression has been particularly useful in the identification of function of proteins that operate in large networks such as transcriptional factors (Zhang, 2003). Flavonoid biosynthesis has been modified previously in studies that overexpress transcription factors (MYB or bHLH) or flavonoid synthesis enzymes to increase levels of these secondary metabolites. This has been useful to increase plant defence responses (Lorenc-Kukuła et al., 2007), improve forage quality (Ray et al., 2003), generate food with improved health benefits (Muir et al., 2001) and to alter flower colour (Katsumoto et al., 2007).

Identified flavonoids in M. truncatula roots and enzymes involved in their conversion

The **Table 2.1** provides a summary of the flavonoid metabolites that have been reported in literature. These metabolites are found in *M. truncatula* hairy root cultures only as this is relevant to this study. Staszków et al. (2011) have previously demonstrated that the flavonoid profiles of *M. truncatula* hairy roots, seedling roots and cell suspension cultures are significantly different. This is important to recognise and take in to account when inferring the specific metabolite's role in symbiotic or pathogenic interactions. Table 2.1 also shows some of the putative functions of different flavonoid metabolite subgroups in their roles in symbiotic and pathogenic interactions.

In this study, I have targeted major enzymes involved in the synthesis of different flavonoid end products for silencing or overexpression. *Chalcone synthase* (*CHS*) was targeted as this represented the first committed step of flavonoid biosynthesis pathway (Wasson et al., 2006, Zhang et al., 2009) and its *Arabidopsis* equivalent is the tt4 mutant where *CHS* is knocked out leading to a complete flavonoid deficiency (Debeaujon et al., 2000). The flavones, catalysed by flavone synthase II (FSII) are *nod* gene inducers in *S. meliloti* (Zhang et al., 2007). The isoflavonoids, catalysed by isoflavone synthase (IFS) were selected because they are likely to play a role in defence (Farag et al., 2008, Subramanian et al., 2005) and may also play some role in controlling auxin transport (Subramanian et al., 2006), although in soybean this was not necessary for nodulation. Flavonol synthase (FLS) catalyses the synthesis of flavonols, that are likely to be the more important auxin transport

regulators in *M. truncatula* (Zhang et al., 2009). The enzyme dihydroflavonol 4-reductase (DFR) is an enzyme controlling the flux into synthesis of anthocyanins, condensed tannins and phlobaphenes (Xie et al., 2004) which are important for pigmentation, allelopathy and as deterrants against herbivory (Peters and Constabel, 2002, Bais et al., 2003). The Figure 2.2 shows a schematic diagram of the flavonoid biosynthesis pathway highlighting major aglycone found in *M. truncatula* roots along with the major enzymes of the pathway. For the purpose of this study I have targeted the following genes for silencing – *CHS*, *FLS*, *IFS*, *DFR* and *FSII*; and for overexpression – *CHS*, *FLS*, *IFS* and *DFR*.

This chapter details the methods used to generate silencing constructs targeting various flavonoid biosynthesis enzyme for RNAi induced silencing or overexpression driven by a constitutive promoter. The model legume *M. truncatula* was used to for studies as a means for studying plant-symbiont associations. The extensive genetic information available for *M. truncatula*, assisted in the designing of experiments. The changes in abundance of the mRNA as well flavonoid metabolites were used to confirm if the strategy was functional.

Table 2.1 – Key flavonoid biosynthesis enzymes, detected metabolites and the putative functions of different classes of flavonoids.

Flavonoid Class	Key biosynthesis enzymes	Reported free aglycones and glycoconjugated flavonoid metabolites in *M. truncatula* hairy roots using LC-MS/MS, HPLC or both detection methods		Putative functions		References for functions
		Aglycone	Glycoconjugate	Symbioses	Pathogeneses	
Chalcones	Chalcone synthase, Chalcone reductase	- Naringenin[1,2] - Liquiritigenin[1,2,3,7] - Isoliquiritigenin[7]	- Naringin# - Prunin#	*nod* gene inducers in rhizobia		Maxwell et al., 1989
Flavonols	Flavonol synthase, Flavaonone 3-hydroxylase	- Myricetin*[6] - Quercetin*[6] - Kaempferol*[6]	- Quercetin 7-O-glucoside# - Kaempferol-3-O-D-glucoside# - Kaempferol 7-O-glucoside#	Auxin transport inhibition	Neutralize free radicles	Zhang et al., 2009, Cao, et al., 1997
Isoflavonoids	Isoflavone synthase, Isoflavone reductase, Isoflavone *O*-methyltransferase, Isoflavone 2'-hydroxylase, Vestitone reductase	- Daidzein[1,5,7] - Genistein[1] - Biochanin A[1,2] - Formononetin[1,2,3,4,5,7] - Afrormosin[1] - Medicarpin[1,5,7] - Vestitone[7]	- Daidzein MalGlc[1] - 2-hydroxyformononetin MalGlc (II)[1] - Biochanin A MalGlcGlc[1] - Biochanin A MalGlc (I)[1] - Biochanin A MalGlc (II)[1] - Genistein MalGlc (I)[1] - Formononetin Glc[1,7] - Formononetin MalGlc (I)[1,7] - Formononetin MalGlc (II)[1] - Formononetin-7-O-β-d-glucoside[3] - Afrormosin Glc[1] - Afrormosin MalGlc (I)[1,7] - Afrormosin MalGlc (II)[1] - Irisolidone MalGlc[1] - Medicarpine MalGlc[1,7]	Some compounds are *nod* gene inducers/ repressors in rhizobia and contribute to auxin transport regulation in soybean. Selected isoflavonoids accumulated at the appresoria formation stage during mycorrhizal infection. Some isoflavonoids are also involved in mycorrhizal autoregulation to prevent excessive colonization.	Inhibit fungal spore germination, elongation of germ tube and hyphal growth by damaging fungal membrane structures. Antifeed against phytophagous insects.	Larose et al., 2002, Higgins, 1978, Subramanian et al., 2005, Caballero et al., 1986, Zuanazzi et al., 1998

Table 2.1 continued– Key flavonoid biosynthesis enzymes, detected metabolites and the putative functions of different classes of flavonoids.

Flavonoid Class	Key biosynthesis enzymes	Reported free aglycones and glycoconjugated flavonoid metabolites in *M. truncatula* hairy roots using LC-MS/MS, HPLC or both detection methods		Putative functions		References for functions
		Aglycone	Glycoconjugate	Symbioses	Pathogeneses	
Flavones	Flavone synthase I/II	- Dimethoxyluteolin[1] - Chrysoeriol[1] - Dihyroxyflavone[2,3] - Apigenin[7]	- Luteolin Glc (I)[1] - Luteolin GlcA[1] - Luteolin Glc[1]	*nod* gene inducers in rhizobia		Peters et al., 1986, Redmond et al., 1986, Zhang et al., 2007
Phlobaphenes, Anthocyanins and Proanthocyanidins (Condensed tannins)	Dihydroflavonol 4-reductase, Leucoanthocyanidin dioxygenase, Leucoanthocyanidin reductase, Anthocyanin reductase	- (-)-epicatechin[6] - (+)-catechin[6] - Delphinidin[6] - Cyanidin[6] - Pelargonidin[6] - Apiferol polymers# - Luteoferol polymers#		*nod* gene inducers	Intensive UV absorption in aerial parts of the plant. Detoxify superoxide radicles. Defense against herbivory. Allelopathic effects	Hungria et al., 1991, Li et al., 1993, Cao, et al., 1997, Peters and Constabel, 2002, Bais et al., 2003
Stilbenes	Stilbene synthase	- Resveratrol#		Unknown	Defense response against *Phoma medicaginis* in *Vitis vinifera*	Hipskind and Paiva, 2000, Langcake and Pryce, 1976

*Detected in Arabidopsis TT2 (ANR) expressing hairy roots of *M. truncatula*.
#Example only. Currently, no reports could be found t of its detection in *M. truncatula* hairy roots.
[1]Staszków et al., 2011, [2]Zhang et al., 2009, [3]Wasson et al., 2009, [4]Laffont et al., 2010, [5]Wasson et al., 2006, [6]Pang et al., 2008, [7]Banasiak et al., 2013

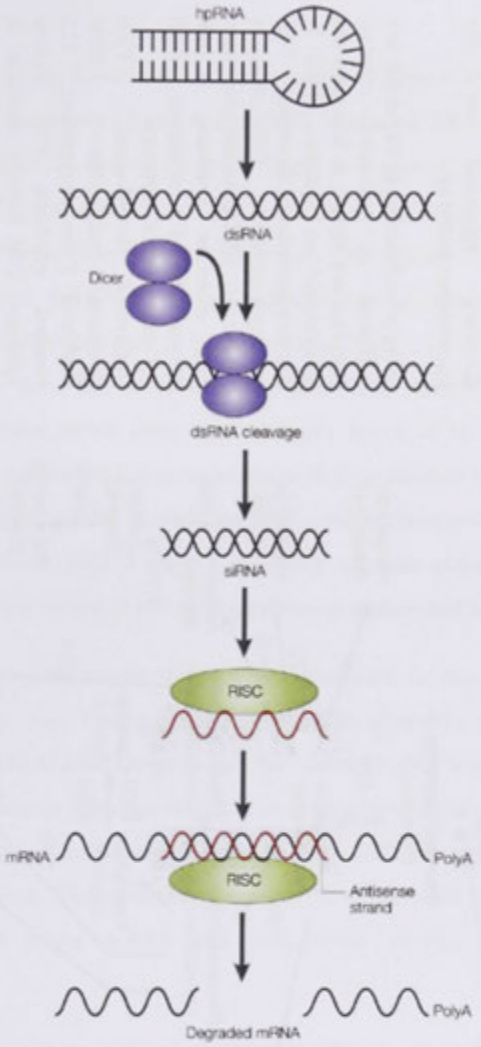

Figure 2.1 – Induction of RNA interference in plants. The hairpin transgene induces the expression of long double stranded RNA (dsRNA) which is recognized by the Dicer proteins. Dicer proteins cleave the dsRNA in to 21 nucleotide dsRNA fragments that are known as short interfering RNAs (siRNAs). The siRNAs are incorporated in to an RNAi silencing complex (RISC) that binds to complementary nucleotides and degrades them. Figure modified from Waterhouse and Helliwell (2003).

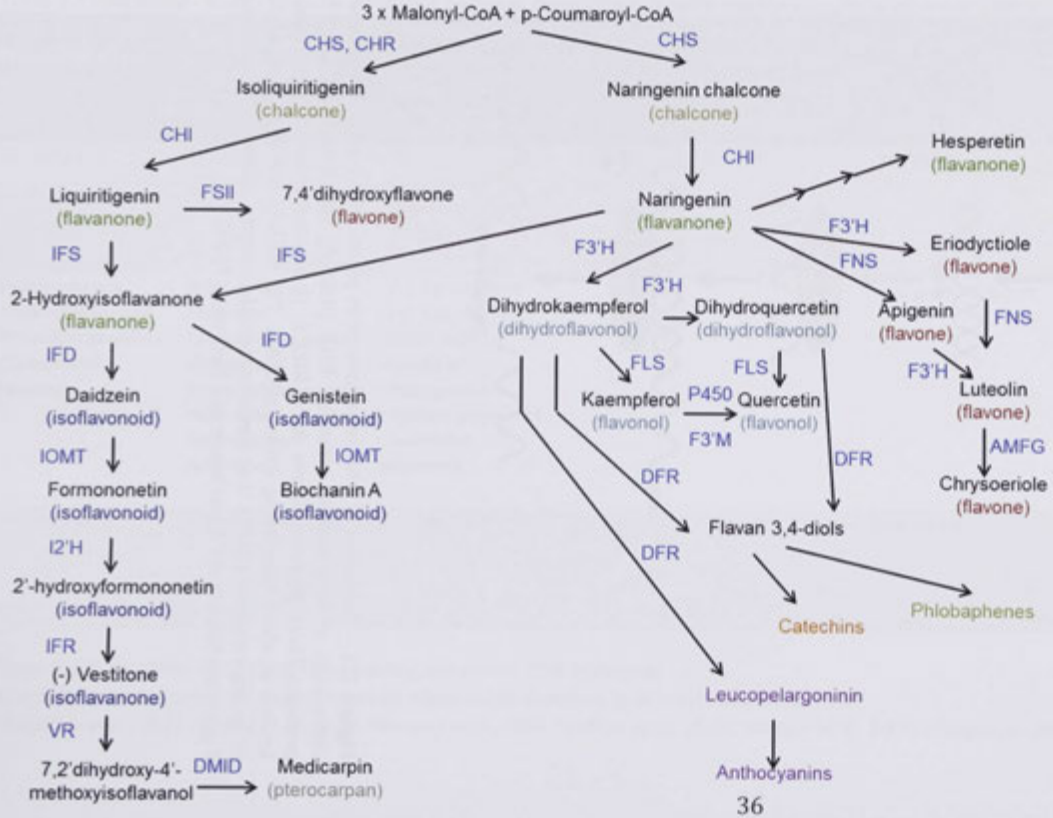

Figure 2.2 – Schematic overview of the flavonoid biosynthesis pathway in *M. truncatula* showing the flavonoid aglycones in the biosynthesis pathway.

Different subclasses of flavonoids are indicated in different colours. Enzymes are shown in blue and are abbreviated as follows: AMFG S-adenosylmethionine:flavonoid 7-O-glucosyltransferase; CHI chalcone isomerase; CHR chalcone reductase; CHS chalcone synthase; DFR dihydroflavonol 4-reductase; DMID 7,2'-dihydroxy-4'-methoxy-isoflavonol dehydratase; F3'H flavonoid-3'-hydroxylase; F3'M flavonoid 3'-monooxygenase; FLS flavonol synthase; FNS flavone synthase; FSII Flavone synthase II; I2'H isoflavone-2'-hydroxylase; IFD 2-hydroxyisoflavanone dehydratase; IFR isoflavone reductase; IFS 2-hydroxyisoflavanone synthase; IOMT isoflavanone-O-methyltransferase; P450 cytochrome P450; VR vestitone reductase.

2.2 Methods

Many of the genes encoding flavonoid synthesis enzymes appear in multiple copies in the genome of *M. truncatula*. I have used siRNA mediated RNA interference for silencing multiple copies of the same gene using a fragment of the conserved region. Two copies of these genes were cloned in to an expression vector where they were placed in reverse direction to each other. This region transcribes in to a double stranded hairpin mRNA as the complementary sequences bind to each other. This dsRNA gets incorporated in to the cellular RNA interference machinery as shown in Figure 2.1. The silencing complex was transferred in to an *Agrobacterium rhizogenes* strain that induced hairy roots in *M. truncatula*. The silencing effects were measured using techniques that quantified the mRNA levels of the target genes (Quantitative Real-Time PCR) and techniques that quantified the flavonoid metabolites (liquid chromatography tandem mass spectrometry, LC-MS/MS) that were the target of the pathway manipulation and techniques.

The same genes were also targeted for overexpression in the hairy roots of *M. truncatula*. The gene copy that was induced in roots according to the *Medicago* Gene Altas data was selected for cloning. The full coding region was transferred to an expression vector where the expression was driven by a strong 35S promoter. This vector was introduced in to the roots of *M. truncatula* through *A. rhizogenes* mediated transformation. The overexpression of the flavonoid synthesis genes were also quantified using mRNA and metabolite quantification methods mentioned above.

The methods in transforming *M. truncatula* to silence of overexpress genes encoding the flavonoid synthesis are shown in Figure 2.3. The seven different stages have been shown which includes – 1) amplification of target genes, 2) generation of entry clones with the target genes, 3) generation of expression clones for RNAi induction or overexpression of genes of interest, 4) transformation of *A. rhizogenes* strains with the expression clones, 5) transformation of *M. truncatula* seedlings with the transformed *A. rhizogenes* 6) callus formation and transformed root emergence in *M. truncatula* and 7) selection of transformed hairy roots of *M. truncatula*.

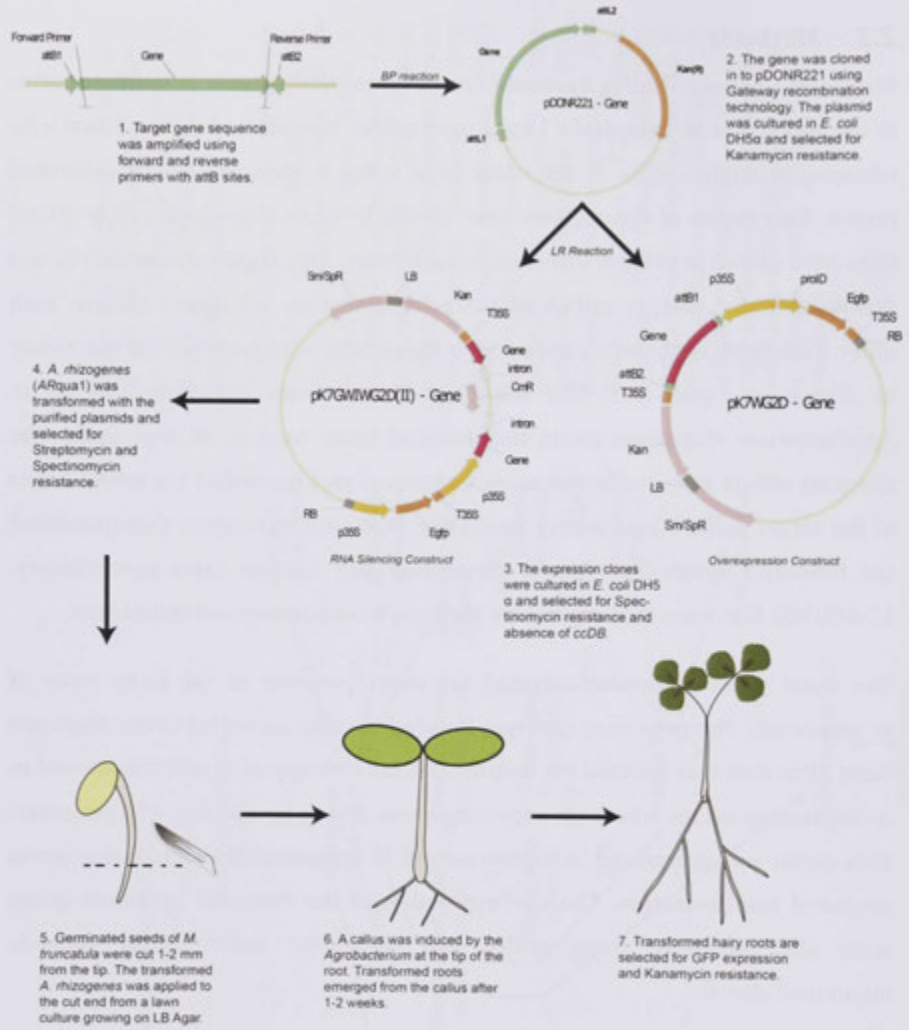

Figure 2.3 – An overview of the methods used to create transgenic hairy roots that were expressing silencing or overexpressing flavonoid constructs.

2.2.1 Construction of RNAi vectors

The RNAi vector pk7GWIWG2D(II) (Karimi et al., 2002) was used to express two copies of the targeted flavonoid synthesis genes in an inverse direction to produce hairpin dsRNA in the transformed plant roots. The mRNA sequences targeted for silencing belonged to *chalcone synthase* (*CHS*), *flavonol synthase* (*FLS*), *isoflavone synthase* (*IFS*), *flavone synthase II* (*FSII*) and *dihydroflavonol-4-reductase* (*DFR*). The *CHS* silencing vector was based on a previously published work by Wasson et al (2006) where the expression vector pHellsgate8 (Helliwell et al., 2002) was used. The vector pk7GWIWG2D(II) was used in my study instead of pHellsgate8 as the latter does not have a GFP marker sequence thus posed difficulties in selection of transformed roots. Regardless, both vectors carried the same *CHS* gene fragment insert and all experiments were carried out with a respective empty vector control.

Homologous sequences for flavonoid synthesis genes downstream of CHS were searched in the *Medicago* Gene Index (DFCI) and several copies of the gene families were identified. These copies were aligned and approximately 200 – 500 bp of conserved sequence was selected. The primers used to amplify these sequences were designed using Primer3 tool (Untergasser et al., 2012, Steve Rozen and Skaletsky, 1998). The attB sites to facilitate gateway cloning were added to the primers (Integrated DNA Technologies, USA). The attB sites recombined with the attP sites on the empty pDONR 201/221 plasmid vector mediated by the BP clonase enzyme (Life Technologies, USA). This entry clone had its *ccd*B gene on the donor vector replaced with the nucleotide sequence of interest. The clones were transformed in to *E. coli* DH5α through freeze thaw method as outlined in section 2.2.4. The vector carrying the *ccd*B fails to replicate in the DH5α strain of *E. coli*. The strain was also cultured in the presence of Kanamycin (100 µg/ml) to select for the correct plasmid. Plasmids were purified out of overnight *E. coli* culture in 2 ml LB media using the GeneElute plasmid miniprep kit (Sigma, USA), which relies on the alkaline lysis method (Bimboim and Doly, 1979). The correct entry clones were sequenced for confirmation (sequencing reactions were carried out at the Australian Genome Research Facility Ltd, Brisbane node).

The confirmed sequences of the entry clones were then recombined into the destination vector pk7GWIWG2D(II) using LR clonase enzyme reaction (Life Technologies, USA). The entry clone containing the attL sites that were generated from the recombination of the attB and attP sites, recombined with the attR sites on the destination vector generating expression clones where *ccd*B was genes were replaced by the nucleotide sequence of interest. This expression clone was also transformed in to *E. coli* DH5α strain and selected on spectinomycin (50 μg/ml).

The plasmid was verified using restriction digestion with *Eco*RI digestion which has three sites present on the vector backbone generating 11081, 2533 and 1798 bp fragments upon digestion of untransformed vector. The *ccd*B inserts were 755 bp each and its replacement with hairpin inducing gene fragments allowed changes in size to be detected. The FSII inserts also had an *Eco*RI site which has been underlined in the sequence data. The confirmed plasmids were transformed in to *A. rhizogenes AR*qua1 strain using the freeze-thaw method (see section 2.2.4).

The sequences used for cloning a region from the *M. truncatula* flavonoid synthesis enzymes are presented in the following sections.

Chalcone synthase (CHS)

The *chalcone synthase* RNA silencing vector was previously created in the laboratory (Wasson et al., 2006). Briefly, 14 copies of the *CHS* gene family were identified in *M. truncatula* and a conserved 543 bp region was amplified using the primers $^{5'}$CGTAAAGCTCAAAGGGCAGA$^{3'}$ and $^{5'}$AACCAACACACGAGCACCTT$^{3'}$ in the forward and reverse directions, respectively. The recombination site attB was attached to the above primers and the fragment (sequence below) was cloned in to pDONR201 (Life Technologies, USA).

```
1       CGTAAAGCTC AAAGGGCAGA AGGTCCTGCA ACTATCTTAG CCATTGGCAC TGCAAATCCA
61      GCAAATTGTG TTGAACAAAG CACTTATCCT GATTTTTACT TTAAAATTAC AAATAGTGAA
121     CACAAAACTG AACTCAAAGA GAAATTTCAG CGCATGTGTG ATAAATCCAT GATCAAGAGG
181     AGATACATGT ATCTAACAGA AGAAATTTTG AAAGAAAATC CTAGTGTTTG TGAATACATG
241     GCCCCTTCAT TGGATGCTAG GCAAGACATG GTGGTGGTAG AGGTACCTAG ACTAGGAAAG
301     GAGGCTGCAG TGAAGGCTAT AAAAGAATGG GGTCAACCAA AGTCAAAGAT TACTCACTTA
361     ATCGTTTGCA CCACAAGTGG TGTAGACATG CCCGGAGCTG ATTATCAACT CACCAAACTC
421     TTGGGTCTTC GCCCATATGT GAAAAGGTAC ATGATGTACC AACAAGGGTG TTTTGCAGGT
481     GGCACGGTGC TTCGTTTGGC CAAAGATCTA GCTGAGAACA ACAAAGGTGC TCGTGTGTTG
541     GTT
```

Flavonol synthase (FLS)

The conserved region from ten identified copies of the *M. truncatula FLS* gene family was amplified using the primers 5'AGGAACAACAACGGTCCAAG3' and 5'CCATCCTCTTTTCCCACTCA3' in the forward and reverse directions (Primer generated from MTR_5g059140). The attB sites were added to the primers in the forward and reverse direction for Gateway Cloning (Life Technologies, USA).

The resulting clone was inserted in to the vector pDONR221 through the BP clonase enzyme and sequenced as shown below.

```
1       GGAACAACAA CGGTCCAAGG TGTGAAACTT GGGGTACCAA TAATAGATTT CAGCAACCCA
61      GATGAGGTAA AGGTGCAAAA TGAGATAATA GAAGCAAGTA AAGAGTGGGG AATGTTTCAA
121     ATTGTGAACC ATGAAATTCC AAATGAAGTT ATAAGAAAGT TGCAAAGTGT TGGTAAAGAG
181     TTTTTTGAGT TACCACAAGA TGAAAAAGAG GTTTATGCTA AACCTGTTAT TGGATCTGAT
241     GTTTCTTCTG AAGGGTATGG TACAAAGCAT CAGAAAGAGT TGAGTGGGAA AAGAGGATGG
```

Isoflavone synthase (IFS)

The conserved region from six identified copies of the *M. truncatula IFS* gene family was amplified using the primers 5'TCTTGCAGGAACAGACTCCA3' and 5'CCCGTCGATCTCACATTCTT3' in the forward and reverse directions (Primer generated from Genbank ID AY939826.1). The attB sites were added to the primers in the forward and reverse direction for Gateway Cloning (Life Technologies, USA).

The resulting clone was inserted in to the vector pDONR221 through the BP clonase enzyme and sequenced as shown below.

```
1       CTTGCAGGAA CAGACTCCAC CGCCGTGTCT ACAGAATGGA CTTTATCAGA GCTCATCAAT
61      AATCCTAGAG TGTTGAAGAA AGCTCGAGAG GAGATTGACT CTGTTGTGGG AAAAGATAGA
121     CTGGTTGATG AATCAGATGT TCAGAATCTT CCTTACATTA AAGCCATCGT AAAAGAAGCA
181     TTTCGCTTGC ACCCACCACT ACCTGTAGTC AAAAGAAAAT GTACACAAGA ATGTGAGATC
241     GACGG
```

Dihydroflavonol-4-reductase (DFR)

The conserved region from four identified copies of the *DFR* gene family was amplified using the primers 5'AGACTTATGGAGCGCGGTTA3' and 5'CTTTGGCAAATTTCCATGCT3' in the forward and reverse directions (Primer generated from Genbank ID AY389346). The attB sites were added to the primers in the forward and reverse direction for Gateway Cloning (Life Technologies, USA).

The resulting clone was inserted in to the vector pDONR221 through the BP clonase enzyme and sequenced as shown below.

```
1       TCTTTGGCAA ATTTCCATGC TTCTTGCTCC GCAAGTGTCT TTGAAACAAA ATACATCCAG
61      CCAGTCATCT TCACTCTCCT ACAAAACTCA ACATCACTCC AACAGCTTTC ATCCCACAAG
121     GGCTTTTGAT CTTCAGTAAC GTTTAGGGTT CCGGCCGATG ATGTGAAAAT AAATCTACGG
181     ACAGTTTTGG CCTTGAGGCA TGCTTTCATG ATGTCTAGCA CCCCTTTTAT GGTAGGCTTG
241     ATCATTTCAT TCTCAGGGTC CTTGGACTCA AAATCCATAG GAGTAGCAAC ATGAAAAACT
301     CCTGTACACC CTTTAATAGC TTCATCAAAA CTACCCTCTT CACCAAGGTC AGCCTTCCAT
361     AGGGACAGTT TGCCCTTTGC ACCTGGCAGT TCTAACAAAT GACTCACCTT CTTCAAGTTT
421     TCTGGGTCGC GGACTGTTGC TCGAACCATG TAACCGCGCT CCATAAGTCT
```

Flavone synthase II (FSII)

The conserved region from three identified copies of the *FSII* gene family was amplified using the primers $^{5'}$AGCTTCCAACACTTGCGTTT$^{3'}$ and $^{5'}$CTCGGCACAATCAAGCAATA$^{3'}$ in the forward and reverse directions (Primer generated from Genbank ID DQ354373.1). The attB sites were added to the primers in the forward and reverse direction for Gateway Cloning (Life Technologies, USA).

The resulting clone was inserted in to the vector pDONR221 through the BP clonase enzyme and sequenced as shown below. *Eco*RI site has been underlined.

```
1       CTTCCAACAC TTGCGTTTAC AAGAGACTCA CAACCTCCTT AAGCTTTTCG CTGATAAAGC
61      GAAAAACTAC GAGGCTGTGA ATGTGACACA AGAGTTGCTA AAGTTGTCAA ACAACGTCAT
121     TTCTAAAATG ATGTTGGGGG AAGCTGAGGA GGCTAGGGAT GTTGTGCGAG ATGTGACCGA
181     GATTTTTGGA GAGTTTAATG TATCGGATTT TATTTGGTTG TTTAAGAAAC TTGATTTGCA
241     AGGGTTTGGG AAGAGGATAG AGGATTTGTT TATGAGGTTT GATACATTGG TGGAAAGGAT
301     TATTAGTAAA AGAGAAGAGT TGAGGAAGAA CAAAGGAAGG AAAGAAAATA AGGGTGAGCA
361     AGGTGCTGAA TTCAGAGACT TTCTTGATAT ATTGCTTGAT TGTGCCG
```

The sequence for attB1 sites in the forward direction was $^{5'}$GGGGACAAGTTTGTACAAAAAAGCAGGCTTA$^{3'}$and attB2 site in the reverse direction was ^{5}GGGGACCACTTTGTACAAGAAAGCTGGGTA$^{3'}$.

2.2.2 Construction of Overexpression vectors

The effects of overexpression of flavonoid biosynthesis enzymes on plant-microbe interactions were studied in this thesis. The targeted genes were overexpressed using the vector pK7WG2D (Karimi et al., 2002). The overexpressed genes included *chalcone synthase, flavonol synthase, isoflavone synthase* and *dihydroflavonol-4-reductase*. The full-length sequences of these genes were

obtained from the *Medicago* Gene Index (DFCI). The expression of the various copies of the same gene was searched in the *Medicago* Gene Expression Atlas (MtGEA, Noble Foundation, USA). The gene copy that was expressed consistently in root samples in multiple experiments was selected for over-expression.

The primers to amplify these sequences were designed using the Primer3 tool (Untergasser et al., 2012, Steve Rozen and Skaletsky, 1998). The recombination attB sites were added to the primers as described previously in section 2.2.1 (Integrated DNA Technologies, USA). The genes were isolated using a proofreading enzyme Platinum Pfx (Life Technologies, USA) in the PCR reaction as per manufacturer's instructions. The isolated fragment was transformed into pDONR221 and sub-cloned in to pK7WG2D vector via Gateway cloning (Life Technologies, USA) as previously described for the silencing constructs. The vectors were confirmed via sequencing (sequencing reactions were carried out at the Australian Genome Research Facility Ltd, Brisbane node) and subsequently transformed in to *A. rhizogenes AR*qua1 strain using freeze-thaw method (see section 2.2.4).

The full-length sequences of *M. truncatula* flavonoid synthesis enzymes that were cloned have been presented in the following section.

Chalcone synthase (CHS)

The primers $^{5'}$ATGGTGAGTGTGTCTGAAAT$^{3'}$ and $^{5'}$TCATATGGTCACACTACGCA$^{3'}$ in the forward and reverse directions were used to amplify the gene sequence for *chalcone synthase* (MTR_7g016800) as shown below. The attB sites were added to the primers in the forward and reverse direction for Gateway Cloning (Life Technologies, USA). The resulting clone was inserted in to the vector pDONR221 through the BP clonase enzyme.

```
1       ATGGTGAGTG TGTCTGAAAT TCGTAATGCT CAAAGAGCAG AAGGTCCTGC AACTATTTTG
61      GCCATTGGTA CTGCAAATCC AGCAAATTGT GTTGAACAAA GCACATATCC TGATTTTTAC
121     TTTAAAATCA CAAATAGTGA ACACAAAACT GAACTTAAGG AGAAATTTCA GCGCATGTGT
181     GATAAATCTA TGATCAAGAG GAGATACATG TATCTAACAG AGGAGATTTT GAAAGAAAAT
241     CCTAGTGTTT GTGAATACAT GGCACCTTCA TTGGATGCAA GGCAAGACAT GGTGGTGGTA
301     GAGGTACCTA GACTAGGAAA GGAGGCTGCA GTGAAGGCTA TAAAAGAATG GGGTCAACCA
361     AAGTCAAAGA TTACTCACTT AATCGTTTGC ACCACAAGTG GTGTAGACAT GCCTGGAGCT
421     GATTATCAAC TCACAAAACT CTTGGGCCTT CGTCCATATG TGAAAAGGTA TATGATGTAC
481     CAACAAGGGT GTTTTGCAGG TGGCACGGTG CTTCGTTTGG CCAAAGATTT GGCTGAGAAC
541     AACAAAGGTG CTCGTGTGTT GGTTGTTTGT TCTGAAGTCA CCGCTGTCAC ATTTCGTGGC
```

```
601       CCCAGTGATA CTCACTTGGA CAGCCTTGTT GGGCAAGCAT TGTTTGGAGA TGGAGCTGCT
661       GCTCTTATTG TTGGTTCTGA CCCAGTACCA GAAATTGAGA AACCTATATT TGAGATGGTT
721       TGGACTGCAC AAACAATTGC TCCTGATAGT GAAGGAGCCA TTGATGGTCA CCTTCGTGAA
781       GCTGGACTAA CATTTCACCT TCTTAAAGAT GTTCCTGGGA TTGTCTCAAA GAACATTACT
841       AAAGCATTGG TTGAGGCTTT CGAGCCATTG GGAATTTCTG ATTACAACTC AATCTTTTGG
901       ATTGCACATC CCGGTGGACC TGCAATTCTA GATCAAGTAG AGCAAAAGTT AGCCTTAAAG
961       CCTGAAAAGA TGAATGCAAC TAGAGAAGTG CTCAGTGAAT ATGGAAATAT GTCAAGTGCA
1021      TGTGTTTTGT TTATCTTAGA TGAAATGAGA AAGAAATCAA CTCAAAACGG ATTGAAGACA
1081      ACGGGAGAAG GACTTGAGTG GGGTGTATTA TTTGGTTTTG GACCAGGACT TACCATTGAA
1141      ACAGTTGTTT TGCGTAGTGT GACCATATGA
```

Flavonol synthase (FLS)

The primers $^{5'}$ATGGAGGTAGAAAGGGTACA$^{3'}$ and $^{5'}$TTATTGAGGGATCTTATTAA$^{3'}$ in the forward and reverse directions were used to amplify the gene sequence for *flavonol synthase* (MTR_5g059140) as shown below. The attB sites were added to the primers in the forward and reverse direction for Gateway Cloning (Life Technologies, USA). The resulting clone was inserted in to the vector pDONR221 through the BP clonase enzyme.

```
1         ATGGAGGTAG AAAGGGTACA AACAATAGCT CATAAATCCA AAAACACTAC AATACCATCC
61        ATGTTCGTTA GGTCAGAAAC TGAGTCACCA GGAACAACAA CGGTCCAAGG TGTGAAACTT
121       GGGGTACCAA TAATAGATTT CAGCAACCCA GATGAGGTAA AGGTGCAAAA TGAGATAATA
181       GAAGCAAGTA AAGAGTGGGG AATGTTTCAA ATTGTGAACC ATGAAATTCC AAATGAAGTT
241       ATAAGAAAGT TGCAAAGTGT TGGTAAAGAG TTTTTTGAGT TACCACAAGA TGAAAAAGAG
301       GTTTATGCTA AACCTGTTAT TGGATCTGAT GTTTCTTCTG AAGGGTATGG TACAAAGCAT
361       CAGAAAGAGT TGAGTGGGAA AAGAGGATGG GTGGACCATT TTTTTCATAT CATATGGCCA
421       CCTTCATCTG TTAATTACAG TTGTTGGCCA AATAACCCTA CTTCCTATAG GGAGGTGAAT
481       GAGGAATATG GCAAGTACCT CCGTAGAGTG TCAAACAAAT TGTTCAATAT CATGTTAGTA
541       GGACTTGGGT TTGAAGAAAA TGAACTCAAG TCAGTTGCAG ATGAAAATGA GTTGATTCAC
601       CTATTGAAAA TCAATTACTA CCCACCATGT CCATGTCCTG ATCTGGTACT AGGTGTGCCA
661       CCACACACAG ATATGTGTTA TATTACCCTT CTCATACCCA ATGAAGTGGA GGGTCTTCAA
721       GCCTCTAGAG ATGGTCAATG GTATGATGTT AAGTATGTCC CCAATGCCCT CATTATTCAC
781       GTTGGTGACC AAATGCAGAT ACTAAGCAAT GGGAAATATA AGGCTGTATT GCACAGAACA
841       ACTGTAAACA AAGATGAGAC AAGAATGTCG TGGCCAGTGT TCATAGAACC CAAGCCAGAA
901       AACGAAGTTG GTCCTCACCC AAAGTTTGTT AACCAAGAGA ATCCTCCAAA GTACAAAACC
961       AAGAAATATA AGGATTATGC TTACTGTAAG CTTAATAAGA TCCCTCAATA A
```

Isoflavone synthase (IFS)

The primers $^{5'}$ATGTTGGTGGAACTTGCAGT$^{3'}$ and $^{5'}$TTAGGAGGAAAGAAGTTTAT$^{3'}$ in the forward and reverse directions were used to amplify the gene sequence for *isoflavone synthase* (AY939826.1) as shown below. The attB sites were added to the primers in the forward and reverse direction for Gateway Cloning (Life Technologies, USA). The resulting clone was inserted in to the vector pDONR221 through the BP clonase enzyme.

```
1         ATGTTGGTGG AACTTGCAGT TACTCTATTG CTCATTGCTC TCTTCTTACA CTTGCGTCCA
61        ACACCTACTG CAAAATCAAA GGCTCTTCGC CACCTTCCAA ATCCACCAAG CCCTAAACCA
121       CGTCTTCCAT TCATAGGTCA TCTTCACCTT TTGGATAACC CACTTCTTCA CCACACTCTT
181       ATCAAGTTAG GAAAGCGTTA TGGCCCTTTG TACACTCTTT ACTTTGGTTC CATGCCTACC
241       GTTGTTGCAT CCACTCCTGA CTTGTTTAAA CTTTTCCTTC AAACCCATGA AGCTACTTCC
301       TTTAACACAA GATTCCAAAC CTCTGCTATT AGTCGTCTTA CCTATGACAA CTCTGTTGCT
```

```
361     ATGGTTCCAT TTGCACCTTA TTGGAAGTTT ATTAGAAAGC TTATCATGAA CGACTTGCTC
421     AACGCCACCA CTGTTAACAA ATTGAGGCCA TTGAGGAGCC GAGAAATCCT TAAGGTTCTT
481     AAGGTCATGG CTAATAGTGC TGAAACTCAA CAGCCACTTG ATGTCACTGA GGAGCTTCTC
541     AAGTGGACAA ACAGCACAAT CTCTACCATG ATGTTGGGTG AGGCCGAAGA GGTTAGAGAT
601     ATTGCTCGTG ATGTTCTTAA GATCTTTGGA GAATATAGTG TTACAAACTT TATTTGGCCT
661     TTGAACAAGT TTAAGTTTGG AAACTATGAT AAGAGAACTG AGGAGATTTT CAATAAGTAT
721     GATCCTATCA TTGAAAAGGT TATCAAGAAA CGACAAGAGA TTGTGAACAA AAGAAAAAAT
781     GGAGAAATCG TAGAAGGCGA GCAGAATGTT GTTTTTCTTG ACACTTTGCT TGAATTTGCA
841     CAAGATGAGA CCATGGAGAT CAAAATTACA AAGGAACAAA TCAAGGGTCT TGTTGTGGAT
901     TTTTTCTCTG CAGGAACAGA CTCCACCGCC GTGTCTACAG AATGGACTTT ATCAGAGCTC
961     ATCAATAATC CTAGAGTGTT GAAGAAAGCT CGAGAGGAGA TTGACTCTGT TGTGGGAAAA
1021    GATAGACTGG TTGATGAATC AGATGTTCAG AATCTTCCTT ACATTAAAGC CATCGTAAAA
1081    GAAGCATTTC GCTTGCACCC ACCACTACCT GTAGTCAAAA GAAAATGTAC ACAAGAATGT
1141    GAGATCGACG GGTATGTGGT TCCAGAAGGA GCACTAATAC TTTTCAATGT CTGGGCAGTG
1201    GGAAGAGACC CAAAATATTG GGTAAAGCCA TTGGAATTTC GTCCAGAGAG GTTCATAGAA
1261    AATGTTGGTG AAGGTGAAGC AGCTTCAATT GATCTTAGGG GTCAACATTT CACACTTCTA
1321    CCATTTGGGT CTGGAAGAAG GATGTGTCCT GGAGTCAATT TGGCTACTGC AGGAATGGCC
1381    ACAATGATTG CATCTATTAT CCAATGCTTC GATCTCCAAG TACCTGGTCA ACATGGAGAA
1441    ATATTGAATG GTGATTATGC TAAGGTTAGC ATGGAAGAGA GACCTGGTCT CACAGTTCCA
1501    AGGGCACATA ATCTCATGTG TGTTCCTCTT GCAAGAGCTG GTGTCGCAGA TAAACTTCTT
1561    TCCTCCTAA
```

Dihydroflavonol-4-reductase (DFR)

The gene sequence for *dihydroflavonol-4-reductase* (MTR_3g005170) could not be amplified through a PCR reaction. This gene sequence was commercially synthesized (Integrated DNA Technologies, USA) with attB sites and cloned through Gateway cloning (Life Technologies, USA) in to the expression vector.

```
1       ATGAGCAGCA GCAACTTGGG AAATGTTGTG TGTGTGACTG GCGCTTCAGG TTACATCGCT
61      TCATGGCTCG TCCGATTGCT TCTTCATCGT GGCTACACTG TTAAAGCCAC CGTTCGCGAT
121     CCAAATGATC CCAAGAAGGT TGACCACTTG GTTAAGCTTG ATGGTGCTAA GGAGAGATTG
181     CAACTGTTCA AGGCAAATCT ACTTGAAGAA GGTGCCTTTG ATTCTGTTGT TCAAGGCTGT
241     CATGGTGTCT TTCACACTGC ATCTCCCTTT TATCATGATG TCAAGGATCC TCAGGCTGAA
301     TTGATTGATC CTGCTCTCAA AGGGACTCTC AATGTTCTCA ACTCATGTGC TAAATCCCCA
361     TCACTCAAAC GTGTTGTTTT AACTTCTTCT ATTGCTGCTG TTGCTTATAA TGGGAAGCCT
421     CGAACTCCTG ATGTTGTTGT TGATGAGACT TGGTTTACAG ATGCTGATTT CTGTGCTAAA
481     TCAAATCTGT GGTATGTGGT TTCAAAGACA TTGGCTGAAG AAGCTGCCTG GAAATTTGTT
541     AAAGAAAACA ACATCGATAT GGTTACTATT AACCCAGCAA TGGTCATAGG GCCTCTCTTG
601     CAACCAGTCC TAAACACAAG TGCTGCTGCA ATTCTAAACC TGATTAATGG TGCACAGACA
661     TTTCCAAATG CTAGTTTTGG ATGGGTCAAT GTGAAAGATG TTGCAAATGC CCATATTCTG
721     GCGTACGAGA ATGCTTCAGC GAGTGGAAGA CATTGTTTAG TTGAGAGAGT AGCACACTAC
781     TCCGAAGTTG TGAGGATTTT ACGTGAACTG TACCCTTCGT TGCAACTCCC AGAGAAGTGT
841     GCGGACGATA AGCCATATGT GCCTATATAT CAGGTTTCCA AAGAAAAGGC GAAAAGCTTG
901     GGACTTGAAT ATACTCCTTT GGAAGTGAGC ATCAAGGAGA CTGTTGAAAG TTTGAAAGAA
961     AAGAAGTTCG CCAACCTTTA A
```

Flavone synthase II (FSII)

The gene for flavone synthase could not be amplified and it was not opted for commercial synthesis as no interesting RNAi phenotypes were observed for this gene.

The sequence for attB1 sites in the forward direction was $^{5'}$GGGGACAAGTTTGTACAAAAAAGCAGGCTTA$^{3'}$and attB2 site in the reverse direction was ^{5}GGGGACCACTTTGTACAAGAAAGCTGGGTA$^{3'}$.

2.2.3 Gene amplification

Routine PCR amplification for amplifying genes of interest in extracted plasmid DNA or bacterial colonies was done using the Econotaq polymerase mix (Lucigen, USA). A typical reaction is shown in Table 2.2. The cycling conditions for the above reaction followed 3 minutes of hot-start at 94 °C followed by 35 cycles of amplification consisting of denaturation at 94 °C for 30 seconds, annealing at 55-60 °C for 30 seconds and extension at 72 °C for 1 minute per kb of DNA. A final extension at 72 °C for 5 minutes was included before the end of the program. For colony PCR, the hot-start stage was extended to 5 minutes to disrupt the bacterial cells and obtain plasmid DNA for amplification. The C1000 Touch Thermo-cycler (BioRad, USA) was used for all PCR amplification reactions.

The PCR amplification of genes for overexpression vectors required proofreading to prevent mistakes; hence, a proofreading enzyme Platinum Pfx polymerase (Life Technologies, USA) was used in this reaction. The 10x Pfx Amplification buffer was used at 2x dilution in final reaction mix and PCR enhancer was added to amplify some templates (*FLS* and *IFS* required enhancer at 1x dilution while *CHS* required enhancer at 2x dilution). A typical reaction's components are shown in Table 2.3.

The cycling conditions for the above reaction followed 3 minutes of hot-start at 94 °C followed by 35 cycles of amplification consisting of denaturation at 94 °C for 15 seconds, annealing at 58 °C for 30 seconds and extension at 68 °C for 1 minute per kb of DNA. A final extension at 68 °C for 5 minutes was included before the end of the program. The C1000 Touch Thermo-cycler (BioRad, USA) was used for all PCR amplification reactions.

Table 2.2 - Components of a routine PCR amplification reaction using Econotaq polymerase mix. The volumes for a typical single reaction are shown.

Components	1x Reaction
2x Econotaq mastermix	10 µl
10 µM Forward Primer	0.2 µl
10 µM Reverse Primer	0.2 µl
Template DNA	100 ng or a bacterial colony
dH_2O	To 20 µl

Table 2.3 – Components of a routine PCR amplification reaction using Platinum Pfx polymerase (proofreading enzyme) mix. The volumes for a typical single reaction are shown.

Components	1x Reaction
10x Pfx Amplification buffer	4.0 µl
10 mM dNTP mix	0.6 µl
50 mM MgSO4	0.4 µl
10 µM Forward Primer	0.3 µl
10 µM Reverse Primer	0.3 µl
Template DNA	100 ng
10 x PCR Enhancer	1.0 - 2.0 µl
dH_2O	Up to 19.84µl
Platinum Pfx polymerase	0.16 µl

PCR product visualization

DNA bands were separated on 1.3-2.0 % Agarose in 1 x TAE buffer as detailed below (Sambrook et al., 2001) and separated using a 100 V electric field. DNA was stained with SYBR-Safe DNA stain (Life Technologies, USA) and visualized on a GelDoc XR transilluminator system (BioRad, USA).

A 50x stock of TAE Buffer was prepared by solubilizing 242 g Tris base ($C_4H_{11}O_3$) with 100 ml of 0.5 M EDTA solution and 57.1 ml glacial acetic acid in distilled water with a total volume of 1 L at pH 8.2 at 25 °C. A 1x dilution was used as a working solution for gel electrophoresis. The final concentration here was 40 mM Tris acetate and 1 mM EDTA at pH 8.2 at 25 °C.

DNA purification

Selected DNA bands were excised on a GelDoc XR transilluminator system (BioRad, USA) using a clean scalpel blade and placed in a pre-weighed, clean 1.5 ml eppendorf tube. The DNA was extracted using the Gel Purification Kit (Qiagen) as per manufacturer's instructions. The concentration of the purified DNA was measured using a NanoDrop ND1000 UV/Vis spectrophotometer (Thermo Fisher Scientific, USA).

Recovery of DNA via ethanol precipitation

DNA was concentrated and recovered from solutions using ethanol precipitation (Sambrook et al., 2001) when higher concentrations were required for cloning and sequencing reactions. A volume of DNA for precipitation was transferred to a fresh 1.5 ml eppendorf tube and three volumes of ethanol were added. This was

followed by an addition of 0.1 volume of 3 M sodium acetate solution. The sample was mixed with gentle inversion and incubated overnight at -20 °C. Subsequently, the tube was centrifuged at maximum speed for 30 minutes at 4 °C. The supernatant was carefully removed without dislodging the pellet. The remaining pellet was dried in a vacuum centrifuge and re-suspended in 10 µl of DNase free water and the concentration was measured on a NanoDrop ND1000 UV/Vis spectrophotometer (Thermo Fisher Scientific, USA).

2.2.4 Transformation of bacterial cells

Preparation of Escherichia coli RbCl competent cells

Competent *E. coli* cells of strains DH5α and DB3.1 were prepared as described by Hanahan and Glover (1985) using rubidium chloride (RbCl) in addition to calcium chloride ($CaCl_2$) to facilitate uptake of foreign DNA. Transformation buffers I and II (TfbI and TfbII) were prepared as shown in Table 2.4.

The pH of TfbI was adjusted to 5.8 with 0.2 M acetic acid and the pH of TfbII was adjusted to 6.8 with 1 M sodium hydroxide solution. The TfbI and TfbII solutions were filter sterilized and stored at 4 °C.

Approximately 300 ml of LB medium with 10 mM $MgCl_2$ and 10 mM $MgSO_4$ was inoculated with 2 ml of an overnight culture of *E. coli* (strain DH5α or DB3.1 as required). The culture was incubated at 37 °C, 260 RPM until OD_{600} of 0.4 - 0.6 was reached. The cells were then chilled on ice for 20 minutes. The cells were centrifuged in a pre-cooled and sterile centrifuge tube (Beckman Coulter, USA) at 3000 RPM for 15 minutes at 4 °C. The supernatant was discarded completely and the cells were re-suspended in 100 mL of cold TfbI solution. The cells were then chilled on ice for 30 minutes and then re-centrifuged at 3000 RPM for 15 minutes at 4 °C. The supernatant was discarded again and the cells were re-suspended in 1.5 mL of cold TfbII solution. Aliquots of 30 µl were prepared in cooled 1.5 mL sterile eppendorf tubes and used for transformation or stored at -80 °C.

Table 2.4 – Components of the transformation buffers used in the preparation of RbCl competent *E. coli* cells

Components	TfbI	TfbII
Rubidium chloride, RbCl	100 mM	10 mM
Manganese chloride, $MnCl_2.4H_2O$	50 mM	-
Potassium acetate, CH_3COOK at pH 7.5	30 mM	-
MOPS, $C_7H_{15}NO_4S$ at pH 6.8	-	10 mM
Calcium chloride, $CaCl_2.2H_2O$	10 mM	75 mM
Glycerol, $C_3H_8O_3$	15 % w/v	15 % w/v

Transformation of Rb-Cl competent E. coli cells

An aliquot of the competent cells was thawed on ice. A volume of 270 µl of ice cold TfbII was added to the thawed cells and gently mixed. A 50 µl aliquot of this solution was mixed gently with 1 µl (or 20-100 ng) of plasmid DNA. The cells were heat-shocked for 45 seconds at 42 °C and 500 µl of LB media (without antibiotics) was added. The cells were regenerated for 1 hour at 37 °C in a shaking incubator. The cells were separated from excess media through centrifugation and plated on LB Agar media with appropriate antibiotics selection. The plates were incubated at 37°C overnight and colonies appeared if the transformation was successful.

Preparation of Agrobacterium rhizogenes competent cells

A 5 ml overnight culture of *A. rhizogenes ARqua1* strain was grown in LB media with streptomycin (100 µg/ml) at 28 °C. A volume of 1 ml of this starter culture was then used to inoculate 100 ml of LB medium with streptomycin (100 µg/ml) in a 1 L Nalgene baffled culture flask (Thermo Fisher Scientific, USA). The culture was grown for 7.5 hours, at which point the OD_{600} was at 0.7, indicating that the culture had reached its log phase. The doubling time was calculated at 1.5 hours using the OD_{600} measurements obtained at regular intervals.

The culture was then chilled on ice for 30 minutes and then centrifuged at 4,000 rpm at 4 °C (Beckmann Coulter, USA). The supernatant was gently removed and the pellet was re-suspended in 5 ml ice-cold 20 mM calcium chloride solution. Aliquots of 50 µl of this suspension were prepared in sterile eppendorf tubes and snap-frozen in liquid nitrogen for storage (Holsters et al., 1978).

Transformation of competent A. rhizogenes ARqua1 cells

An aliquot of chemically competent *ARqua1* cells were thawed on ice. Up to 5 µl (or 100 ng) of plasmid DNA was added to these cells and gently mixed. The cells were snap-frozen in liquid nitrogen and heat-shocked by incubating at 37°C for 5 minutes. 500 µl of LB medium (no antibiotics) was then added to this mixture and the cells were regenerated for 2 hours at 28 °C in a shaking incubator. The cells were separated from excess media through centrifugation and plated on LB Agar media with streptomycin (100 µg/ml) and spectinomycin (50 µg/ml) selection. The plates were incubated at 28 °C for two days and colonies appeared if the transformation was successful.

2.2.5 Agrobacterium-mediated gene silencing in M. truncatula roots

The *M. truncatula* roots were transformed with *A. rhizogenes AR*qua1 carrying silencing or overexpression plasmids using the hairy root transformation method as described previously (Boisson-Dernier et al., 2001). Briefly, the seeds of wild-type cultivar A17 Jemalong were lightly scarified using sand paper and surface sterilized for 10 minutes with 6 % (wt/v) sodium hypochlorite solution. The sterilized seeds were washed five times with sterile water to remove all traces of sodium hypochlorite. The seeds were then imbibed in sterile water for 4 hours and transferred onto water agar plates for stratification at 4 °C for 2 days. The seeds were then germinated at 25 °C overnight.

Approximately 1-2 mm of the root tips of the germinated seedlings were excised using a sterile scalpel blade and a small amount of *A. rhizogenes* expressing appropriate plasmid for transformation was applied from a fresh lawn culture grown on LB agar medium with streptomycin (100 µg/ml) and spectinomycin (50 µg/ml) selection. The seedlings were placed on 15 cm ø slanted modified-Fåhraeus agar medium (Table 2.4) containing 25 µg/ml kanamycin for selection.

The roots were grown for one week at 20 °C with 16 hour photoperiod and 140 µE light flux. This was followed by a change in temperature to 25 °C while maintaining the other parameters for growth for 1 week. At the end of two weeks since the initial transformation, the seedlings had formed callus and hairy roots emerged.

The roots were selected using GFP as a visual selection marker under a stereomicroscope (M205FA - Leica Microsystems, Germany) with excitation at 470 nm and emission at 515 nm. The transformed roots were transferred onto 15 cm ø Fåhraeus medium (Table 2.4) agar plates without antibiotics and grown at 25 °C for an additional week.

2.2.6 Media composition

Fåhreus and modified Fåhreus medium

The composition of modified and unmodified Fåhreus media is listed in Table 2.5 (Somasegaran and Hoben, 1994, Fåhraeus, 1957, Boisson-Dernier et al., 2001). The media were supplemented with 12 g of J3 Agar (Gelita Australia, Australia), sterilized by autoclaving and poured on 150 mm ø sterile petri dishes. Kanamycin (25 µg/ml) was also added to cooled modified-Fåhreus media prior to pouring onto petri dishes to select for transformed plant roots expressing a kanamycin resistance gene.

Table 2.5 – Composition of Fåhreus and modified-Fåhreus growth media

	Fåhreus media	Modified-Fåhreus media
Macro elements	**Concentration (mM)**	**Concentration (mM)**
Calcium chloride $CaCl_2$	0.9	0.9
Magnesium sulphate $MgSO_4$	0.5	0.5
Potassium dihydrogen phosphate KH_2PO_4	0.7	0.7
Di-sodium hydrogen phosphate Na_2HPO_4	0.8	0.8
Ferric citrate $C_6H_6FeO_7$	0.02	0.02
Ammonium nitrate NH_4NO_2	-	0.5
Micro elements	**Concentration (µM)**	**Concentration (µM)**
Boric acid H_3BO_3	46.26	1.63
Manganese chloride $MnCl_2$	-	0.5
Manganese sulphate $MnSO_4$	9.11	-
Copper sulphate $CuSO_4$	0.32	0.4
Zinc chloride $ZnCl_2$	-	0.72
Zinc sulphate $ZnSO_4$	0.77	-
Sodium molybdate Na_2MoO_4	0.58	0.4

General media used for bacterial cultures

The *A. rhizogenes* and *E. coli* cultures were grown in low salt LB medium (typtone 10 g/L, sodium chloride 5 g/L and yeast extract 5 g/L). J3 Agar (12 g/L) (Gelita

Australia, Australia) was added for solid media. *S. meliloti* cultures were grown in Bergensen's modified medium (Rolfe et al., 1980) or BMM (Table 2.6)

All media were autoclaved prior to use.

Table 2.6 – Composition of Bergensen's modified medium

Component	Concentration /L
$Na_2PO_4.12H_2O$	360 mg
$MgSO_4.7H_2O$	80 mg
$FeCl_3$	3 mg
$CaCl_2.2H_2O$	40 mg
H_3BO_3	3 mg
$MnSO_4.4H_2O$	10 mg
$ZnSO_4.7H_2O$	7 mg
$CuSO_4.5H_2O$	0.25 mg
$CoCl_2.6H_2O$	0.25 mg
$Na_2MoO_4.2H_2O$	0.25 mg
Biotin	0.2 mg
Thiamine	2 mg
Na-glutamate	0.5 g
Yeast extract	0.5 g
Mannitol	3 g (solid medium)/ 10 g (liquid medium)
Agar	15 g

2.2.7 Confirmation of RNA silencing or overexpression through quantitative real-time PCR

The root samples were snap frozen in liquid nitrogen and ground to a fine powder using a mortar and pestle. Approximately 80-100 mg of ground material was transferred to a fresh eppendorf tube for RNA extraction using the Spectrum Plant Total RNA kit (Sigma, USA) as per manufacturer's instruction. The on-column DNase digestion set (Sigma, USA) was used to remove traces of DNA from the RNA bound to the column during the extraction process. The extracted RNA was quantified on a NanoDrop ND1000 UV/Vis spectrophotometer (Thermo Fisher Scientific, USA). The first strand cDNA was synthesized from an equal amount of RNA from all the samples using the Superscript III First Strand cDNA synthesis kit (Life Technologies, USA). The synthesized cDNA was further diluted 5 times in DEPC treated water.

The relative transcript abundance was measured using quantitative real-time PCR in a 10 µl reaction volume (Table 2.7). The primers for the reactions are listed in Table 2.5 and used at 2 pM each. Each reaction had 2.5 µl of synthesized cDNA added to it. A mix of ABI Power SYBR Green PCR mastermix and cDNA solution was aliquoted in the 384 well PCR plate (Applied Biosystems, USA) followed by the mix of primers and water. This was done to ensure that the cDNA was distributed evenly across the different wells while the primers were in excess to not limit the reaction.

Table 2.7– Components of a quantitative real-time PCR reaction

Components	Volume per reaction (µl)
ABI Power SYBR Green PCR Mastermix	5.0
Forward Primer (10 µM)	0.2
Reverse Primer (10 µM)	0.2
DEPC H_2O	2.1
cDNA solution	2.5

The gene fragments were amplified using ABI Power SYBR Green PCR Master Mix kit (Applied Biosystems, USA) on the ABI 7900HT Sequence Detection System (Applied Biosystems, USA). A part of the *M. truncatula* GAPDH gene (MTR_3g085850) (Kakar et al., 2008) was used as a reference control. The primer pairs used to amplify the various gene fragments are listed in Table 2.8. Amplification with the primers to amplify *DFR* transcripts was not successful despite several attempts and primer redesigns. One of the pair of primers with the best efficiency is listed. The transcript abundance was calculated using the Pfaffl method (Pfaffl, 2001).

The designed primers listed in Table 2.8 amplified a conserved region separate from the region that was targeted for RNAi silencing to avoid any competitive binding with ihpRNA.

Table 2.8 – Primer pairs used for quantitative real-time PCR reactions

Gene	Orientation	Primer sequence
CHS	F	5′ CGCTGTCACATTTCGTGG 3′
	R	5′ AACACACCCCATTCAAGTCC 3′
FLS	F	5′ CACCATGTCCATGTCCTGAT 3′
	R	5′ GCCACGACATTCTTGTCTCA 3′
IFS	F	5′ GATCGACGGGTATGTGGTTC 3′
	R	5′ CTGCTTCACCTTCACCAACA 3′
DFR	F	5′ TGAAGATGACTGGCTGGATG 3′
	R	5′ TAGGGACAGTTTGCCCTTTG 3′
FSII	F	5′ GCCACGACATTCTTGTCTCA 3′
	R	5′ CACCATGTCCATGTCCTGAT 3′
GAPDH	F	5′ TGCCTACCGTCGATGTTTCAGT 3′
	R	5′ TTGCCCTCTGATTCCTCCTTG 3′

F – Forward primer; R – Reverse primer

2.2.8 Confirmation of metabolite changes through LC-MS/MS

Root samples for analysis on the Liquid Chromatography Tandem Mass Spectrometry (LC-MS/MS) were freeze-dried (VirTis Benchtop Freeze Dryer, SP Scientific, USA) and ground to a fine powder using a mortar and pestle. A sample of 5 mg (± 0.1 mg) of the ground powder was transferred to a clean eppendorf tube and flavonoids were extracted in 1 ml of 80 % methanol (Acros Organics, USA). The samples were dissoved in a sonic bath for 30 minutes at 4 °C and centrifuged at 13 000 RPM for 15 minutes. The supernatant was dried in a vaccum centrifuge at room temperature and resuspended in 50 µl of 80 % methanol supplemented with internal standard umbelliferone, $C_9H_6O_3$ (Sigma, USA) at 0.4 ppm. The solution was filtered using Nanosep MF GHP 0.45 µm cellulose filter (Pall Life Sciences, USA) and 7 µl of the extract was injected in to the chromatographic column for separation.

Absolute standards for MS/MS analysis were prepared as follows – chemical standards were obtained from Indofine (USA) and Sigma-Aldrich (USA) as listed in Appendix Table A2.1 and stocks were prepared in absolute methanol at 1000 to 2000 ppm using 5 ml volumetric flasks. These standards were combined in to a

mix where all the standards were at 10 ppm. Standard mix at 5, 2, 1, 0.5, 0.1, 0.05, 0.01, and 0 ppm were subsequently prepared through serial dilutions.

Mass spectrometry was performed using an Agilent 6530 Accurate Mass LC-MS Q-TOF (Santa Clara, CA, USA). Samples were subjected to ESI in the Jetstream interface in the negative mode as the flavonoids were better detected in this mode. The conditions for the negative mode were as follows – Gas temperature 300 °C, drying gas 9 L/min, nebulizer 25 psig, sheath gas temperature 350 °C and flow rate 11 L/min, capillary voltage 3000 V, nozzle voltage 500 V and fragmentor voltage 140 V. Samples were injected (7 µl) in to an Agilent Zorbax Eclipse 1.8 µm XDB-C18 2.1 x 50 mm column at 35 °C. Solvent A consisted of 0.1 % aqueous formic acid and solvent B consisted of 80 % methanol/water with 0.1 % formic acid. Flavonoids aglycones and glucosides were eluted with the following ratios of Solvent A to B – 90:10 for 0 - 2 minutes, 75:25 for 2 - 7 minutes, 50:50 for 7 – 10 minutes, 30:70 for 10 – 15 minutes, 10:90 for 20 – 24 minutes, 90:10 for 24 – 35 minutes. The instrument was run in the extended dynamic mode over a range of m/z 50-1000 using targeted collision induced dissociation (CID; N_2 collision gas supplied at 18 psi) MS/MS (3 spectra/s). Analysis of data was done using the Agilent MassHunter software (Agilent, USA). Limit of Detection (LOD) and Limit of Quantitation (LOQ) was calculated for all the standards.

Limit of Detection (LOD) and Limit of Quantitation (LOQ)

The detection and quantitation of metabolites are dependent on the limits of these parameters. The Limit of Detection (LOD) which represents the minimum detectable value and the Limit of Quantitation (LOQ) which represents the minimum quantifiable value was calculated for all the analyte standards at 0.5 ppm using measured Signal to Noise (S/N) ratio, as follows –

$$LOD = 3 \times S/N \times 0.5\, ppm$$

$$LOQ = 5 \times S/N \times 0.5\, ppm$$

The LOD is the level that can be reliably distinguished from the background noise or the signal produced in the absence of an analyte. The LOQ defines the sensitivity

and analytes with concentrations above it produce sufficient signals with suitable precision (Armbruster and Pry, 2008).

Metabolite quantification

Metabolite concentration was calculated as follows –

$$Concentration\ of\ analyte\ \left(\frac{ng}{g}\right) = RF \times \frac{Sample\ area}{ISTD\ Area} \times \frac{Amount\ ISTD\ (ng)}{sample\ dry\ biomass\ (g)}$$

The response factor for instrument detector for each analyte was calculated using peak areas from 0.1 ppm standard mix that included 0.4 ppm internal standard.

$$RF = \frac{Analyte\ concentration\ (ppm)}{ISTD\ concentration\ (ppm)} \times \frac{ISTD\ Area}{Analyte\ Area}$$

$$RF = \frac{0.1\ ppm}{0.4\ ppm} \times \frac{ISTD\ area}{Analyte\ area}$$

The RF and R^2 values were calculated from the calibration curves are shown in Appendix Table A2.1. The calculated values for LOD and LOQ are also provided.

2.3 Results

2.3.1 Transformation efficiencies in M. truncatula roots expressing RNAi or overexpression constructs

The transformation of roots to generate materials for performing assays was done in batches of 140 plants per construct. Therefore, for each repeat, a total of 840 germinated seedlings were transformed with *A. rhizogenes* carrying the RNAi constructs and 700 germinated seedlings were transformed with the *A. rhizogenes* carrying the overexpression constructs.

Variations in the transformation efficiencies of these constructs were observed. Therefore, the transformation event was replicated three times and the results are presented in Figure 2.4 and 2.5.

There was no significant difference in the transformation efficiency in the roots that was differentially silenced for genes encoding flavonoid synthesis enzymes (Figure 2.3). Transformation of roots with the overexpression vectors showed slightly lower transformation efficiencies (Figure 2.4). In particular, the roots transformed to overexpress gene encoding DFR showed a significant decrease in the proportion of transformed roots, where roots emerged from the callus 3 weeks post induction.

2.3.2 Quantification of transcript levels of genes encoding flavonoid biosynthesis enzymes in silenced and overexpressing hairy roots

The relative abundance of the genes encoding the flavonoid biosynthesis enzymes was determined in roots transformed with RNA silencing inducing plasmid or overexpression plasmids. Figure 2.6 shows that all the roots targeted for silencing showed reduction in the abundance of the gene transcript encoding flavonoid biosynthesis enzyme. Data in Figure 2.7 shows the transcript abundances of *CHS*, *FLS* and *IFS* in respective roots expressing overexpression constructs The *FLS* and *IFS* overexpressing roots showed an increase in the target transcript; however, this was not observed in *CHS* overexpressing roots.

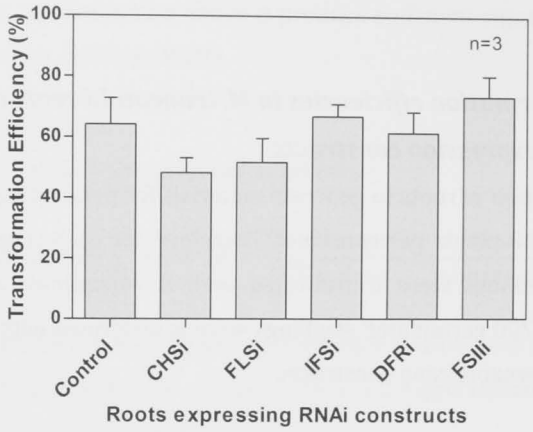

Figure 2.4 – The efficiency of transformation for the *M. truncatula* roots transformed with *A. rhizogenes* carrying the RNAi constructs. The results indicate mean ±SD of three independent repeats with 140 plants per construct. No significant difference ($P<0.05$) was found through one-way ANOVA.

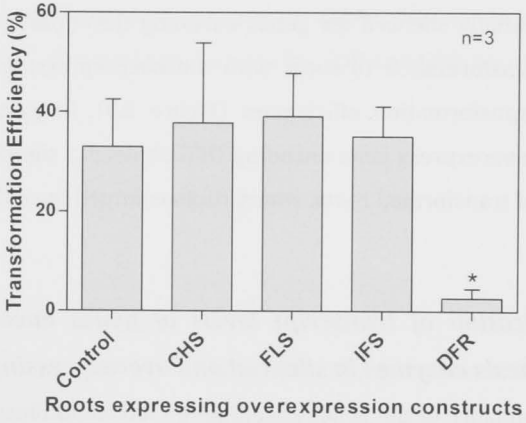

Figure 2.5 – The efficiency of transformation for the *M. truncatula* roots transformed with *A. rhizogenes* carrying the overexpression constructs. The results indicate mean ±SD of three independent repeats with 140 plants per construct. Significance of difference was measured through one-way ANOVA at $P<0.05$ and significant difference to the control is shown with an asterisk.

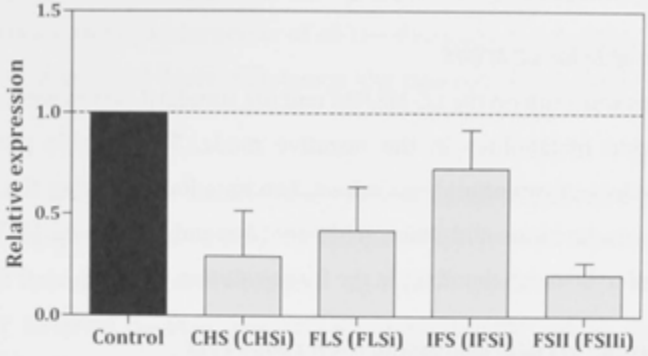

Figure 2.6 – The relative transcript abundance (mean ±SD of two biological repeats with 30 roots each) of silenced genes in respective transformed roots compared to empty vector transformed roots (set at 1, dashed line). The expression of all the genes targeted for silencing (in *CHS*i, *FLS*i, *IFS*i and *FSII*i transformed roots) showed reduced transcript levels compared to control. The DFR transcript could not be reliably amplified.

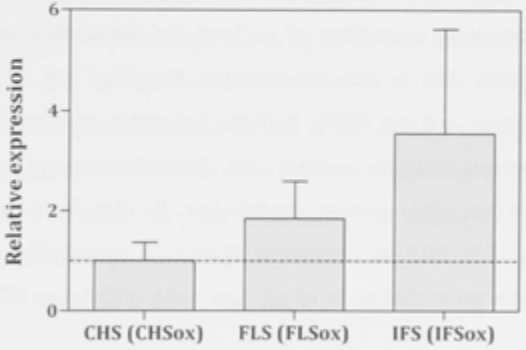

Figure 2.7 – The relative transcript abundance (mean ±SD of two biological repeats with 30 roots each) overexpressed genes in respective transformed roots compared to empty vector transformed roots (set at 1, dashed line). The *CHS* expression was unchanged in roots transformed with *CHS* overexpression (*CHS*ox) construct. Both *FLS* and *IFS* showed increased expression in roots that were transformed with the FLS and IFS overexpressing constructs (*FLS*ox and *IFS*ox respectively).

2.3.3 LC MS/MS Quantification for flavonoid aglycones and glucosides

Standards profile for LC MSMS

The standards were run on the LC-MS/MS and the standard curves were generated for all targeted metabolites in the negative mode. The data is presented in increasing orders of retention-time values. The ions for qualifying the standards are listed as product ions and other qualifiers (Appendix Table A2.1). These ions were detected to be most abundant in the fragmentation patterns.

Flavonoid profile of roots expressing RNAi constructs

While all the compounds listed in Appendix Table A2.1 were targeted for quantification, I did not detect all of them in *M. truncatula* hairy root samples. This could be due to their absence or low abundance preventing their detection. The Figures 2.8 and 2.9 show selected flavonoid metabolite profiles that were consistently detected in *M. truncatula* hairy roots. These figures show flavonoid profiles of uninoculated roots that are expressing the silencing or overexpression constructs targeting genes encoding the flavonoid biosynthesis enzymes. The graphs show the absolute quantities of each of the metabolite as measured per gram of dry biomass. There was no absolute standard for some metabolites (Formononetin isomer and n,n DHF), and the inference was made based on the m/z values of the parent and the product ions. Quantifications of these metabolites were made based on the known metabolite it closely resembled namely Formononetin and 7,4'-DHF. A change in flavonoid metabolite content is also presented along with roots that were challenged with pathogens (Chapter 6).

Silencing of gene encoding CHS enzyme was expected to have a direct effect on all the metabolites as this enzyme targets the first committed step in the pathway. The metabolites Formononetin, Quercetin, Prunetin/Biochanin A, Apigenin, Genistin, Coumestrol, n,n DHF and an isomer of Formononetin all show a reduction in absolute contents when compared to empty vector control. A few other metabolites such as Isoliquiritigenin, Prunin, 7,4' DHF and Luteolin failed to show any silencing.

It was hypothesized that the overexpression of the gene encoding CHS enzyme would increase the concentrations of all the flavonoid metabolites, however, this was not observed and roots maintained the concentrations close to the control levels.

The flavonol branch was silenced and overexpressed in the hairy roots through targeting the gene encoding the FLS enzyme. The flavonol Quercetin showed a significant decrease in concentration compared to control in *FLS* silenced roots. The other targeted flavonol aglycone Kaempferol could not be detected in *M. truncatula* hairy roots. In these RNAi roots, the following metabolites also showed a decrease – 7,4'DHF, Formononetin, Isomer of Formononetin and Genistin. Other metabolites such as Isoliquiritigenin and Prunetin/Biochanin A showed an increase in these roots. In roots overexpressing the *FLS* gene, the concentration of Quercetin (a flavonol) was slightly higher than control and Kaempferol aglycone was not detected.

The isoflavonoid branch was targeted through the silencing or overexpression of the gene encoding the IFS enzyme. Silencing of the branch showed reduction in the concentration of the isoflavonoids Formononetin, Prunetin/Biochanin A and Genistin. The flavonol Quercetin and the flavone 7,4'DHF also showed a decrease. The following metabolites showed an increase or no change in their concentrations – Isoliquiritigenin, Prunin, Apigenin and Luteolin. When overexpressing the *IFS* gene the concentration of Formononetin (an isoflavonoid) showed a significant increase.

The anthocyanin synthesis branch was targeted by silencing or overexpression of gene encoding the DFR enzyme. No anthocyanin metabolites were available so the indirect effects on other metabolites were measured. The silencing of this branch led to an increase in Prunin concentration. The metabolites showing a reduction were 7,4'DHF, Genistin and Coumestrol.

The roots overexpressing the *DFR* gene could not be generated sufficiently to test the concentration of metabolites. This was due to the inefficiency of transformation as shown in Figure 2.5.

The silencing of *flavone synthase II* (*FSII*) was aimed at the flavones present in the hairy roots of *M. truncatula*. However, none of the flavone metabolites showed any silencing. The *FSII* gene was not targeted for overexpression.

A summary table combining the qRT-PCR and metabolite analysis is presented in the following section (*Discussion 2.4*).

Figure 2.8 – Selected flavonoid metabolite concentrations as mean ±SD of five repeats with 30 roots each that were expressing RNAi constructs to silence genes encoding flavonoid biosynthesis enzymes. Significant differences (P<0.05, 1-way ANOVA) from Control are indicated with asterisks (n.d. – not detected).

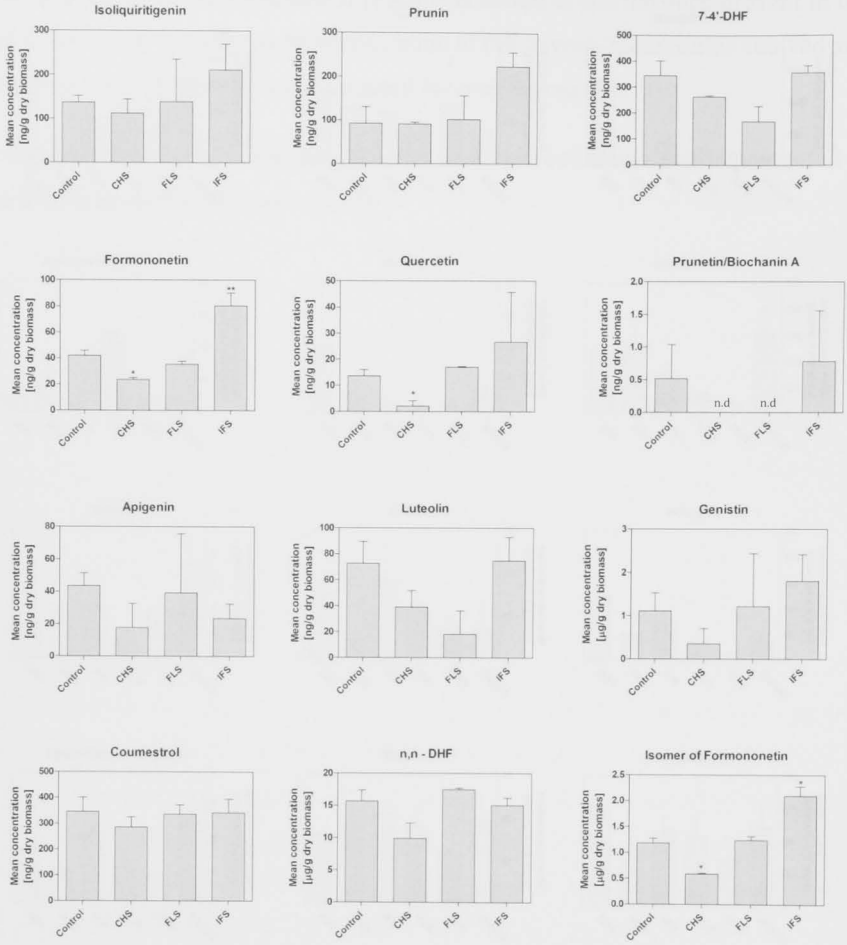

Figure 2.9 – Selected flavonoid metabolite concentrations as mean ±SD of five repeats with 30 roots each that were expressing overexpression constructs to overexpress genes encoding flavonoid biosynthesis enzymes. Significant differences ($P<0.05$, 1-way ANOVA) from Control are indicated with asterisks (n.d. – not detected).

2.4 Discussion

The objective of this chapter was to create a systematic way of generating *M. truncatula* roots that were selectively silencing or overexpressing genes encoding key flavonoid biosynthesis enzymes. This would generate roots that could be studied for roles of different flavonoid branches in symbiosis and defence in the model legume *M. truncatula.* In this chapter, I have demonstrated how the different genes for silencing and overexpression constructs were cloned.

Generating the plant materials that had altered flavonoid metabolite profile presented a number of challenges. The *M. truncatula* genome is diploid and most genes are present in multiple copies (Cannon et al., 2006, Blanc and Wolfe, 2004). Therefore, an approach that silences a single gene could not be used. A siRNA mediated RNA interference mechanism was used to silence multiple copies of the genes, which shared conserved sequences. The siRNA was induced from the gene specific dsRNA that was transcribed from the RNAi inducing vector. The host cell's own RNA interference machinery could be used to process and produce the silencing 21nt RNAs (Waterhouse and Helliwell, 2003).

I have used the GATEWAY™ technology (Life Technologies, USA) to insert two copies of a gene fragment in reverse orientations in a vector that induces a hairpin DNA formation due to complementary sequences (Karimi et al., 2002). This hairpin DNA is recognised by the cellular RNAi machinery that subsequently processes it to 21nt siRNA (Waterhouse et al., 1998) capable of fragmenting target gene transcript in a sequence specific manner. This is particularly useful for silencing multiple copies of the same genes as found in the *M. truncatula* transcriptome.

For overexpression, I have used the cauliflower mosaic virus 35s promoter (p35s) (Odell et al., 1985) to increase the expression of a copy of flavonoid gene that was consistently expressed in the root samples across multiple root-microbe interactions (accessed using the *Medicago Gene Altas MtGEA* http://mtgea.noble.org/). This strategy has been utilised successfully in the past to modify the flavonoid biosynthesis pathway (Muir et al., 2001, Ray et al., 2003, Katsumoto et al., 2007, Lorenc-Kukuła et al., 2007, Hichri et al., 2011).

A. rhizogenes mediation hairy root transformation was selected for generation of root material (Boisson-Dernier et al., 2001). This method allows for rapid and efficient generation of composite plants with transformed root material that could be used for root-microbe interaction studies. Therefore, a large number of genes can be effectively functionally tested for different biological processes such as symbiotic interactions with rhizobia and/or fungi, and pathogenic interactions with disease inducing bacteria, fungi, oomycete and parasites (Kereszt et al., 2007).

Hairy roots generated using this method showed normal root-nodule development (Boisson-Dernier et al., 2001). However, they may have altered content or sensitivities to the plant hormone auxin (Shen et al., 1990) (see Chapter 3). Therefore, all the experiments presented in this thesis always included an empty vector transformed control to ensure that the changes were independent of the inherent differences between hairy roots and seedling roots.

Flavonoids are important plant metabolites that regulate a number of processes in plants (see Chapter 1 for detailed discussion). These could include plant root-development during the *Agrobacterium* mediated plant-transformation processes (Taylor and Grotewold, 2005). The low rate of emergence of hairy roots from the callus of *M. truncatula* transformed with DFR overexpression construct (Figure 2.6) indicates a likely role for DFR processed metabolites such as anthocyanins and condensed tannins as a developmental regulator. No report exists yet implicating these metabolites in developmental roles. Alternatively, it may be the perturbations of metabolic flux directing flavonoids to other branches could be responsible for the low rate of root emergence.

The plant material generated using the methods described in this chapter form the basis for the studies detailed in Chapters 3-5. Therefore, these roots were tested for the level of transcript abundances as a result of the silencing or overexpression. In addition, the flavonoid metabolite profile was also determined. A summary of the changes in these quantities is shown in Table 2.9.

The differentially silenced roots all showed a reduction in the targeted transcript abundance. In addition, they also showed a reduction in the respective metabolite

levels (with exception for *DFR* silenced roots as a suitable flavonoid standard was unavailable).

The overexpression of genes was more challenging. The overexpression of *CHS* did not yield in an increase in transcript abundance or the flavonoid metabolites. The overexpression of *FLS* showed an increase in transcript abundance of *FLS* however, only a slight increase in the flavonol Quercetin level could be detected. *IFS* overexpression led to increases in the concentrations of isoflavonoids Formononetin and Genistin. Together, this suggests that even though the transcript abundances could be increased, there may be other restrictions such as abundance of transcription factors or transporters that prevent an increase in accumulation of flavonoid end product (Dixon and Steele, 1999).

Table 2.9 – Summary of the changes in transcript and metabolite levels in uninfected *M. truncatula* roots transformed with RNA silencing constructs (*CHS*i, *FLS*i, *IFS*i, *DFR*i, and *FSII*i) or overexpression constructs (*CHS*ox, *FLS*ox, *IFS*ox, *DFR*ox). The changes show the increase or decrease in transcript of gene encoding the respective targeted enzyme compared to its levels in control roots. The changes in the flavonoid end product concentration in these same roots are also shown. The DFR transcript in DFR silenced roots (DFRi) could not be amplified in qRT-PCR and insufficient roots samples overexpressing DFR (DFRox) were collected due to low transformation efficiency (Figure 2.4) (not determined = n.d.). Significantly different (1-way ANOVA) changes are shown with asterisks ($P<0.05$)

	Relative transcript abundance measured using qRT-PCR	Metabolite level relative to control as measured using LC MS/MS											
		Isoliquiritigenin/ Liquiritigenin	Prunin (Naringenin 7-O-glucoside)	Quercetin	7,4'-DHF	Apigenin	Luteolin	n,n- DHF	Formononetin	Formononetin isomer	Prunetin/ BiochaninA	Genistin	Coumestrol
		Flavanone	Flavanone	Flavonol	Flavone	Flavone	Flavone	Flavone	Isoflavone	Isoflavone	Isoflavone	Isoflavone	Coumestans
*CHS*i	↓	↑	↑	↓	≈	↓	≈	↓	↓	↓	↓	↓	↓
*FLS*i	↓	↑	↑	↓***	↓	≈	≈	≈	↓	↓*	↑	↓*	≈
*IFS*i	↓	↑	≈	↓	↓	↑	↑	≈	↓	≈	↓	↓	≈
*DFR*i	*n.d.*	≈	↑	≈	↓**	≈	≈	≈	≈	↓	≈	↓	≈
*FSII*i	↓	↑	↑*	↑	≈	↑	↑	≈	≈	↓	≈	↓	≈
*CHS*ox	≈	≈	≈	↓*	↓	↓	↓	↓	↓*	↓*	↓	↓	≈
*FLS*ox	↑	≈	≈	≈	↓	≈	↓	≈	≈	≈	↓	≈	≈
*IFS*ox	↑	↑	↑	↑	≈	↓	≈	≈	↑**	↑*	≈	↑	≈
*DFR*ox	*n.d.*												

2.5 Conclusion

This chapter details the generation of plant material for subsequent studies in plant-microbe interactions as discussed in Chapters 3-6. The rapid and high-throughput generation of hairy roots expressing gene-silencing or gene-overexpressing constructs made it feasible to systematically study the flavonoid biosynthesis pathways in *M. truncatula*. Here I have shown the method used to generate roots silenced in *CHS, FLS, IFS, DFR* and *FSII*. The enzymes encoded by these genes are key regulators of various branches of flavonoid synthesis. The genes *CHS, FLS, IFS* and *DFR* were also targeted for overexpression. The *CHS* overexpression did not yield any significant increase in flavonoid products while the overexpression of *DFR* significantly reduced normal hairy root development. The genes encoding the enzymes FLS and IFS were shown to increase the accumulation of certain flavonols and isoflavonoids respectively.

Chapter 3. Flavonols and isoflavonoids control auxin transport and accumulation during nodule development in M. truncatula

Summary

Specific flavonoids have long been implicated as auxin transport regulators in plants. The study presented in this chapter aims to investigate the role of specific branches of the flavonoid pathway in controlling auxin transport and accumulation during nodulation in *M. truncatula.* Silencing of flavonoids led to a significant reduction in nodule numbers in the roots. The *CHSi* roots also failed to inhibit auxin transport when inoculated with rhizobia. An investigation of auxin content found that the *M. truncatula* hairy roots contained free IAA and several amino acid conjugates of IAA at very high concentrations. Even though the acropetal transport of auxin was inhibited in the presence of rhizobia, auxin concentration at the site of inoculation was unexpectedly reduced. This could indicate that the inoculation of these roots with rhizobia might have triggered a metabolic process that reduced the active IAA concentration as well as conjugated IAA.

It was found that flavonols and isoflavonoids mediate auxin transport inhibition (ATI) as a result of inoculation with rhizobia during indeterminate nodule formation. The silencing of flavonols also led to a significant reduction in root-nodules suggesting that the flavonols could be essential as inhibitors. Conversely, silencing of isoflavonoids did not reduce the number of root-nodules, implying that they may not be vital in indeterminate nodule formation in *M. truncatula*.

Finally, it was investigated if the role of flavonoids in controlling auxin transport could be replaced using a synthetic auxin transport inhibitor (TIBA) to rescue nodulation in flavonoid deficient roots. TIBA could only induce uninfected pseudo-nodules in flavonoid silenced roots and this would imply that flavonoids not only control auxin transport during nodulation, but also play additional roles in infection. This question was further investigated in Chapter 4.

3.1 Introduction

Flavonoids have long been implicated as auxin transport inhibitors and mediators of it its breakdown through peroxidases. Here the aim was to identify specific flavonoid groups involved in the auxin transport inhibition activity and the resulting changes in auxin accumulation and response at the site of rhizobia infection. A narrow window of auxin is likely responsible for the induction of the cortical cell divisions in nodule primordia (Ferguson and Mathesius, 2014). Therefore, it is important to identify the flavonoids responsible for this activity and attempt to rescue flavonoid silenced roots with the exogenous application of synthetic auxin transport inhibitors. This would illustrate whether the transport modulation activity is the essential role flavonoids play during symbiotic nodulation.

While previous studies with *M. truncatula* have shown that flavonoids are required for auxin transport control during nodulation (Wasson et al., 2006) this study did not identify which flavonoids are necessary for auxin transport control. A subsequent study by Zhang et al. (2009) showed that flavonols were most likely the flavonoids required for nodulation. However, their effects on auxin transport and accumulation were not studied.

Polar auxin transport

Polar auxin transport is catalysed by the PIN and LAX proteins (Schnabel and Frugoli, 2004). The authors identified ten PIN proteins and five LAX proteins in *M. truncatula*. It has also been shown that the intracellular cycling of PIN proteins under the control of cellular flavonoids is responsible for the transport of auxin to sink tissue (Peer et al., 2004). Peer et al. (2004) also showed that expression of *PIN* and *LAX* changed in the *Arabidopsis* flavonoid mutants. However, it is unclear if the gene expression of PIN and LAX transporter proteins are also regulated by flavonoids in *M. truncatula*.

3.1.1 Auxin metabolism and homeostasis during plant-development

An overview of auxin metabolism is shown in Figure 3.1. Auxin is a major plant hormone and can occur in several active forms. The most abundant active free-

form of auxin in most land plants is the indole-3-acetic acid or IAA (Bajguz and Piotrowska, 2009). A number of other small molecules such as indole-3-butryic acid (IBA), 4-Cl-IAA, indole-3-pyruvic acid (IPA) and phenylacetic acid (PAA) also show auxin activities (Bajguz and Piotrowska, 2009).

Auxin is mainly synthesized from the precursor tryptophan (Trp) through a Trp-dependent pathway (Figure 3.2). The IPA pathway catalyzed by the YUCCA family of proteins is likely the major synthetic pathway as shown in *Arabidopsis* (Mashiguchi et al., 2011).

Auxin is believed to be synthesized in all dividing tissue but mainly in the shoot (Zhao, 2010). The long distance transport from shoot to the root is via the phloem, but cell-to-cell auxin transport occurs through active polar auxin transport mechanisms (Rosquete et al., 2012). The chemiosmotic hypothesis (Rubery and Sheldrake, 1974) proposes that the IAA is protonated in the acidic environment of the apoplast (pH~5.5) and deprotonated in the cytosol (pH~7). The deprotonated IAA (IAA^-) carries a negative charge and requires a carrier driven mechanism to exit the cell (Figure 3.1).

The spatio-temporal distribution of auxin is dependent on the rate of influx and efflux of IAA from the cell as mediated by the transporter proteins. The short distance cell-to-cell auxin transport is mediated by PGP, AUX, PIN and LAX proteins located on the plasma membrane (Schnabel and Frugoli, 2004). PIN proteins have been observed to undergo cycling between plant membrane and an endosomal vesical. In *Arabidopsis* and *Medicago* it has been shown that flavonoids act as natural auxin transport inhibitors (Brown et al., 2001, Wasson et al., 2006).

Flavonoids target both influx and efflux of auxin by modulating several transport proteins. The auxin importer PGP belongs to the ATP-binding cassette subfamily B (ABCB) transport family which depends on the hydrolysis of ATP for its activity (Terasaka et al., 2005). In *Arabidopsis*, the aglycone flavonols have been suggested to regulate the activity of several PGP transporter proteins in shoot and root apices (Peer et al., 2004), likely through inhibition or phosphorylation of ATPase or through allosteric binding.

The auxin efflux carriers such as the members of PIN-Formed proteins are also modulated by cellular flavonoids. In addition to altering the expression of multiple *PIN* genes in *Arabidopsis*, flavonoids also have direct effect on membrane cycling of PIN transporter proteins (Peer et al., 2004). This mechanism likely involves flavonoids as kinase and phosphatase inhibitors which target auxin transport regulatory proteins such as serine/threonine kinase PINOID and PINOD-related WAG kinases (Peer and Murphy, 2007). These regulatory proteins direct the subcellular localization of PIN proteins.

Flavonoids may also influence the fluidity of the cellular membranes which could indirectly result in altered cellular trafficking of auxin (Peer and Murphy, 2006). The hydrophobic flavonoids may integrate and intercalate with the lipid bilayer and alter the rigidity of the membranes (Scheidt et al., 2004).

Inhibition of auxin transport leads to a buildup of auxin in the cell and an auxin gradient is established in the tissue (Rubery and Sheldrake, 1974). The increased IAA activates auxin signaling proteins that activate several downstream events such as activation of stress response (Tognetti et al., 2012), ROS generation (Cook et al., 1995) and early nodulation genes (ENODs). The application of synthetic auxin transport inhibitors such as NPA (1-N-naph- thylphthalamic acid) and TIBA (2,3,5-triiodobenzoic acid) on *Medicago* roots under laboratory conditions is also able to induce cell-divisions in the cortex to produce pseudonodule-like structures (Rightmyer and Long, 2011, Hirsch et al., 1989).

Auxin can be stored within the cells or marked for degradation (IAAsp and IAGlu) through conjugation with small sugar molecules or amino acids (Ludwig-Müller, 2011). The composition of the conjugates vary between plant species and amide linked amino acid conjugates have been shown to be more abundant in leguminous plants (Bandurski and Schulze, 1977).

Conjugated auxin has several roles in plant development but its precise function is yet to be elucidated (Ljung, 2013). At present knowledge, the conjugates are thought to be storage forms of active auxin however, evolutionary studies have indicated that the conjugated auxins were developed first as the auxin hydrolases

are found in moss ferns (Ludwig-Müller, 2011). There may be other roles of auxin conjugates including roles that antagonize auxin effects (Rosquete et al., 2012), however, this needs to be further explored.

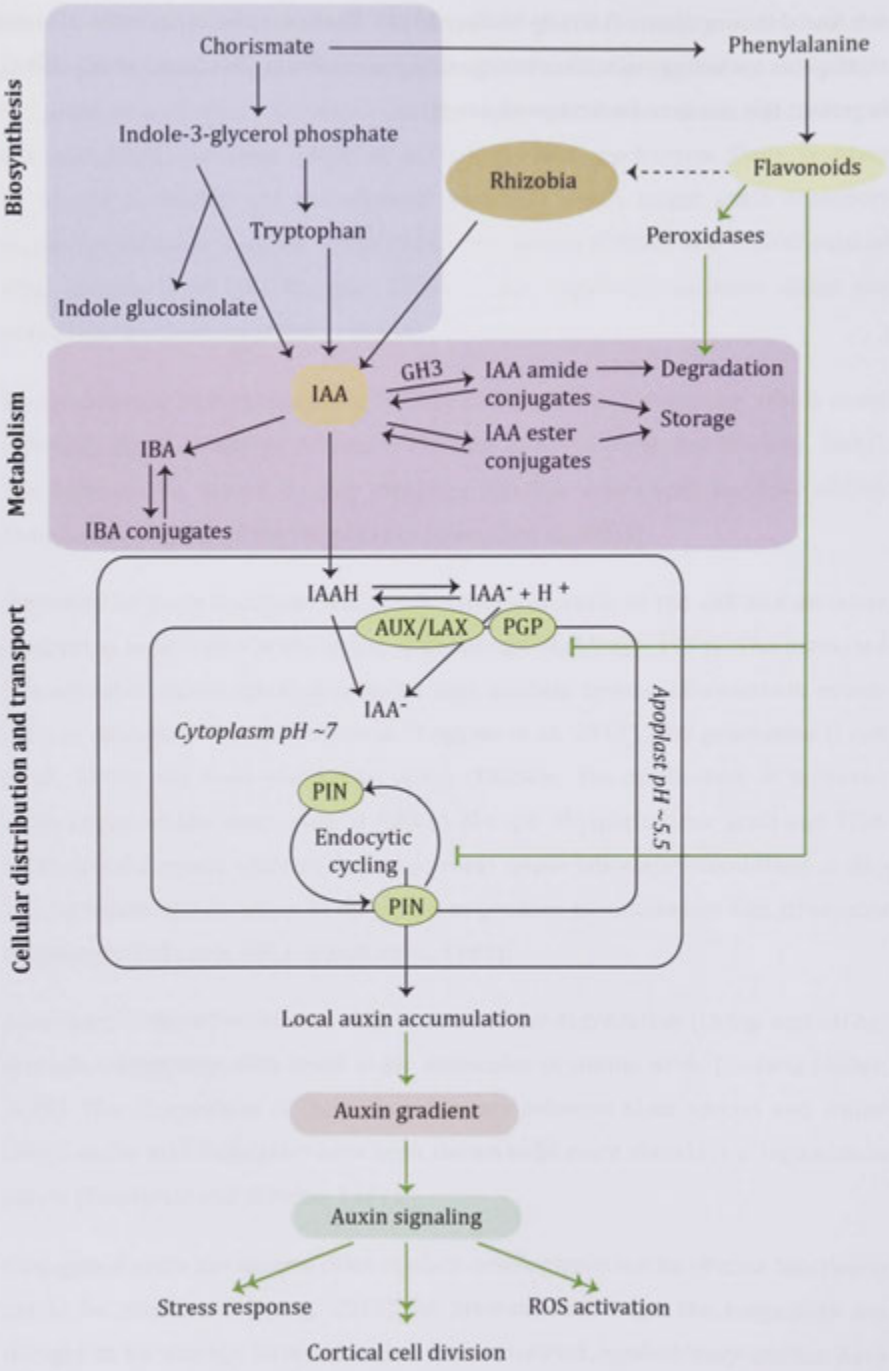
Biosynthesis
Chorismate
Phenylalanine
Indole-3-glycerol phosphate
Rhizobia
Flavonoids
Tryptophan
Peroxidases
Indole glucosinolate
Metabolism
IAA
GH3
IAA amide conjugates
Degradation
Storage
IAA ester conjugates
IBA
IBA conjugates
Cellular distribution and transport
IAAH
IAA⁻ + H⁺
AUX/LAX
PGP
IAA⁻
Cytoplasm pH ~7
Apoplast pH ~5.5
PIN
Endocytic cycling
PIN
Local auxin accumulation
Auxin gradient
Auxin signaling
Stress response
ROS activation
Cortical cell division

Figure 3.1 – Auxin fate in plant root cells and interactions with rhizobia. This figure shows an overview of the synthesis of IAA from the precursor chorismate. Chorismate is also a precursor to phenylalanine that leads to the formation of secondary metabolites such as flavonoids. IAA is normally synthesized in young leaf tissue and it can be converted to Indole-3-butryic acid (IBA) through β-oxidation. Rhizobia can also synthesise IAA and it is thought that it contributes to the cellular auxin levels during the nitrogen fixation stage (Theunis et al., 2004). IAA and IBA can be converted to their ester or amide conjugates. Some IAA amide conjugates such as IAA conjugated to aspartic acid and glutamic acid are irreversible and leads to degradation through peroxidases. Flavonoids have regulatory control over these peroxidases. Other amide and ester conjugations are reversible and the metabolites can readily be converted to free IAA. IAA is negatively charged in the apoplastic pH of 5.5 so requires importer proteins such as PGP and LAX. The exporter proteins such as PIN and PGP mediate the transport of IAA out of the cell in a directionally controlled manner. The cycling of the PIN proteins is affected by some flavonoids, which lead to its accumulation in specific tissues. An auxin gradient is created could contribute to the cortical cell divisions required at to form a nodule primordia. The black arrows shows actual metabolite conversion or movement, green arrows show regulatory control and dashed arrow show activation of Nod factor synthesis genes in rhizobia by plant secreted flavonoids. IAA metabolism and biosynthesis also occurs in the cytoplasm but have been shown outside for convenience. The Figure has been modified from Tognetti et al. (2012).

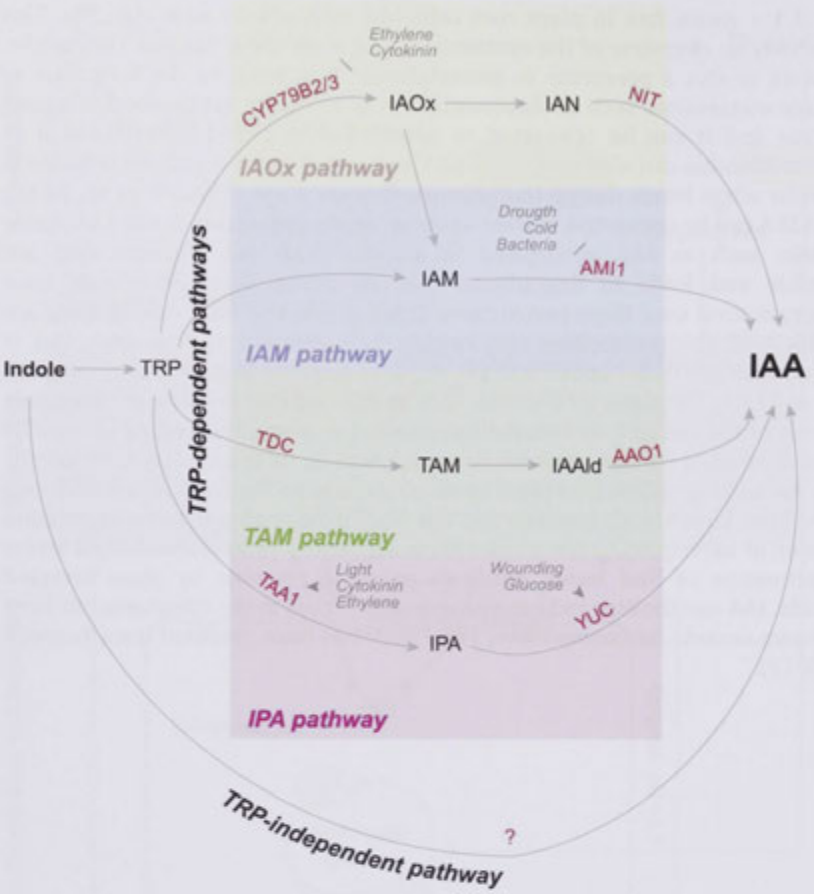

Figure 3.2 – Simplified auxin biosynthesis pathway. The The IAOx, IAM, and IPA pathways are derived from Tryptophan. The intermediates of the pathway are shown in black while the biosynthesis enzymes are shown in red. The IPA/YUCCA pathway has recently been suggested to be the major IAA synthesis pathway in *Arabidopsis* (Mashiguchi et al., 2011). IAA can also be synthesized through tryptophan independent pathways, however, the process has not been elucidated. AAO, ACETALDEHYDE OXIDASE; AMI1, AMIDASE 1; CYP79B2/3, CYTOCHROME P450, FAMILY 79, SUBFAMILY B, POLYPEPTIDE 2/3; IAA, Indole-3-acetic acid; IAAld, Indole-3-acetaldehyde; IAM, Indole-3-acetamide; IAN, Indole-3-acetonitrile; IAOx, Indole-3-acetaldoxime; IPA, Indole-3-ylpyruvic acid; NIT, NITRILASE; TAA1, TRYPTOPHAN AMINOTRANSFERASE OF ARABIDOPSIS; TAM, Tryptamine; TDC, TRYPTOPHAN DECARBOXYLASE; TRP, Tryptophan. The figure has been adapted from Rosquete et al. (2012).

Silencing of flavonoids through RNA interference of *chalcone synthase* transcript in *M. truncatula* has been achieved previously (Wasson et al., 2006). Here it was shown that auxin transport inhibition was mediated by flavonoids similar to the action of synthetic auxin transport inhibitor NPA. It was also reported that *CHS*i roots showed increased auxin transport compared to control roots. This provided the genetic evidence that flavonoids were involved in modulating auxin transport within the roots during nodule organogenesis. Therefore, it was rational to further study the impact of flavonoids on the gene expression of the auxin transporter proteins, identify the class of flavonoids responsible for auxin transport inhibition phenotype and rescue nodulation in flavonoid-deficient roots by exogenous application of synthetic auxin transport inhibitor.

3.2 Methods

Strain and growth conditions for rhizobia, inoculation technique

The Nod factor overexpressing plasmid E65 was isolated from *S. meliloti* A2102 (Barnett et al., 2004) and ligated with the open reading frame of *gfp* that was excised from the pHC60 vector (Cheng and Walker, 1998). The resulting vector was electroporated into *S. meliloti* strain 1021 (Meade et al., 1982). A detailed description has been provided in Chapter 4.2. The E65 and E65-gfp rhizobia strains were grown overnight in liquid BMM culture with 10 µg/ml tetracyclin supplements to select for the Nod factor overexpressing plasmid.

Plant growth and nodulation measurements and analysis

Seeds of A17 Jemalong were scarified and surface sterilized with 6 % (w/v) sodium hypochlorite for 10 minutes and washed five times with sterile water. Subsequently the seeds were stratified at 4 °C for two days and then germinated overnight at 25 °C. The seedlings were transformed using hairy root transformation method as described previously (Boisson-Dernier et al., 2001) using the *A. rhizogenes* strain *AR*qua1 carrying the respective RNAi vectors as described in Chapter 2. The transformed seedlings were cultured on modified Fåhreaus medium (Table 2.4) for one week at 20 °C followed by one week at 25 °C. Untransformed roots were discarded after screening for the presence of flavonoid auto-fluorescence under UV excitation (excitation 365 nm, emission 420 nm) for pHellsgate8 and pHellsgate8-*CHS* transformed roots, or gfp fluorescence (excitation 470 nm, emission 515 nm) for pk7GWIWG2D(II), pk7GWIWG2D(II)-*FLS*, pk7GWIWG2D(II)-*IFS*, pk7GWIWG2D(II)-*DFR* and pk7GWIWG2D(II)-*FSII* transformed roots under a stereomicroscope (M205FA – Leica Microsystems, Germany). The remaining plantlets were transferred to Fåhreaus medium and cultured for 1 week at 25 °C with 16 hour photoperiod (with 140 µE light intensity).

The silencing vector for *CHS* was used as described previously (Wasson et al., 2006) and labelled as 'Control' (empty vector pHellsgate8) or '*CHS*i' (pHellsgate8 carrying *CHS* silencing hairpin). Gene fragments for RNAi silencing vectors of *FLS*

(TC198603), *IFS* (TC175803), *DFR* (AY389346) and *FSII* (TC172770) were amplified using the primers detailed in Chapter 2 and transformed in to pk7WGIGW2D(II) vector (see section 2.2.1 for details). An empty vector control was also used for all comparisons. All vectors were transformed in to *A. rhizogenes* using the freeze-thaw method (Weigel and Glazebrook, 2005) where competent *A. rhizogenes* bacteria was mixed gently with plasmid DNA, snap-frozen in liquid N_2 and immediately thawed at 37°C for 5 minutes with occasional shaking. The cells were regenerated in LB media for 4 hours and subsequently on LB agar plates at 28 °C for two days.

Quantitative Real-Time PCR analysis to measure expressions of genes encoding IAA transporter proteins PIN and LAX; and IAA synthesis proteins YUCCA1, 2 and 3

Control and *CHS*i roots were inoculated with *S. meliloti* A2102 carrying *nodD3* overexpression plasmid (E65) and a 5 mm long root section around the zone of inoculation site was collected from 50 roots each at 6 hours and 24 hours post inoculation and immediately frozen in liquid N_2. Samples were collected in three biological replicates. The roots were ground using a mortar and pestle on dry-ice and the RNA was extracted using the Spectrum Total Plant RNA isolation kit (Sigma, USA) and treated with DNAase (On-column DNAseI digestion set, Sigma, USA) to digest contaminating DNA. Subsequently the cDNA was synthesized using Superscript III First strand cDNA synthesis kit (Life Technologies, USA). The synthesized cDNA was further diluted 5 times in DEPC treated water.

The relative transcript abundance was measured using quantitative real-time PCR (see section 2.2.7) in a 10 µl reaction volume (Table 2.7). The primers for the reactions are listed in Table 3.1 and used at 2 pM each. Each reaction had 2.5 µl of synthesized cDNA added to it. A mix of ABI Power SYBR Green PCR mastermix and cDNA solution was aliquoted in the 384 well PCR plate (Applied Biosystems, USA) followed by the mix of primers and water. This was done to ensure that the cDNA was distributed evenly across the different wells while the primers were in excess to not limit the reaction.

Quantitative real time PCR analysis was carried out using the ABI 7900HT Real-Time PCR System (Applied Biosystems, USA) and data were analyzed using Sequence Detection Systems version 2.4 (Applied Biosystems, USA) following the ΔΔCt method corrected for primer efficiencies (Schmittgen and Livak, 2008).

Three putative YUCCA genes (MTR_1g011630, MTR_3g109520 and MTR_7g099330) were identified by Ng et al. (unpublished) through homology with *Arabidopsis* genes. Primers were designed and used to quantify their levels in the control and *CHS* silenced roots at 6 and 24 hpi with rhizobia as shown in Table 3.2. The Pfaffl method (Pfaffl, 2001) was used to quantify the changes in transcript abundance of these genes.

Table 3.1 – The primers used to amplify the *PIN* and *LAX* genes in *M. truncatula*

Gene	GenBank ID	Orientation	Primer Sequences
PIN1	AY115836.1	F	5'TGCCCTGAACAAGCTAGGAG3'
		R	5'GAGACGGGTCATAACACTTGC3'
PIN2	AY115837.1	F	5'AGCCTAAGCTGATTGCATGTGG3'
		R	5'TGCTATTGAGGTTGCCGCAATC3'
PIN3	AY115838.1	F	5'CTTCGCCGGTTTCGGAAAG3'
		R	5'GTTCATCAGCCACCACCATC3'
PIN4	AY115839.1	F	5'GCATGGCTATGTTCAGTCTTGG3'
		R	5'GACCAACAAGGAATCTCACACC3'
PIN5	AY115840.1	F	5'CGAGCATTATCGGCCTAAC3'
		R	5'CCTGCATCCGACAATATGG3'
PIN6	AY553209.1	F	5'CAGCCTCGTATCATTGCTTGT3'G
		R	5'CGGCAATCGAGGATAAGGAC3'
PIN7	AY553210.1	F	5'TGTGATTGCGGCAACCTC3'
		R	5'TGGCAAACACAAAGGGAACG3'
PIN8	BK005119.1	F	5'GGAATCGGCGAGTGAAATAC3'
		R	5'CCCACTGTGACAAGAATG3'
PIN9	AY553211.1	F	5'ATGGGTGTGGATCTTGTG3'
		R	5'CCCTCTATTCCCGTTCTTC3'
PIN10	AY553212.1	F	5'TGCCACCTGCTAGTGTTATG3'
		R	5'GGGACCAGGTAAGACCAATAAG3'
LAX1	AY115841.1	F	5'CTTGGCCTTGGCATGACTAC3'
		R	5'TCTTTGGACCCGAGTGAACC3'
LAX2	AY115843.1	F	5'TGGGTTTGGGTTTGGAGGATGG3'
		R	5'GACTGGTGGTGGTTTGCATTGG3'
LAX3	AJ299399.1	F	5'GACAGGCTGAGGATGTGAAG3'
		R	5'AACAGCATGTCCACCAAAGG3'
LAX4	AY115844.1	F	5'TGGAGGATGGGCTAGTATGACC3'
		R	5'ATGGTGCTTGAGGTGGTGTTGG3'

F – Forward primer; R – Reverse primer

Table 3.2 – The primers used to amplify the *YUCCA* genes in *M. truncatula*

Gene	Locus		Primer Sequences
YUCCA1	MTR_1g011630	F	5'GGTGATGGAAGGTGTGAAAGAG3'
		R	5'TGCTCTTGTACCCTGTTGCT3'
YUCCA2	MTR_3g109520	F	5'GATTCAGTACACGTCCTACC3'
		R	5'CCTATCGACAAGTCCCAATG3'
YUCCA3	MTR_7g099330	F	5'TCCAATGCCTGAAGATTTCCC3'
		R	5'CTCGTTGAATTGCGGGTTGA3'

F – Forward primer; R – Reverse primer

Auxin transport measurements

An overnight culture of *Sinorhizobium meliloti A2102* carrying the pE65 vector for Nod factor overexpression was prepared in liquid BMM with 10 µg/ml tetracycline for selection. The culture was subsequently diluted with BMM whilst still in its log phase to an OD_{600} between 0.1 - 0.2. Transformed hairy roots of at least 1.5 cm length were spot inoculated 4mm from the root-tip at the zone of root hair emergence. One root was selected for inoculation per plant. The plants were grown at 20 °C for 24 hours in a 16 hour photoperiod with 140 µE light intensity. The radioactive auxin was then applied on the roots as follows –

To prepare the agar block containing radiolabeled auxin, 8.0 µl of a 1 mCi/ml ^{3}H-IAA (American Radiolabeled Chemicals, Inc.) was added to 30 µl of ethanol under sterile conditions. The mixture was then added to 1.5 ml of melted and cooled 1 % agarose (at pH 4.8), poured on a 35mm ø petri dish and swirled vigorously to mix. Once the agar solidified, blocks of 2 x 2 x 2 mm "donor" agarose were cut.

The roots that were spot inoculated were cut at a fixed distance of 1.2 cm from the root-tip 24 hours later. On a fresh Fåhreaus medium plate, strips of parafilm were laid. The cut end of the root was placed on the parafilm strip's edge so that the majority of the root was in contact with the agar medium. A donor bock of ^{3}H-labelled IAA was positioned on top of the parafilm and placed in contact with the cut end of the root. This was confirmed under a microscope. Several trials with hairy roots and different ^{3}H-IAA stocks were conducted to obtain this optimum time required to transport the ^{3}H-IAA in hairy roots. It was determined that 14 hours of transport was required to obtain a measurable radioactivity in the

segments. Therefore, the roots were incubated vertically and in the dark for 14 hours at room temperature.

Two 3 mm segments above (A) and below (B) the site of inoculation were cut (schematic shown in Figure 3.3), solubilized in 2 ml scintillation fluid (Emulsifier-safe, Perkin Elmer) overnight and the radioactivity was measured using Beckman Coulter LS6500 Scintillation Counter for 1 minute per sample.

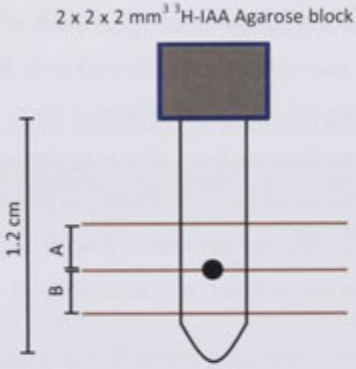

Figure 3.3 – Schematic diagram showing the placement of 3H-IAA block on a 1.2 cm root at 24 hpi with rhizobia. The position of rhizobia applied through a fine needle is shown as a black circle. 3 mm segments above (A) and below (B) the inoculation site were collected after 14 hours of transport.

Rescue of auxin transport inhibition with the exogenous application of flavonoids

Following hairy root transformation on modified Fåhreaus media, the *CHSi*, *FLSi*, *IFSi* and Control roots were grown on Fåhreaus media supplemented with 100 nM of flavonoids Isoliquiritigenin or Quercetin. Auxin transport was measured in these samples as described above.

Auxin extraction and quantification via liquid chromatography – mass spectrometry

Approximately 3000 seedlings of *M. truncatula* A17 Jemalong were transformed with *A. rhizogenes* carrying the Control and *CHS*i vectors in five replicates. One root from each plant was selected for inoculation with *S. meliloti A2102* carrying the Nod factor overexpression plasmid (E65) at OD_{600} between 0.1 and 0.2. The roots were spot-inoculated 3 mm from the root-tip. The seedlings were cultured at 20 °C for exactly 24 hours and 5 mm region around the point of inoculation (excluding the root-tip) was excised and snap frozen in liquid nitrogen.

Auxin was extracted from ground tissue in 1 ml extraction solvent (Methanol:Propanol:Glacial Acetic Acid 20:79:1) in a sonic bath for 15 minutes at 4 °C. The debris was removed through centrifugation and extracted solution was vacuum dried at room temperature. The samples were re-suspended in 60% methanol (Acros Organics, USA) and filtered through Nanosep MF GHP 0.45 µm cellulose filter (Pall Life Sciences, USA) prior to injection of 7 µl of the sample. The extraction method was adapted from Müller and Munné-Bosch (2011).

Auxin quantification was carried out on Agilent 6530 Accurate Mass LC-MS Q-TOF (Sante Clara, CA, USA). Calibration curves with known standards (IA-Phenylalanine, IA-Leucine, IA-Valine, IA-Tryptophan, 4-Cl-IAA was obtained through OlChemim, Czech Republic; IA-Aspartate, IA-Alanine, IA-Isoleucine, IA, IBA, PAA was obtained from Sigma, USA; and Indole-2,4,5,6,7-d_5-3-acetic acid was obtained from Cambridge Isotope Laboratories, USA) were established.

Quantification was carried out in the positive mode and developed in-house with the following conditions: Gas sheat temperature 250 °C, drying gas 5 L min^{-1}, nebulizer 30 psig, sheath gas temperature 350 °C and flow rate of 11 L min^{-1}, capillary voltage 2500V, nozzle voltage 500V and fragmentor voltage 140 V. 7 µl of the samples were injected in to Agilent Zorbax Eclipse 1.8 µm XDB-C18 2. 1 x 50 mm column. The solvent A was 0.1 % aqueous formic acid and solvent B was 90 % methanol/ water with 0.1 % formic acid. Free Auxin and conjugates were eluted at a flow rate of 200 µl min^{-1} with a linear gradient from 10 – 50 % solvent B from 0-8 minutes, 50-70% solvent B from 8-12 minutes, hold from 12-20 minutes, 70-10 %

solvent B from 20-21 minutes, hold from 21-30 minutes. The instrument was run on extended dynamic mode over a range of m/z 50-1000 using targeted collision induced dissociation (CID) MS/MS. Data analysis was carried out using Agilent MassHunter software. Internal standard of deuterium labeled IAA was used for quantifications.

The response factors (RF) of instrument detector for each standard analyte was calculated using peak areas from 0.1 ppm standard mix that included 0.4 ppm internal standards (ISTD).

$$RF = \frac{Analyte\ concentration\ (ppm)}{ISTD\ concentration\ (ppm)} \times \frac{ISTD\ Area}{Analyte\ Area}$$

$$RF = \frac{0.1\ ppm}{0.4\ ppm} \times \frac{ISTD\ area}{Analyte\ area}$$

$$Concentration\ of\ analyte\ \left(\frac{ng}{g}\right) = RF \times \frac{Sample\ area}{ISTD\ Area} \times \frac{Amount\ ISTD\ (ng)}{sample\ fresh\ weight\ (g)}$$

Where-

RF = Response factor

ISTD = Internal Standard, D5-IAA

and

Standard concentrations of 0.1 ppm was used to calculate the response factor with the coefficient of determination, R^2 values were calculated from the calibration curves and shown in Table 3.3.

Table 3.3 – The response factors and regression coefficient of determination of the standard curves for the four auxin analytes that were detected in *M. truncatula* hairy root samples

Analyte	Response factor	R^2
IAA	0.2633	0.9985
IA-Ala	0.2302	0.9989
IA-Ileu	0.08	0.937
IA-Val	0.1481	0.9272

Auxin responsive GH3 accumulation through β-glucuronidase reporter activity

M. truncatula cv. Jemalong 2HA having β-glucoronidase (GUS) reporter gene fused to 722 bp region upstream of the ATG start codon of the GH3 gene from *Glycine max* (an auxin responsive promoter)(Hagen et al., 1991, van Noorden et al., 2007) was used for visualizing auxin response (full transgenic plants generated by Dr. Flavia Pellerone, unpublished). Hairy root transformation with *CHS* silencing construct and empty vector control was carried out in these plants. Roots were screened as previously described.

Roots were harvested at various time points and stained for β-glucoronidase (GUS) as described previously (Vitha et al., 1995). Root tissue was fixed in ice cold fixative (4 % formaldehyde in 100 mM phosphate buffer pH 7) for 30 minutes at 4 °C in vacuum, rinsed 3 times in ice cold water, and stained with X-gluc solution (0.1 mM 5-bromo-4chloro-3-indolyl β-D-Glucoronide, 50 mM methanol, 0.1 M phosphate buffer pH 7, 1% (v/v) 0.1 M potassium ferrocyanide, 1 % (v/v) 0.1 M potassium ferricyanide, 150 mM Triton X-100 in distilled water) at 37 °C for several hours until distinct blue colour appeared. Roots were imaged under brightfield conditions using a stereomicroscope (MF205FA, Leica Microsysthems, Germany). Images were captured using 12.5 megapixel digital camera (DFC 550 – Leica Microsystems, Germany).

Induction of pseudonodules in M. truncatula hairy roots

The synthetic auxin transport inhibitor TIBA was dissolved in methanol to achieve a concentration of 1 mM and filter sterilized through a 0.45 µM syringe filter (Merk Millipore, Germany). It was subsequently diluted in sterile water to concentrations

ranging from 25 to 200 µM as described in Section 3.3.8. Approximately 25 ml of this solution was flooded on the plate with the hairy roots. The solution was left for 30 seconds and the residual liquid was removed and discarded. The plates were then dried under the laminar flow prior to inoculation with rhizobia. This method has been adapted from Rightmyer and Long (2011). Separate samples of roots were also supplemented with 100 nM of Naringenin and Isoliquiritigenin each as a control.

The roots were then inoculated with Nod factor overexpressing rhizobia (E65) tagged with gfp at OD_{600} between 0.1 and 0.2 (see Chapter 4.2). Nodulation on these roots were assessed and the results are described in section 3.3.8. Nodules and pseudonodules were embedded in 3 % Agarose (Astral Scientific, Australia) and sectioned at 100 µM thickness using a Vibratome 1000 Plus Tissue sectioning system (Intracel, UK). Sections were observed under brightfield and epifluorescence (excitation 480 nm, emission 505 nm) using a compound microscope (DM5500 – Leica Microsystems, Germany). Images were captured using 12.5 megapixel digital camera (DFC 550 – Leica Microsystems, Germany).

Bioinformatic searches for flavonoid and auxin synthesis protein sequences

To determine the evolution of flavonoid and auxin synthesis pathways, sequence alignment searches were performed on major plant orders (Savolainen and Chase, 2003) with protein sequences from *M. truncatula* and *A. thaliana* using NCBI BLASTP tool (www.blastncbi.nlm.nih.gov). The *M. truncatula* sequences for flavonoid synthesis enzymes (and their UniProt IDs) used were CHS (G7KR31), FLS (G7J3J8), DFR (Q6QT1), FSII (Q0ZM38) and IFS (Q49BZ0). The *A. thaliana* sequences for auxin synthesis proteins used were AMI1 (Q9FR37), AAO1 (Q7G193), YUC1 (Q9SZY8), CYP71A13 (O49342), CYP79B2/B3 (O81346) and NIT1/2 (P32961) (Mano and Nemoto, 2012).

A cladogram of these plant orders was simultaneously constructed using the NCBI taxonomy data obtained through phyloT (www.phylot.biobyte.de) and visualized using TreeGraph 2 (Stöver and Müller, 2010). These data are presented in Chapter 6 – General Discussion.

Statistical analysis

All data plots and statistical analysis was carried out using GraphPad Prism (version 5.02, USA).

3.3 Results

3.3.1 Silencing of flavonoids reduces the number of nodules in *M. truncatula* roots

The enzyme chalcone synthase forms the first committed step of flavonoid biosynthesis. Silencing of this enzyme leads to a knockdown of flavonoid biosynthesis. The *CHS* silenced roots were inoculated with Nod factor overexpressing rhizobia expressing a constitutive *nodD3* gene to study the role of flavonoids independent of *nod* gene induction. The number of nodules on these roots is shown in Figure 3.4. The silencing of flavonoids leads to a significant reduction in number of nodule per root as expected from previous studies (Wasson et al., 2006, Zhang et al., 2009).

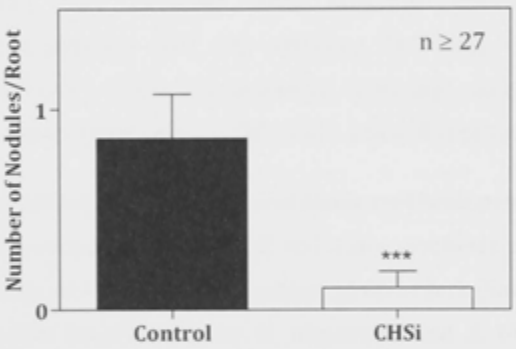

Figure 3.4 – Average nodule numbers in Control and *CHS*i roots 14 dpi with rhizobia (Mean ±SEM). The two groups were compared using an unpaired t-test showed significant reduction ($P<0.001$) in number of nodules in *CHS*i roots compared to Control.

3.3.2 Flavonoid silenced roots fail to inhibit auxin transport in response to rhizobia inoculation

During a successful root-rhizobia interaction the perception of Nod factors in the roots leads to an inhibition of polar auxin transport, PAT (Wasson et al., 2006, Mathesius et al., 1998b). This is thought to lead to the initial cortical cell divisions required to form a nodule. The inhibition of auxin transport is therefore, a critical aspect of formation of the symbiotic nodule. Some flavonols such as a kaempferol

glycoside have been shown to affect the PAT through changes in the cycling of PIN proteins in *Arabidopsis* (Yin et al., 2013b).

Auxin responses, indirectly indicating auxin accumulation during rhizobia inoculation of Control and *CHS*i roots were demonstrated using an auxin responsive promoter GH3 (van Noorden et al., 2007, Hagen et al., 1991) fused to β-glucuronidase (GUS) reporter system (Figure 3.5). Here, the staining of the GUS reporter shows that after 24 hpi (B), auxin accumulates at the site of inoculation while lack of staining below the inoculation site in control roots (A and B) indicates inhibition of acropetal auxin transport as found in white clover previously (Mathesius et al., 1998b). GUS staining of the flavonoid silenced roots 6 and 24 hpi (C and D) did not show any accumulation of stain at a specific site in the root. Roots also stained more intensely possibly indicating higher auxin content.

To test whether changes in GH3:GUS expression can be explained by the changes in acropetal auxin transport, radiolabelled auxin transport was measured. The Figure 3.6 demonstrates a significant difference in radioactively labelled IAA (^{3}H-IAA) concentration above and below the inoculation site. The flavonoid silenced roots generally were able to transport much more ^{3}H-IAA than control roots and failed to show any inhibition above and below the site of inoculation. This was similar to the changes in GH3:GUS expression as shown in Figure 3.5 and also concurred with the previously published results (Wasson et al., 2006).

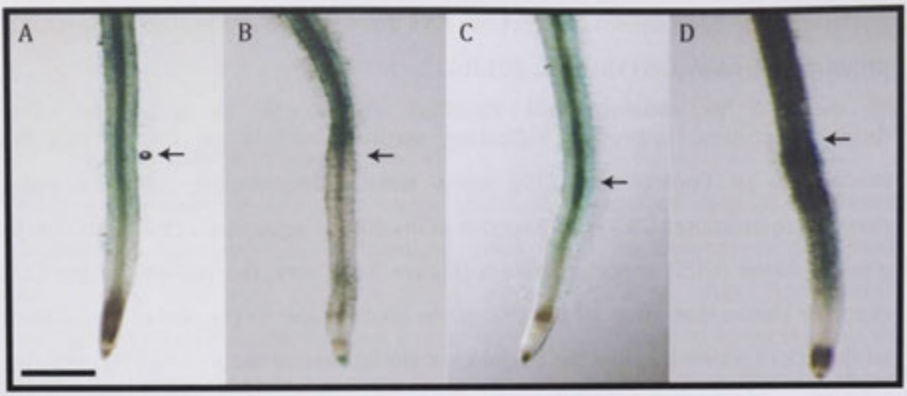

Figure 3.5– Expression of the auxin responsive promoter GH3 fused to β- glucuronidase (GUS) reporter system in Control (A, B) and *CHS*i (C,D) transformed hairy roots at 6 hpi (A, C) and 24 hpi (B, D). The sites of inoculations are indicated with arrows. The GH3 expression indicates a localised accumulation of auxin above the inoculation site compared to below in control roots 24 hpi (B). No such change was observed for flavonoid-deficient roots at a similar time-point (D). More intense staining of flavonoid-deficient roots (D) possibly indicated higher auxin content in these roots. Approximately 10 roots were stained per sample group. Scale bar represents 3 mm length.

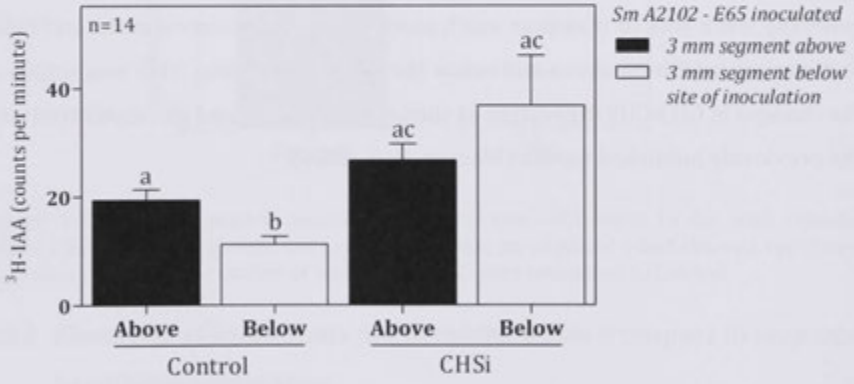

Figure 3.6 – Auxin transport measurements in Control and flavonoid silenced (*CHS*i) roots 24 hpi with rhizobia (E65). The sections above and below represent 3 mm zones above and below the point of inoculation. Significantly different CPMs are depicted by different alphabets (ANOVA, $P<0.05$).

3.3.3 *Silencing of flavonoids alters the accumulation of auxin in roots inoculated with rhizobia*

To test whether the changes in auxin response and auxin transport resulted in changes in the auxin content at the inoculation site, the absolute quantities of the IAA and its conjugates were measured using LC-MS/MS shown in Figure 3.7 and Table 3.4 as ng/g fresh weight of the root sample. The roots were either transformed with empty vector control (pHellsGate8) or vector carrying *CHS* silencing complex (pHellsGate8-*CHS*i). Roots were inoculated with BMM culture medium (Mock) or *Sinorhizobium meliloti* A2102 carrying the Nod factor overexpression vector (E65) and a 5 mm long root segment around the site of inoculation was harvested 24 hours post inoculation. At least 50-80 root samples for each were collected in five separate repeats collecting at least 50 mg of fresh weight for each sample.

IAA and IA-Ala was identified positively in the root samples by comparing with the retention times and fragmentation patterns of pure standards. IA-Ileu and IA-Val standards eluted at a different retention times when compared with the root samples. The fragmentation intensity patterns for the unknown compound in the root sample did not match the fragmentation pattern intensities of the standard compounds; however, the major peaks of IAA were common in all. This discrepancy could be explained by the presence of an isomer of the same analyte in the hairy root samples. Therefore, these IAA conjugates in the root samples are referred to as IA-Ileu-like and IA-Val-like compounds. The response factors of the standards were used to calculate the concentrations of its isomers.

In addition to the above, other standards were also eluted through the column. These were IBA, PAA, 4Cl-IAA, IA-Asp, IA-Phe, IA-Trp, and IA-Leu. The compounds extracted from the hairy roots of *M. truncatula* and eluted through the column did not match with the retention times and fragmentation patterns of any of these analytes.

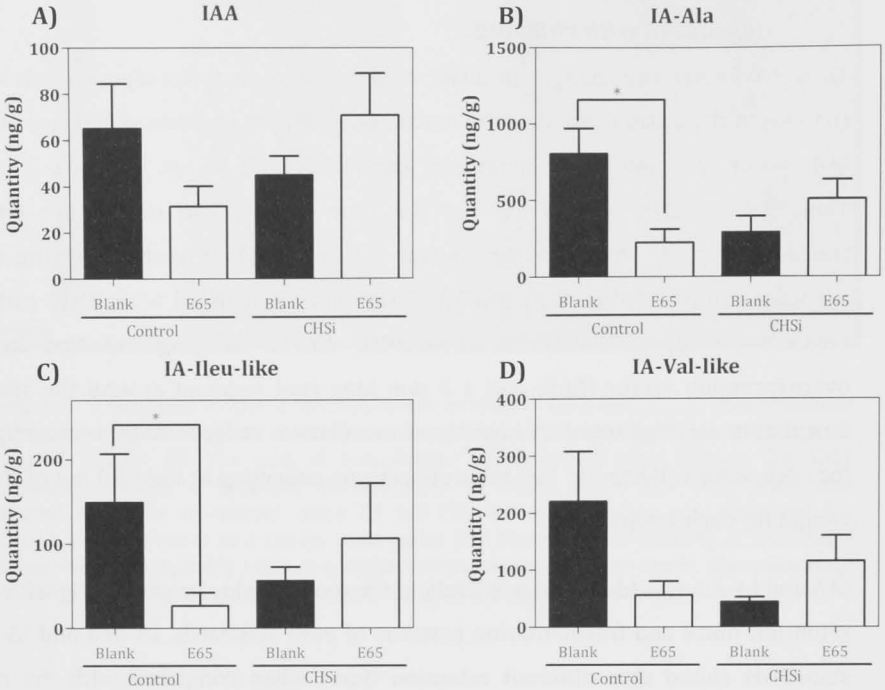

Figure 3.7 – The concentrations of IAA and its conjugates as detected in Control and *CHS*i roots 24 hpi with E65 rhizobia. Mean ±SEM of Auxin concentrations in 5 biological replicates with 50-80 root segments each are shown. Significant differences were calculated through Student t-test.

Table 3.4 – The mean concentrations of the IAA and its conjugates that were detected in Control and *CHS*i roots 24 hpi.

Sample	Inoculation	Concentration (ng per g fresh weight)			
		IAA	IA-Ala	IA-Ileu -like	IA-Val-like
Control	Mock	65.18 ±19.27	803.96 ±166.76	149.16 ±57.61	220.64 ±87.54
	E65	31.58 ±8.66	221.72 ±87.05	26.50 ±15.58	56.16 ±24.30
***CHS*i**	Mock	44.86 ± 8.34	286.28 ±108.00	56.24 ±16.26	43.69 ±8.95
	E65	70.89 ±18.06	506.75 ±125.07	40.59 ±10.09	115.53 ±44.78

Mean concentration with SEM from 5 biological repeats of 50-80 roots each.

The quantities of the IAA and conjugates found in *M. truncatula* hairy roots were observed to be higher compared to whole seedlings as investigated by Jason Ng (unpublished results) following the same method of isolation and quantifications. In *M. truncatula* A17 seedling roots, the IAA concentration was approximately 10 ng/g fresh weight while IA-Ala was found at 25 ng/g fresh weight. The isomers of IA-Ileu and IA-Val were only observed in the hairy roots and not in the seedling roots.

There was a significant impact of inoculation in control roots where the presence of rhizobia reduced the concentration of IA-Ala and IA-Ileu-like compounds in the zone of inoculation. This trend was maintained for IA-Val-like compounds, although not significantly. It was also expected that the reduction in the IAA conjugates would increase the concentration of free IAA as a result of conversion to active forms. However, this was not observed. The concentration of free IAA was halved after inoculation of the control roots; although this was not statistically significant. In addition, the concentrations of IAA conjugates also reduced upon rhizobia inoculation.

In *CHS*ī roots, the opposite trend to Control roots was observed where the concentration of both free IAA and conjugates consistently increased in response to rhizobia inoculation. However, these changes were not statistically significant.

3.3.4 Silencing of flavonoids does not alter the PIN or LAX gene expression in M. truncatula

It has been suggested that flavonoids may affect the cycling of the auxin transporter proteins PIN (Geldner et al., 2001) and possibly LAX (Peer et al., 2011). Studies showing effects of flavonoids in this expression has been shown in *Arabidopsis* (Peer et al., 2004). However, a similar expression study has not been done in legumes. Legumes almost exclusively contain the isoflavonoids that may be important for the expression of genes encoding auxin transporter proteins.

Therefore, to test whether changes in auxin transport were due to changes in *PIN* and *LAX* gene expression the relative expressions of the *PIN* and *LAX* genes in the inoculation zone were investigated in control and flavonoid silenced roots at 6 and

24 hpi with Nod factor overexpressing rhizobia (E65). The results are presented in Figures 3.8 – 3.9 and Tables 3.5 – 3.6. The *LAX5* gene could not be amplified and has been omitted. The results indicate that flavonoids did not affect the expression of any of the tested *PIN* or *LAX* genes except *PIN9*. However, in my experiments, the amplification of *PIN9* gene was inconsistent and only a single biological replicate represents the results.

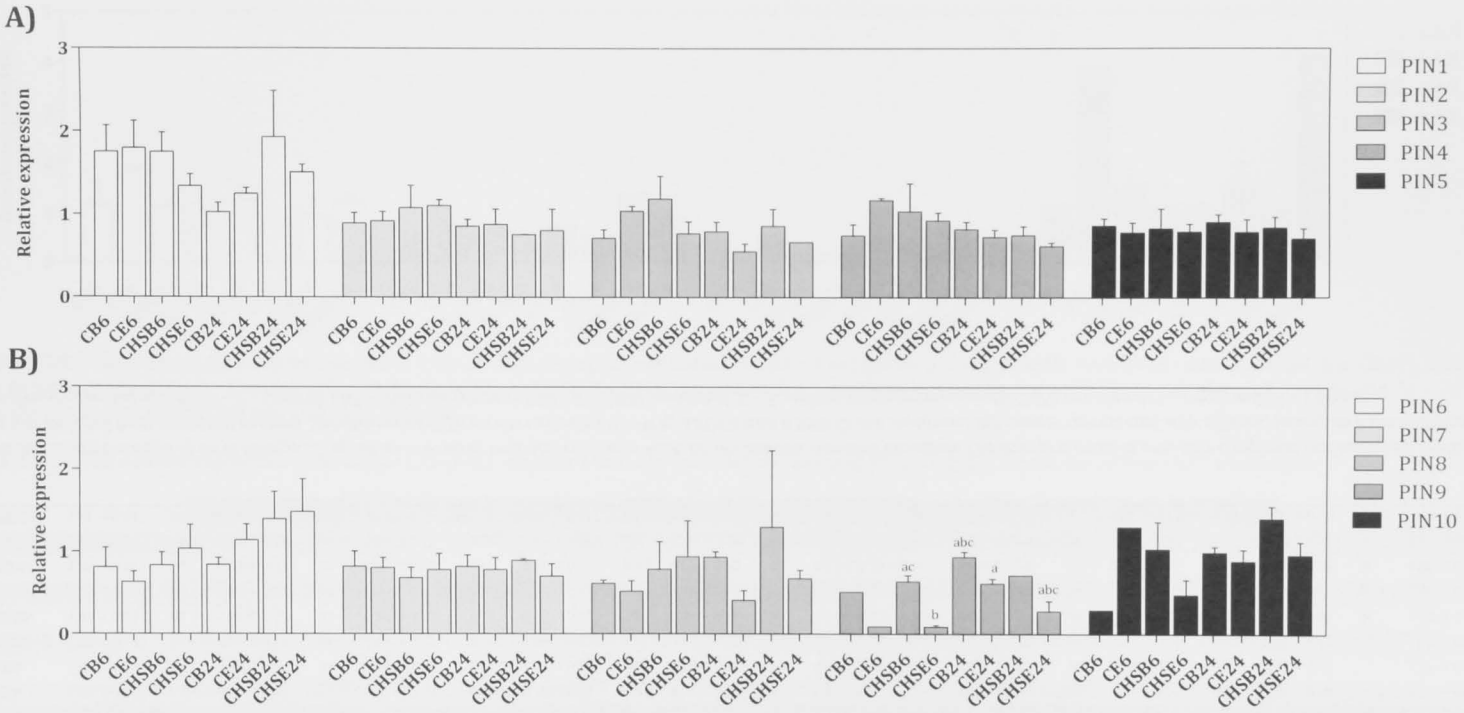

Figure 3.8 – The relative gene expressions (Mean ± SD of three biological replicates) of *PIN 1-10* compared to Control BMM inoculated roots at 24 hpi (i.e. CB24). Samples are denoted as follows – C – Control; CHS – *chalcone synthase* RNAi; B – BMM inoculated; E – *S. meliloti* overexpressing nodD (E65) inoculated; 6 – 6 hpi; and 24 – 24 hpi. Results of one-way ANOVA are also shown in Table 3.4.

Table 3.5 – The relative expression of *Medicago PIN* genes measured through quantitative real-time PCR using ΔΔCt method corrected for efficiencies

	PIN1		*PIN2*		*PIN3*		*PIN4*		*PIN5*		*PIN6*		*PIN7*		*PIN8*		*PIN9*		*PIN10*	
CB6	1.75 ± 0.45	ns	0.89 ± 0.22	ns	0.72 ± 0.18	ns	0.75 ± 0.23	ns	0.87 ± 0.15	ns	0.81 ± 0.42	ns	0.82 ± 0.32	ns	0.61 ± 0.06	ns	*0.51 ± 0.00*	-	*0.29 ± 0.00*	-
CE6	1.80 ± 0.47	ns	0.92 ± 0.19	ns	1.04 ± 0.08	ns	1.17 ± 0.04	ns	0.78 ± 0.21	ns	0.63 ± 0.22	ns	0.81 ± 0.22	ns	0.52 ± 0.23	ns	*0.09 ± 0.00*	-	*1.31 ± 0.00*	-
CHSB6	1.75 ± 0.33	ns	1.08 ± 0.47	ns	1.19 ± 0.39	ns	1.04 ± 0.59	ns	0.83 ± 0.41	ns	0.83 ± 0.28	ns	0.68 ± 0.22	ns	0.79 ± 0.48	ns	0.64 ± 0.11	ac	1.03 ± 0.58	ns
CHSE6	1.34 ± 0.25	ns	1.11 ± 0.13	ns	0.77 ± 0.25	ns	0.93 ± 0.17	ns	0.80 ± 0.16	ns	1.04 ± 0.51	ns	0.78 ± 0.34	ns	0.94 ± 0.62	ns	0.09 ± 0.03	b	0.48 ± 0.32	ns
CB24	1.03 ± 0.20	ns	0.86 ± 0.14	ns	0.80 ± 0.20	ns	0.82 ± 0.15	ns	0.91 ± 0.13	ns	0.84 ± 0.15	ns	0.82 ± 0.24	ns	0.94 ± 0.09	ns	0.94 ± 0.09	abc	1.00 ± 0.12	ns
CE24	1.25 ± 0.12	ns	0.88 ± 0.32	ns	0.55 ± 0.16	ns	0.73 ± 0.15	ns	0.79 ± 0.26	ns	1.14 ± 0.33	ns	0.78 ± 0.25	ns	0.41 ± 0.16	ns	0.61 ± 0.08	a	0.89 ± 0.24	ns
CHSB24	1.93 ± 0.97	ns	0.76 ± 0.01	ns	0.86 ± 0.29	ns	0.75 ± 0.15	ns	0.84 ± 0.18	ns	1.40 ± 0.46	ns	0.89 ± 0.03	ns	1.31 ± 1.32	ns	*0.71 ± 0.00*	-	1.41 ± 0.21	ns
CHSE24	1.51 ± 0.14	ns	0.81 ± 0.45	ns	*0.67 ± 0.00*	-	0.62 ± 0.07	ns	0.71 ± 0.21	ns	1.49 ± 0.69	ns	0.70 ± 0.26	ns	0.67 ± 0.15	ns	0.28 ± 0.18	abc	0.96 ± 0.23	ns

Data shown are the mean of three biological replicates with three technical replicates each. Errors indicate standard deviation. The data presented in grey only comprised one biological replicate and was excluded from statistical analysis. Significance of difference tested using One-Way ANOVA with a 95% CI and significant differences represented with different letters, ns = not significant. Samples are denoted as follows – C – Control; CHS – chalcone synthase RNAi; B – BMM inoculated; E – S. meliloti overexpressing nodD (E65) inoculated; 6 – 6 hpi; and 24 – 24 hpi.

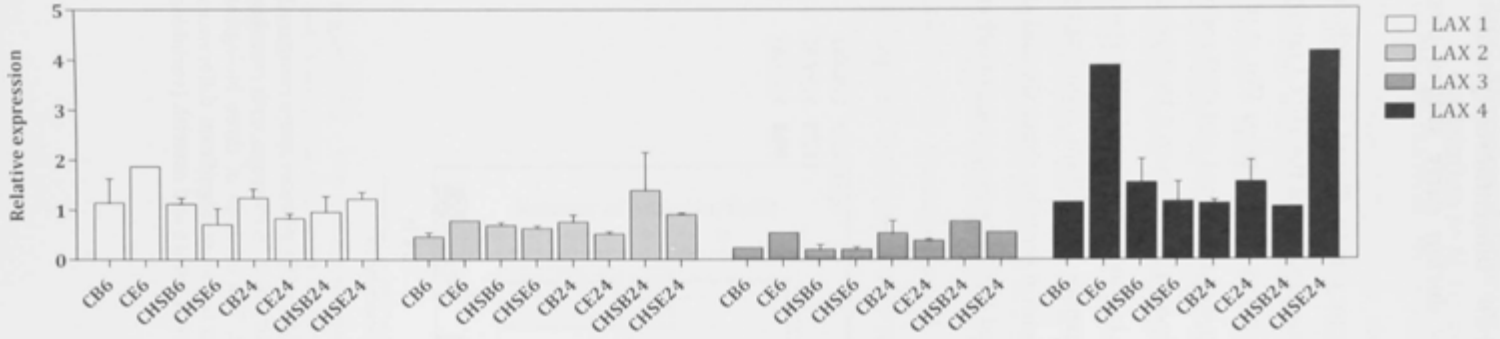

Figure 3.9 – The relative gene expression (Mean ± SD of three biological replicates) of LAX1-4 compared to Control BMM inoculated roots at 24 hpi. (i.e. CB24). Samples are denoted as follows – C – Control; CHS – chalcone synthase RNAi; B – BMM inoculated; E – S. meliloti overexpressing nodD (E65) inoculated; 6 – 6 hpi; and 24 – 24 hpi. Results of one-way ANOVA are also shown in Table 3.5.

Table 3.6 – The relative expression of *Medicago LAX* genes measured through quantitative real-time PCR using ΔΔCt method corrected for efficiencies

	LAX 1		***LAX 2***		***LAX 3***		***LAX 4***	
CB6	1.14 ± 0.69	ns	0.46 ± 0.11	ns	*0.24 ± 0.00*	-	*1.15 ±0.00*	-
CE6	*1.87 ± 0.00*	-	*0.78 ± 0.00*	-	*0.54 ± 0.00*	-	*3.88 ± 0.00*	-
CHSB6	1.12 ± 0.20	ns	0.69 ± 0.10	ns	0.20 ± 0.14	ns	1.54 ± 0.66	ns
CHSE6	0.71 ± 0.55	ns	0.63 ± 0.09	ns	0.20 ± 0.09	ns	1.16 ± 0.68	ns
CB24	1.24 ± 0.32	ns	0.76 ± 0.24	ns	0.53 ± 0.43	ns	1.12 ± 0.11	ns
CE24	0.83 ± 0.17	ns	0.52 ± 0.07	ns	0.38 ± 0.06	ns	1.55 ± 0.74	ns
CHSB24	0.96 ± 0.44	ns	1.39 ± 1.32	ns	*0.77 ± 0.00*	-	*1.05 ± 0.00*	-
CHSE24	1.22 ± 0.23	ns	0.91 ± 0.54	ns	*0.55 ±0.00*	-	*4.15 ± 0.00*	-

Data shown are the mean of three biological replicates with three technical replicates each. Errors indicate standard deviation. The data presented in grey only comprised one biological replicate and was excluded from statistical analysis. Significance of difference tested using One-Way ANOVA with a 95% CI and significant differences represented with different letters, ns = not significant. Samples are denoted as follows – C – Control; CHS – chalcone synthase RNAi; B – BMM inoculated; E – S. meliloti overexpressing nodD (E65) inoculated; 6 – 6 hpi; and 24 – 24 hpi.

3.3.5 *Expression of genes encoding auxin biosynthesis proteins increases in flavonoid silenced roots during early stages post rhizobia inoculations*

To test whether changes in auxin accumulation were due to altered synthesis of auxin, three putative genes encoding auxin synthesis proteins of the *YUCCA* family were identified through homology with the *Arabidopsis YUCCA* genes (Ng et al., unpublished). The expression of these genes was tested in Control and *CHS*i roots at 6 and 24 hpi with Nod factor overexpressing rhizobia (E65). Figure 3.10 showed that the expression of *YUCCA1* slightly increased in mock-inoculated *CHS*i roots compared to mock-inoculated control roots. Rhizobia inoculation significantly induced *YUCCA1* expression in *CHS*i compared to control roots by about six-fold at 6 hpi. No changes were also observed in *YUCCA2* and *YUCCA3* expressions in either rhizobia-inoculated or mock-inoculated roots.

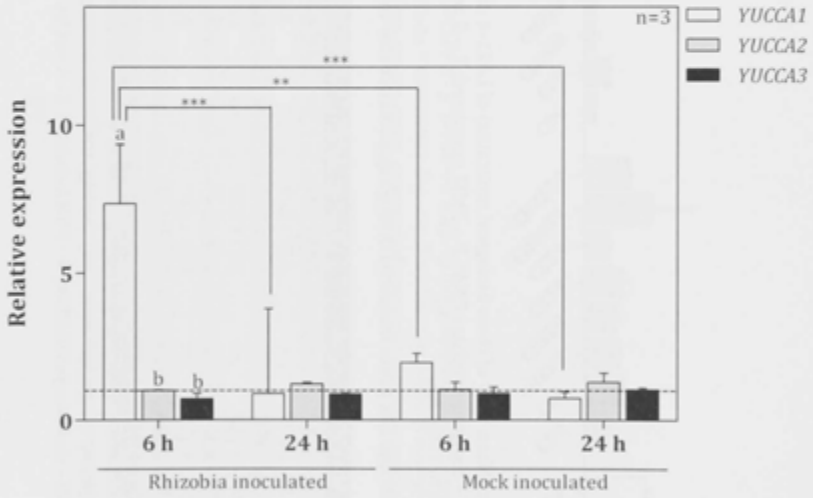

Figure 3.10 – The relative expression of *YUCCA1, 2* and *3* in *CHS* silenced roots compared to control roots (Expression level at 1) at 6 and 24 hours post inoculation with rhizobia and 6 and 24 hour post mock inoculation with BMM. The average of three biological replicates with each comprising of 50-60 root segments is shown. Significant differences measured through two-way ANOVA are shown by different letters and asterisk (variables gene and time post inoculation).

3.3.6 *Silencing of different branches of the flavonoid biosynthesis alters nodulation in M. truncatula*

To identify the most critical class of flavonoids required for nodulation, transgenic *M. truncatula* hairy roots that were silenced in genes encoding flavonoid biosynthesis enzymes were inoculated with rhizobia (E65). Figure 3.11 shows the average number of nodules that appear in differentially silenced roots for other flavonoid biosynthesis enzymes. Although these results did not indicate any statistically significant differences between the Control and any of the RNAi silenced lines, the number of nodules found on *FLS* silenced roots showed a negative trend. Therefore, the nodulation assay was repeated with a larger pool of samples, and the results are shown in Figure 3.12. This reconfirmed that the silencing of flavonols led to a significant reduction in nodule numbers ($P < 0.05$). This agreed with the findings of Zhang et al. (2009) who showed that *CHS* RNAi roots of *M. truncatula* could be rescued with the application of the flavonol kaempferol in the presence of Nod factor overexpressing *S. meliloti* E65.

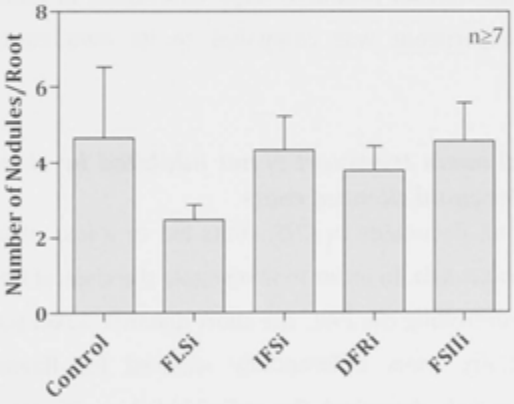

Figure 3.11 – The average number of nodules found in empty-vector Control hairy roots and hairy roots that were differentially silenced in genes encoding flavonoid synthesis enzymes 14 dpi with rhizobia. Mean ±SEM shown above. An ANOVA did not identify any significant changes.

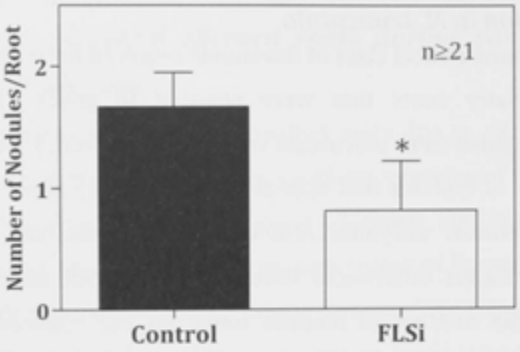

Figure 3.12 – The average number of nodules found in control and *FLS* silenced hairy roots 14 dpi with rhizobia. Mean ±SEM shown above. Silencing of *FLS* led to a significant ($P<0.05$) reduction in number of nodules per roots (unpaired t-test).

It should also be noted that large variations were observed in the nodulation efficiencies between experimental replicates. The hairy roots are likely more susceptible to the ethylene accumulation (Shen et al., 1988) in plate growth assay, therefore, two experiments produced large differences in number of nodules in controls. Each experiment was compared to its own control for statistical differences.

3.3.7 Acropetal auxin transport is not inhibited by rhizobia in flavonol and isoflavonoid silenced roots

The silencing of all flavonoids in *CHS*i roots led to a loss of inhibition of auxin transport in *M. truncatula*. In order to investigate the class of flavonoids that were responsible for controlling the PAT, the short distance auxin transport assay was repeated with hairy roots differentially silenced for flavonoid biosynthesis enzymes. As previously described, the radiolabeled auxin was detected in 3 mm zones above and below the inoculation site after 24 hours. The results are presented in the Figure 3.13 (A) and (B).

In Figure 3.13 (A) there is a significant difference in ^{3}H-IAA in the zones above and below the inoculation site in control, *DFR* silenced and *FSII* silenced roots. This difference was absent in *FLS* and *IFS* silenced roots suggesting that the mechanism that inhibits the auxin transport in these roots was defective.

The differences in the auxin transported in 3 mm segments above and below the site of inoculation with only BMM growth media served as a control (Figure 3.13 B). The results clearly indicate that in the absence of rhizobia, there is no significant difference in the accumulation of ^{3}H-IAA above or below the inoculation site, although auxin transported into the segment above the inoculation site was consistently higher that in the segment below.

Rescue of the auxin transport inhibition phenotype in *FLS*i and *IFS*i roots with the exogenous application of Isoliquiritigenin and Quercetin is shown in Figure 3.14. Isoliquiritigenin is a precursor to isoflavonoid metabolites whilst Quercetin was a flavonol detected in *M. truncatula* hairy roots (see Chapter 2). The auxin transport could be inhibited in *FLS*i roots by supplementing the growth media with Isoliquiritigenin which likely increases the overall root-isoflavonoid concentrations. Quercetin was also able to rescue the auxin transport inhibition phenotype in rhizobia inoculated roots however, this was not statistically significant. This result required further confirmation.

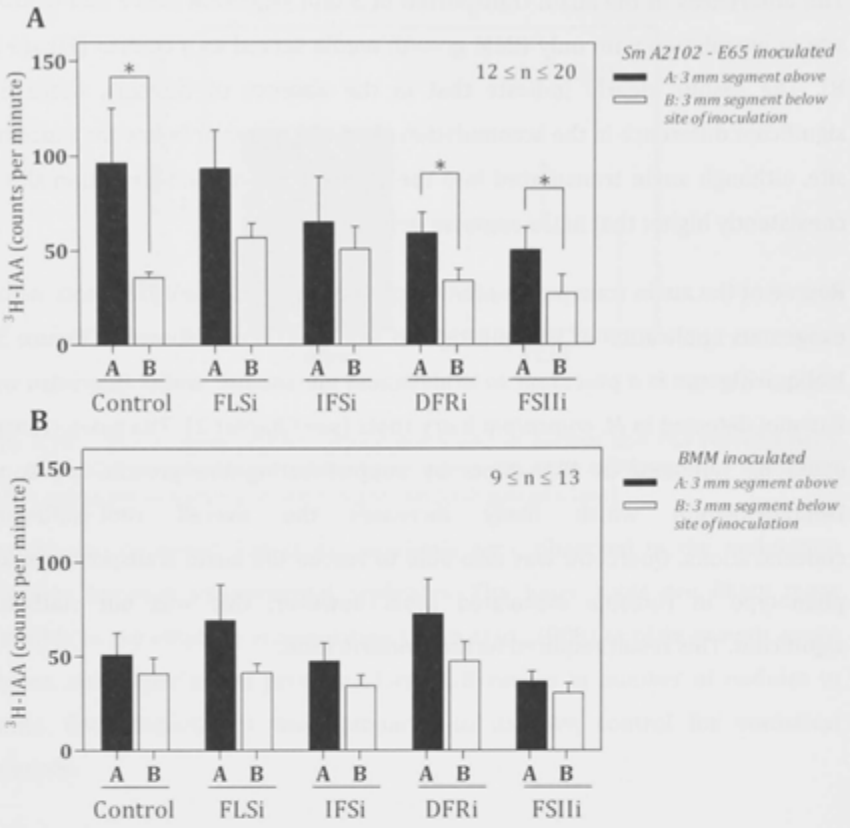

Figure 3.13 – Acropetal auxin transport measurements in 3 mm root segments above and below the inoculation site reflecting ^{3}H-IAA content (Mean ± SEM) in differentially silenced roots. The roots in A) were inoculated with Nod factor overexpressing rhizobia strain E65 and the roots in B) were mock inoculated with only the media (BMM) used to grow the rhizobia strain. There were no significant differences between the segments above and below the inoculation site in any of the BMM inoculated roots. Significant differences (P<0.05) between CPM above and below the inoculation site was determined using 1-way ANOVA and marked with asterisks.

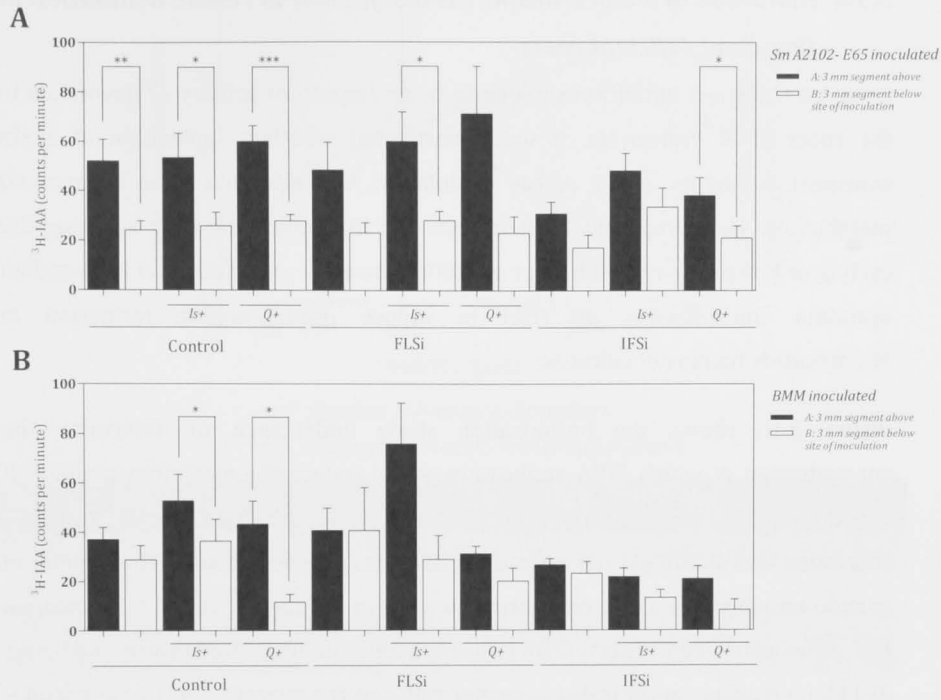

Figure 3.14 – Acropetal auxin transport measurements showing the rescue of auxin transport inhibiton phenotype in *FLS*i and *IFS*i roots with supplements of Isoliquiritigenin (Is+) or Quercetin (Q+) in the growth medium. Significant differences ($P<0.05$) between CPM above and below the inoculation site was determined using 1-way ANOVA and marked with asterisks.

In graph A where the roots were inoculated with rhizobia - the transport of auxin was inhibited in all control roots treated with or without flavonoid supplements. Only application of Isoliquiritigenin could induce a significant difference in 3 mm root segment above (A) and below (B) the inoculation site 24 hpi with *S. meliloti A2102 E65.* No significant change was observed with Quercetin supplements in *FLS*i roots. However, in *IFS*i roots Quercetin was able to rescue the auxin transport inhibition phenotype.

In graph B, the roots were inoculated with growth medium (BMM) without rhizobia – the transport of auxin was inhibited by Isoliquiritigenin and Quercetin in control roots where a significant difference in 3 mm root segment above (A) and below (B) the inoculation site 24 hpi was observed. No significant changes were observed in any other constructs.

3.3.8 *Inhibition of auxin transport is insufficient to rescue nodulation in flavonoid deficient roots*

As auxin transport inhibition showed to be an important activity of flavonoids in the roots of *M. truncatula*, it was investigated whether application of auxin transport inhibitors could rescue nodulation in roots that lacked flavonoid metabolites. The compound TIBA inhibits the IAA anion efflux by affecting the cycling of PIN proteins (Geldner et al., 2001). However, no study had reported an optimum concentration of TIBA to induce pseudo-nodule formation in *M. truncatula* hairy root cultures.

Figure 3.15 shows the optimization study undertaken to determine the concentration at which TIBA application would induce the maximum number of pseudo-nodules in a high proportion of *M. truncatula* hairy root samples tested. It was found that at 100 µM concentrations the roots showed a peak in the number of pseudo-nodules. The same concentration used in seedling roots of *M. truncatula* has previously been reported to induce pseudo-nodules (Rightmyer and Long, 2011). Increasing concentrations further reduced the average number of pseudo-nodules per roots even through there was an increase in the percentage of roots that formed pseudo-nodules. Therefore, TIBA at 100 µM concentration was determined to be ideal for inducing pseudo-nodules in the following experiments.

In both Control and *CHS*i roots, TIBA was applied prior to inoculation with Nod factor overexpressing rhizobia (TIBA + E65). The experimental treatments in Control and *CHS*i roots included rhizobia only treatment (E65), TIBA only treatment (TIBA) and rescuing nodulation with the application of flavonoids (Isoliquiritigenin and Naringenin at 100 nM each) along with rhizobia (Fl+E65). Naringenin and Isoliquiritigenin are precursors of the 5-hydroxyflavonoids (such as flavonols, flavones, anthocyanins etc.) and 5-deoxy(iso)flavonoids (such as isoflavonoids), respectively. Naringenin and Isoliquiritigenin are also products of enzymatic reaction of CHS enzyme and are able to fully complement the lack of flavonoids-metabolites in *CHS* silenced roots. Naringenin was previously shown to rescue nodulation in *CHS*i roots (Wasson et al., 2006).

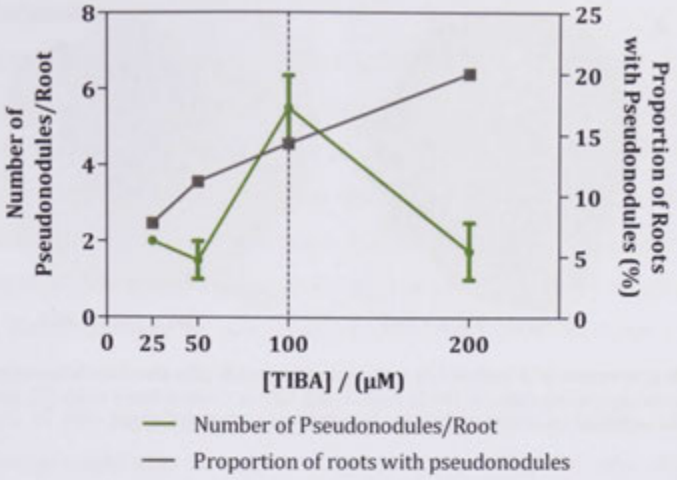

	TIBA concentrations			
	25 µM	50 µM	100 µM	200 µM
Average pseudonodule numbers	0.154 ± 0.55	0.167 ± 0.51	0.786 ± 2.04	0.350 ± 0.93
Percentage of roots with pseudonodules	7.69	11.11	14.29	20.00
Number of pseudonodule/nodulating root	2 ±0.0	1.5 ± 0.7	5.5 ± 1.7	1.75 ±1.5

Figure 3.15 – Optimization of TIBA-induced pseudonodule formation in *M. truncatula* hairy root cultures 28 dpi. The graph and table show the changes in the average number of pseudonodules formed per root and the proportion of roots forming pseudonodules as a function of varying concentrations of TIBA applied to the roots.

Figure 3.17 shows the proportion of roots that formed nodules (including pseudo-nodules) in Control and *CHS*i roots. In Control roots, the application of rhizobia (E65), rhizobia with TIBA (TIBA + E65) (Figure 3.16 A) and rhizobia with flavonoids (Isoliquiritigenin and Naringenin) (Fl + E65) produced normal nodulation phenotype. TIBA alone in these roots induced uninfected pseudo-nodules only.

In *CHS*i roots, the application of E65 did not produce any nodules. The application of TIBA alone and TIBA with E65 (Figure 3.16 B) produced only uninfected pseudo-nodules. Only the exogenous application of flavonoids with E65 could rescue the formation of infected nodules. This suggests that flavonoids may have a role in nodule infection beyond their role as auxin transport inhibitor during nodule development.

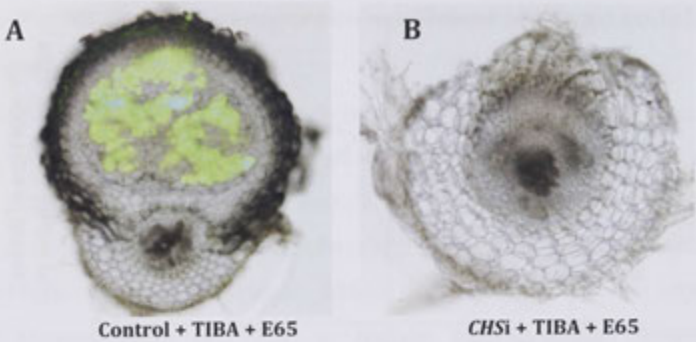

Figure 3.16 – Structure of a nodule (A) and a pseudo-nodule (B). The formation of nodules with Nod factor overexpressing rhizobia (E65) tagged with GFP in Control hairy roots (A) and *CHS*i roots (B) that were supplemented with auxin transport inhibitor TIBA at 100 μM.

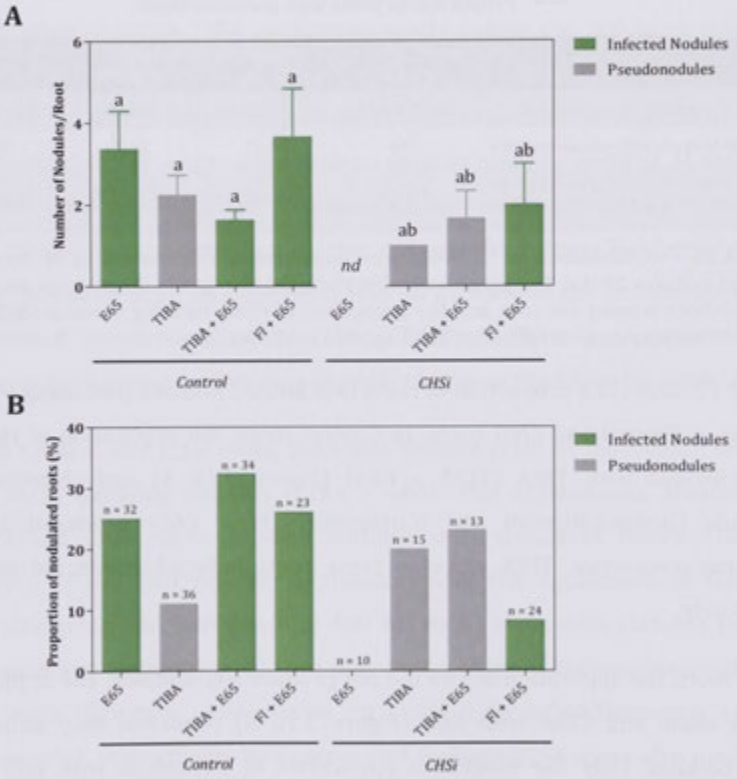

Figure 3.17 – The average number of nodules or pseudo-nodules per nodulating root is shown as mean ± SEM in A) and percentage of roots that nodulated in Control and *CHS*i roots shown in B). TIBA and flavonoid (Isoliquiritigenin and Naringenin) treatments were applied prior to E65 inoculation and nodule number were counted 28 dpi with rhizobia (E65) or BMM. Statistically significant differences measured through ANOVA are represented with different letters, *nd* = not detected.

3.4 Discussion

Silencing of flavonoids led to a decrease in number of nodules that formed on roots of *M. truncatula*. The regulation and coordination of nodule organogenesis is dependent on the chemical signals that are transported from one part of the plant to another. Auxin is one such chemical messenger or hormone that is primarily synthesized in the shoot apical meristem and young leaves, and transported to the roots to induce growth and development of root organs such as nodules (Peer et al., 2011). However, roots are not completely dependent on shoot derived auxins. Auxin has been also shown to be synthesized in root meristematic regions as well as upwards of the root tip to a smaller extent (Ljung et al., 2005). These root-derived auxins could also be used in conjunction or independently of the shoot derived auxin for root development (Bhalerao et al., 2002). However, computational studies have indicated that an auxin maximum is achieved at the site of nodule initiation through inhibition of auxin export (Deinum et al., 2012). This chapter investigated which mechanisms might be responsible for alteration of auxin transport and accumulation during nodule initiation and studied their dependence on root flavonoids.

3.4.1 Flavonoids regulate polar auxin transport in response to rhizobia

The transport of auxin occurs from the shoot to the root and the changes in auxin concentration likely induce cell divisions at the nodule primordia. This trafficking of auxin occurs through the active cell-to-cell movement known as polar auxin transport (PAT). The PAT is mediated by a number of transporters which include the auxin influx and efflux transporters. Although the influx of auxin can occur passively through diffusion, it is thought that diffusion is insufficient to maintain the cellular demands (Peer et al., 2011). A family of symporters (AUX1/LAX) are located on the cell membrane and they cotransport two protons along with an IAA anion. These influx carrier proteins are often polarly distributed on opposite sides of the cell to the PIN family of auxin efflux proteins (Rosquete et al., 2012). The PIN family of proteins mediates the tissue-specific flow of auxin out of the cell alongside a subset of ABCB transporters (Peer et al., 2011). The source of energy

for their operation is unknown as none of the PIN proteins have been shown to contain ATP binding domains (Zažímalová et al., 2010).

It has been found that during root nodule initiation, the exudation of flavones leads to Nod factor synthesis in the rhizobia (Redmond et al., 1986, Peters et al., 1986). The perception of Nod factors by the roots and development of the infection thread is believed to induce the synthesis of flavonols such as kaempferol and quercetin in the roots (Zhang et al., 2009). A bis-glycoside of the flavonol kaempferol inhibits polar auxin transport in *Arabidopsis* shoots (Yin et al., 2013b). Similar function may be important for cell divisions and initiation of nodule primordia in *Medicago* as nodulation could be restored in flavonoid-silenced roots treated with kaempferol (Zhang et al., 2009). This evidence has been derived from the exogenous application of specific flavonoid compounds and observations in its ability to inhibit auxin transport (Jacobs and Rubery, 1988). In my results, I made similar observations where *CHS*i roots failed to inhibit auxin transport (Figure 3.6) and did not show an auxin accumulation at the site of rhizobia inoculation (Figure 3.5) measured indirectly through the auxin responsive GH3 expression.

3.4.2 Local abundance of IAA and conjugates reduces at 24 hpi with rhizobia in M. truncatula hairy roots and this is regulated by flavonoids

Auxin exists in multiple forms in plants and their abundance seems to vary by the species (Korasick et al., 2013). The active forms of auxin include IAA, 4-Cl-IAA and PAA (Korasick et al., 2013). In *M. truncatula* hairy roots, only IAA was detected amongst the active auxins. Interestingly, the IAA concentration at the inoculation site was reduced as a result of inoculation as opposed to increasing (Figure 3.7). It would have been expected that inhibition of auxin transport in vector control roots through flavonoids would increase the concentration of IAA as it is normally found in seedling roots (Ng et al, unpublished). It should also be noted that the 5 mm segments where the auxin concentrations was quantified spanned above and below the site of rhizobia-inoculation, whereas auxin transport was measured in the 3 mm segment above and 3 mm segment below the site of rhizobia-inoculation.

Auxin sensitivity of hairy roots is also significantly different compared to untransformed roots (Shen et al., 1988). Separate experiments that measured IAA concentration in seedling roots of *M. truncatula* by Ng et al. (unpublished) showed its concentration to be much lower than hairy roots. In seedling roots, the inhibition of auxin transport caused by rhizobia inoculation also led to an increase in local auxin content.

Auxin homeostasis is maintained in roots through various metabolic processes (Rosquete et al., 2012). It is therefore, possible that the IAA content in hairy roots of *M. truncatula* was reduced when inoculated with rhizobia to create a biologically active balance of auxin to induce cell divisions.

The studies with radioactive tracer auxin showed that flavonoids, specifically flavonols and isoflavonoids inhibited auxin transport in hairy roots after rhizobia inoculation. Therefore, it was not surprising that loss of flavonoids resulted in no change in IAA concentration at the inoculation site when compared to uninoculated flavonoid deficient hairy roots (Figure 3.7).

Interestingly, the hairy roots of *M. truncatula* showed very high concentrations of IAA amino acid conjugates. It has been speculated that auxin conjugates are present to act as a storage form to prevent toxic effects of excessive IAA or serve as an intermediary molecule before its breakdown by catabolism (Ludwig-Müller, 2011). The reduction in local IAA as well as IAA conjugate concentrations as a result of rhizobia inoculation suggests that excessive IAA may have been converted to other metabolites or completely broken down. Further investigations are required to determine what these breakdown products might be or if they serve any other purposes within the roots.

3.4.3 Root flavonoids do not alter the expression of PIN or LAX genes in response to rhizobia

The cell-to-cell polar auxin transport is mediated through auxin influx and efflux proteins. The LAX family and the PIN family of proteins are prominent auxin influx and efflux carriers. While influx of IAA into the cells can occur passively, the presence of LAX transporters likely accelerates that process. Conversely, the

deprotonated IAA requires a transporter to move out of the cell and thus require proteins such as the PIN transporters (Zažímalová et al., 2010). Although several studies have shown changes in localization of LAX and PIN in the direction of auxin flow (Santelia et al., 2008, Peer et al., 2011), I tested if the expression of these genes were affected by cellular flavonoid content in the legume *M. truncatula*. With the aid of quantitative real-time PCR, I showed that the expression of 10 *PIN* genes and 4 *LAX* genes were not affected by root-flavonoids or rhizobia inoculation at 6 and 24 hpi. It would suggest that the intracellular cycling or activity changes of these proteins forms the major mechanism controlling PAT and the transcription of the gene encoding the transporter proteins does not change due to flavonoids or rhizobia inoculation. This is in contrast to *PIN* gene expression in a *CHS*-deficient mutant of *Arabidopsis* (Peer et al., 2004). Further studies into localization of these transporter proteins *in situ* would be required to confirm this hypothesis.

3.4.4 Flavonoids regulate YUCCA1 synthesis during early stages of rhizobial infection

The principle naturally occurring auxin is indole-3-acetic acid (IAA) (Bandurski and Schulze, 1977). It is derived from the precursor tryptophan and indole-3-glycerol phosphate molecules in the tryptophan dependent and independent pathways. In *Arabidopsis*, it has been proposed that the indole-3-pyruvic acid (IPA) pathway is the main auxin biosynthesis pathway (Mashiguchi et al., 2011). This pathway is catalyzed by the family of *YUCCA* genes which encode flavin monooxygenase-like enzymes that convert IPA to IAA in the IPA pathway and oxidize tryptamine (TAM) to N-hydroxytryptamine in the TAM pathway (Mano and Nemoto, 2012) (Figure 3.2).

The gene expression of the *YUCCA* family was determined to test whether it was influenced by the root flavonoid contents. There was no significant change in *YUCCA* gene expression in the Control roots in response to rhizobia. However, in rhizobia-inoculated *CHS*i roots *YUCCA1* was expressed at significantly higher levels compared to mock inoculated *CHS*i roots at 6 hpi. This suggested that the lack of flavonoids influenced the induction of auxin synthesis genes as a response to rhizobia. The probe Mtr.50586.1.S1_at corresponded to the *YUCCA1* on the

Medicago Gene Atlas (www.MtGEA.noble.org). Expression profiles of a number of gene expression experiments showed that the *YUCCA1* is highly expressed in the aerial tissues such as vegetative buds, flowers and seeds (Figure 3.18) which are suggested to sites of high auxin synthesis (Zhao, 2010). It is interesting that lack of flavonoids in these tissues is inducing *YUCCA1* due to rhizobial inoculations.

In *Arabidopsis*, studies indicate that *YUCCA1* overexpression is not necessarily correlated with increase in free IAA or conjugated IAA contents (Stepanova et al., 2011). It would suggest that the differences in auxin synthesis is concealed by the transport and catabolism of IAA and conjugates. Indeed, as it is discussed in this chapter that the local auxin content of roots inoculated with rhizobia did not show an increase in IAA in *M. truncatula* hairy roots and it is likely tightly controlled through other processes. However, in flavonoid-silenced *M. truncatula* hairy roots, an opposite trend of increasing IAA content, although not statistically significant, was observed when roots were inoculated with rhizobia. This would suggest that flavonoid controlled auxin homeostasis was affected in regulating IAA synthesis and breakdown.

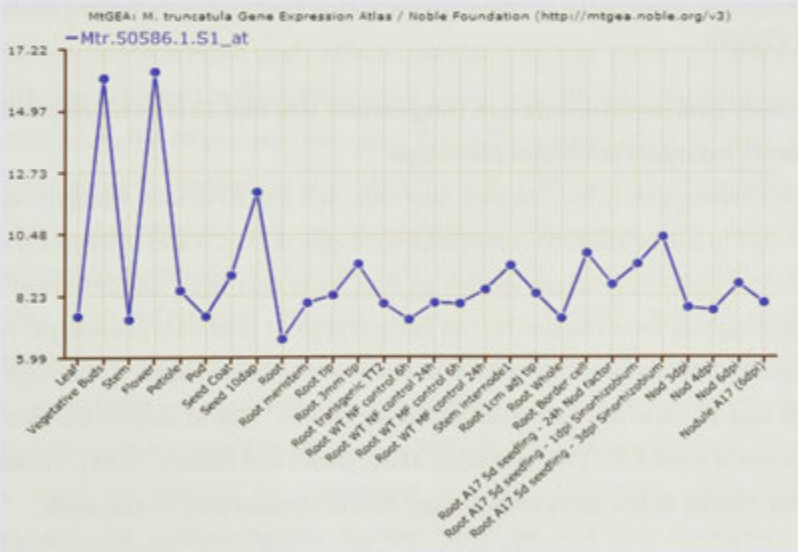

Figure 3.18 – Medicago Gene Expression Atlas details the expression levels of YUCCA1 in different anatomical parts and treatments. The expression is primarily induced in the vegetative buds, flowers and seeds. Inoculation with rhizobia also show an increase in expression but at lower levels.

3.4.5 *Isoflavonoid regulated auxin-transport inhibition is not essential for indeterminate nodule formation in M. truncatula roots*

- *Auxin transport inhibition induced by flavonols is needed for nodulation*

It has been reported that isoflavonoids are accumulated during the early stages of determinate nodule formation in soybean (Subramanian et al., 2007). It was speculated that isoflavonoids accumulated at the site of rhizobia infection and it could modulate polar auxin transport in soybean roots. However, accumulation of these metabolites was also shown to be non-essential as the roots nodulated normally even in the absence of isoflavonoids (Subramanian et al., 2007).

The roots of *M. truncatula* form indeterminate nodules with rhizobia. Isoflavonoids were also found to modulate auxin transport during the establishment of these nodules but silencing of these metabolites did not have an effect on the number of nodules that formed on the roots. Conversely, the loss of flavonols significantly reduced the number of nodules per root (Figure 3.12). This suggested that flavonols are essential for auxin transport control and nodule development and this result agrees with the rescue of *CHS*i roots with flavonol kaempferol by Zhang et al. (2009).

Flavonols and Isoflavonoids can complement IFSi and FLSi roots respectively for auxin transport inhibition phenotype

It was investigated if the flavonol quercetin and the flavanone isoliquiritigenin were able to rescue auxin transport inhibition effects in *FLS*i and *IFS*i roots (Figure 3.14). The radioactive tracer studies on *FLS*i roots that were supplemented with isoliquiritigenin were rescued for the auxin transport inhibition phenotype. Auxin transport inhibition was also achieved when quercetin was applied, although this result was not statistically significant in my results. This is despite the fact that quercetin is a good ATI (Murphy et al., 2000, Jacobs and Rubery, 1988). Therefore, further repeats of this assay with a larger pool of samples may be required.

Isoliquiritigenin is a metabolite upstream of the isoflavonoid biosynthesis pathway whose products were shown to induce auxin transport inhibition (Figure 2.2).

Isoliquiritigenin could also be channeled into isoflavonoid metabolites but not flavonols in the *FLS* silenced roots as the *flavonol synthase* transcription was reduced. Conversely, the flavonol quercetin cannot be rechanneled into any other metabolite in the plant as the metabolite is not a precursor for other flavonoid synthesis enzymes. This would suggest that flavonol metabolites up-stream of quercetin may be responsible for the stronger auxin inhibition phenotype important for nodulation. One candidate could be kaempferol or its glycoside as previously suggested to be an important auxin transport inhibitor (Zhang et al., 2009). Therefore, in future this rescue experiment could be repeated with the application of other flavonols such as kaempferol and its glucosides to narrow the compound responsible for ATI in *M. truncatula* during nodule formation.

3.4.6 Auxin transport inhibition by TIBA was insufficient to rescue nodulation in CHSi roots

Application of kaempferol in *Medicago* roots has previously been shown to rescue nodulation in flavonoid-deficient roots (Zhang et al., 2009) possibly through inhibiting auxin transport. It was examined if the application of synthetic auxin transport inhibitors would alter the accumulation of auxin required in the zone of inoculation and as a result could rescue nodulation in *CHS*i roots. The application of TIBA was optimized in hairy roots and it concurred with the concentration used in previous studies (Rightmyer and Long, 2011). The Control and *CHS*i hairy roots were subjected to treatments with rhizobia and TIBA as well as rhizobia and flavonoids (naringenin and isoliquiritigenin). TIBA was able to induce pseudonodule formation in Control and *CHS*i roots, however, when applied together with GFP-tagged rhizobia, it failed to produce infected nodules. Pseudonodule structure is different from normal nodules where pseudonodules have more dispersed meristem and the vascular tissue does not extend to the distal parts of the nodule (Hirsch et al., 1989). In the same experiment, the *CHS*i roots could be rescued for nodulation with the exogenous application of naringenin and isoliquiritigenin together with the rhizobia. Naringenin and isoliquiritigenin are flavonoid metabolites that could be converted in to a majority of the flavonoids found in plants (Winkel-Shirley, 2001). This would suggest that

kaempferol as previously shown to rescue nodulation (Zhang et al., 2009) may have been responsible for other functional interactions with the rhizobia and not just auxin transport inhibition. An effective way to identify various roles was to conduct a transcriptome analysis of flavonoid-deficient roots inoculated with rhizobia and compare it to appropriate controls (see Chapter 4).

3.5 Conclusion

The results in this chapter show that silencing of flavonoids by silencing the expression of *chalcone synthase* led to a significant reduction in nodule numbers. The *CHS*i roots failed to inhibit auxin-transport when inoculated with Nod factor overexpressing rhizobia. This suggested that root-flavonoids were responsible for changes in auxin homeostasis. The direct measurements of IAA concentrations in *M. truncatula* hairy roots showed an overall decrease in bioactive and conjugated IAA when inoculated with rhizobia. In *CHS*i roots, inoculation with rhizobia had no effect on IAA concentration. As flavonoids are involved in peroxidase mediated auxin catabolism, it is speculated that this may be a major mechanism in maintaining the auxin balance required for nodule formation in *M. truncatula* hairy roots. The concentrations of IAA and IAA conjugates were also observed to be higher in Control hairy roots compared to seedling roots of *M. truncatula* suggesting that hairy roots have different auxin sensitivities.

Previous studies in *Arabidopsis* had showed that gene expression of auxin transporter proteins of the PIN family was modulated by cellular flavonoids, however, I did not find any similar evidence for *PIN* and *LAX* genes in *CHS*i hairy roots of *M. truncatula*.

The changes in IAA concentrations can also be attributed to its synthesis through the YUCCA pathway which forms the major IAA biosynthesis pathway in plants. I found that *YUCCA1* gene expression was significantly up-regulated in *CHS*i roots inoculated with rhizobia compared to mock-inoculated *CHS*i roots. This could explain the increased concentrations of IAA observed in *CHS*i roots.

The silencing of other flavonoid biosynthesis branches led to the observation that FLS products were likely to be crucial for nodulation even though the auxin transport inhibition was modulated by both IFS and FLS product.

The *CHS*i roots were complemented by a synthetic auxin transport inhibitor TIBA, which led to the formation of pseudo-nodule structures on the roots. These pseudo-nodules were not colonized by rhizobia, which led to the hypothesis that

flavonoids play additional roles in facilitating the infection with rhizobia. This is further investigated in Chapter 4.

Chapter 4. Additional roles of flavonoids in symbiotic nodule organogenesis

Summary

It was established that flavonoids, in particular flavonols and isoflavonoids are inhibitors of polar auxin transport (PAT) during nodule organogenesis. An inhibition of PAT by the synthetic auxin transport inhibitor TIBA was insufficient to rescue nodulation in flavonoid-silenced (*CHS*i) roots. Therefore, it was hypothesized that flavonoids play additional roles during the root-rhizobia interactions, in particular the infection pathway.

To discover the pathways that were modulated by flavonoids, I identified the changes in the transcriptomic abundances in *CHS*i and Control roots at 6 and 24 hpi with rhizobia (E65) or blank media (B) through a microarray based approach.

It was found that extensive changes occurred as a result of the absence of flavonoids, in the abundances of mRNAs encoding enzymes involved in plant-hormone synthesis and breakdown. At 6 hpi, flavonoids altered transcripts of genes that are involved in the synthesis and breakdown of ethylene, auxin, cytokinin and gibberellin, but not strigolactones. There was also evidence of extensive changes in the transcript abundance of the enzymes involved in reactive oxygen species (ROS) generation and scavenging, and I tested whether this modulates the infection thread progression.

It was successfully demonstrated that ROS accumulation and not scavenging is important for IT formation. Many flavonoids are anti-oxidative molecules and their absence increased the expression of other ROS scavenging molecules. This could be affecting the oxido-reductive balance of the cell and preventing successful infection of rhizobia.

4.1 Introduction

Chapter 3 presented a detailed study of the changes in auxin response mediated by flavonoids during the early stages of the legume-rhizobia symbioses. It was further considered that the flavonoids were modulating auxin by affecting the polar auxin transport. I also established that the application of a synthetic auxin transport inhibitor, TIBA, in *M. truncatula* hairy roots could induce cell divisions leading to the formation of a pseudo-nodule like structure. In the absence of endogenous flavonoids, these pseudo-nodules could not be infected with rhizobia, suggesting additional roles of these secondary metabolites. In this chapter, I identified these roles through a whole transcriptome study of *CHS*i hairy roots compared to Control hairy roots of *M. truncatula.*

4.1.1 Early symbiotic interactions between legumes and rhizobia

The interaction between legumes and their rhizobia symbiont is initiated by a chemical cross-talk where root exuded flavonoids are recognized by the compatible rhizobia (Peters et al., 1986, Redmond et al., 1986). This leads to the induction of nod-gene synthesis in the bacteria. This synthesis generates the proteins involved in synthesis and export of lipochito-oligosaccharides or Nod factors (NFs). NFs are perceived by roots by LysM-receptors (Limpens et al., 2003) and an immediate increase in intracellular calcium levels is observed in the root hairs. This is followed by a series of calcium spikes and changes in the root hair cytoskeleton so that they curl around the bacteria to encapsulate them (Miwa et al., 2006). At the same time, the NF perception also stimulates cell division in the pericylce and inner cortex to form the nodule primordium (Marino et al., 2009).

Subsequently, an infection thread (IT) grows in the root hairs, which the rhizobia use to travel inwardly towards the inner cortex. This infection thread is preceded by the formation of trans-cellular cytoplasmic bridges known as pre-IT (van Brussel et al., 1992). The growth and elongation of the infection thread is under the control of the host plant, which guides the symbiotic bacteria to release them into an organelle-like structure (symbiosome) in the specific inner cortical cells. Within the symbiosomes, the bacteria differentiate into nitrogen fixing bacteroids housed within the developed nodules (Marino et al., 2009).

Plant-hormone biosynthesis and responses during nodulation

The classical plant hormones are required during nodulation to regulate and activate multiple processes. These processes range from initiation to senescence of a nodule and include regulation of cell division and differentiation as well as infection and control of defence responses. For the purpose of this study, the focus is on the early interactions between the plant and rhizobia.

The biosynthesis pathways for Gibberellic acid (GA), Ethylene, Cytokinin and Auxin are shown in Figure 4.1 and discussed below.

A) Gibberellin

In the semiaquatic legume *Sesbania rostrata* it has been demonstrated that GAs are involved in infection pockets and infection thread formation, as well as primordium development during nodulation (Lievens et al., 2005). In Pea, Ferguson et al. (2005) further showed that GA stimulated nodule formation at low concentrations but inhibited it at higher concentrations suggesting an optimal concentration requirement for nodule organogenesis.

There are as many as 130 isoforms of GA that are considered as inactive or their activity has not been understood at present. The major bioactive GAs (GA_1 and GA_4) are synthesised via a parallel pathway diverging from GA_{12}.The major enzymes involved in first stage of conversion of geranylgeranyl diphosphate to GA_{12} are *ent* - copalyl diphosphate synthase (CPS), *ent*-kaurene synthase (KS), *ent*-kaurene oxidase (KO) and *ent*-kaurenoic acid oxidase (KAO). The next stage is catalysed by 2-oxoglutarate-dependent dioxygenases namely GA 20-oxidase ($GA20_{ox}$) and GA 3β-hydroxylases ($GA3_{ox}$). Bioactive GA is degraded by GA2-oxidases ($GA2_{ox}$) (Lievens et al., 2005, Hayashi et al., 2014), thus maintaining its required concentrations in the cells.

B) Ethylene

Ethylene is a strong inhibitor of nodule formation in *M. truncatula* (Peters and Crist-Estes, 1989). It has been suggested that ethylene acts upstream or at the calcium spiking point in the nodulation signalling pathway (Oldroyd et al., 2001). Ethylene is also shown to be inhibited by GA_1 in pea (Ferguson et al., 2011).

The synthesis of S-adenosyl methionine (SAM) is catalysed by SAM synthetase. SAM is also a precursor for polyamine (Spermidine/Spermine) synthesis pathway and can function as a methyl donor. The conversion of SAM to 1-aminocyclopropane-1-carboxylic acid (ACC) is the rate limiting step in ethylene biosynthesis and is catalysed by the enzyme ACC synthase. 5'-methylthioadenosine (MTA) is a by-product that is generated as a result of this conversion. MTA is recycled back to methionine to conserve the methylthio group. ACC oxidase catalyses the final step of ethylene biosynthesis. ACC synthase and ACC oxidase are transcriptionally regulated by biotic and abiotic stimulus, while ACC synthase may also be regulated by the cellular calcium and ROS balance. Ethylene responses are mediated through Ethylene Response Factors (ERFs such as ERN and ERD) (Wang et al., 2002, Desbrosses and Stougaard, 2011).

C) Cytokinin

Cytokinins mimic the morphogenic effects of Nod factors (Cooper and Long, 1994, Frugier et al., 2008). Similar to the effects of Nod factors, the exogenous application of cytokinin induces cortical cell divisions, amlyplast deposition and expression of early nodulin in several legumes (reviewed by Frugier et al., 2008). It is proposed that cytokinin acts downstream of Nod factor perception (Murray et al., 2007, Gonzalez-Rizzo et al., 2006) while repressing lateral root formation to induce nodule formation (Frugier et al., 2008). The gene expression of *NIN* is also regulated by cytokinins and this could be important as epidermal response to rhizobia (Murray et al., 2007, Frugier et al., 2008). NIN is important for infection thread formation and bacterial entry in a spatially regulated mechanism (Marsh et al., 2007).

The MEP (methylerythritol phosphate) pathway for biosynthesis of isoprenoid (iP) and *trans*-zeatin (tZ) cytokinins is initiated by adenosine phosphate-isopentenyltransferases (IPT) that form iP-nucleotides. These are subsequently converted to active free bases by cytokinin nucleoside 5'-monophosphate phosphoribohydrolases (LONELY GUY or LOGs) (Mortier et al., 2014). iP nucleotides can also be converted to the tZ-nucleotides through cytochrome P450 monooxygenases (CYP735As). The *cis*-zeatin (cZ) cytokinin is derived from the

MVA (mevalonate) pathway. The bioactive cytokinins can be inactivated by cytokinin oxidase dehydrogenases (CKXs) or can be conjugated with sugar moieties by glucosyltransferases (UGTs) (Werner and Schmulling, 2009).

D) Auxin

Auxins have profound effect on plant growth and development. In roots, auxin influences its morphology, elongation, lateral root and nodule formations (Woodward and Bartel, 2005). Auxin is mainly synthesised in the aerial tissue and transported in a polar direction towards the root (Ljung et al., 2005). This auxin transport is inhibited by root-flavonoids in response to rhizobia (Wasson et al., 2006), which may lead to auxin accumulation at the site of nodule organogenesis (Mathesius, 2001).

There are four proposed pathways for auxin synthesis in plants. These are the tryptophan dependent indole-3-pyruvic acid (IPA) pathway, the indole-3-acetamide (IAM) pathway and the indole-3-acetaldoxime (IAOx) pathway; and an unknown tryptophan independent pathway (Figure 3.2). Of these, the IPA pathway is demonstrated to be the major biosynthesis pathway for IAA in *Arabidopsis* (Mashiguchi et al., 2011) as well as in pea roots (Quittenden et al., 2009). This pathway is catalysed by TRYPTOPHAN AMINOTRANSFERASE OF ARABIDOPSIS (TAA1) and a family of Flavin monoxygenase-like proteins (YUCCAs). The YUC enzymes also mediate the rate-limiting step in this conversion.

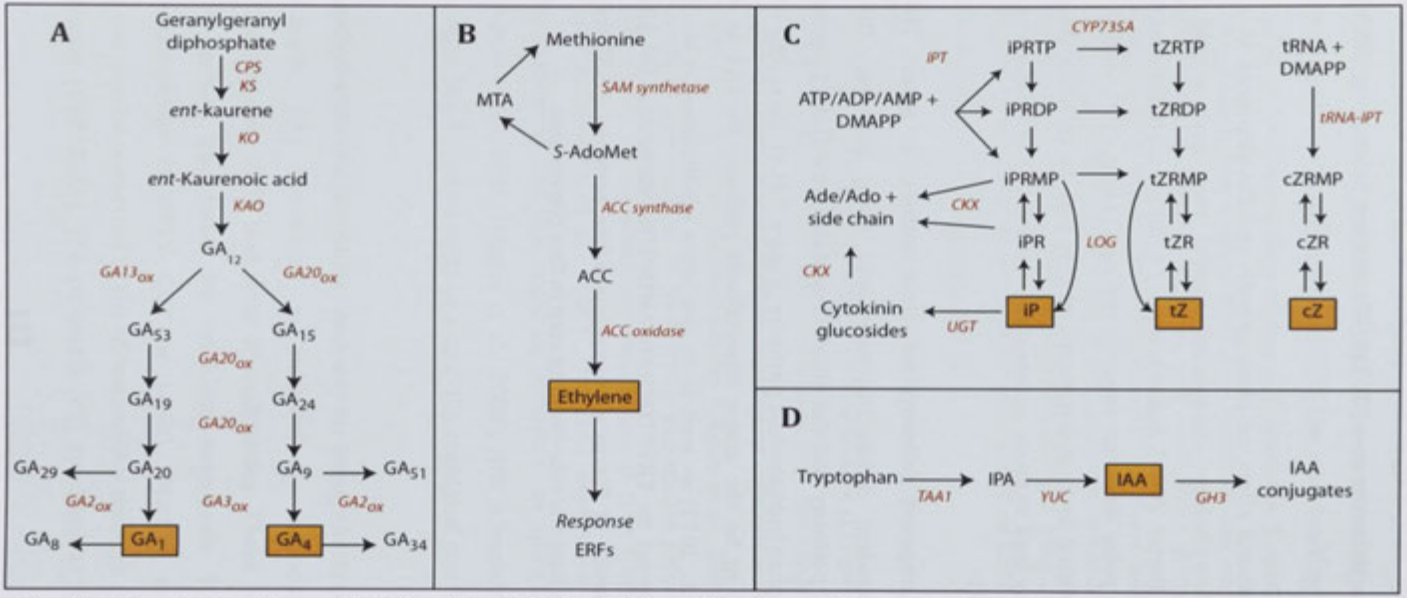

Figure 4.1 – Major biosynthesis pathways of A) Gibberellic acid (GA), B) Ethylene, C) Cytokinin and D) Auxin (modified from Wang et al., 2002, Werner and Schmulling, 2009, Desbrosses and Stougaard, 2011, Mashiguchi et al., 2011, Hayashi et al., 2014). The bioactive forms of the enzymes are highlighted in orange box and the key enzymes involved in the conversion are labelled in red. GA synthesis enzymes are *ent*-copalyl diphosphate synthase (CPS), *ent*-kaurene synthase (KS), *ent*-kaurene oxidase (KO), *ent*-kaurenoic acid oxidase (KAO) and GA oxidases. Ethylene synthesis enzymes are S-adenosyl methionine synthetase (SAM synthetase), 1-aminocyclopropane-1-carboxylic acid synthase (ACC synthase) and ACC oxidase, while response is mediated by the ethylene response factors (ERFs). Cytokinin (isoprenoid (iP), *trans*-zeatin (tZ) and *cis*-zeatin (cZ)) synthesis requires the enzymes adenosine phosphate-isopentenyltransferases (IPT), LONELY GUY (LOG), cytokinin oxidase dehydrogenases (CKXs), cytochrome P450 monooxygenases (CYP735As) and glucosyltransferases (UGTs). Major auxin biosynthesis is mediated by TRYPTOPHAN AMINOTRANSFERASE OF ARABIDOPSIS (TAA1) and Flavin monoxygenase-like proteins (YUCCAs). Auxin can be conjugated by the Gretchen Hagen 3 (GH3) family of enzymes.

The interplay of hormones and molecular processes during nodulation

The Nod factor signalling cascade is shown in Figure 4.2 and was reviewed extensively by Ferguson et al. (2010). A summary of the key elements of the cross-talk and hormonal regulation of the molecular processes is presented here.

The molecular events during early nodulation are initiated by the exudation of flavonoids into the rhizosphere. This leads to the synthesis and export of Nod factors (NF) from the rhizobia that are perceived by the LysM Receptor-like kinase proteins (Limpens et al., 2003) located on the epidermal cells. Another RLK with leucine rich repeat (LRR RLK) are also involved in the NF signal perception and downstream signal transduction. However, activation of LysM RLK was demonstrated to be a prerequisite to activation of LRR RLK (Cárdenas et al., 1998).

Activation of RLK leads to changes in Ca^{2+} fluxes where there is an initial rapid influx of Ca^{2+} ions followed by the membrane depolarization efflux of Cl^- and K^- from the root hair cells. Subsequently, a characteristic oscillation in the cytosolic Ca^{2+} concentration is induced (Oldroyd and Downie, 2008). The ion-channel proteins and nucleoproteins are required for these calcium-spiking events that are perceived by a Ca^{2+}/calmodulin-dependent protein kinase (CCaMK) (Hayashi et al., 2010).

Downstream of CCaMK several transcription factors are required including Nodulation signal pathway (NSP1), NSP2, Ethylene response factor required for nodulation (ERN) and Nodule inception (NIN). The NSP1/2 transcription factors are likely activated by the Ca^{2+} spiking in the nucleus, and this directs the expression of early nodulation (ENOD) genes in the epidermal cells. The binding of NSP1 to promoters of ERN1 and NIN is also essential for expression of some ENODs (Hirsch et al., 2009, Ferguson et al., 2010).

The activation of NF LRR RLK also triggers the expression of 3-hydroxy-3-methyl glutaryl CoA reductase 1 (HMGR) that may be involved in the synthesis of cytokinins, brassinosteroids and other isoprenoid-derived hormones (Kevei et al., 2007). Other proteins that interact with LRR RLK are *Rhizobium*-directed polar

growth (RPG) in *Medicago* (Arrighi et al., 2008) and Sym-RK interacting protein (SIP1) in *Lotus* (Zhu et al., 2008). RPG is reportedly required for polar tip growth of the infection threads (Arrighi et al., 2008) whilst SIP1 is a transcription factor that regulates infection through binding with the NIN protein (Zhu et al., 2008).

Other transcription factors such as Ethylene response factor (ERF1) in *Lotus* and Ethylene response factor required for nodule differentiation (ERD) in *Medicago* are also localized in the nucleus and are required for nodulation (Vernie et al., 2008). However, their precise roles are yet to be identified. Similarly the U-box protein CERBERUS in *Lotus* also commands an unknown role during nodulation (Yano et al., 2009).

Nodule organogenesis requires co-ordinated responses from the cortex as well as the epidermal cells of the roots. This co-ordination is likely mediated through a cytokinin receptor (MtCRE1/LjLHK1) (Gonzalez-Rizzo et al., 2006), however, the real mobile signal is unknown. CCaMK appears to play a role in activation of downstream genes in the cortex. NSP1/2 activated by CCaMK regulate the cortical cell divisions while NIN functions as a negative regulator of ENOD11 thus directing its spatial expression. NIN expression is induced by cytokinin or NF application thus suggesting that NIN acts as a positive regulator of cortical cell divisions (Hirsch et al., 2009, Soyano et al., 2013).

In addition to cytokinin being a possible candidate for a mobile signal coordinating the epidermal and cortical events, the hormone abscisic acid (ABA) is also suggested as a candidate for this role (Ding et al., 2008). Other plant hormones such as auxin, brassinosteroids and gibberellins are reported as positive regulators of nodule development while reactive oxygen species (ROS), jasmonic acid (JA) and ethylene are considered to be negative regulators of these processes (Ferguson et al., 2010).

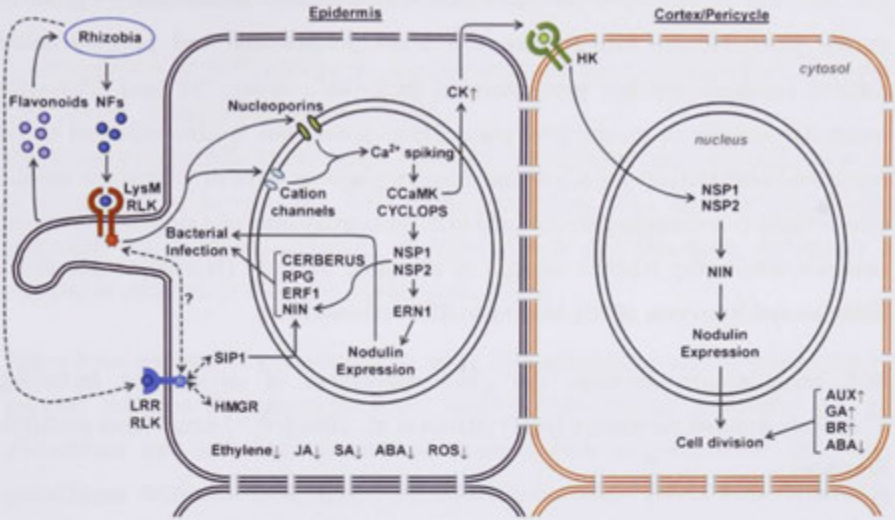

Figure 4.2 – The molecular events in early nodule organogenesis in legumes (adapted from Ferguson et al., 2010). Nodulation is initiated by the exudaton of flavonoids in to the rhizosphere which attracts and induces Nod factor (NF) synthesis in compatible rhizobia. The NF is perceived by the LysM receptor-like kinases (LysM-RLKs) and leucine-rich receptor-like kinases (LRR-RLKs) on the root epidermis. The perception triggers a number of NF signalling cascade, cortical/pericycle cell divisions, and bacterial infection events. A signal, possibly cytokinin is perceived in the cortex/pericycle which further induces transcription factors (NSP1/2, NIN) involved in expression of nodulins. The figure also show the speculated changes (increase or decrease of concentrations) in auxin (AUX), ethylene, jasmonic acid (JA), salicylic acid (SA), abscisic acid (ABA), gibberellic acid (GA), brassinosteroids (BR), and reactive oxygen species (ROS). Further abbreviations – SIP1 (SymRK-interacting protein), HMGR (3-hydroxy-3-methylglutaryl CoA reductase1), cytokinin (CK), CCaMK (calcium and calmodulin-dependent protein kinase), RPG (*Rhizobium*-directed polar growth), ERF1 (ethylene response factor 1), NIN (nodule inception), NSP1/2 (nodulation signaling pathway 1/2), ERN1 (ERF required for nodulation), HK (receptor with a histidine kinase domain/Cre1).

Role of Reactive Oxygen Species (ROS) in legume-rhizobia symbiosis

The ROS are secondary messengers that are important in the early signalling during plant-rhizobia interactions. The plant peroxisomal and plasmalemmal NADPH oxidases are key generators of ROS ($O_2^{\bullet -}$, H_2O_2, $^{\bullet}OH$ and $^{\bullet}O_2$) with molecular oxygen O_2 as the precursor. Their generation is also reported to be associated with the release of calcium into cytoplasm as a result of biotic or abiotic interactions. It is thought that Ca^{2+} and ROS are constituents of a singular signalling network where the NADPH oxidase is activated by Ca^{2+} (Marino et al., 2009, Glyan'ko and Vasil'eva, 2010), leading to ROS accumulation.

ROS accumulation activates the gene expression of *peroxidases* including *Rhizobium induced peroxidase* (*rip1*) (Ramu et al., 2002). RIP1 could have multiple functions –

1) It could detoxify the H_2O_2 produced by the NADPH oxidase thus preventing oxidative damage to the cellular machinery at the site of infection (Ramu et al., 2002).

The accumulation of ROS in roots triggers a hypersensitive response (HR) that protects the roots from pathogenic attacks. This is important as the rhizobia could be intially perceived as a pathogen. The detoxification of ROS only at the site of infection allows the host to prevent indiscriminate rhizobial penetration into the roots (Glyan'ko and Vasil'eva, 2010) while facilitating successful infection at a specific site.

2) RIP1 could be involved in peroxidase-mediated cell-wall modifications during infection thread progression and nodule organogenesis (Ramu et al., 2002, Marino et al., 2009).

ROS and cell-wall bound peroxidases activate a number of early nodulation genes such as *ENOD10, ENOD 11* and *MtPRP4.* These genes encode proline-rich proteins (PRPs) that are members of a superfamily of cell wall proteins known as extensins (Kieliszewski and Lamport, 1994, Rathbun et al., 2002). These nodule-specific PRPs comprise of a series of tyrosine-containing pentameric motifs that are associated with cross-linking of cell wall proteins. Therefore, RIP1 accumulation at

the site of infection thread development could be central in the early stages of nodule organogenesis (Ramu et al., 2002, Nanda et al., 2010).

3) Modulation of ROS activity to directly regulate the plant-signalling proteins (Ramu et al., 2002, Ivashuta et al., 2005).
ROS accumulation affects the redox potential in a cell that could affect the activity of transcription factors and GTP binding proteins. The RIP1 activity could modulate this potential, affecting phosphorylation and therefore, activity of a number of proteins in the roots (Ramu et al., 2002).

Apart from peroxidases, a number of other ROS scavenging mechanisms exist to prevent oxidative damage in the roots. Some of these include molecules such as glutathione and ascorbate as well as enzymes such as glutathione reductase, glutathione S-transferases (GSTs) ascorbate peroxidase (APX) and superoxide dismutase (SOD) to mediate this defence against high ROS presence (Marino et al., 2009). Table 4.1 summarises the activities of various antioxidants systems during nodulation.

Table 4.1 – Summary of activities of various antioxidant systems in rhizobia-infected nodules (modified from Marino et al., 2009)

Antioxidant	Activity
Substrates	
Ascorbate (ASA)	Substrate of APX
Glutathione (GSH)	Substrate of Gpx, GST, GR Provides reducing capacity for dehydroascorbate reductase Post-translational protein regulation
Enzymes	
Ascorbate-Glutathione (ASA-GSH) cycle enzymes	Detoxification of H_2O_2
Thioredoxins (Trxs)	Post-translational protein regulation
Glutaredoxins (Grxs)	Post-translational protein regulation
Glutatione S-transferases (GSTs)	Tagging of oxidative degradation products for removal Acting as Gpxs to directly scavenge for peroxides
Peroxiredoxins (Prxs)	Detoxification of H_2O_2, peroxynitrate and alkyl hydroperoxides
Glutathione peroxidases (Gpxs)	Reduction of lipid peroxides and other organic peroxides

Antioxidative activity of flavonoids

Flavonoids play an important role in maintenance of the ROS homeostasis through their ability to scavenge for free radicles. This antioxidative property of flavonoids are attributed to their structural ability to participate in the reaction below –

$$F - OH + R \cdot \rightarrow F - O \cdot + RH$$

Where the hydroxyl group on the flavonoid (F) reacts with the free radical (R·) to produce a relatively stable flavonoid radicle (F-O·) (Heim et al., 2002). The nuclear structure of flavonoids is shown in Figure 4.3. Their antioxidant function is a resultant of the number of hydroxyl groups attached to the ring structures shown (Gill and Tuteja, 2010).

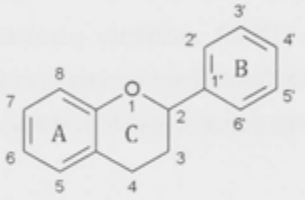

Figure 4.3 – The nuclear structure of flavonoids. The B-ring hydroxyl groups strongly enhances the ROS scavenging ability of the flavonoids.

The three determinants of radical scavenging has been described by Rice-Evans and colleagues (1996) as follows –

1 – Higher stability of the flavonoid radical and electron delocalisation is contributed by the o-dihydroxy structure on the B-ring.

2 – Electron delocalisation in the B-ring and resulting antioxidative potency was promoted by the 2,3 double bond and a 4-oxo function in the C-ring.

3 – Maximum radical scavenging potential is determined by the 3- and 5-OH groups with 4-oxo function in the A and C rings.

In Chapter 3, the changes in auxin synthesis, transport and accumulation were studied in detail. As it was found that synthetic auxin transport inhibitors were insufficient to rescue nodule formation in the flavonoid-deficient roots, the aim of this chapter was to identify the wider changes in plant-hormone and oxidoreductive balances in early plant-rhizobia interactions through a whole transcriptome analysis. I have analysed the changes at 6 and 24 hpi with Nod factor overexpressing rhizobia (E65) in Control and *CHS*i roots. A multiple comparison with 3-way interactions was included in the study. To identify the pathways that were highly affected as a result of flavonoid silencing a GO enrichment analysis was undertaken.

4.2 Methods

Bacterial strains

To generate a *gfp*-labelled E65 strain, the plasmid pTE3 containing *nodD3* expression cassette driven by the *tcp* promoter was isolated from *S. meliloti* A2102 (Barnett et al., 2004), linearized using *Bgl*II (New England Biolabs, USA) and treated with Antartic phosphatase (New England Biolabs, USA) to remove 5' phosphate and prevent self-ligation. A 957 bp region from the plasmid pHC60 containing *gfp* under a constitutive promoter (Cheng and Walker, 1998) was excised using *Bgl*II and ligated into the linear pTE3 vector containing *nodD3* expression cassette using T4 DNA ligase (New England Biolabs, USA). The resulting 24 kB plasmid (pTE3-E65-gfp) was electroporated into competent *S. meliloti* 1021 as described below. The colonies were cultured in BMM with 10 µg/ml tetracyclin (Sigma, USA) and screened for GFP fluorescence to confirm insertion of *gfp* fragment.

The *S. meliloti* 1021 strain was made electrocompetent as follows – A 250 ml culture of *S. meliloti* 1021 was grown to OD_{600} of 0.6 at 28 °C at 170 RPM. The culture was chilled on ice for 30 minutes and centrifuged at 9000 RPM for 10 minutes at 4 °C in 500 ml sterile centrifuge tube (Beckman Coulter, USA). The pellet was washed four times in sterile ice-cold deionized water, finally with 10 % (v/v) sterile ice-cold glycerol solution. The pellet was resuspended in 1 ml of 10 % (v/v) sterile ice-cold glycerol solution and aliquoted on ice. A final concentration of 10^{10} – 10^{11} CFU/ml was achieved.

Approximately 2.5 µg of pTE3-E65-gfp vector was electroporated into 50 µl of competent *S. meliloti* 1021 at 21 kV/cm and 200 Ω. The colonies were recovered in 1 ml of BMM media for four hours at 28 °C at 170 RPM and selected on BMM agar with 10 µg/ml tetracyclin (Sigma, USA) cultured at 28 °C for two days. The resulting colonies were screened for GFP fluorescence to confirm tagging of the pTE3-E65 vector with GFP.

S. meliloti expressing pTE3-E65 (E65) was used to inoculate plants in preparation of material for the transcriptomic analysis while *S. meliloti* expressing pTE3-E65-gfp (E65-gfp) was used to visualize the infection thread.

Sample generation, preparation and microarray analysis

M. truncatula cv. Jemalong A17 was scarified and surface sterilised in 6 % sodium hypochlorite for 10 minutes, washed 5 times to remove all traces of sodium hypochlorite and plated on water agar plates as described in Chapter 2. Seeds were stratified at 4 °C for 2 days before germinating overnight at 25 °C. Seedlings were transformed with *A. rhizogenes* carrying an empty vector Control (pHellsGate 8 or C) or *CHS* silencing construct (pHellGate-*CHS*i) as described previously (Wasson et al., 2006). The roots were selected for an absence of auto-fluorescence due to the presence of flavonoids under UV excitation wavelength (365 nm).

Selected roots were spot inoculated at the zone of root hair emergence with Nod factor overexpressing rhizobia (E65) (Barnett et al., 2004) at OD_{600} between 0.1 and 0.2 (inoc+ or E) or the BMM culture medium representing mock inoculation (inoc- or B). Approximately 5 mm segments were cut at the site of inoculation at 6 h and 24 h post inoculation from 50 - 60 roots in 3 biological replicates while ensuring to remove the root-tip. The segments were snap-frozen in liquid N_2, ground using mortar and pestle and RNA was isolated using the RNeasy RNA extraction kit (Qiagen, USA). The RNA was purified using RNeasy columns (Ambion) and quality was assessed on Agilent 2100 Bioanalyzer prior to cDNA synthesis. The chip hybridization and scanning (Affymetrix 61K Medicago GeneChip) was carried out at the ACRF Biomolecular Resource Facility (John Curtin School of Medical Research, ANU) on the Affymetrix GeneChip DNA array system (Affymetrix Inc., USA).

Statistical Analysis

Microarray Statistical analysis was performed using Partek Genomics Suite (Partek). The Gene chip Robust Multiarray Averaging (GC-RMA) method was used to normalise all expression data and to correct for background errors. Analysis of variance (ANOVA) in One-way (Genotype), Two-way (Genotype * Inoculation) and Three-way (Genotype * Inoculation * Time) interactions were calculated with

significance at $P<0.05$ and $FDR<0.1$. The run date (Scan Date) of the samples generated a random effect. The model details are provided in Appendix A4.1. Singular GO Enrichment Analysis (SEA) was performed using AgriGO analysis tool (Du et al., 2010) probed using Medicago Affymetrix Genome Array identifiers. The Fisher statistical method with Yekutieli multi-test adjustment (Benjamini and Yekutieli, 2001) at $P<0.05$ and $FDR<0.05$; and a minimum of 5 mapping entries on the complete gene ontologies was used to confirm significant enrichment. Transcriptional changes of selected genes were confirmed using qRT-PCR on an ABI 7900HT system. The cDNA for qRT PCR was synthesised using the SuperScript III First-Strand synthesis Kit (Life Technologies, USA) and the $\Delta\Delta Ct$ method corrected for primer efficiencies was used to calculate the fold change using Sequence Detection Systems software version 2.4 (Applied Biosystems, USA).

Quantitative real-time PCR was performed on selected genes to confirm the transcriptional data. The ABI Power SYBR mix (Applied Biosytems, USA) was used to amplify the sequences using primers as listed in Table 4.2 on the ABI 7900HT PCR system (Applied Biosystems, USA).

Table 4.2 – The primers used to amplify genes for confirmation of transcriptional data from microarray

Gene	Tentative consensus		Primer Sequences 5'-3'
Chalcone synthase	TC119999	F	CGCTGTCACATTTCGTGG
		R	AACACACCCCATTCAAGTCC
LysM domain containing receptor like kinase 3	TC172631	F	TGGGCATGCTACTGGTAGTG
		R	ACAGCTCCAAATCCACCTTG
Peroxidase	TC183217	F	GGTCTTCTTCAAACGGACCA
		R	TGGACTGAACAAAGGCTTCA
Rhizobium induced peroxidase rip-1	TC113389	F	GTTTGCCCTCAAGCATTACC
		R	GCAGGACTGATCCATCACAA
Auxin responsive GH3 Product	TC125691	F	TGGCACGTCCAGTTCTAACA
		R	AGGCCACAAAGCATCTGAGT
Type A response regulator	TC176233	F	GAATTGCATGTGCTTGCTGT
		R	CGCTGTTCTCTCCATCCAAT
Pathogenesis related protein 5-1	TC180277	F	GGTGGCGGTAAGCAACTAAA
		R	GTTCCCTGAACCGTCAAAGT
2,4-D inducible Glutathione S-transferase	TC168199	F	AAGAGCAAGAAGCTGCCAAG
		R	TGATGTTGCCAAAGGTCTCA

F – Forward primer; R – Reverse primer

ROS inhibition in roots

Hairy roots were transformed and grown as described previously. Two ROS inhibitors were used – Diphenyleneiodonium chloride or DPI and chloro[[2,2'-[1,2-ethanediylbis[(nitrilo-κN)methylidyne]]bis[6-methoxyphenolato-κO]]]-manganese or EUK-134 (Sigma, USA). 10 mM stock solutions were prepared for each inhibitor in DMSO. For the treatment of the roots (*CHS*i and Control), the plantlets were transferred to a freshly prepared Fåhreus media agar plate supplemented with DPI (1 µM) or EUK-134 (2 µM) (Zhang et al., 2014). The roots were flood inoculated with Nod factor overexpressing rhizobia (E65) (Barnett et al., 2004) and observed after 14 dpi for their nodulation phenotype.

Histochemical staining to visualise ROS accumulation

Histochemical staining was done to visualize accumulation of ROS in the roots in response to the rhizobia inoculations. The general oxidative stress indicator 5-(and-6)-chloromethyl-2',7'-dichlorodihydrofluorescein diacetate (CM-H_2DCFDA, Life Technologies, USA) which detects several ROS species (HO·, H_2O_2, NO, ROO·, $ONOO^-$, $\cdot O2^-$) was used as per manufacturer's instructions. Roots were carefully removed from the growth medium ensuring they sustained minimum mechanical damage. These were subsequently submerged in 5 µM H_2-DCFDA made in 0.1 M potassium phosphate buffer solution. The samples were covered with foil and incubated in vacuum for 30 minutes at room temperature, followed by three washes with ice-cold 0.1 M potassium phosphate buffer. The accumulation of ROS in the roots was imaged immediately after staining under 495 nm excitation and 520 nm emission using stereomicroscope (Olympus SZX9, USA) microscopes and images were taken using Olympus DP70 (12.5 megapixel) imaging system.

4.3 Results and Discussion

A microarray analysis was used to unravel the various functions of flavonoids in the *M. truncatula-S. meliloti* symbiosis. The data here compared the changes in transcript levels in Control and flavonoid deficient (*CHS*i) roots that were inoculated with Nod factor overexpressing rhizobia (E65) or BMM culture media at 6 and 24 hpi. Therefore, the changes observed are independent of nod-gene activation by flavonoids exuded by the roots. In the following sections, the results of the experiment as well as a rescue strategy are presented and discussed.

4.3.1 Verification of gene expression levels using qRT-PCR

The probes that detected significant transcript changes amongst all the experimental comparisons are presented in Appendix Table A4.1. A large number of *CHS* transcripts were significantly down-regulated in *CHS*i roots providing a first confirmation that the RNAi silencing approach was successful in the sampled roots. In addition, the genes marking early nodulation events such as *ENOD11* (TC 123589) and *Vapyrin* (TC132783) were up regulated in Control hairy roots 24 hpi with rhizobia compared to Control hairy roots that were mock inoculated with BMM. This confirmed that nodule organogenesis was functional in these roots.

The data obtained from the microarray were then verified using qRT-PCR of selected genes (Table 4.3) chosen for their roles in nodulation and pathogenesis. The results largely confirmed that the changes were comparable and validated this experimental approach.

Table 4.3 – Verification of expression patterns of seven tentative consensus sequences (TC) through quantitative real-time PCR across four comparison groups

Tentative Consensus Number	Gene	Fold change		Group
		Chip	qPCR	
TC119999	*Chalcone synthase*	-8.80	-11.39	1
TC172631	*LysM domain containing receptor like kinase 3*	-2.58	-1.82	2
TC183217	*Peroxidase*	3.00	2.75	2
TC113389	*Rhizobium induced peroxidase rip-1*	-2.50	-1.60	2
TC125691	*Auxin responsive GH3 Product*	3.21	2.15	2
TC176233	*Type A response regulator*	2.06	1.02	3
TC180277	*Pathogenesis related protein 5-1*	2.61	3.42	4
TC168199	*2,4-D inducible Glutathione S-transferase*	5.31	2.83	4

1 - CHSB6vCB6; 2 - CHSE6vCE6; 3 - CHSE24vCHSB24; 4 - CHSE24vCE24

4.3.2 *Silencing of flavonoids leads to extensive changes in transcript levels*

The analysis of the transcript abundances through microarray analysis indicated a large number of probesets that showed a significant difference in gene expression when roots were flavonoid deficient and/or inoculated with rhizobia.

Two-way ANOVA analysis between *CHS*i and Control roots that were inoculated or mock-inoculated yielded interesting results as shown in Figure 4.4. The Venn diagram here shows the overlap of transcripts that were either up- or down-regulated in the selected comparisons. This includes the effects of inoculation in *CHS*i and Control roots as well as changes in transcript abundance due to loss of flavonoids.

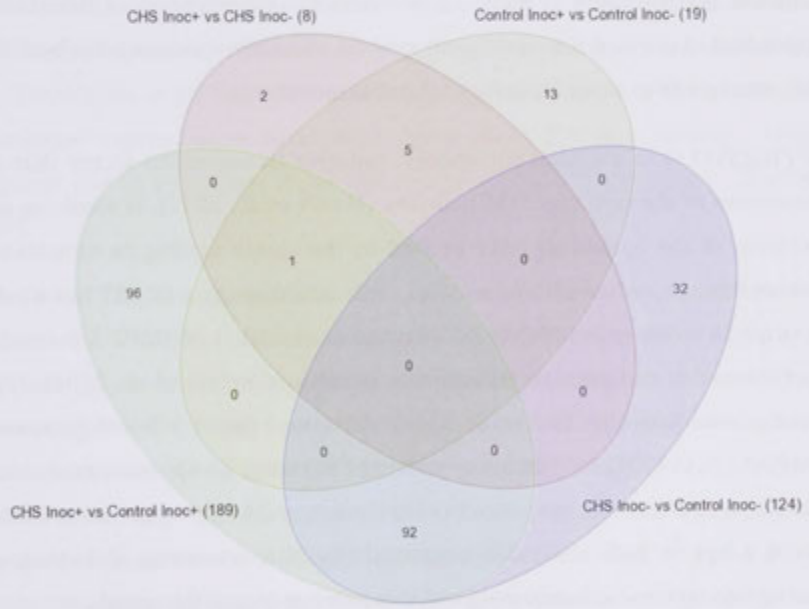

Figure 4.4 – Venn diagram showing the overlap of the differentially expressed genes in Two-Way Interaction (Genotype*Inoculation) comparisons for ANOVA.

There were six transcripts that showed up-regulation in both *CHS* silenced and Control roots due to inoculation with rhizobia (Table 4.4). These genes included a *Receptor like kinase* (*RLK*), *Nodule inception* (*NIN*) and *Vapyrin* (*VPY*) whose roles are discussed below. The three other transcripts' role in nodulation is yet unknown.

Plant receptor-like kinases are transmembrane proteins that are involved in signal perception from biotic or abiotic stimulus. RLKs are defined by their presence of a signal sequence, an amino-terminal with a transmembrane region, and a carboxyl-terminal kinase region (Shiu and Bleecker, 2001). Several RLKs have been found in *M. truncatula* that are specifically involved in rhizobia infection processes (Limpens et al., 2003). However, the RLK (TC113229) that was up regulated has not been studied in detail and its functions are currently unknown. It could be speculated that this RLK is likely to be involved in perception of the rhizobia independent of the root flavonoid content as its abundance increased in both *CHS*i and Control roots as a consequence of rhizobia inoculation.

NIN (TC131714) is a nodulation-specific putative transcription factor that acts downstream of the common SYM pathway (Marsh et al., 2007). It mediates gene expression in the epidermal layer as well as the cortex leading to formation of infection threads and eventually nodules. NIN acts through a CCAAT box binding transcription factor called MtHAP2-1 (Soyano et al., 2013). MtHAP2-1 is involved in persistence of meristem in inderminate nodules (Combier et al., 2006). It is a transcriptional activator that leads to cell division. I found a 3-fold increase in *MtHAP2-1* (TC117738) in rhizobia inoculated *CHS*i roots 24 hpi compared to *CHS*i roots 6 hpi; and rhizobia inoculated Control roots at 24 hpi compared to Control roots at 6 hpi. In both cases this suggested that NIN activation of downstream transcription factor was functioning and was independent of flavonoids.

Vapyrin (*VPY*) (TC132783) has recently been discovered as an essential gene involved in the progress of symbiotic interactions with rhizobia and mycorrhiza (Murray et al., 2011). VPY is involved in membrane trafficking and biogenesis and it is required for normal infection thread formation. There was an increase in its

expression in both Control and *CHS*i roots upon inoculation with rhizobia, suggesting that the expression of *VPY* was also independent of flavonoids.

One of the genes that did show a large fold change in transcript abundance in control roots due to inoculation was similar to a metal transporter CNNM4 (NP7257575). There was also an increase in this transcript in *CHS*i roots upon inoculation but this increase was more than 2-fold less than the Control roots. Metal transporters are integral to establishment of root-nodules as manganese and calcium facilitate the bacterial colonisation and binding of lectins to the tip of root hairs (Kijne et al., 1988, González-Guerrero et al., 2014). Subsequently, the calcium-calmodulin kinases (CCaMKs) are activated which then induces NSP1/2 or NIN transcription factors (Singh and Parniske, 2012, González-Guerrero et al., 2014). Despite this, little is known about the CNNM family of proteins that are evolutionarily conserved Mg^{2+} transporters (Hirata et al., 2014). In *Arabidopsis* Mg^{2+} has been implicated in root hair elongation (Niu et al., 2014) and an increase in accumulation of Mg^{2+} may be involved in a similar role. Despite the increase in transporter expression in flavonoid-deficient roots, it may represent a reduced response due to a decrease in hormonal or oxidoreductive responses (discussed later).

There were 13 other transcripts that only showed an increase in Control roots as a response to rhizobia inoculation. These included transporters and defence response genes likely to regulate the bacterial infection by the host plants. Interestingly two transcripts belonging to flavonoid synthesis enzymes downstream of chalcone synthase (TC179864 and TC130349) were up-regulated in *CHS*i roots only upon inoculation. This would suggest that the synthesis of flavonoids was crucial for nodulation and the cells were compensating for a lack of metabolites by up-regulating the downstream flavonoid-synthesis genes.

Table 4.4 – The subset of genes that showed a transcriptional up regulation as a result of inoculation in Control and/or *CHS*i roots

ProbesetID	TC #	Description	Fold change	
			Control * inoc+ vs. Control * inoc-	*CHS* * inoc+ vs. *CHS* * inoc-
Mtr.16214.1.S1_at	TC113229	*Receptor-like kinase*	5.27	3.27
Mtr.28094.1.S1_at	TC131714	*Nodule inception (NIN)*	4.89	3.44
Mtr.42828.1.S1_at	TC132783	*Vapyrin*	4.66	2.90
Mtr.4797.1.S1_s_at	AL383715	*Mt Dwarf 27*	3.12	2.96
Mtr.8357.1.S1_s_at	TC124041	*Helix-loop-helix DNA-binding*	3.27	2.44
Mtr.23516.1.S1_at	NP7257575	*Similar to Metal transporter CNNM4 (MTR_6g051860)*	5.28	2.81
Mtr.11288.1.S1_at	TC132637	*Ripening-related protein-like*	2.03	–
Mtr.11343.1.S1_at	TC128669	*Mt Dwarf 27*	2.96	–
Mtr.11507.1.S1_at	TC131018	*Taxane 13-alpha-hydroxylase*	2.04	–
Mtr.13963.1.S1_at	TC134627	*Putative uncharacterised protein*	3.69	–
Mtr.17272.1.S1_at	TC128588	*Tubulin beta chain*	3.16	–
Mtr.20144.1.S1_at	TC121454	*Multi antimicrobial extrusion protein MatE*	3.81	–
Mtr.28784.1.S1_at	BM813243	*Partially similar to LOB domain-containing protein*	2.08	–
Mtr.35511.1.S1_at	TC135762	*Trypsin inhibitor (Pathogenesis related)*	7.28	–
Mtr.37912.1.S1_at	TC122080	*Putative uncharacterised protein*	5.17	–
Mtr.41028.1.S1_at	TC177697	*Putative uncharacterised protein*	3.53	–
Mtr.45719.1.S1_at	TC124041	*Helix-loop-helix DNA-binding*	3.15	–
Mtr.46524.1.S1_at	TC126222	*Cyclic peptide transporter*	2.13	–
Mtr.47095.1.S1_x_at	NP7260213	*ABC transporter, Pleitropic drug resistance protein*	2.32	–
Msa.2558.1.S1_at	TC179864	*Isoliquiritigenin 2'-O-methyltransferase*	–	2.73
Mtr.40868.1.S1_at	TC130349	*isoliquiritigenin 2'-O-methyltransferase*	–	2.70

Furthermore, a large number of genes were differentially expressed in *CHS*i roots compared to Control roots. These included genes involved in hormonal as well as oxidoreductive responses. These changes are described at in detail in the following sections.

Figure 4.5 shows a series of Venn diagrams that specify the number of probes showing at least a 2 fold change across four comparisons with $P<0.05$ and $FDR<0.1$ (A-D). In Figure 4.5 A) and B) the overlapping change in transcript abundance with respect to time post inoculation is shown in either E65 (Figure 4.5 A); inoc+) or BMM (Figure 4.5 B); inoc-) inoculated roots. The comparison of *CHS*i inoc+ roots to Control inoc+ showed that the majority of the change in transcript abundance appeared early in the interaction between roots and rhizobia (6 hpi). It should be noted that a conservative approach was taken to determine the transcripts that were differentially expressed in order to minimize the number of false positives.

In Figure 4.5 B), *CHS*i inoc- roots were compared with Control inoc - roots. Fewer changes in transcript abundance were observed in these groups of samples compared to rhizobia inoculated roots. These changes reflected the genes that are differentially expressed in the absence of flavonoids. Many of these included several copies of the *CHS* transcript that was the target of the RNAi silencing.

In Figure 4.5 C) and D) the effects of inoculation at 6 and 24 hpi were shown for *CHS*i roots compared to Controls. This comparison confirmed that the majority of change in transcript abundance was due to inoculation of rhizobia at 6 hpi.

Together these data strongly implicate flavonoids in the very early stages of rhizobia infection in *M. truncatula* hairy roots. Plant hormones mediate growth and development of nodules (Oldroyd, 2007). There have been several studies suggesting auxin regulation by flavonoids as a likely contributor to nodule organogenesis (as discussed in Chapter 3). In the following section, the evidence from the microarray analysis was used to identify other possible targets that are modulated by flavonoids.

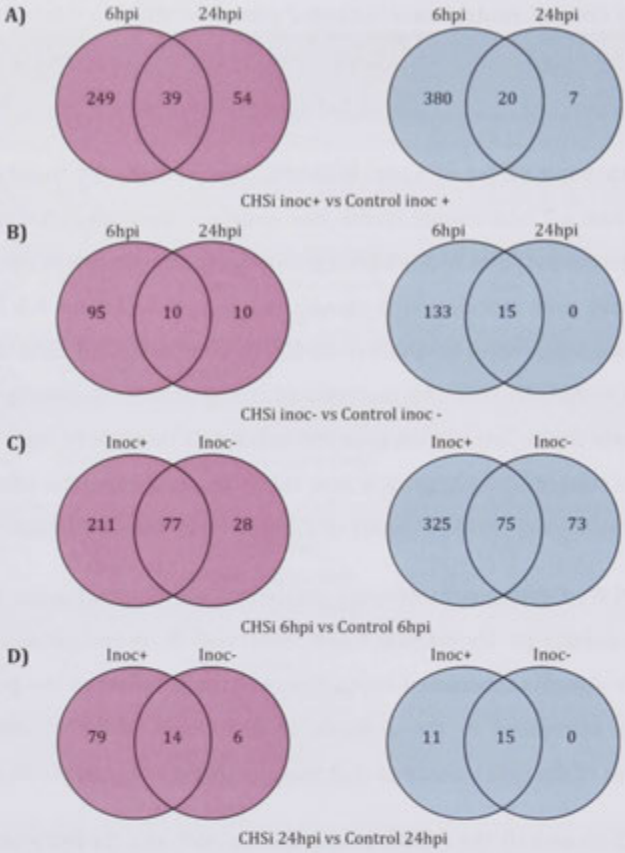

Figure 4.5 – Venn diagrams showing the transcript abundance changes with greater than 2 fold increase represented on the left in red and greater than 2 fold decrease are shown on the right in blue. A) and B) compare the changes in *CHS*i vs Control roots that were inoculated (A) and mock-inoculated (B) at 6 and 24 hpi. C) and D) show the changes with respect to inoculation 6 hpi (C) and 24 hpi (D).

4.3.3 Transcriptional changes observed in plant-hormone responsive genes

Ethylene

Ethylene plays a crucial role in nodulation. Studies in *Medicago* have shown that ethylene sensitivity regulates nodule numbers independent of autoregulation (Penmetsa and Cook, 1997, Penmetsa et al., 2003, Penmetsa et al., 2008). Part of its mode of action might be mediated through the control of PIN-mediated auxin transport (Prayitno et al., 2006). It has been observed in legumes that ethylene production is higher in nodulating roots (Lee and Larue, 1992, Hunter, 1993) but this hormone is a repressor of nodulation (Lee and Larue, 1992), thus acting in a feedback inhibition loop. Lee and Larue (1992) also noted that repression of nodulation occurred through arrested development of infection threads.

A major precursor of ethylene is 1-aminocyclopropane-1-carboxylic acid (ACC). The first committed step in ACC synthesis from S-adenosylmethionine (S-AdoMet) is catalysed by 1-aminocyclopropane-1-carboxylate synthase (ACC synthase). Subsequently, the enzyme 1-aminocyclopropane-1-carboxylate oxidase (ACC oxidase) converts ACC into gaseous ethylene (Wang et al., 2002) (Figure 4.1).

The results shown in Table 4.5 indicated one copy of ACC synthase (TC119108) was up regulated at 6 hpi in rhizobia-inoculated Control roots compared to rhizobia-inoculated *CHS*i roots at 6 hpi. This suggested that the roots with WT flavonoid content respond to the infecting rhizobia by increasing the synthesis of the precursor ACC or that *CHS*i roots inhibit the synthesis of ethylene during infection. Since there was no significant change observed in Control roots rhizobia inoculate vs. mock-inoculated at 6 hpi, this second possibility is the more likely scenario.

The transcript encoding ACC oxidase (TC131421), which catalyses the conversion of ACC to ethylene, increased in rhizobia-inoculated Control roots at 24 hpi compared to the same roots at 6 hpi. This transcript was also overexpressed in rhizobia-inoculated *CHS*i roots compared to rhizobia-inoculated Control roots, both at 6 hpi, thus suggesting an increase in ethylene production in the presence of

rhizobia in the absence of flavonoids. An increase in ethylene would be expected to suppress infection thread formation and reduce the number of nodules in flavonoid-silenced roots. In Control roots, it appears that transcription of some of the genes encoding ethylene synthesis proteins increased after 24 hpi with rhizobia compared to rhizobia-inoculated roots at 6 hpi, possibly as response to control the number of growing ITs.

Ethylene acts as a signalling molecule and its perception leads through a signal transduction machinery that initiates specific biological responses (Wang et al., 2002). The family of plant-specific transcription factors called Ethylene Response Factor (ERF) are capable of binding to ethylene responsive element motif (Vernié et al., 2008, Riechmann and Meyerowitz, 1998). Many of the ERFs are responsive to biotic and abiotic stresses (Vernié et al., 2008) but a few are also involved in regulating plant processes such as organ development, cell division and cell differentiation. Several ERFs have been reported to be involved in the nodulation processes. Transcriptomic studies in *Lotus japonicus* has shown components of ethylene signalling are important in regulating nodule numbers (Desbrosses and Stougaard, 2011). ERN1 or ERF required for nodulation 1 has been demonstrated to be critical for Nod factor signal transduction (Middleton et al., 2007) while a few other ERNs have been found to bind to the *cis* element driving NF induction of early nodulation marker gene *ENOD11* (Andriankaja et al., 2007). An ERF required for nodule differentiation, or ERD, is required at a later stage during nodule organogenesis. EFD regulates the primary cytokinin response regulator Mt*RR4* and is involved in the feedback inhibition of nodulation (Vernié et al., 2008).

The results did not show any change in transcript abundance of ERN, but ERD (TC131878) was up regulated at 6 hpi in rhizobia-inoculated *CHS*i roots compared to rhizobia-inoculated Control at 6 hpi. ERD is a negative regulator of nodulation as it arrests cell division and promotes differentiation instead (Vernié et al., 2008). Therefore, an increase in its concentration at 6 hpi would inhibit the cortical cells from dividing and arrest infection threads in rhizobium inoculated flavonoid-deficient roots.

Auxin and Cytokinin

Auxin and cytokinin are two major plant hormones and have been the subjects of numerous studies. However, according to a previous transcriptomic profiling study, syntheses of these hormones were not highly altered during *M. truncatula* root endosymbiosis (Manthey, et al., 2004). However, as discussed in Chapter 3, I found that the local auxin content is altered at the site of rhizobia inoculation through inhibition of auxin transport, auxin breakdown and/or conversion. Wasson et al. (2006) demonstrated that PAT inhibition is linked to flavonoids in the hairy roots of *M. truncatula*.

Despite a higher concentration of auxin measured in the *CHS*i roots at 24 hpi compared to Control roots at 24 hpi (Figure 3.10), a majority of the auxin responsive genes showed a reduction in fold change in inoculated *CHS*i roots compared to inoculated Control (Table 4.5). This would suggest that the auxin response is reduced early in the interaction with rhizobia in the *CHS*i roots.

Cytokinins are also crucial to nodule organogenesis and they may be key signals for cell differentiation (Frugier et al., 2008). Glucosides of cytokinin are believed to be stable storage forms of this hormone (Sakakibara, 2006). The reduction in at least one copy of the enzyme involved in conversion of cytokinin in to one of its glucosides (TC115341) was found in *CHS*i roots compared to Control roots both at 6 hpi. This could be important in regulating a balance of auxin and cytokinin to induce a nodule meristem. However, detailed quantification of cytokinins and their derivatives would be needed to confirm this result in the future.

Cytokinin feedback signalling is mediated by two-component response regulators. Studies in *Arabidopsis* have divided the functionality of these proteins into at least ten type A ARRs that collectively control feedback regulation of cytokinin signalling, regulation of circadian rhythm, regulation of phytochrome functions as well as inhibition of meristem development (To and Kieber, 2008). The response regulator ARR8, found mainly in roots of Arabidopsis, has been described as a negative regulator of cytokinin signalling (Osakabe et al., 2002) and regulator of circadian rhythm (To and Kieber, 2008). An ARR8 transcript (TC127591) was found to be reduced in rhizobia-inoculated *CHS*i roots compared to rhizobia-

inoculated Control roots at 6 hpi. The reduction could reflect an increase in cytokinin response early in the interaction with rhizobia in flavonoid-deficient roots; however, other molecular events could be required to induce cortical cell divisions. So far no other studies have implicated ARR8 in nodulation.

Gibberellin

Gibberellins are another class of classical plant hormones that are required for nodulation. Their concentration is tightly controlled through metabolic processes. The enzyme *ent*-kaurene oxidase catalyses an early step in the synthesis of this hormone, however, the rate limiting step is considered to be catalysed by Gibberellic acid 20-oxidase (GA20ox) with GA 3-oxidase (GA30ox or GA 3β-hydroxylase) (Middleton et al., 2012, Hayashi et al., 2014) (refer to Figure 4.1 in introduction). Higher expression of the genes encoding these enzymes has also been observed to increase the concentration of bioactive GA (Ogawa et al., 2003, Yamaguchi, 2008, Hayashi et al., 2014).

Transcriptomic studies in soybean showed a transient increase in gibberellin synthesis genes at 12 hpi with rhizobia and then declining (Libault et al., 2010, Hayashi et al., 2012). GA synthesis is also increased during the later stages of nodule formation (Hayashi et al., 2012), thus showing that this hormone is required at distinct stages of nodulation.

Table 4.4 shows that the transcript abundance for *ent*-kaurene oxidase (TC131702) is higher at 6 hpi compared to 24 hpi in rhizobia-inoculated Control roots. No significant changes were observed in the flavonoid silenced roots in comparison. The GA30ox (TC123648), involved in later stages of gibberellin synthesis, showed a decrease in rhizobia-inoculated *CHS*i roots compared to inoculated Controls, both at 6 hpi. The transcript encoding the rate-limiting enzyme GA20ox's was increased 24 hpi in rhizobia-inoculated *CHS*i roots compared to rhizobia-inoculated Control roots also at 24 hpi. These results suggest that flavonoids may directly or indirectly alter GA biosynthesis during nodulation.

Strigolactones

Strigolactones (SLs) are a newly discovered class of hormones that are increasingly implicated in a number of plant-developmental responses (Ruyter-Spira et al., 2013). SLs are derived from carotenoids and are well-known stimuli for symbiotic arbuscular mycorrhiza fungi (Xie et al., 2010). Recently these molecules have been shown to reduce shoot branching (Gomez-Roldan et al., 2008) and promote nodulation in the roots of pea (Foo and Davies, 2011). Currently, the biosynthesis and mode of action of SLs in nodulation are poorly understood in *M. truncatula*. However, two transcription factors from this model legume NODULATION SIGNALING PATHWAY1 (NSP1) and NSP2 have been shown to be essential for SL biosynthesis (Liu et al., 2011). In legumes NSP1/2 are also crucial in the Nod factor induced signalling pathway leading to activation of early nodulation genes (ENODs) and induction of cortical cell division (Oldroyd and Downie, 2008).

It was found that NSP2 expression was reduced in rhizobia-inoculated *CHSï* roots at 6 hpi compared to rhizobia-inoculated Controls at the same timepoint (Table 4.5). This could potentially indicate that higher NSP2 expression in the latter sample could be a result of 1) an increase in the biosynthesis of SLs during nodulation or 2) an increase due to a functioning Nod factor signalling pathway in these roots, which could increase SL synthesis.

In rice and *Arabidopsis*, DWARF27 (D27) is essential for synthesis of SLs and acts upstream of CCD7 and CCD8 (Waters et al., 2012) that belong to the SL synthesis pathway. D27 converts *trans*-β-carotene to 9-*cis*-β-carotene, the substrate for CCD7. Notably, for the gene *MtDWARF27*, increases in fold change were observed for the following comparisons - CHSE24/CHSB24, CHSE24/CHSE6, CE/CB and CHSE/CHSB (Appendix Table A4.1). This reflects that that the early pathways of SL biosynthesis increases as a result of rhizobia inoculation but this was not affected by the absence of flavonoids in the roots.

The synthesis of and response to auxin, cytokinin, ethylene and gibberellins were modulated by the presence of flavonoids in the roots during early stages of rhizobia inoculations while strigolactone synthesis appeared to be independent of

flavonoids' presence. The changes in plant-hormone synthesis could lead to changes in their concentrations, but this will need to be confirmed in the future by mass spectrometric analysis of the hormones. This could reflect multiple targets and modes of action. An enrichment of reactive pathways through GO enrichment analysis was used to further understand these processes.

Table 4.5 – Changes in expression of selected hormone related genes in flavonoid silenced (*CHS*) and control roots (C) at 6 and 24 hpi with rhizobia (E) or blank media (B). Only significant changes are shown. No significant changes were observed in the listed genes in CE vs CB comparison.

Identifier	TC#	Gene	*CHSE-6 vs CE-6*	*CHSE-24 vs CE-24*	*CE-24 vs CE-6*	*CHSB vs CB*	*CHSE vs CE*	*CHS vs C*
Ethylene								
Mtr.20234.1.S1_at	TC119108	*1-aminocyclopropane-1-carboxylate synthase*	-2.40		-2.43			
Mtr.14782.1.S1_at	TC119510	*1-aminocyclopropane-1-carboxylate oxidase*				-2.11		
Mtr.38034.1.S1_at	TC131421	*1-aminocyclopropane-1-carboxylate oxidase-like*	5.64		3.07	2.93	3.26	3.09
Mtr.41581.1.S1_at	TC131878	*Ethylene response factor required for nodule differentiation (ERD)*	2.41					
Auxin								
Mtr.40263.1.S1_at	TC125691	*Auxin-responsive GH3 product*	3.21			2.80		2.15
Mtr.33354.1.S1_at	BF651172	*GH3 family protein*			-2.32			
Mtr.16954.1.S1_at	TC127344	*Auxin-induced protein 6B*	-2.60					
Mtr.166.1.S1_at	NP7259676	*Auxin-induced protein 6B*	3.31					
Mtr.4658.1.S1_at	AL373405	*Weakly similar to Auxin induced protein 6B*	-2.11		-2.18			
Mtr.33402.1.S1_at	TC133428	*Auxin-induced protein 5NG4*	-2.45		-2.32			
Mtr.11938.1.S1_at	TC115989	*Auxin-induced protein 5NG4*	-2.50		-2.36			
Mtr.45199.1.S1_at	TC139158	*Auxin-induced protein 5NG4*	-2.11		-2.01			
Mtr.11717.1.S1_at	TC119939	*Auxin-induced protein 5NG4*			2.47			
Mtr.32635.1.S1_at	BE247944	*Auxin-induced protein 5NG4*			-2.36			
Mtr.27937.1.S1_at	BF520859	*Weakly similar to auxin induced protein 5NG4*	2.00					
Mtr.49789.1.S1_at	TC136337	*Auxin-induced protein-like protein*	-2.25		-2.07			
Mtr.25935.1.S1_x_at	TC128097	*Auxin-induced SAUR-like protein*	-2.08					
Mtr.25935.1.S1_at	TC128097	*Auxin-induced SAUR-like protein*	-2.02					
Mtr.49764.1.S1_at	TC113258	*Auxin Efflux Carrier PIN9*						2.57
Mtr.1633.1.S1_x_at	TC168199	*2,4-D inducible glutathione-S-transferase*	4.50	5.31		4.40	4.89	4.64
Cytokinin								
Mtr.44246.1.S1_at	TC120060	*Cytokinin-O-glucosyltransferase*			-2.13			
Mtr.38043.1.S1_at	TC115341	*Cytokinin-O-glucosyltransferase*	-2.45		-2.42			
Mtr.174.1.S1_at	TC127591	*Two-component response regulator ARR8*	-2.05					

Table 4.5 continued– Changes in expression of selected hormone related genes in flavonoid silenced (*CHS*) and control roots (C) at 6 and 24 hpi with rhizobia (E) or blank media (B). Only significant changes are shown. No significant changes were observed in the listed genes in CE vs CB comparison.

Identifier	TC#	Gene	*CHSE-6 vs CE-6*	*CHSE-24 vs CE-24*	*CE-24 vs CE-6*	*CHSB vs CB*	*CHSE vs CE*	*CHS vs C*
Gibberellin								
Mtr.38633.1.S1_at	TC131702	*ent-kaurene oxidase*			-2.77			
Mtr.13370.1.S1_at	TC123648	*Gibberellin 3-beta-hydroxylase*	-3.28					
Mtr.15436.1.S1_at	TC113415	*Gibberellin 20 oxidase*		2.21				
Mtr.34199.1.S1_at	TC126191	*Gibberellin 20 oxidase*		2.32				
Strigolactone								
Mtr.44789.1.S1_at	TC112920	*Nodulation-signalling pathway 2 (NSP2)*	-2.81					

4.3.4 *GO enrichment analysis shows a significant over-representation of genes involved in an oxidoreductive response in flavonoid silenced roots*

The genes involved in biological processes in plants were mapped according to their gene ontologies. Selected comparisons of the GO are shown in Appendix Figures A4.2 – A4.8 and the significant pathways are discussed here.

Comparisons of inoculated flavonoid silenced root with inoculated control roots at 6 hpi showed a significant down regulation of 400 transcripts (Figure 4.4 A). GO pathway enrichment analysis mapped these changes to a wide range of functionalities. Among the highly enriched pathways were those that were involved in a response to stimulus (Figure A4.2). This suggests that the flavonoid silenced roots failed to alter gene expression as a response to rhizobia. Other genes involved in metabolic processes relating to metabolism of carbohydrates, nitrogen, amino acids and lipid also showed silencing in flavonoid deficient roots. At 24 hpi, the flavonoid silenced roots showed a sustained reduction in metabolic processes such as synthesis of amino acids and small molecules (Figure A4.3). At 24 hpi, defence response pathways in flavonoid silenced roots were up-regulated (Figure A4.4).

The comparisons of the molecular functions revealed interesting results. The rhizobia-inoculated flavonoid silenced roots at 6 hpi compared to rhizobia-inoculated Control roots also at 6 hpi showed a reduction in oxidoreductase activity and calcium ion binding (Figure A4.5). There were also reduction in transferase activities and these could be implicated in flavonoid biosynthesis. However, contradictorily, the flavonoid deficient roots showed an even larger proportion of gene representations involved in the oxidoreductase activity that were up regulated at 6 hpi with rhizobia (Figure A4.6). This could suggest an up-regulation of defence response activity from the roots. Many of the flavonoid biosynthesis genes downstream of *chalcone synthase* possess transferase activity and therefore, represented an enriched pathway that was up regulated at 6 hpi in *CHS*i roots. At 24 hpi, the molecular function enriched in the flavonoid silenced roots continues to show an increase in oxidoreductase activity (Figure A4.7), and a

decrease in transferase activity that is likely associated with flavonoid biosynthesis (Figure A4.8).

Changes in redox related transcript abundance show multiple changes

A detailed exploration of the microarray data showed multiple changes to redox related transcript abundances as shown in Table 4.6. NADPH oxidases have been suggested to be a major source of ROS production in plants. In root hairs, they have been demonstrated to activate Ca^{2+} influx channels for ABA signalling as a stress response (Coelho et al., 2002, Foreman et al., 2003, Kwak et al., 2006). The data in Table 4.6 show that expression of transcripts encoding NADPH oxidase was up-regulated in *CHS*i roots compared to Control roots. Up-regulation of these genes suggests that ROS generation by NADPH oxidase was higher in *CHS*i roots. A comparison of Control roots between 6 and 24 hpi also showed a higher expression of transcript encoding NADPH oxidase at 24 hpi with rhizobia. Although the literature has reported that increases in ROS production in *M. truncatula* occurred as early as 3 hpi (Cárdenas et al., 2008), the differences in the physiological properties of *M. truncatula* hairy roots could imply that the timeline for induction is different from seedling roots.

Flavonoids are also antioxidative molecules (Hernández and Van Breusegem, 2010) and their absence could be responsible for an increase in other antioxidative enzymes such as peroxidases, glutathione S-transferases, thioredoxins and lipoxygenases to prevent a hypersensitive response and cell death in infected roots Hérouart et al., 2002.

Peroxidase enzymes are a major group of anti-oxidative enzymes in plants. While some transcripts of peroxidase genes were increased in *CHS*i roots compared to control roots, a few others were decreased. Interestingly, one of the genes that was silenced in flavonoid deficient roots encoded *rhizobium induced peroxidase* or *RIP1* (TC113389). RIP1 is crucial for nodule formation (Cook et al., 1995, Ramu et al., 2002) and therefore, the expression of this gene was explored further using qRT-PCR (as discussed in the following section). RIP1 is involved in the cross-linking of

the cell walls and development of infection threads at the site of rhizobia infection (Ramu et al., 2002).

Glutathione S-transferases (GSTs) are a versatile group of enzymes involved in the tagging of products for oxidative breakdown (Marrs, 1996). They also have the ability to directly scavenge for peroxides. Several copies of the *GSTs* show an increased expression in *CHS*i roots (rhizobia-inoculated or BMM-inoculated) at 6 and 24 hpi compared to Control roots. Some *GST* transcripts (TC123031 and TC178462) changes were only observed in rhizobia-inoculated control roots. The increase in GST activity in the *CHS*i roots suggests an increased scavenging activity. This increase could be to compensate for lack of the antioxidative flavonoids. In addition, the increased GST activity would likely alter the redox signalling and H_2O_2 mediated cross-linking of infection thread formation.

Two isoforms of thioredoxins (TC119349, TC125417) were found to show differential expression. The symbiotic specific s-type thioredoxin (TC119349) (Alkhalfioui et al., 2008) showed a decrease in the rhizobia-inoculated *CHS*i roots compared to rhizobia-inoculated control roots. The h-type thioredoxin that has been reported to be induced due to stress exposure (Alkhalfioui et al., 2008), was up-regulated in the *CHS*i roots. This suggested that *CHS*i roots were not responding to rhizobia as a symbiont but perceived it as a biotic stress agent. This is not surprising as symbionts and pathogenic responses share many commonalities in infection pathways (Zamioudis and Pieterse, 2012) and flavonoids might serve to differentiate one from the other.

Another source of ROS in the roots could result from the enzyme activity of lipoxygenases. These enzymes are involved in the oxidation of polyunsaturated fatty acids by oxygen and results in the production of hydroperoxides and O_2^- radicles (Lynch and Thompson, 1984, Becana et al., 2000). It was observed that the lipoxygenases were down regulated in inoculated flavonoid silenced roots compared to inoculated control roots. Therefore, this would decrease the amount of cellular ROS production (in contrast to NADPH oxidases). The overall changes in redox potential of the cell dependent on opposing ROS generations and scavenging

could be important for establishment and progress of bacterial infection in the roots.

To test whether changes in redox status of *CHSi* roots would affect infection thread formation, the changes to development of infection threads in the root hairs were examined (Figure 4.6). Control and *CHSi* roots were inoculated with GFP-labelled rhizobia that overexpressed Nod factors (E65-gfp). The Control roots showed root hair curling (a) and infection thread formation (b) 48 hpi. While *CHSi* roots were observed to form curled root hairs (c), as also found by Wasson et al. (2006), *CHSi* roots were not found to harbour any infection threads (d). The changes in the redox signalling as previously discussed could be responsible for the lack of infection threads in rhizobia inoculated *CHSi* roots.

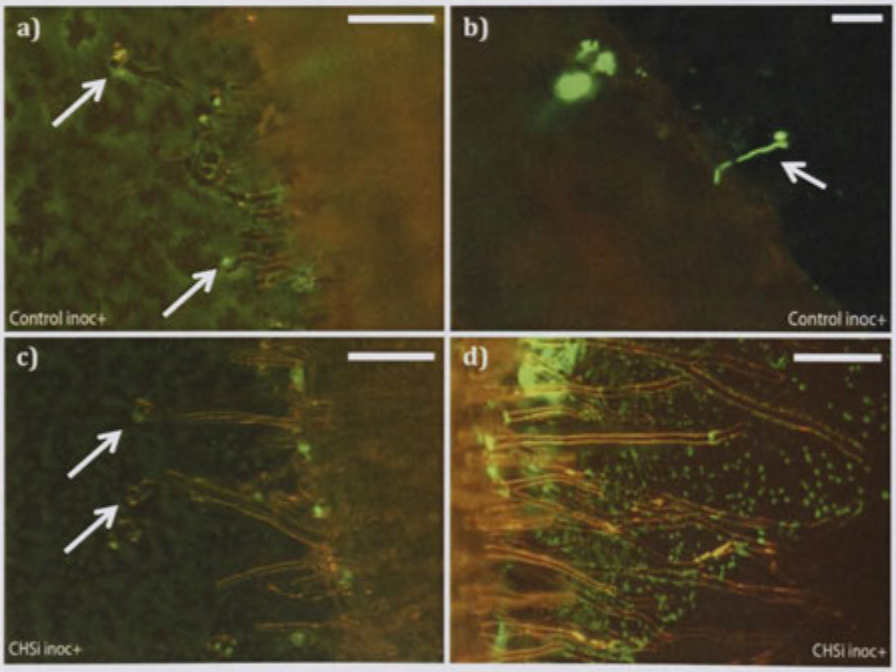

Figure 4.6 – The changes in root-hairs observed in Control (a-b) and *CHSi* (c-d) roots after inoculation with E65-gfp. Curling of root hairs was observed in both Control (a) and *CHSi* (c) roots (arrows) but infection threads only formed in Control (b) (arrow) and not in *CHSi* (d) roots. At least 10 roots were screened for each sample at 48 hpi with E65-gfp. Bars represent 100 μm.

Table 4.6 – Significant fold-changes in expression of redox related genes in flavonoid silenced (CHS) and Control roots (C) at 6 and 24 hpi with rhizobia (E) or blank media (B). Only significant changes are shown. No significant changes were observed in the listed genes in CE vs CB comparison.

Identifier	TC#	Gene	CHSE-6 vs CE-6	CHSE-24 vs CE-24	CE-24 vs CE-6	CHSB vs CB	CHSE vs CE	CHS vs C
Glutathione S-transferase								
Mtr.38111.1.S1_at	TC123357	*Glutathione S-transferase 19*	4.74	2.46	3.17	2.52	3.42	2.93
Mtr.35335.1.S1_s_at	CX550152	*Glutathione S-transferase 12*	4.37	2.56		2.58	3.35	2.94
Mtr.40293.1.S1_at	TC119881	*Weakly similar to Glutathione S transferase*	3.82			2.95	2.80	2.87
Mtr.1633.1.S1_x_at	TC168199	*2,4-D inducible glutathione-S-transferase*	4.50	5.31		4.40	4.89	4.64
Mtr.6489.1.S1_at	TC123131	*Glutathione S-transferase, C-terminal; Thioredoxin-like*		3.61		2.14	2.77	2.44
Mtr.43621.1.S1_at	TC175901	*Glutathione S-transferase*	3.42	2.20		2.29	2.74	2.51
Mtr.12316.1.S1_at	TC121824	*Glutathione S-transferase*	2.60				2.12	
Mtr.39734.1.S1_at	TC124916	*Glutathione S-transferase*			-2.31			
Mtr.10494.1.S1_x_at	TC123031	*Glutathione S-transferase*	2.92		2.14		2.21	
Msa.1760.1.S1_at	TC113984	*Partially similar to glutathione S-transferase-like*			-2.08			
Mtr.11377.1.S1_at	TC178462	*Similar to Glutathione S-transferase*	2.98		2.23		2.14	
Peroxidase								
Mtr.43507.1.S1_at	TC182277	*Seed coat peroxidase precursor*	3.51		2.80	2.28	2.83	2.54
Mtr.41137.1.S1_at	TC179440	*Partially similar to Peroxidase 11 precursor*	2.06		2.94			
Mtr.12601.1.S1_at	TC183217	*Peroxidase 5*	3.00				2.08	
Mtr.25211.1.S1_s_at	TC113389	*Rhizobium induced peroxidase, rip1*	-2.72		-2.02			
Mtr.25211.1.S1_at	TC113389	*Rhizobium induced peroxidase, rip1*	-2.50					
Mtr.46628.1.S1_s_at	TC127622	*Peroxidase*	-2.27					
Mtr.38220.1.S1_at	TC115891	*Peroxidase*	-2.14					
Mtr.42141.1.S1_at	TC128539	*Peroxidase*		2.07				
Mtr.18570.1.S1_at	NP7267887	*Peroxidase*			3.39			
Mtr.14592.1.S1_at	TC114005	*Peroxidase*			3.37			
Mtr.10373.1.S1_at	TC129282	*Peroxidase*			2.72			
Mtr.46047.1.S1_at	BG585312	*Peroxidase*			-2.39			
Mtr.15379.1.S1_at	TC113407	*Peroxidase*			-2.01			
Mtr.40970.1.S1_at	TC129031	*Weakly similar to cationic peroxidase 1-like*				2.84		2.23
Mtr.31637.1.S1_at	AL373292	*Partially similar to Peroxidase*						-2.05

Table 4.6 continued – Significant fold-changes in expression of redox related genes in flavonoid silenced (CHS) and Control roots (C) at 6 and 24 hpi with rhizobia (E) or blank media (B). Only significant changes are shown. No significant changes were observed in the listed genes in CE vs CB comparison.

Identifier	TC#	Gene	*CHSE-6 vs CE-6*	*CHSE-24 vs CE-24*	*CE-24 vs CE-6*	*CHSB vs CB*	*CHSE vs CE*	*CHS vs C*
NADPH oxidase								
Mtr.38954.1.S1_at	TC125263	*NADPH oxidase*	8.68		2.22	2.56	3.59	3.03
Mtr.12656.1.S1_at	TC176766	*NADPH:quinone oxidoreductase*	2.47	3.48		2.57	2.93	2.75
Thioredoxin (TRX)-like superfamily								
Mtr.48820.1.S1_at	TC141262	*Glutathione peroxidase (GPx)*	-2.59		-2.58			
Mtr.12557.1.S1_at	TC130088	*Weakly similar to L-ascorbate oxidase homolog*			2.06			
Mtr.40666.1.S1_at	TC119349	*Thioredoxin s2*	-2.20					
Mtr.9679.1.S1_at	TC125417	*Thioredoxin H2*	3.34		2.76			
Lipoxygenase								
Mtr.46868.1.S1_s_at	TC122215	*Lipoxygenase*	-4.81			-2.89		-2.40
Mtr.46870.1.S1_at	TC118775	*Lipoxygenase*	-4.39			-3.19		-2.48
Mtr.8427.1.S1_at	TC122096	*Lipoxygenase*	-2.85	2.22	-6.01			
Mtr.46863.1.S1_s_at	TC119040	*Lipoxygenase*	-2.26					
Mtr.50427.1.S1_at	TC132688	*Seed lipoxygenase*	-2.01					
Mtr.50430.1.S1_at	TC112628	*Lipoxygenase*			-4.12			

Transcript abundance of Rhizobium induced peroxidase (RIP1) increases during early interactions with rhizobia and is dependent on flavonoids

The expression of *RIP1* (TC113389) transcript measured through the microarray analysis showed distinct reduction when flavonoid-silenced roots were compared to control roots after rhizobia inoculation (Table 4.6). These changes were confirmed using quantitative RT-PCR as shown in Figure 4.7. The data presented show the fold change in transcript abundance at 6 and 24 hpi in Control and *CHS*i roots relative to the respective BMM-inoculated roots (dashed line at 1). Gene expression of *RIP1* was significantly increased in rhizobia-inoculated Control roots at 6 hpi compared to mock-inoculated Control roots at 6 hpi. There was also a significant difference of expression of *RIP1* between rhizobia-inoculated Control roots at 6 and 24 hpi. Comparatively there was no change in expression due to rhizobia inoculation in flavonoid-silenced roots. However, there was a difference in relative expression of *RIP1* in rhizobia-inoculated Control and *CHS*i roots at 6 hpi confirming the previous results.

The enzyme RIP1 is an early nodulin gene and its sequence analysis indicates the presence of sequence motifs that are homologous to ROS binding *cis*-elements (Ramu et al., 2002). Infection with rhizobia and NF leads to a rapid generation of ROS in a localised region of the root likely through Ca^{2+} signalling. NF perception has been reported to induce *RIP1* transcription in the epidermal cells that is at its maximum levels 3 hpi in *M. truncatula* seedling roots (Passardi et al., 2005, Ramu et al., 2002).

Plant peroxidases possess a variety of functions in many plant-developmental processes (see introduction 1.3). In the context of symbiosis, the peroxidases are required for cross-linking and alterations of the cell walls to assist in infection thread formation (Salzwedel and Dazzo, 1993, Ramu et al., 2002). Alternatively, peroxidases are mediators of ROS levels that contribute to signalling events. Subtle alterations of the cell's redox states are crucial for plant-signalling processes that trigger pathways for successful development of nodules in the roots (Marino et al., 2009). These pathways include activation of GTP binding proteins and transcription factors that could be influenced in their phosphorylation state

through changes in redox potential, consequently leading to a myriad of functional changes (Ramu et al., 2002). In my results, I observed a significant increase in *RIP1* transcript at 6 hpi in control roots but not in flavonoid silenced roots. This could imply that flavonoids interfere with the Nod factor perception pathway at the early stage thus preventing RIP1 activation.

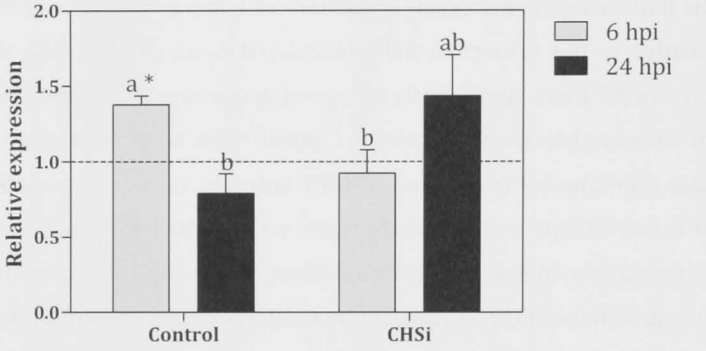

Figure 4.7 – Relative expression of *RIP1* transcript when inoculated roots were compared with un-inoculated roots at 6 and 24 hpi. The asterisk (*) shows significant difference in expression of *RIP1* transcript compared to un-inoculated roots (indicated by a dashed line). The differences between groups are indicated by different letters. All comparisons were made with One-Way ANOVA with Tukey-Kramer multiple comparison tests (Mean ±SEM shown for 3 biological repeats each with 3 technical replicates).

Nodulation in flavonoid-silenced (CHSi) roots could not be rescued with redox inhibitors

The extensive increase as well as decrease in oxidoreductase activity justified an enquiry if application of redox inhibitors were sufficient to rescue nodulation in *CHS*i roots. The synthetic chemical EUK and diphenylene iodonium (DPI) were used to prevent generation of ROS which might be causing a defence response against the rhizobia in *CHS*i roots. EUK-134 is a scavenger of $O_2^{\bullet -}$ as it mimics the activity of superoxide dismutase (SOD) and DPI is an inhibitor of NADPH oxidases (Zhang et al., 2014). The concentrations of DPI and EUK-134 used in this study were chosen based on the effects in *M. truncatula* measured by Zhang et al. (2014).

Application of either EUK or DPI reduced the nodulation capacity of Control roots and did not increase any nodule numbers in *CHS*i roots (Figure 4.8). In addition, it was observed that the application of ROS inhibitors also had inhibitory effects on root growth (not measured). This showed that ROS play a crucial role in not just nodule organogenesis, but other developmental processes as well.

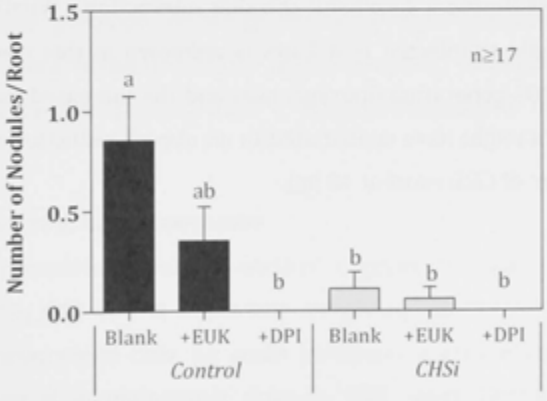

Figure 4.8 – Number of nodules 14 dpi with E65 in the presence of ROS inhibitors EUK and DPI is shown for Control and flavonoid deficient (*CHS*i) roots. Different letters indicate significant difference based on One-Way ANOVA with Bonferroni Multiple Comparison Test (Mean ±SEM shown).

ROS accumulated in the root hairs of control roots but not CHSi during root-rhizobia interactions

To test the whether the changes in the expression of genes related to the generation of ROS resulted in the changes in the accumulation of ROS during early stages of nodulation, a histochemical staining method was used to visualize the ROS in Control and *CHS*i roots.

Figure 4.9 shows the ROS accumulation in control and *CHS*i transformed hairy roots of *M. truncatula* after inoculation with E65 through H_2-DCFDA staining. The images show a time course of the accumulation of ROS at 6 hpi (a,d), 24 hpi (b,e) and 48 hpi (c,f) with rhizobia in Control (a-c) and *CHS*i (d-f) roots.

In both control and *CHS*i-transformed roots, strong ROS staining was located in the epidermal cells of the zone of root-elongation and the zone showing ROS staining was more extensive in *CHS*i roots, although this was not quantified.

However, staining was found in the Control roots hairs at 48 hpi (c) while this was absent in *CHS*i roots (f). This confirmed the up-regulation of the accumulation of ROS in the roots during a successful rhizobia interaction. Whether this staining was confined only to infected root hairs is unknown at this stage. The reduced expression of ROS generating lipoxygenases and the increased expression of ROS scavenging GSTs might have contributed to an overall reduction in ROS observed in the roots hairs of *CHS*i roots at 48 hpi.

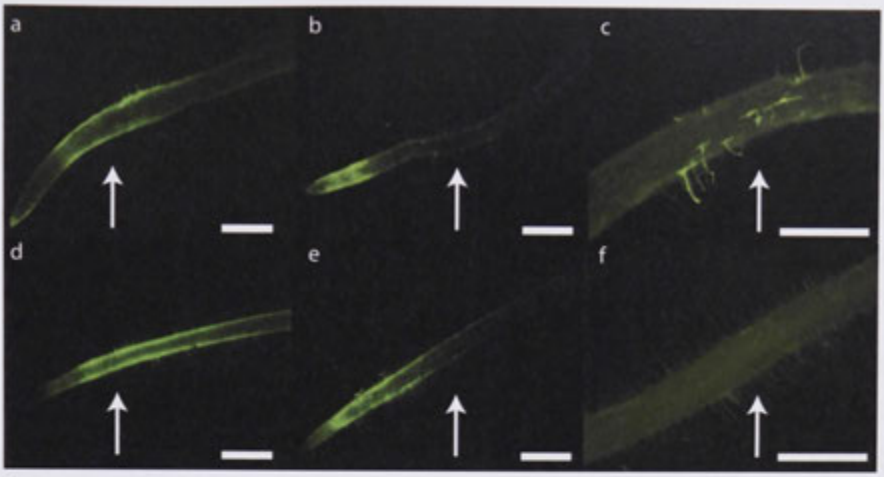

Figure 4.9 – A time course of images showing the accumulation of ROS in the Control roots (a-c) and *CHS*i roots (d-f) at 6 hpi (a,d), 24 hpi (b,e) and 48 hpi (c,f). All roots were stained with 2',7'-dichlorodihydrofluorescein diacetate (H_2DCFDA) that is converted to highly fluorescent 2',7'-dichlorofluorescein (DCF) in the presence of ROS. Bars represent 1 mm. At least 10 roots were stained to show the presence of ROS for each time-point and genotype. The white arrow indicates the location of the spot inoculation with rhizobia.

The ROS in roots were also stained using a) nitroblue tetrazolium (NBT) that detects superoxide anions and b) diaminobenzidine tetrahydrochloride (DAB) that identifies hydrogen peroxide. Although the roots were stained, there was no observable difference between Control and *CHS*i roots. However, ROS staining methods require further quantification in future to accurately determine these changes.

ROS regulation of root apical meristem

The root apical meristem (RAM) contains a group of slowly dividing cells (Quiescent Centre, QC) and is important for giving rise to root structures in response to environmental cues. An auxin maximum is critical at the QC for cell specifications and it is maintained through PAT, auxin synthesis and auxin breakdown. Although the mechanism of action of auxin on QC is unknown, it is thought that this hormone acts through modifying the cellular redox state (Mathesius et al., 2011).

High auxin concentrations have been correlated with generation of ROS such as H_2O_2 and $O_2^{\cdot-}$ (Joo et al., 2001, Pfeiffer and Höftberger, 2001, Schopfer, 2001, Schopfer et al., 2002). It may be that peroxidase catalysed oxidation of IAA might be responsible for free radicle generation (Kawano, 2003) or ROS generation could be linked to activity of auxin on other redox-associated systems (Jiang et al., 2003, Kisu et al., 1997, Kawano, 2003, Pignocchi and Foyer, 2003, Jiang and Feldman, 2005).

As discovered in maize, there is a difference in the redox states of QC and adjacent RAM; where QC is highly oxidizing and RAM is highly reducing. Interestingly, the pattern of redox state could shifted by changing the location of the auxin maximum (Jiang et al., 2003, Kerk and Feldman, 1995). More importantly, the redox state influences the cell division actvity in plants (Vernoux et al., 2000).

As *CHS*ì roots lacked crucial flavonoids mediating auxin transport and accumulation, it is likely to have influence on cell division in the meristematic tissue. In future, it would be useful to use techniques such as immunolocalisation of IAA and laser capture microdissection of the RAM to understand more specific influences of flavonoids in this region.

4.4 Conclusions

A lack of flavonoids due to silencing of the *CHS* gene family led to a strong reduction in nodule numbers. While exogenous application of auxin transport inhibitors could induce pseudonodules in *CHS*i roots, these were not infected, suggesting plant flavonoids play additional roles in infection of rhizobia. Findings in this chapter confirmed that no infection threads were formed in *CHS*i roots inoculated with rhizobia. Therefore, the microarray based transcript abundance analysis was undertaken to discover additional roles of flavonoids in plant-rhizobia symbioses.

Hormonal response and redox response are likely targets of flavonoids during nodulation

The classical hormones ethylene, auxin, cytokinin and gibberellin showed changes in abundances of several genes encoding enzymes that are involved in hormone synthesis. Suppression of ethylene signalling is important for the initiation of infection thread formation during nodule development (Oldroyd et al., 2001). This event is closely followed by changes in auxin and cytokinin signalling to initiate cortical cell divisions (Ferguson and Mathesius, 2014). Even though the PAT could be inhibited and cell divisions induced with TIBA application in *CHS*i roots, this did not produce infected nodules. It is likely that the ethylene and gibberellin signalling at early stages is central for IT formation. It is also proposed that in addition to affecting auxin transport, flavonoids affect the expression of other proteins of the common nodulation signalling pathway at the infection site. The cross-talk and interplay of these proteins with plant hormones provides further basis to study the roles of flavonoids further in future.

ROS accumulation rather than inhibition is important for nodule initiation

The GO enrichment analysis of differentially expressed genes in *CHS*i roots showed a significant enrichment of oxidoreductive pathways. The decrease in concentrations of several peroxidases in rhizobia-inoculated *CHS*i roots compared to rhizobia-inoculated Controls perhaps pointed to increases in accumulation of ROS as a defence response in *CHS*i roots. However, a rescue attempt blocking the

ROS generation did not increase the number of nodules formed on the *CHS*i roots. It is likely that a constant decrease in ROS does not initiate IT formation. A specific timing for up- and down-regulation of ROS-relating enzymes may be required that is difficult to mimic using exogenously applied inhibitors.

The cellular machinery is a constant source of ROS generation in plant cells. The antioxidative properties of flavonoids may be important as a detoxifying mechanism to prevent damage to the cellular components. In addition, there are a number of other ROS scavenging enzymes that are able to subtly control the redox activity of the cells.

ROS accumulation is an important requirement during nodulation to trigger pathways in nodule organogenesis. Co-localisation of ROS and RIP1 in the root hairs could be important for mediating the growth of an infection thread that rhizobia traverse through as they move towards the dividing inner cortex (Ramu et al., 2002). Therefore, the lack of flavonoids may be contributing to – 1) inability of roots to distinguish a symbiotic bacteria from a pathogen thus preventing the access of all microbes towards the inner cortex or 2) the increased synthesis of redox scavenging enzymes to compensate for loss of antioxidative activity in the cells.

The increased expression of NADPH oxidase and reduction in lipoxygenase and *RIP1* suggested that the ROS generation was altered in flavonoid-silenced roots. The changes in antioxidative activity could be preventing successful host-colonization. Staining of the roots showed that there was no accumulation of ROS in the root hairs at 48 hpi at the infection site in *CHS*i roots, and no successful infection threads were found. This supports the hypothesis that IT progression is dependent on flavonoids.

Given the importance of ROS in the multiple developmental activities during nodule organogenesis at the RAM, it was expected that inhibition of ROS did not yield in a successful colonization of *CHS*i roots with rhizobia. Therefore, it is likely that ROS mediated processes in activation of nodulation related genes, as well as

changes in the cytoskeleton play a central role in nodule organogenesis. Crucially, ROS activity is potentially facilitated by the flavonoids whose antioxidative properties may allow it to manipulate the cellular events. The role of flavonoids in manipulating auxin concentrations may have indirect roles in maintaining an active QC at the RAM.

Appendix

A4.1 Microarray Statistical Analysis

Figure A4.1 Sources of variations in 4-way ANOVA comparisons

Table A4.1 – Fold changes in transcripts across the ANOVA comparisons in *CHS*ï and Control roots 6 and 24 hpi with E65 rhizobia or Blank media.

Results of GO enrichment analysis

Figure A4.2 *CHS*E6 vs CE6 Down-regulated genes showing enrichment of biological processes

Figure A4.3 *CHS*E24 vs CE24 Down-regulated genes showing enrichment of biological processes

Figure A4.4 *CHS*E24 vs CE24 Up-regulated genes showing enrichment of biological processes

Figure A4.5 *CHS*E6 vs CE6 Down-regulated genes showing enrichment of molecular functions

Figure A4.6 *CHS*E6 vs CE6 Up-regulated genes showing enrichment of molecular functions

Figure A4.7 *CHS*E24 vs CE24 Up-regulated genes showing enrichment of molecular functions

Figure A4.8 *CHS*E24 vs CE24 Down-regulated genes showing enrichment of molecular functions

Chapter 5. The roles of flavonoids in plant-pathogen interactions

Summary

Many flavonoids are known to play defensive roles in plant-pathogen interactions. In both symbiotic and pathogenic interactions, flavonoids appeared to act via auxin and redox modulation. In this chapter, I discuss the implications of silencing or overexpressing different genes encoding enzymes of the flavonoid biosynthesis pathway on the metabolic flux changes that accompanies root responses to pathogenic fungi and oomycete.

Here, I have discussed experimental studies where I challenged roots with altered flavonoid profiles to the pathogenic fungi *Rhizoctonia solani* AG8 and oomycete *Aphanomyces euteiches*. *R. solani* AG8 represents a major challenge in agriculture with significant losses to productivity. By overexpressing *IFS*, I have demonstrated that root growth improved in *R. solani* infected plants. This has not been reported before as *R. solani* AG8 is considered particularly good at detoxifying phytoalexin flavonoid compounds.

Flavonols and isoflavonoids emerged as prime candidates for regulating auxin accumulation likely through PAT inhibition in *M. truncatula*. Flavonols and isoflavonoids also regulated the plant defence response and this may be through their effect on auxin homeostasis.

One of the mechanisms through which roots evade pathogen is through secondary root formation and ROS accumulation. The flavonoids are likely to have roles in both these processes as they have been demonstrated to be ATI (Chapter 3) and ROS modulator (Chapter 4).

5.1 Introduction

The role of flavonoids in interactions between plant and pathogens is described in this chapter. The studies focused on the role the different flavonoid branches play in enhancing plant protection or making the roots more susceptible to infections. The root pathogens used in this study were the fungi *Rhizoctonia solani* AG8 and the oomycete *Aphanomyces euteiches*.

Rhizoctonia solani causes extensive field damage

The fungal pathogen *Rhizoctonia solani* causes major yield limitation for no-till cereal crops such as wheat or barley. The root-rot disease caused by this fungus creates bare patches on the ground with plants that produce little or no grains. There have not been any cultivars of wheat or barley that show resistance to *Rhizoctonia* (Yin et al., 2013a). The annual yield losses experienced by Western Australia in cereal due to *R. solani* induced root rot disease are estimated to be up to 5 % and up to $ 27 million in wheat and barley alone (Hüberli et al., 2013).

The fungus *R. solani* is a basidiomycete that reproduces asexually primarily through a vegetative mycelium or uniformily textured sclerotia. The fungus occasionally produces sexual spores (basidiospores) that are not enclosed in a fruiting body. The groups of *Rhizoctonia* are also subdivided based on hyphal anastomosis reactions determined by the vegetative compatibility between isolates (Carling and Sumner, 1992). Eleven anastomosis groups have been described ranging from AG-1 to AG 10 and AG-BI. The isolate of *R. solani* responsible for root-rot of cereal crops in Australia belongs to the anastomosis group 8 (AG-8) and it has been observed to be the most destructive of all other groups (Ogoshi et al., 1990).

The damage caused by *R. solani* is not limited to cereal crops and its damaging effects are seen in legumes and brasiccas as well (Hane et al., 2014). *R. solani* severely affects the roots of *M. truncatula* where it causes necrosis of the roots leading to stunted growth and bare-patches are observed in the field (Streeter et al., 2001). It is particularly damaging to the seedling roots where its invasion leads

to disintegration of root cortex, causing a characteristic spear tipping (Ogoshi et al., 1990).

The oomycete Aphanomyces euteiches

Oomycetes are a diverse group of eukaryotes that have often been mistaken for fungi to which they are phylogenetically unrelated. The oomycete *Aphanomyces euteiches* has been shown to have a biotrophic association with legumes (Nyamsuren et al., 2003). This pathogen is reported as a major limitation in cultivation of economically important legume crops (Gaulin et al., 2007) with up to 80 % yield losses reported in Pea crops (Djébali et al., 2013).

The lifecycle of this oomycete commences from germination of oospores close to the host roots leading to the release of bi-flagellate zoospores that are attracted to root exudates. Once the zoospores adhere to the surface of the roots, they penetrate possibly through the formation of a specialized appressorium. The mycelium grows through the root cortex and eventually producing the next generation of oospores that are released into the soil as the roots decay (Kjoller and Rosendahl, 1998, Nyamsuren et al., 2003).

It has been shown that several isoflavones including 5,4' –dihydroxy -7-methoxy-isoflavone or prunetin, genistein and biochanin A as well as their glycosides strongly attract zoospores of *A. euteiches* (Sekizaki and Yokosawa, 1988, Yokosawa et al., 1986). Contradictory to this, it was also reported that phenolics such as isoflavonoids accumulated in resistant *M. truncatula* lines could contribute towards resistance, however, this was not directly shown (Djébali et al., 2009).

M. truncatula wild type A17 plants are shown to be resistant to *A. euteiches* infection. The roots showed browning due to accumulation of phenolic compounds but no effect on plant growth have been reported (Gaulin et al., 2007). It was shown that the increased pericycle cell divisions of the root in resistant lines provide extra structural barriers that prevent stele colonization and produce additional secondary roots. This provided a useful system to study if alteration of

flavonoid metabolites in *M. truncatula* A17 roots varied its ability to protect against *A. euteiches* infection.

It was found that *CHS*i roots' gene expressions of defence response including changes in antioxidative genes and pathogenesis response genes were widespread as a result of rhizobia interactions (as shown in Chapter 4). Therefore, in this chapter, the aim was to challenge the roots with altered flavonoid profiles with root pathogens *R. solani* and *A. euteiches* and identify if the flavonoid content is related to an increase in disease tolerance. The disease resistance in this case is measured by the changes in root growth, which has been shown previously to be useful determinant of disease severity (Schneebeli et al., 2014).

Flavonoids as plant defence compounds

Plant defence related flavonoids are often categorized as phytoanticipin or phytoalexins (Dixon, 2001). The phytoanticipin flavonoids are pre-formed during normal plant-developmental processes and contribute to the innate immunity of the plants against pathogenic attacks. The phytoalexin flavonoid synthesis is induced due to a challenge or stress.

Surveys of plant defence compounds have revealed many flavonoids possessing antimicrobial (Ostroumova et al., 2013, Cushnie and Lamb, 2005) and antifungal properties (Grayer and Harborne, 1994). Cushnie and Lamb (2005) extensively reviewed the anti-microbial mechanisms of action of flavonoids that includes inhibition of DNA gyrase, cytoplasmic membrane function and energy metabolism. Jiménez-González et al. (2008) also hypothesise that flavonoids induce cellular membrane degradation of the microorganism and act as either bacteriostatic or bactericidal agents. In addition, Jiménez-González et al. (2008) also summarise the antifungal activities of several isoflavonoids that suppress germination of fungal spores and penetrate fungal cell to inhibition its growth. In barley, flavonoids such as proanthocyanidins and dihydroquercetin interfere with the cross-linking of enzymes; inhibit microbial cellulases, xylases and pectinases; inactivate enzyme by chelation of metals required for their activity; and possibly form a physical barrier

like structure to prevent hyphal penetration (Skadhauge et al., 1997, Treutter, 2005).

The abovementioned defence mechanisms induced by flavonoids are also likely to constitute a hypersensitive response and programmed cell death during a pathogen infection (Beckman, 2000). Flavonoids and other phenolics are often located in specific cell layers. For instance, catechin and gallocatechin have been observed to be located in all root cap and endodermal cells and in cells around emerging secondary roots of cotton (Mace et al., 1978). In *Arabidopsis*, similar localisation studies showed the accumulation of quercetin in the subcellular nuclear area, plasma membrane and endomembrane systems; and kaempferol in the nuclear regions and plasma membranes (Peer et al., 2001).

This compartmentalisation of flavonoids is hypothesised by Beckman (2000) to assist in engaging rapid protection against stress stimulus and form the first line of defence. In addition, if the stress persists, the phenolic compounds localised elsewhere could sustain a further metabolic cascade through IAA and ethylene to produce a peridermal defence (Beckman, 2002).

Exudation of flavonoids in to the rhizosphere attracts and induces Nod factor synthesis in nitrogen fixing bacteria capable of forming symbiotic relationship with most legume plants (Peters et al., 1986, Redmond et al., 1986). Flavonoids have also been reported to be elevated in roots interacting with mycorrhizal fungus (Lagrange et al., 2001, Siqueira et al., 1991). These have been addressed in detail in Chapter 1.

Interestingly, some pathogenic plant-interacting microorganisms such as the oomycete *Phytophthora sojae* and the fungal pathogen *Fusarium solani* have also adapted to be attracted to root-exuded flavonoids (Morris and Ward, 1992, Ruan et al., 1995). Several species of *Botrytis* and *Colletotrichum* have also been reported to hydroxylate and metabolise flavonoids such as medicarpin into 6a,7-dihydroxymedicarpin that does not possess any antifungal activity (Ingham, 1976).

Metabolic engineering for plant disease resistance

Engineering the flavonoid biosynthesis pathway presents an exciting opportunity to improve plant disease resistance. Although many of the antimicrobial and antifungal compounds are produced through a cascade of enzymes, it is possible to engineer single step conversion of ubiquitous metabolites into potent defence compounds. For example, naringenin could yield sakuranetin through o-methylation; isoflavonoids could be isoprenylated; or stilbenes could be produced from malonyl co-A (Dixon, 2001).

Complex manipulation of the flavonoid biosynthesis pathway is more challenging as it presents several restrictions to generation of desired end products. This has been discussed further in Chapter 1. In overexpressing a biosynthesis enzyme, many of the flux control points are not well understood and could yield completely different end results as found in Chapter 2. However, as this study is designed to systematically silence or overexpress different flavonoid synthesis branches, it serves as an initial point of understanding how these fluxes could be diverted. In this chapter, the aim was to ascertain if the manipulation of flavonoid synthesis enzymes yielded in any significant changes in growth and susceptibility of engineered roots towards pathogen attack.

5.2 Methods

Media and growth conditions for R. solani and A. euteiches

The oomycete *A. euteiches* was cultured on cornmeal agar as described below. 15 g of cornmeal polenta (purchased from local supermarket) was added to a muslin cloth bag and placed in 1 L of distilled water. The water was gently boiled for 30 minutes. The cloth bag with the cornmeal polenta was discarded and the remaining water was brought up to 1 L again with distilled water and adjusted to pH 7.0. 12 g of J3 agar (Gelita Australia) was added to this and autoclaved before pouring on to sterile 9 cm ø petri dishes.

The culture medium for the fungus *R. solani* was potato dextrose agar (PDA). 39 g of commercially available PDA mixture (Sigma, USA) was added to 1 L of distilled water and autoclaved. The media was poured on sterile 9 cm ø petri dishes for subsequent use.

Inoculation methods for R. solani and A. euteiches

Roots were transformed as previously described in Chapter 2, to express gene silencing constructs for *CHS, FLS, IFS, DFR* and *FSII* in pK7GWIWG2D(II) vector and gene overexpression constructs for *CHS, FLS, IFS* and *DFR* in pK7WG2D vector. *DFR* overexpression led to very low transformation efficiency (Figure 2.5) and only a limited number of roots could be generated for investigating root-pathogen interactions.

The plant roots were inoculated with a uniformly sized mycelial plug from a plate that actively grew *R. solani* or *A. euteiches*. For the *R. solani* culture, sterile 9 cm plates with PDA were prepared. A hyphal plug was used to inoculate the center of this plate and grown at 25 °C in the dark for 1 week. Approximately 3 mm x 3 mm x 3 mm hyphal plugs from the edges of the plate, where the hyphae were actively growing, were excised and used for plant root inoculation. One root per plant was selected for inoculation. A similar method was used to inoculate roots with mycelia of *A. euteiches*. The *A. euteiches* was cultured on corn meal agar and grown at 25 °C in the dark for 2 weeks prior to inoculation of the roots.

Root growth measurements

Prior to inoculation with the pathogenic fungi or oomycete, the tips of the roots were marked at the back of the culture dish. The inoculum was placed next to the root tip and the change in growth of the roots was measured relative to this point. After 7 and 14 days, the plants on the agar plates were photographed using a digital camera (Nikon Coolpix P500, Japan) along with a marked ruler for scale. The total root length was measured using ImageJ software (NIH, USA) from photographed roots.

Flavonoid content analysis

One infected *Medicago* root per plant was harvested and snap-frozen in liquid N_2. They were subsequently lyophilized (VirTis Benchtop Freeze Dryer, SP Scientific, USA) for 2 days prior to analysis. The roots were ground using a mortar and pestle. The flavonoid content analysis was performed as described in Chapter 2.2.8.

Statistical analysis

All root growth measurements were compared using one-way ANOVA on GraphPad InStat software (USA) and plotted on GraphPad Prism software (USA). Tukey pairwise comparisons were done to compare multiple data groups. Chi-square test was conducted for proportional analysis of root-growth using GraphPad Prism (USA).

Two way ANOVA was used to compare effects of Genotype vs. Treatment on flavonoid content changes as measured using targeted MS/MS as previously described in Chapter 2. The data were analyzed and plotted using GraphPad Prism (USA).

5.3 Results

The perturbations in flavonoid synthesis led to changes in the growth and susceptibility of the *M. truncatula* hairy roots to the oomycete *A. euteiches* and the fungus *R. solani*. In this section, the response of differentially silenced or overexpressing flavonoid roots to challenges by the two pathogens was assessed. Subsequently the absolute changes in the flavonoid contents of the roots are discussed.

5.3.1 The silencing of FLS reduced the root growth following an infection with A. euteiches

The transgenic hairy roots expressing the hairpin for silencing genes encoding flavonoid biosynthesis enzymes were subjected to root growth assays. This was done to identify the effect of silencing of a particular branch of flavonoid biosynthesis on infection with pathogenic oomycete. Figure 5.1 shows the effects of challenging the transgenic *M. truncatula* plants with *A. euteiches*. The wild type *M. truncatula* A17 is partially resistant to *A. euteiches* and shows slight browning of the roots which could be due to root-rot symptoms or accumulation of phenolics as previously reported (Djébali et al., 2013).

The change in root lengths following infection with a hyphal plug of *A. euteiches* was measured at 7 and 14 days post inoculation as shown in Figure 5.2. At 7dpi the root growth was retarded in *CHS*i roots, however, it was significantly reduced in *FLS*i roots when compared to controls. At 14 dpi the effects were variable and did not identify a significant difference in root length changes.

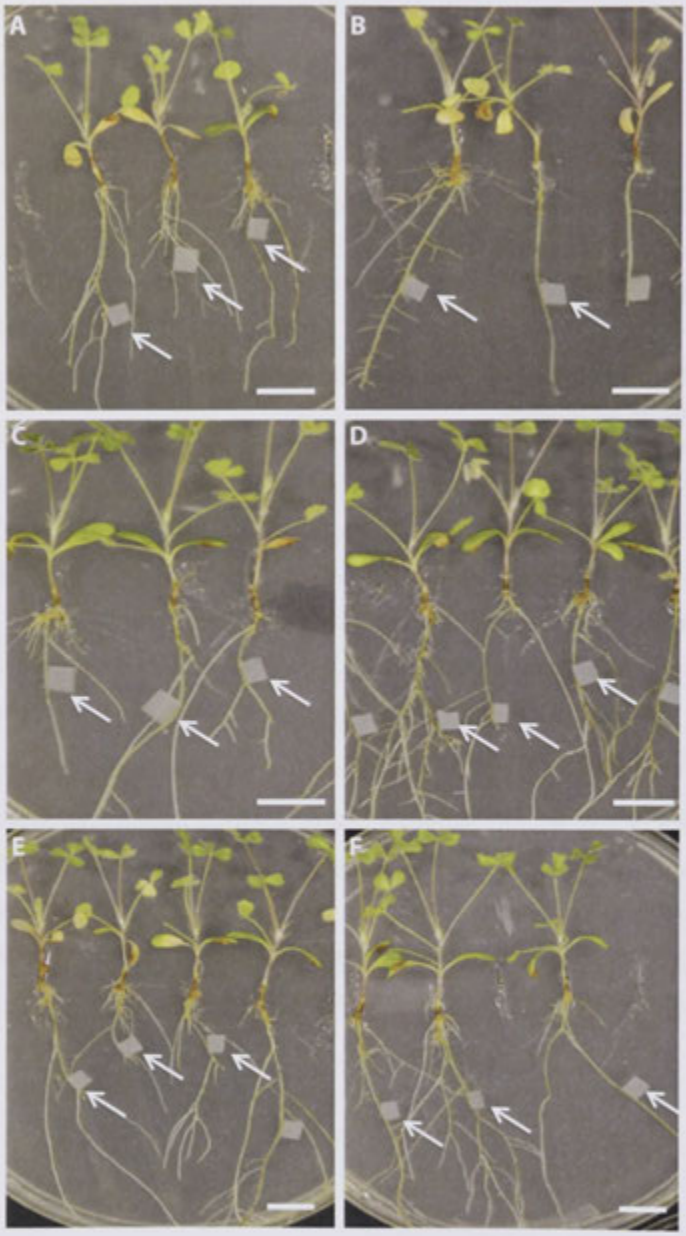

Figure 5.1 – Transgenic hairy roots of *M. truncatula* infected with *A. euteiches* hyphal plug (14 dpi). Letters A-F in order denote the following RNAi hairpin expressing roots – Empty Vector Control, *CHSi*, *FLSi*, *IFSi*, *DFRi*, and *FSIIi*. Scale bars represent 1.5 cm length. The arrows show the *A. euteiches* inoculum.

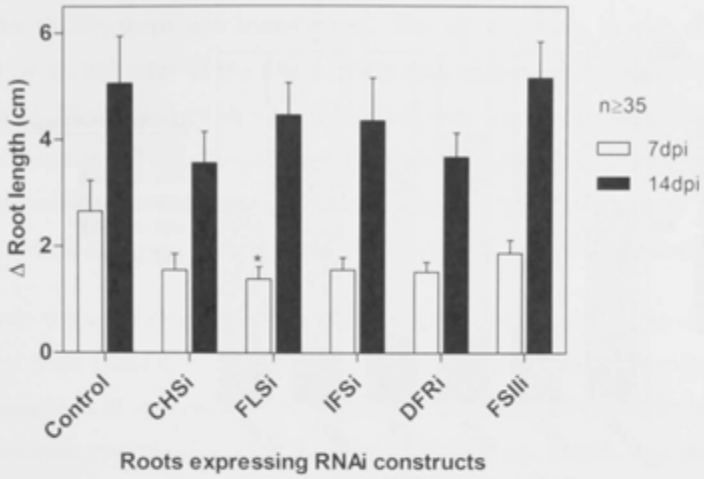

Figure 5.2 – Changes in root length 7 and 14 dpi with *A. euteiches* of roots expressing different RNAi constructs. Mean with SEM shown. Statistically significant difference with the Control is indicated with an asterisk ($P<0.05$ in a one-way ANOVA).

Large variations were observed in the way the roots responded to the infection with *A. euteiches*. Therefore, the changes in root lengths were classified into five categories showing varying degrees of growth (Figure 5.3). At 7 dpi, the distribution of *CHS*, *FLS* and *DFR* silenced hairy roots were significantly different to empty vector control. In all three flavonoid silenced hairy roots, there were a lower proportion of roots that showed greater than 2 cm change in root length. In *DFR* silenced hairy roots, the proportion of roots that showed little or no growth was diminished, while larger proportions were showing moderate levels of growth (0.5 - 2 cm) changes. The distribution of roots at 14 dpi according to changes in root lengths showed that in *CHS* and *FLS* silenced hairy roots there was a larger proportion of roots that showed little or no growth. This suggests that the *CHS* and *FLS* products are necessary for maintaining root growth following infection with *A. euteiches*.

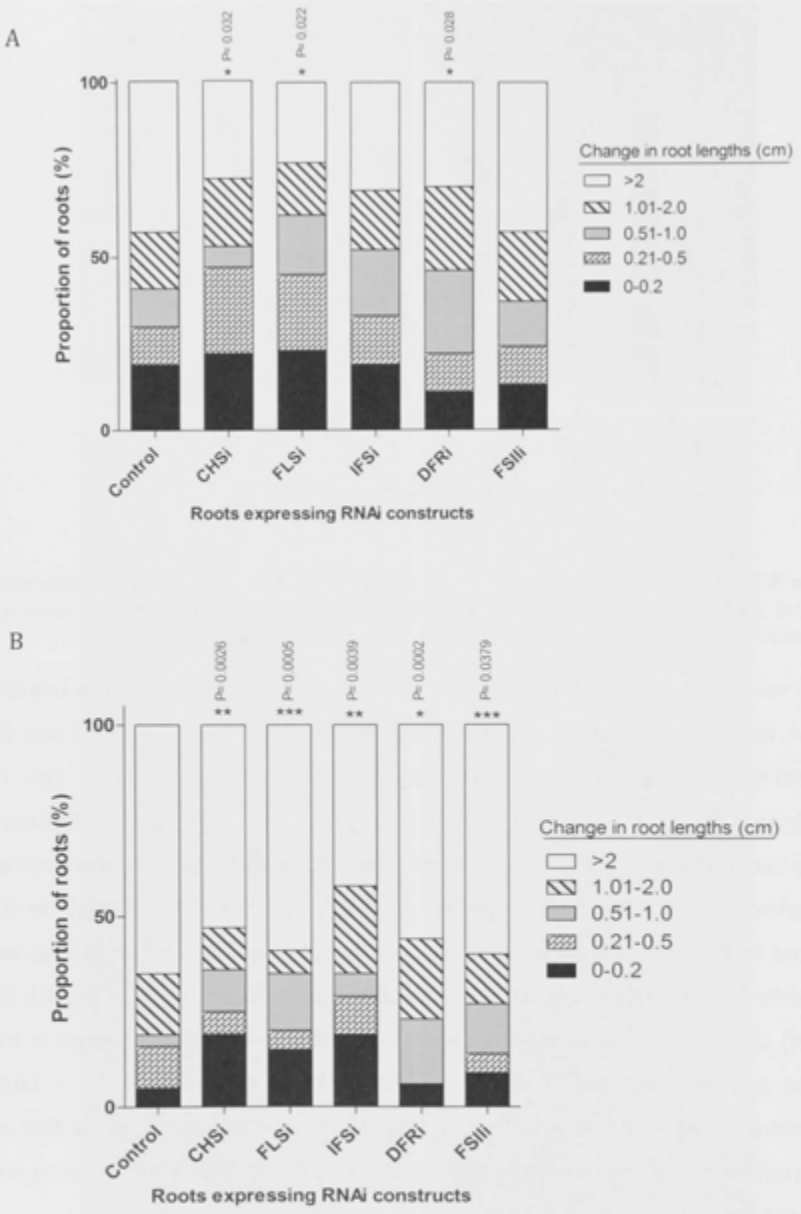

Figure 5.3 – Catogorised changes in root lengths 7 and 14 dpi with *A. euteiches* shown in A and B respectively. The *P*-values indicate significant difference from the control roots based on a χ^2 test.

The roots of these composite plants expressed gene silencing RNAi constructs whilst the shoots were not transformed. The fresh weight of the shoot was recorded as an indicator of the effect of the root pathogenic infection driven by *A. euteiches* (Figure 5.4) 14 dpi. No significant difference was observed between the control and any of the shoot weights of the composite plants in which the roots were expressing flavonoid-silencing constructs. A significant change in shoot weight was only observed in comparisons with *FLS* and *IFS* silenced plants.

It has been reported that roots damaged by pathogens increase the number of secondary roots (Gaulin et al., 2007) and it was suggested that enhanced lateral root formation in *M. truncatula* A17 compared to a susceptible genotype was likely one mechanism contributing to resistance (Djébali et al., 2009). The number of secondary roots that emerged from below the site of inoculation was recorded as shown in Figure 5.5. Although no significant difference was observed, the average number of secondary roots was lower in infected *FLS*i, *IFS*i and *DFR*i roots compared to control roots.

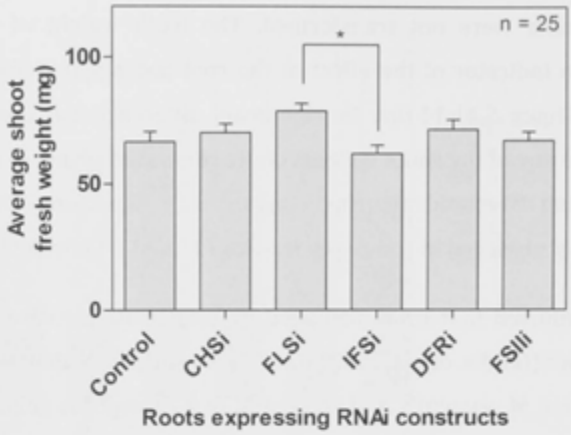

Figure 5.4 – Graph shows the shoot weights of all the composite plants with RNAi expressing roots 14 dpi with *A. euteiches*. Mean with SEM shown. Significant difference was observed only when comparing between FLS and IFS silenced roots (one-way ANOVA)

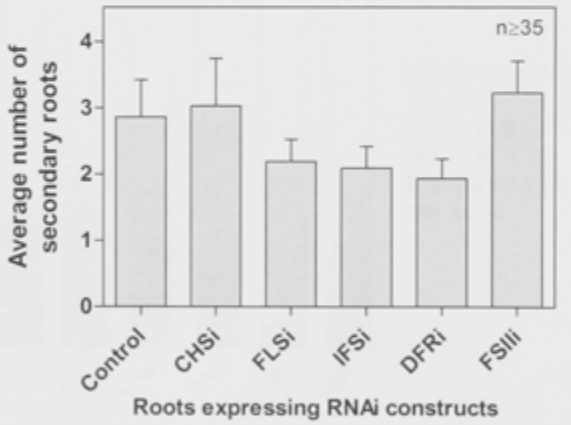

Figure 5.5 – Graph shows the differences in the number of secondary roots that emerged below the site of infection in of all the composite plants with RNAi expressing roots 14 dpi with *A. euteiches*. Mean with SEM shown. No significant difference were observed (one-way ANOVA)

5.3.2 *The overexpression of DFR gene increased the roots' tolerance to A. euteiches*

The transgenic hairy roots overexpressing flavonoid biosynthesis enzymes were investigated for changes in root growth upon inoculation with *A. euteiches*. Figure 5.6 shows the characteristic browning of the roots in a similar manner as seedling roots (Figure 5.6 F) and also large variations in how the roots survived the infection. The total root length showed no significant changes in any of the flavonoid overexpressing roots from Control roots subjected to *A. euteiches* infection (Figure 5.7). This was further investigated by categorizing the root length changes according to classifications (Figure 5.8) where 0-0.2 cm representing little of no change, 0.21-0.5 cm representing low increases, 0.51-1.0 cm representing modest increases, 1.0-2.0 cm representing high growth and more than 2 cm representing excellent root growth phenotypes. It was observed that in *IFS* overexpressing hairy roots 7 dpi, a larger proportion of roots showed between 0.2-0.5 cm growth compared to control hairy roots. The *DFR* overexpressing roots consistently showed a larger proportion of roots with the highest growth rate of more than 2 cm at 7 and 14 dpi.

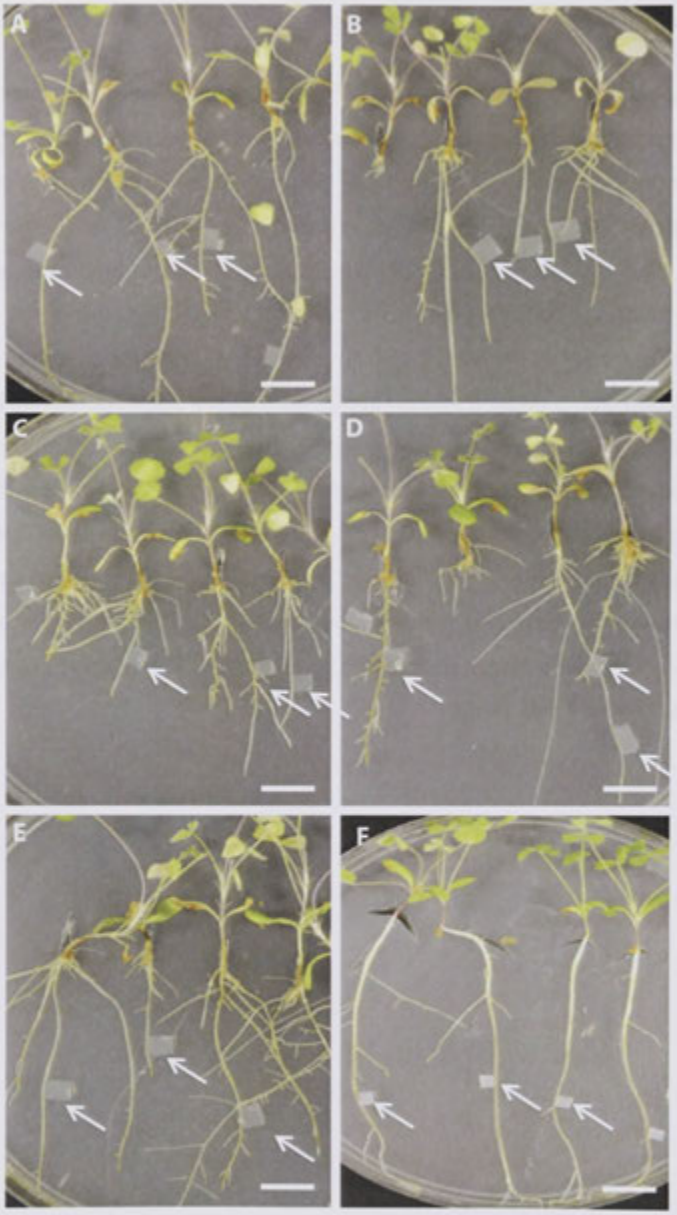

Figure 5.6 – Transgenic hairy roots of *M. truncatula* infected with *A. euteiches'* hyphal plug (14 dpi). Letters A-E in order denote the following gene overexpressing roots – Empty Vector Control, *CHS*, *FLS*, *IFS* and *DFR*. A-E Scale bars represent 1.5 cm length. Typical infection of *M. truncatula* seedling root is shown in F with scale bar representing 2 cm length. The arrows show the *A. euteiches* inoculum

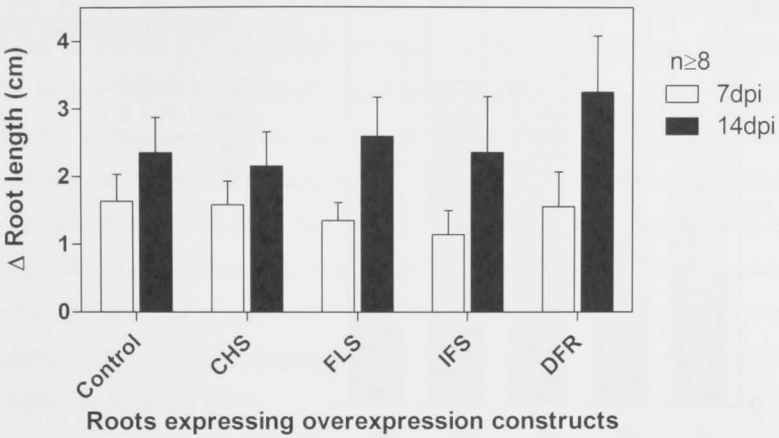

Figure 5.7 – Changes in root length 7 and 14 dpi with *A. euteiches* of roots expressing different flavonoid overexpression constructs. Mean with SEM shown. No significant differences were observed (one-way ANOVA).

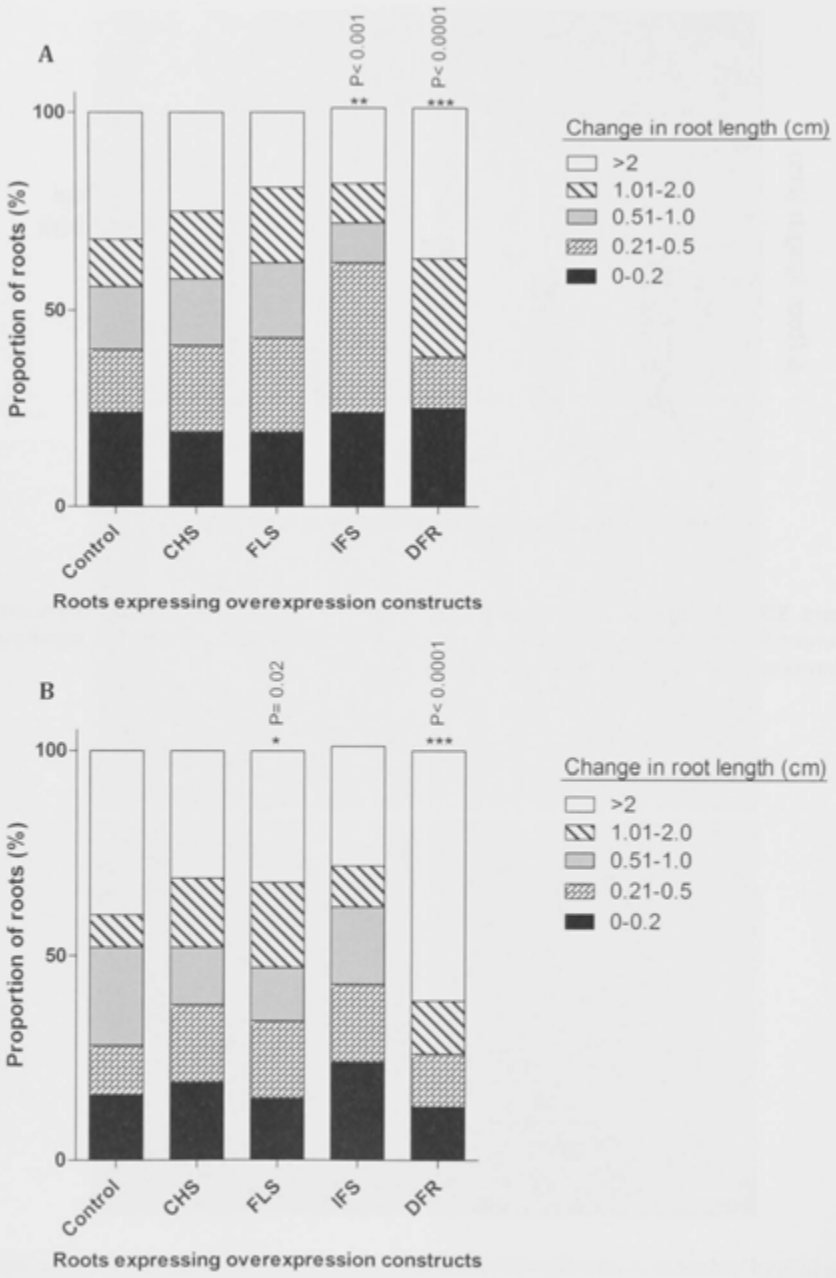

Figure 5.8 – Categorical changes in root lengths 7 (A) and 14 (B) dpi with *A. euteiches* shown in A and B respectively. The *P*-values indicate significant difference from the control roots based on a χ^2 test.

Resistant plants also produced more lateral roots during infection with *A. euteiches* (Gaulin et al., 2007, Djébali et al., 2009). Therefore, the number of secondary roots emerging 14 dpi from below the infection site with *A. euteiches* hyphal plug is presented in Figure 5.9. The hairy roots overexpressing *FLS* and *DFR* showed slightly higher number of lateral roots that emerged from below the site of inoculation, although this was not statistically significant. The distinction was made when the roots were categorized according to the number of secondary roots (Figure 5.10). It showed that the *IFS* and *DFR* overexpressing roots had a significant difference in secondary root emergence pattern compared to control. While the *IFS* overexpressing roots showed a higher proportion of roots with no secondary roots, the *DFR* overexpressing roots showed a higher proportion of roots with 3 to 6 lateral roots.

The shoot fresh weights of these composite flavonoid-overexpressing plants infected with *A. euteiches* were measured (Figure 5.11). The composite plants with roots overexpressing *DFR* showed an increase in shoot weight compared to Control, which could be related to increases in its tolerance to the pathogen.

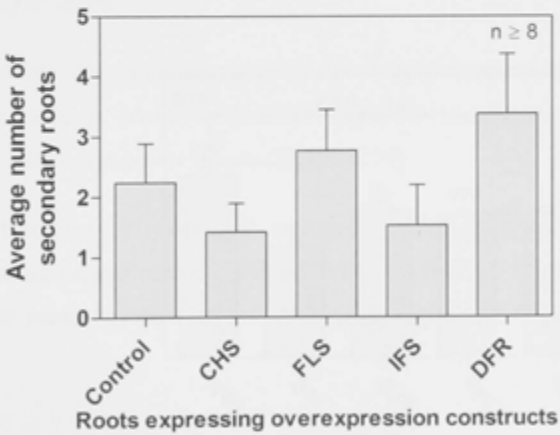

Figure 5.9 – Differences in the number of secondary roots that emerged below the site of infection in of all the composite plants with RNAi expressing roots 14 dpi with *A. euteiches*. Mean with SEM shown. No significant difference were observed (one-way ANOVA)

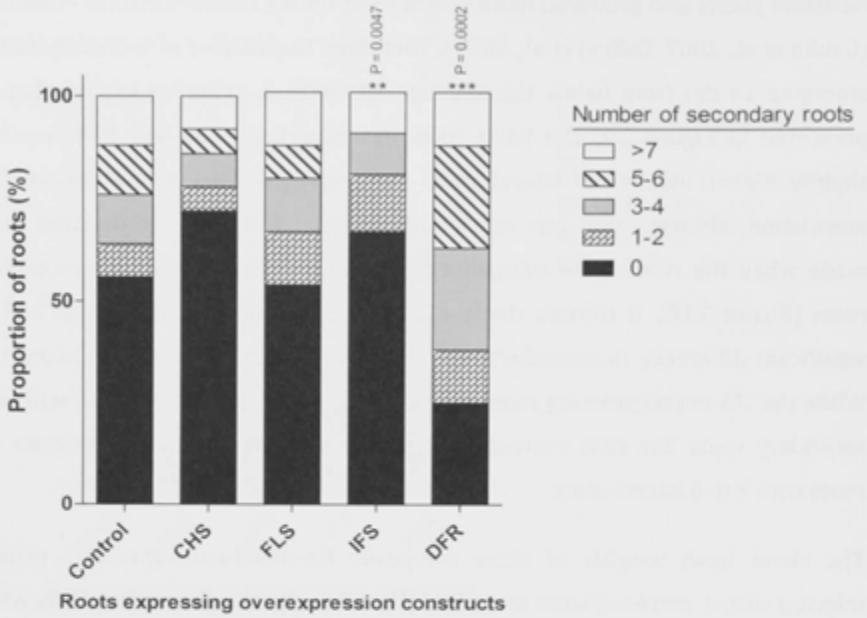

Figure 5.10 – The distribution of emergence of secondary roots from below the site of infection 14 dpi with *A. euteiches* shows significant differences between control and *FLS* as well as *IFS* overexpressing roots ($P<0.005$, χ^2 test).

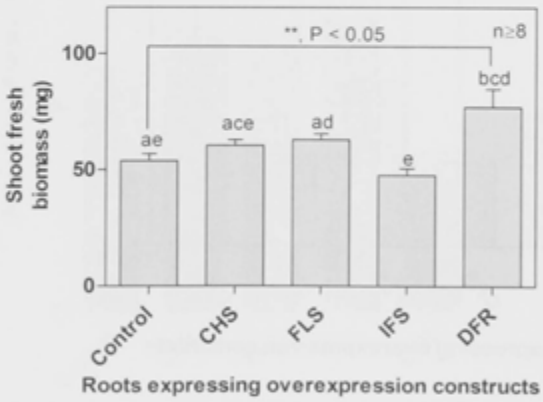

Figure 5.11 – Shoot fresh weights of the composite plants with RNAi expressing roots 14 dpi with *A. euteiches*. Mean with SEM shown. A significant difference was observed between control and *DFR* silenced roots (one-way ANOVA).

5.3.3 *The silencing of FLS and DFR genes significantly reduces roots' tolerance to R. solani*

The transgenic hairy roots expressing flavonoid silencing RNAi constructs were subjected to infection with pathogenic fungi *R. solani* (AG8) (Figure 5.12). A close look at the infection site shows the presence of prolific amounts of hyphae emerging from the agar plug. The infection with these hyphae led to browning of the roots and reduction in its growth in Control roots (Figure 5.12 A). Compared to the control roots, all other transgenic roots expressing flavonoid-silencing constructs showed an increase in root browning (Figure 5.12 B-F). In *DFR*i roots this change was highly visible (Figure 5.12 E) while *FLS*i and *IFS*i also showed increased browning (Figure 5.12 C, D).

The changes to root length were recorded at 7 and 14 dpi with a mycelial plug of *R. solani* (Figure 5.13). The root growth was retarded in all the flavonoid silenced roots, but significantly at 7 dpi in *FLS* and *DFR* silenced roots, and at 14 dpi in *DFR* silenced roots. These roots showed as much as 50 % reduction in change of root length when compared to control hairy roots at the respective time post inoculation. This indicates that the *FLS*i and *DFR*i lines showed stronger damage from infection by *R. solani*.

Surprisingly, the average shoot weight at 14 dpi in these composite plants showed a significant increase in plants with *DFR*i roots. No significant difference was observed in any other composite plants (Figure 5.14).

The number of secondary roots that emerged 14 dpi from below the site of inoculation showed a significant suppression in the *FLS*i roots. A decrease was also observed in *DFR*i roots, but this was not statistically significant (Figure 5.15).

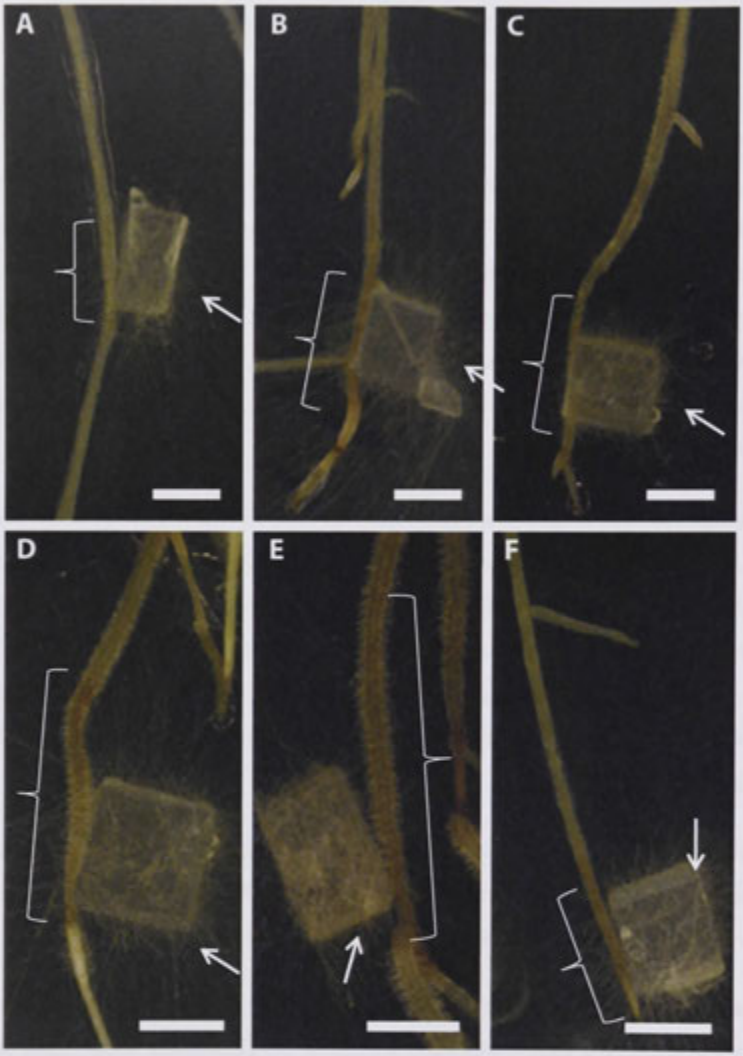

Figure 5.12 - Transgenic hairy roots of *M. truncatula* infected with *R. solani* mycelial plug (14 dpi). Letters A-F in order denote the following RNAi hairpin expressing roots – Empty Vector Control, *CHSi*, *FLSi*, *IFSi*, *DFRi*, and *FSIIi*. Scale bars represent 4mm length. The arrows show the *R. solani* inoculum. Brackets show areas of significant root browning.

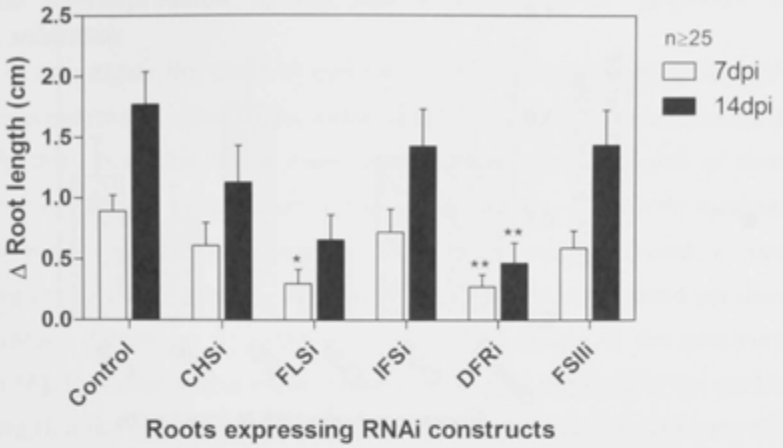

Figure 5.13 – Changes in root length 7 and 14 dpi with *R. solani* in hairy roots expressing different RNAi constructs. Mean with SEM shown. Significance of differences compared to Control indicated with asterisk shows $P<0.05$ in a one-way ANOVA.

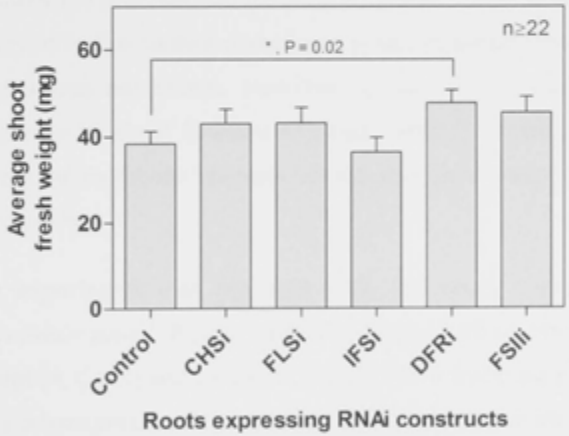

Figure 5.14 – Shoot fresh weights of the composite plants with RNAi expressing roots 14 dpi with *R. solani*. Mean with SEM shown. Significant difference (P=0.02) was observed between control and DFR silenced roots (one-way ANOVA).

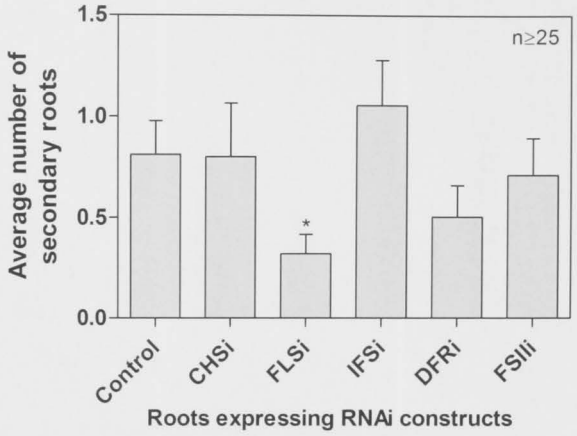

Figure 5.15 – Number of secondary roots that emerged below the site of infection in of all the composite plants with RNAi expressing roots 14 dpi with *R. solani*. Mean with SEM shown. Significant difference compared to Control indicated with asterisk shows $P<0.05$ in a 1-way ANOVA.

5.3.4 The overexpression of IFS increased the roots' tolerance to R. solani

In order to investigate the effect of overexpression of genes encoding flavonoid biosynthesis enzymes on plant roots, a root length change assay was performed as previously described. The initial experiment included overexpression of three flavonoid biosynthesis enzymes encoding genes namely – *chalcone synthase*, *flavonol synthase* and *isoflavone synthase*. These roots were compared to roots expressing empty vector controls at 7 and 14 dpi. The first attempt did not show any significant differences in changes in root length in any of the constructs (Figure 5.16). However, it was evident from the changes observed in the control hairy roots, that the infection with *R. solani* was not severe and the roots were able to grow on average > 2 cm after 7 or 14 dpi.

To confirm that the pathogenic interaction was not severe, the effects on shoot biomass changes were also recorded as in Figure 5.17. Here, the average shoot fresh weight was compared between different composite plants at 14 dpi between *R. solani* inoculated (+) and mock-inoculated (-) plants. There was no significant difference observed in the control plants as a result of pathogenesis, confirming that the infection was not severe. However, it was noticed that there was a significant difference in shoot biomass of plants with *FLS* overexpression. This could be a result of metabolic changes within the plant and requires further investigation in future.

Therefore, the experiment was repeated with the roots overexpressing the flavonoid biosynthesis genes (Figure 5.18). The Figure 5.18 shows the severity of infections at 7 dpi (A, C & E) and 14 dpi (B, D & F). The transformation efficiency of plants with *CHS* overexpression was very low and could not be used in the assay. However, the comparisons were made between Control, *FLS* and *IFS* overexpressing roots as shown in Figure 5.19. The Control hairy roots showed little growth and extensive spread of infection was evidenced by the small change in root growth over time. The roots that overexpressed *IFS* showed significant increase in root growth compared to Control at both 7 and 14 dpi. Although there was a significant increase in root growth observed in the previous assay, the

change was not observed when the pathogenicity of infection with *R. solani* was high.

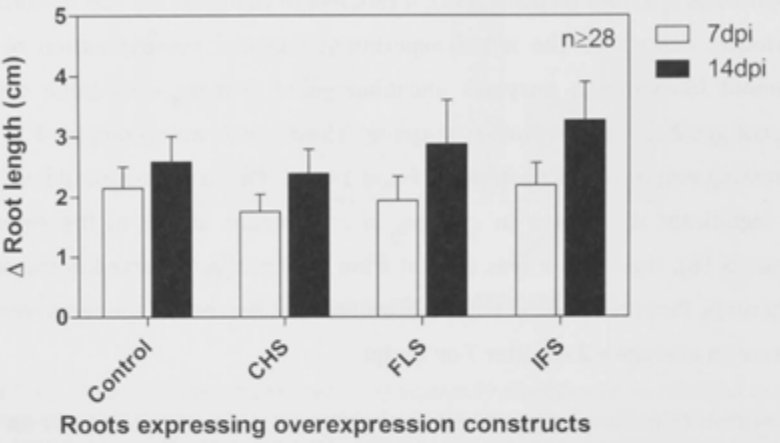

Figure 5.16 – Changes in root length 7 and 14 dpi with *R. solani* of roots expressing different flavonoid overexpression constructs. Mean with SEM shown. No significant differences were observed (one-way ANOVA).

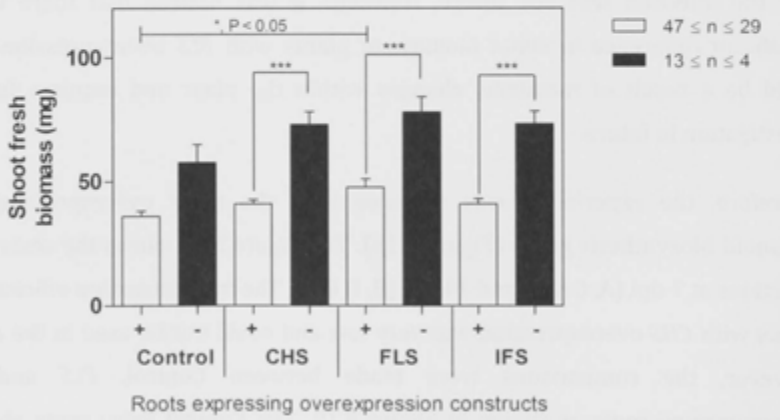

Figure 5.17 – Changes in shoot biomass compared 14 dpi with between *R. solani* inoculated (+) and mock inoculated (-) plants. Mean with SEM shown. Asterisks indicate significant difference compared through one-way ANOVA with post-test.

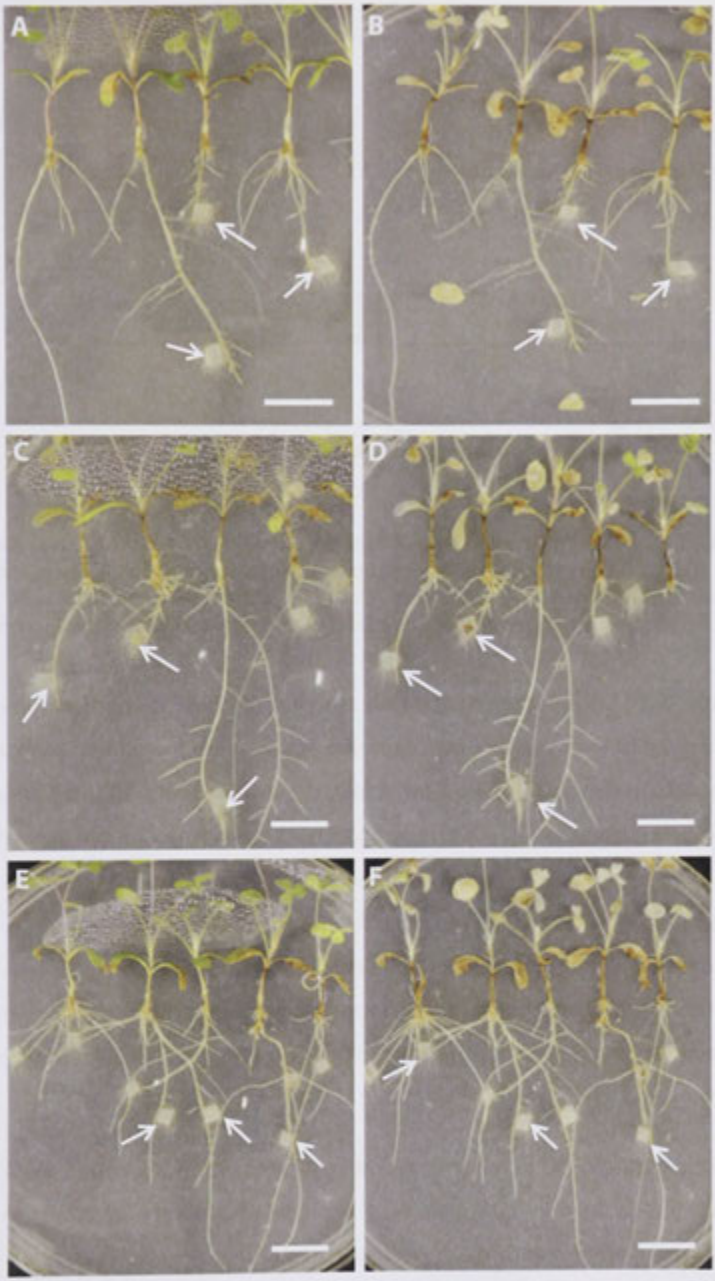

Figure 5.18 – Transgenic hairy roots of *M. truncatula* infected with *R. solani* mycelial plug (7 and 14 dpi). Roots in A, C and E are at 7 dpi. Roots in B, D and F are at 14 dpi. The images represent Empty Vector Control (A&B), *FLS* overexpressing roots (C&D) and *IFS* overexpressing roots (E&F). Scale bars represent 1.5 cm length. The arrows show the *R. solani* inoculum.

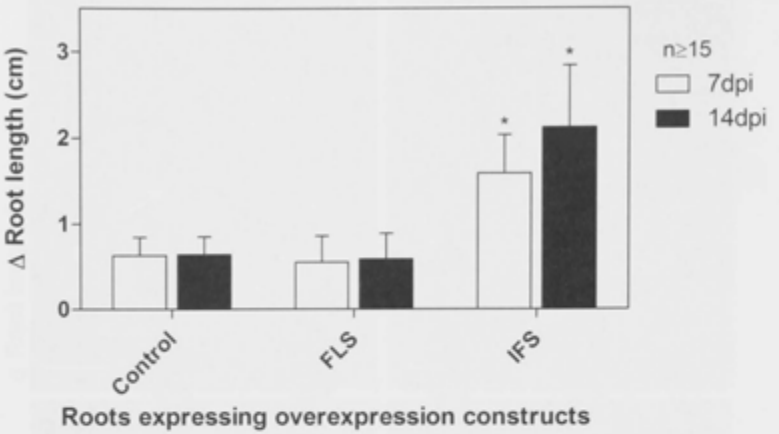

Figure 5.19 - Changes in root length 7 and 14 dpi with *R. solani* of roots expressing different flavonoid overexpression constructs. Mean with SEM shown. Significant differences as indicated with asterisks ($P<0.05$) were observed (one-way ANOVA) between *IFS* overexpressing roots compared with Controls at respective time points.

The Figure 5.20 shows the shoot fresh weights of these composite plants with flavonoid biosynthesis enzyme overexpression that were inoculated with *R. solani*. The comparison was made with uninoculated control plants' shoot. The infection with *R. solani* caused severe reduction in shoot biomass in control as well as *FLS* and *IFS* overexpression plants' shoot biomass compared to uninoculated control thus confirming the severity of the infection. The increase in root length induced in the IFS overexpressing roots was not reflected in the change in biomass of the shoot as no significant difference was found when compared to control. However, there was a decrease in shoot biomass ($P<0.05$) of *FLS* overexpressing composite plants compared to control.

As previously noted, the number of secondary roots emerging from below the site of inoculation site with pathogen may indicate the ability of roots to induce structural reinforcements through pericycle divisions to prevent infection (Djébali et al., 2009). In Figure 5.21, the number of secondary roots that emerged below the site of inoculation is shown. There was a significant increase ($P<0.01$) in the

number of secondary roots in *IFS* overexpressing roots compared to empty vector controls.

Categorising the change in root length 7 and 14 dpi with *R. solani* (Figure 5.22 A and B) indicated a larger proportion of *FLS* overexpressing roots that were unable to grow more than 0.2 cm. However, *IFS* overexpressing roots showed larger proportion that grew more than 2 cm.

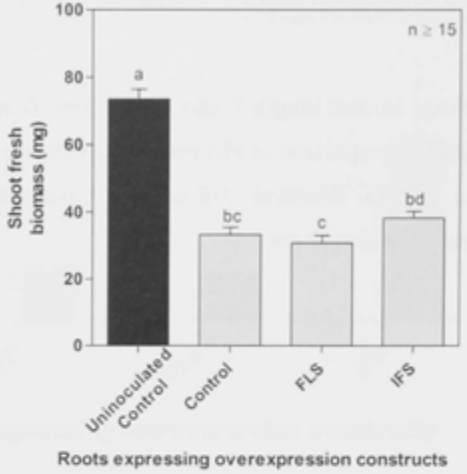

Figure 5.20 – Changes in shoot biomass compared 14 dpi with between *R. solani* inoculated (grey) and uninoculated plants. Mean with SEM shown. Significantly different root samples have been differentially marked with letters (one-way ANOVA).

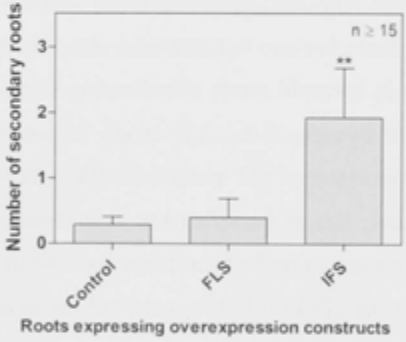

Figure 5.21 – Number of secondary roots that emerged below the site of infection in all the composite plants with RNAi expressing roots 14 dpi with *R. solani*. Mean with SEM shown. Significant changes from Control were observed in *IFS* overexpressing roots (asterisks indicate $P<0.01$, 1-way ANOVA).

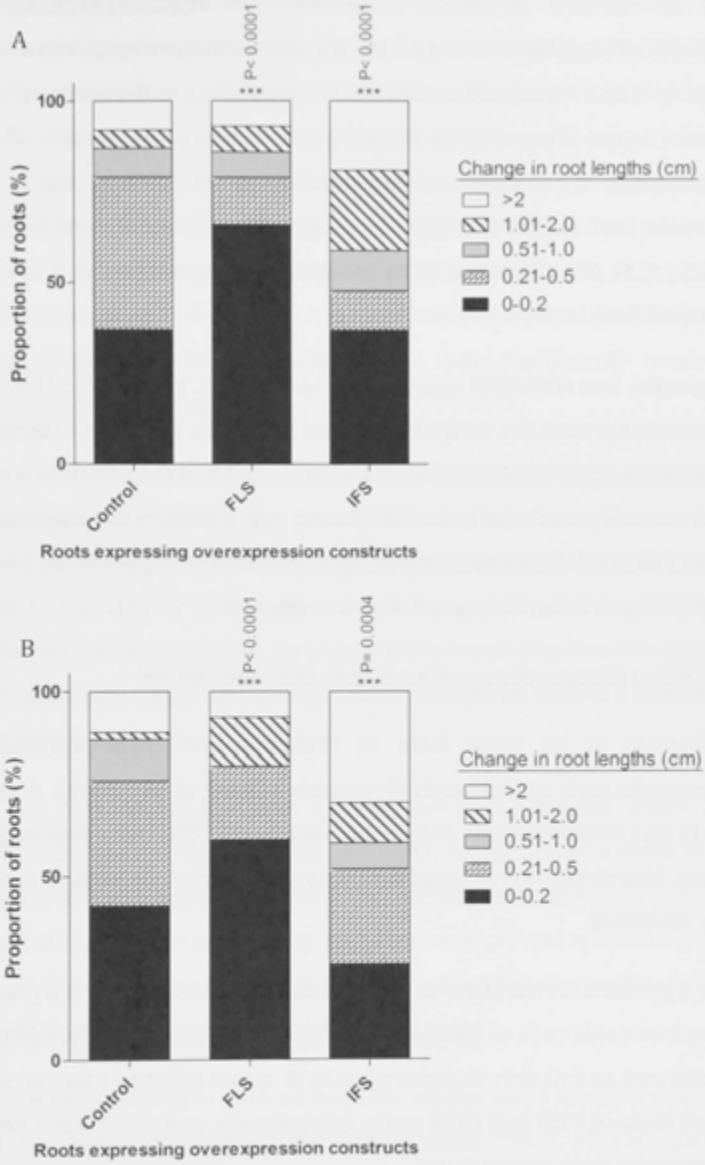

Figure 5.22 – Categorical change in root lengths 7 and 14 dpi with *R. solani* are shown in A and B, respectively. The *P*-values indicate significant difference from the control roots based on a χ^2 test.

Changes in selected flavonoid metabolites in roots expressing various differentially silenced or overexpressed flavonoid biosynthesis enzymes

The Figures 5.23 – 5.25 show the fold-change (FC) differences in flavonoid metabolite content compared to empty vector Control. Three sets of data are shown indicating the changes in uninfected, *R. solani* infected and *A. euteiches* infected roots. Each set has five samples representing FC in different RNAi silenced roots (*CHS*i, *FLS*i, *IFS*i, *DFR*i and *FSII*i) compared to Control (set at 1 and depicted with a dashed line).

In these graphs, two statistical comparisons were made. These were 1) within each of the treatment groups the ANOVA showed if any of the RNAi line differed in their response to pathogen, and 2) ANOVA comparison of FC of flavonoids in a particular RNAi line was also made between uninfected and pathogen treated groups. This comparison showed if a particular pathogen was able to suppress the plant roots' ability to synthesis flavonoids as a defensive response.

The interesting changes observed have been described below –

Isoliquiritigenin is an early form of chalcone that is a precursor to 5-deoxyflavonoids such as 5-deoxyisoflavonoids (Zhang et al., 2009). A significant increase in this compound was detected in uninfected *FSII*i line compared to other RNAi roots. This increase was significantly down regulated by both *R. solani* and *A. euteiches* infections.

Prunin is a glycoside of naringenin. Naringenin is a flavonone that is a precursor to 5-hydroxyflavonoids such as flavonols and flavones (Winkel-Shirley, 2001). Prunin content showed an increase in expression in *R. solani* infected roots compared to uninfected roots in *FLS*i and *DFR*i roots. Interestingly, prunin was not detected in *CHS*i roots in the same comparisons.

Apigenin, luteolin, 7, 4'-dihydroxyflavone (7-4' DHF) and its isomer (n,n DHF) are flavones that may be important in nodulation. Flavones such as luteolin and 7-4' DHF have previously been shown to induce Nod factor biosynthesis in compatible rhizobia (Peters et al., 1986, Redmond et al., 1986, Djordjevic et al., 1987).

However, during a pathogen attack there was no significant change observed in the accumulation of apigenin, luteolin or 7-4' DHF in infected versus uninfected roots. Additionally, in *CHS*i roots infected with *R. solani*, luteolin could not be detected at all. Luteolin biosynthesis was also significantly higher in *R. solani* infected *IFS*i roots compared to other experimental groups. It suggested that the metabolic flux in *IFS*i could be channelled to produce higher amounts of luteolin when isoflavonoid synthesis was suppressed. However, accumulation of the isomer n,n DHF was increased in *R. solani* infected *CHS*i roots compared to uninfected *CHS*i roots suggesting that this unknown isomer may significantly contribute to tolerance against the pathogen.

Formononetin is an isoflavonoid and have been shown to increase in concentration during pathogen attack (Ravnskov et al., 2008). An increase in formononetin was observed in *R. solani* infected *CHS*i roots compared to uninfected *CHS*i roots. This was despite silencing of *CHS*, which led to an overall silencing of the entire flavonoids biosynthesis pathway. An isomer of formononetin was also detected but it did not show any significant changes when compared between uninfected and pathogen infected groups.

Genistin is a glycoside of genistein, an isoflavonoid (Grotewold, 2006). Prunetin and biochanin A are also derived from genistein. A significant increase in genistin accumulation was observed in *R. solani* infected *CHS*i roots compared to uninfected roots, suggesting that this compound must impart important protective advantage to the roots. Similarly, prunetin or biochanin A accumulation was also much higher in *R. solani* infected roots (significantly for *DFR*i roots).

The flavonoid coumestrol is derived from the isoflavonoid daidzein and has been reported as a potent phytoalexin (Gnanamanickam, 1979). This metabolite was induced significantly in *CHS*i and *FSII*i roots infected with *R. solani* when compared to respective uninfected RNAi roots. Together, these data reinforces the importance of isoflavonoids during pathogenesis.

Table 5.1 summarizes the changes in flavonoid content in all the RNAi lines compared to empty vector Control for all three treatment groups (Uninfected, *R. solani* and *A. euteiches* infected). The individual data graphs are shown in Appendix Figure A5.1-A5.2. A coloured arrow represents a significant increase or decrease in accumulation while black arrows represent a change that was statistically insignificant. No change is represented by a '=' symbol while undetectable signal has been shown with the abbreviated 'n.d.'. Three columns have been highlighted in red to show the experimental groups where the infection with *A. euteiches* or *R. solani* retarded the root growth.

Observations in this table show that the silencing of *CHS* led to an overall decrease in several metabolites in all samples. However, in *R. solani* infected roots, some flavonoids were up regulated. The microarray analysis in Chapter 4 showed that the plant compensates for a lack of chalcone metabolites by up-regulating downstream flavonoid biosynthesis genes. It is also crucial to highlight that RNAi silencing does not lead to a complete silencing of the gene expression. During a significantly damaging pathogen attack, the roots managed to produce some flavonoids.

The *FLS* silenced roots showed the highest reduction in root-growth and significant incidence of infection. The *R. solani* and *A. euteiches* infected roots also showed reduction in the flavonol quercetin contents. In addition, a majority of other flavonoids were reduced during the *A. euteiches* infection.

The *DFR* silenced roots infected with *R. solani* were also phenotypically affected in root growth responses. The silencing of *DFR* leads to the silencing of anthocyanin and phlobaphenes as shown in Chapter 1. These metabolites were not targeted during the metabolite analysis due to resource restrictions. It was interesting to observe that silencing of *DFR* significantly decreased metabolite flux to the flavone 7,4'-DHF in uninfected roots. Several other metabolites were also reduced significantly during *A. euteiches* infection but no significant change was observed during *R. solani* infection.

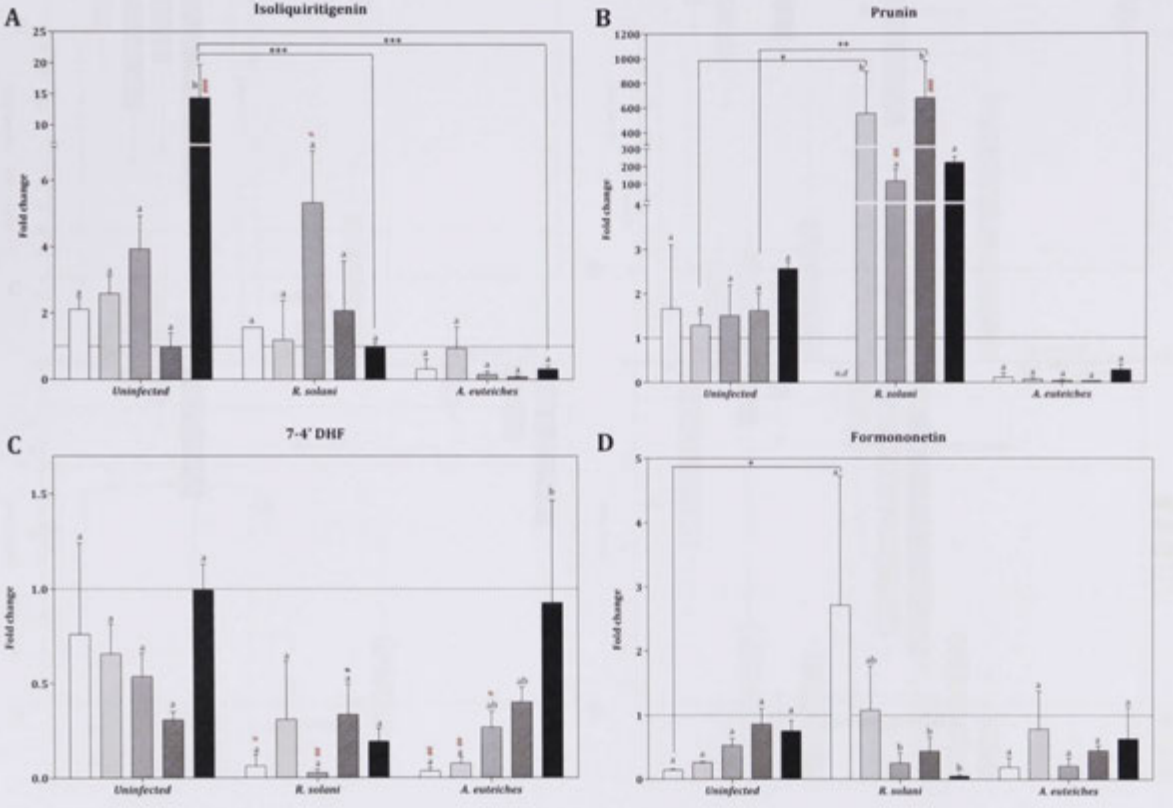

Figure 5.23 – Fold change differences in flavonoid concentrations between control roots, set at 1 (dashed line) and uninfected, *R. solani* infected and *A. euteiches* infected roots expressing RNAi constructs ($P<0.05$ shown by #). All measurements were made 14 dpi. Different alphabets show significant differences in compound FC within each treatment group. Asterisks (*) indicate significant differences between same compounds in different treatment groups.

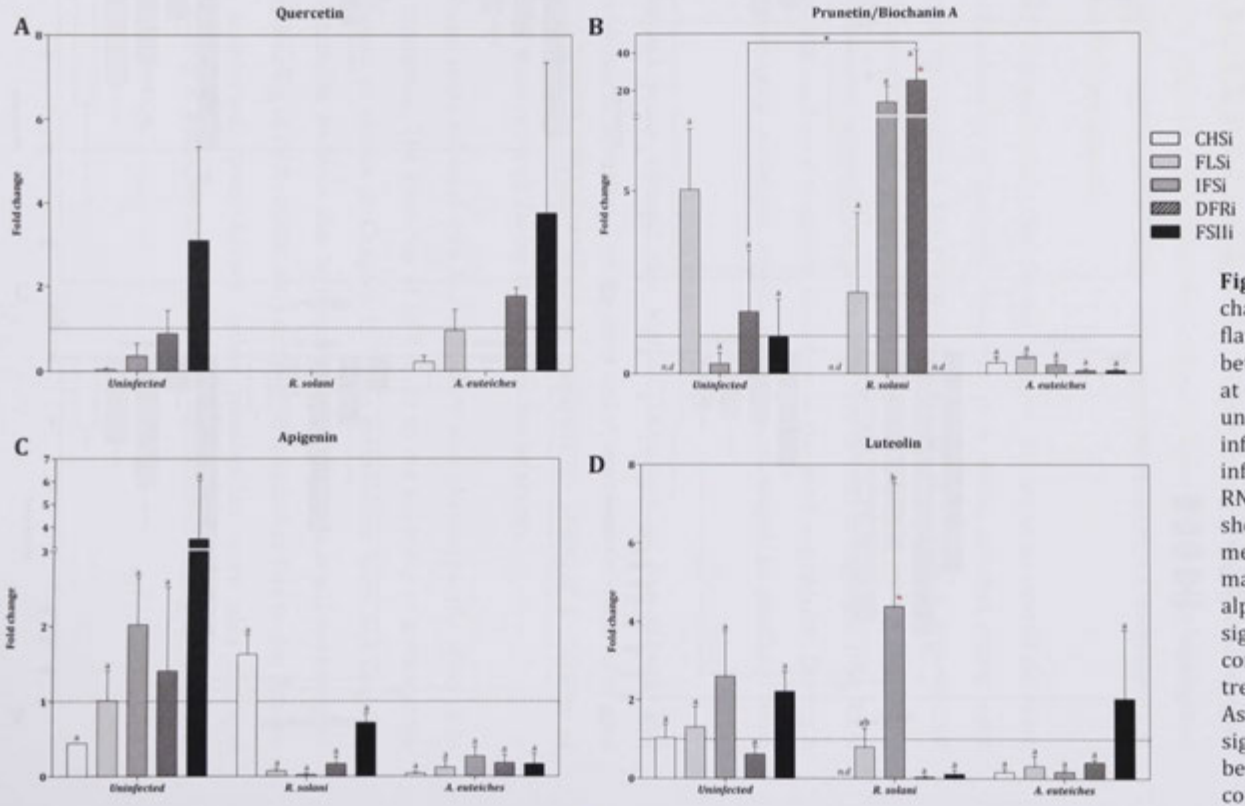

Figure 5.24 – Fold change differences in flavonoid concentrations between control roots, set at 1 (dashed line) and uninfected, *R. solani* infected and *A. euteiches* infected roots expressing RNAi constructs ($P<0.05$ shown by #). All measurements were made 14 dpi. Different alphabets show significant differences in compound FC within each treatment group. Asterisks (*) indicate significant differences between same compounds in different treatment groups.

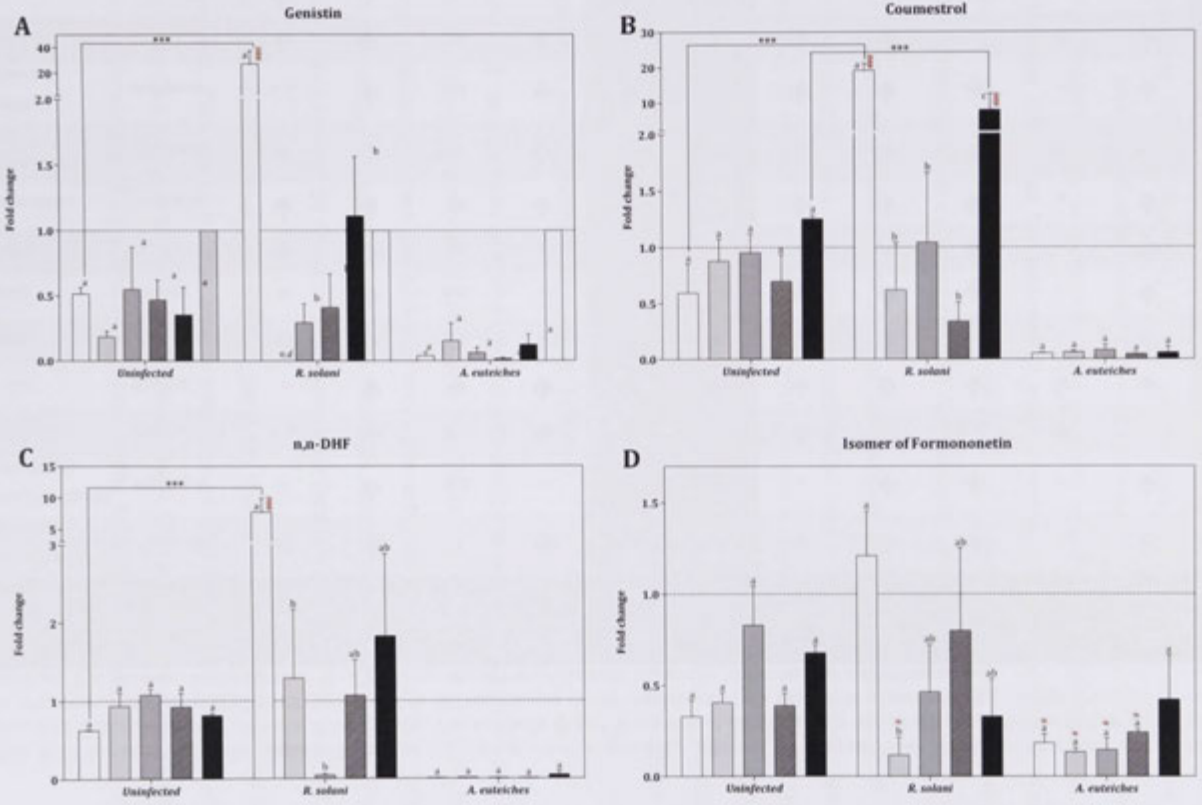

Figure 5.25 – Fold change differences in flavonoid concentrations between control roots, set at 1 (dashed line) and uninfected, *R. solani* infected and *A. euteiches* infected roots expressing RNAi constructs ($P<0.05$ shown by #). All measurements were made 14 dpi. Different alphabets show significant differences in compound FC within each treatment group. Asterisks (*) indicate significant differences between same compounds in different treatment groups.

Table 5.1– A summary of the flavonoid content changes in roots expressing different RNAi constructs compared to empty vector control (EV) expressing roots and challenged with *A. euteiches (Ae)* and *R. solani (Rs)*. The symbols ↑ and ↓ represent significant up and down regulation whilst ↑ and ↓ represent up and down regulation that was not statistically significant compared to EV expressing roots challenged with the same organisms. No change from EV is marked with = and n.d. shows no detection. The columns highlighted in pink show genotypes with reduced tolerance to the respective pathogens.

		CHSi			*FLSi*			*IFSi*			*DFRi*			*FSIIi*		
Flavonoids	**Class**	*Uninfected*	*Ae*	*Rs*	*Uninfected*	*Ae*	*Rs*	*Uninfected*	*Ae*	*Rs*	*Uninfected*	*Ae*	*Rs*	*Uninfected*	*Ae*	*Rs*
Isoliquiritigenin/ Liquiritigenin	Flavanone	↑	↓	=	↑	=	=	↑	↓	↑	=	↓	=	↑	↓	↑
Prunin (Naringenin 7-O-glucoside)	Flavanone	=	↓	n.d.	=	↓	↑	=	↓	↑	=	↓	↑	↑	↓	↑
Quercetin	Flavonol	n.d.	↓	n.d.	↓	↓	n.d.	↓	n.d.	n.d.	↓	=	↑	↑	↑	n.d.
7,4'-DHF	Flavone	=	↓	↓	↓	↓	↓	↓	↓	↓	↓	↓	↓	=	=	↓
Apigenin	Flavone	↓	↓	↑	=	↓	↓	=	↓	↓	=	↓	↓	↑	↓	↓
Luteolin	Flavone	=	↓	n.d.	=	↓	=	↑	↓	↑	=	↓	↓	↑	=	↓
n,n- DHF	Flavone	↓	↓	↑	=	↓	=	=	↓	↓	=	↓	=	=	↓	=
Formononetin	Isoflavone	↓	↓	↑	↓	=	=	↓	↓	↓	=	↓	↓	=	↓	↓
Formononetin isomer	Isoflavone	↓	↓	=	↓	↓	↓	=	↓	↓	↓	↓	=	↓	↓	↓
Prunetin/ Biochanin A	Isoflavone	n.d.	↓	n.d.	↑	↓	=	↓	↓	↑	=	↓	↑	=	↓	n.d.
Genistin	Isoflavone	↓	↓	↑	↓	↓	n.d.	↓	↓	=	↓	↓	=	↓	↓	=
Coumestrol	Coumestans	↓	↓	↑	=	↓	=	=	↓	=	=	↓	=	=	↓	↑

Figures 5.26 – 5.27 show a similar fold-change comparison as Figures 5.23-5.25 before, but here the roots overexpressing genes encoding flavonoid biosynthesis enzymes were investigated for their metabolite changes. The changes in metabolite levels of DFR overexpressing roots are not included due to lack of transformed roots for uninfected and *R. solani* infected sample collections.

With the exception of an isomer of the isoflavonoid formononetin, there was no significant change observed in any of the metabolite fold-change in the three *R. solani* and *A. euteiches* infected overexpression lines compared to uninfected roots. Fold-changes in quercetin and genistin could not be determined, as the metabolite could not be detected in empty vector control hairy roots. However, genistin accumulation was increased in *R. solani* infected *FLS* and *IFS* overexpressing roots compared to *CHS* overexpressing roots.

The isomer of formononetin showed an increase in fold changes in all *R. solani* overexpressing roots compared to uninfected roots. The accumulation was also significantly higher in *FLS* overexpressing roots compared to *CHS* overexpressing roots, whilst *IFS* overexpressing roots showed an even higher fold change in this metabolite. Interestingly, the *IFS* overexpressing roots recorded a significantly lower metabolite accumulation in *A. euteiches* infected roots compared to uninfected roots. This could be due to the inability of *A. euteiches* to induce significant pathogenesis in *M. truncatula* roots.

Table 5.2 summarizes the changes in metabolite levels compared to the empty vector control as described previously for Table 5.1. The columns highlighted in green indicate the root samples that were phenotypically more resistant compared to their empty vector control roots towards infection by the pathogen. This has been demonstrated by the growth assays described previously in this chapter.

The overexpression of *CHS* did not yield an increase in metabolite levels as was expected. This could be due to the presence of *CHS* high up in the biosynthesis pathway that may not be the rate-limiting step in the downstream conversions. The overexpression of *FLS* yielded an increase in the flavonol quercetin but this was not

significant. The overexpression of *IFS* led to a significant increase in isoflavonoids formononetin and its isomer in uninfected roots.

The *R. solani* infected *IFS* roots also showed more tolerance and had increased root growth compared to the empty vector control transformed hairy roots. These roots showed significantly higher accumulation of isoflavonoids as well as coumestrol, which is also derived from the isoflavonoid daidzein. Coumestrol as previously mentioned is a potent phytoalexin and protects the plants from pathogenic infections (Gnanamanickam, 1979).

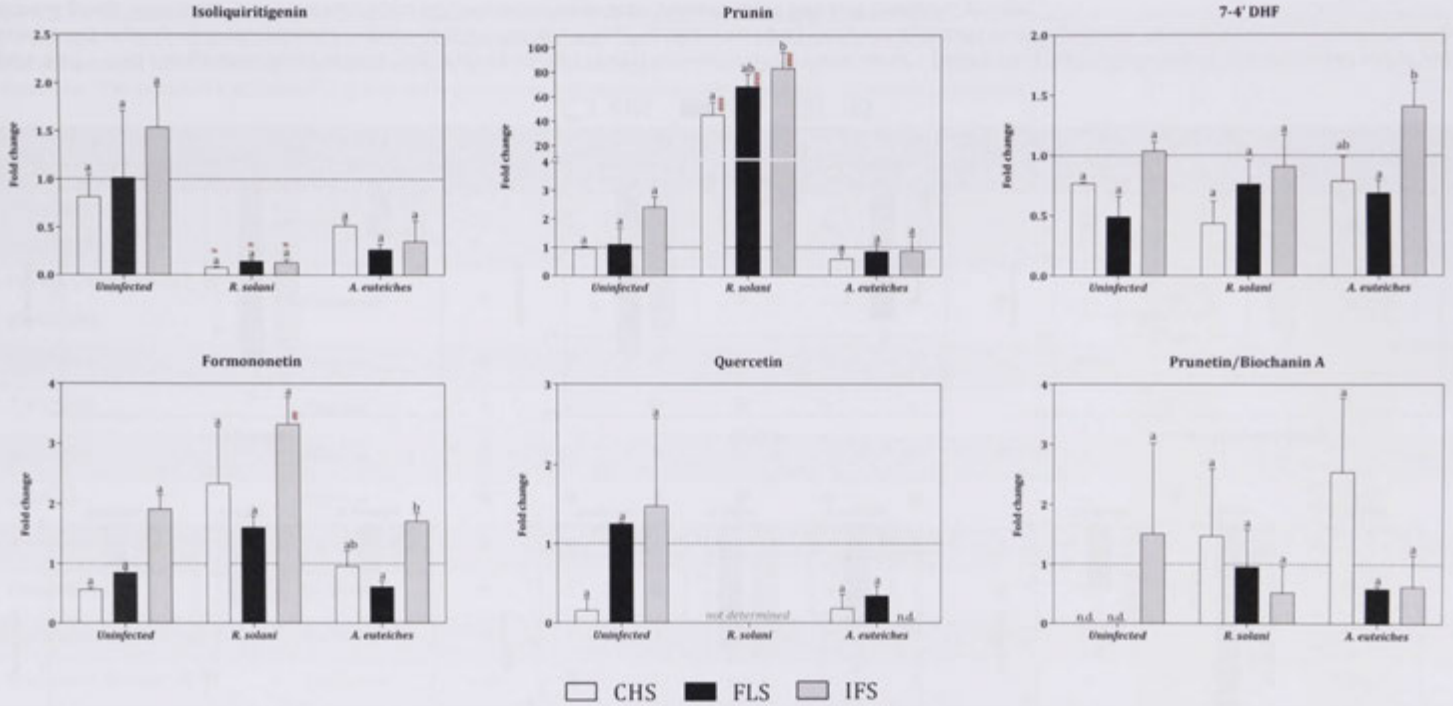

Figure 5.26 –Fold change differences in flavonoid concentrations (14 dpi) between control roots, set at 1 (dashed line) and uninfected, *R. solani* infected and *A. euteiches* infected roots expressing overexpression constructs (CHS, FLS and IFS) ($P<0.05$ shown by #). Different alphabets show significant differences in compound FC within each treatment group. Asterisks (*) indicate significant differences between same compounds in different treatment groups.

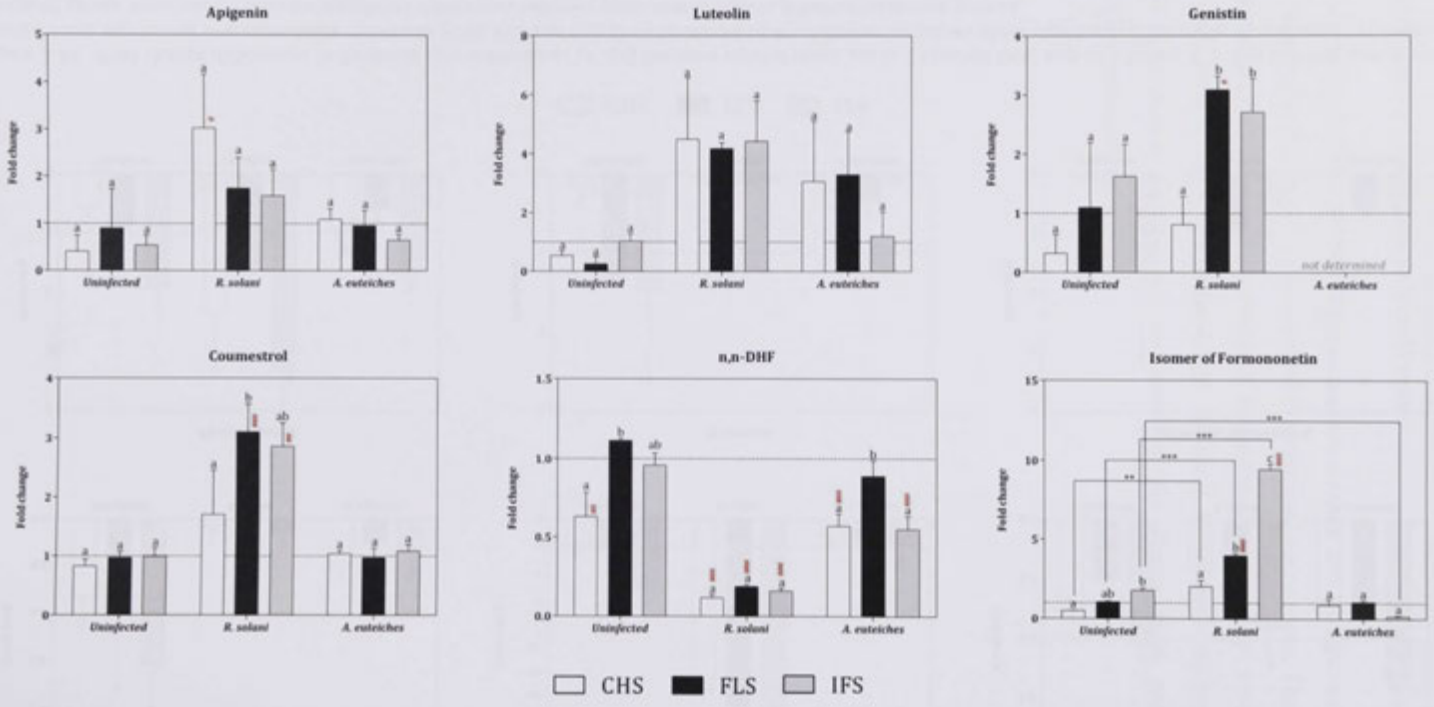

Figure 5.27 – Fold change differences in flavonoid concentrations (14 dpi) between control roots, set at 1 (dashed line) and uninfected, *R. solani* infected and *A. euteiches* infected roots expressing overexpression constructs (CHS, FLS and IFS) ($P<0.05$ shown by #). Different alphabets show significant differences in compound FC within each treatment group. Asterisks (*) indicate significant differences between same compounds in different treatment groups.

Table 5.2 – A summary of the flavonoid content changes in roots expressing different overexpression constructs compared to empty vector control (EV) expressing roots and challenged with *A. euteiches (Ae)* and *R. solani (Rs)*. The symbols ↑ and ↓ represent significant up and down regulation whilst ↑ and ↓ represent up and down regulation that was not statistically significant compared to EV expressing roots challenged with the same organisms. No change from EV is marked with = and n.d. shows no detection. The columns highlighted in green show genotypes with increased tolerance to the respective pathogens.

Flavonoids	Class	CHS*ox*			FLS*ox*			IFS*ox*			DFR*ox*		
		Uninfected	Ae	Rs	*Uninfected*	Ae	Rs	*Uninfected*	Ae	Rs	*Uninfected*	Ae	Rs
Isoliquiritigenin/ Liquiritigenin	Flavanone	=	↓	↓	=	↓	=	=	↓	=		↑	
Prunin (Naringenin 7-O-glucoside)	Flavanone	=	=	↑	=	=	↑	↑	=	↑		↑	
Quercetin	Flavonol	↓	↓	↑	↑	↓	↑	=	n.d.	↑		=	
7,4'-DHF	Flavone	=	=	↓	↓	=	=	=	=	=		=	
Apigenin	Flavone	↓	=	↑	=	=	=	↓	=	=		=	
Luteolin	Flavone	↓	↑	↑	↓	↑	↑	=	=	↑		↑	
n,n- DHF	Flavone	↓	↓	↓	=	=	↓	=	↓	↓		=	
Formononetin	Isoflavone	↓	=	↑	=	=	=	↑	↑	↑		↑	
Formononetin isomer	Isoflavone	↓	=	=	↓	=	↑	↑	↓	↑		↑	
Prunetin/ Biochanin A	Isoflavone	n.d.	↑	=	n.d.	=	=	=	=	=		↑	
Genistin	Isoflavone	↓	↑	=	=	↑	↑	=	n.d.	↑		↑	
Coumestrol	Coumestans	=	=	↑	=	=	↑	=	=	↑		↑	

5.4 Discussion

The study presented in this chapter aimed to discover if common pathways were engaged between the symbiotic and pathogenic root-microbe interactions. It has been shown that the flavonoid profile exuded by a host root during nodulation is specific to the symbiotic bacteria where it induces Nod factor synthesis while other flavonoids possess phytoalexin activity (e.g. Zuanazzi et al., 1998). This offers selectivity for the host roots in establishing the relationship with only the compatible microorganisms.

As discussed in Chapter 4, the lack of flavonoids in *CHS*i roots increased the gene expression of many antioxidative and pathogenesis related genes in roots in the presence of rhizobia. The aim of the study presented in this chapter was to better understand if altering specific groups of flavonoids had an effect on the extent of pathogenicity caused by a nectrophic fungi and a biotrophic oomycete. It was anticipated that the altered expression of flavonoids might increase the plant's tolerance to these organisms. Additionally, it was aimed that the important flavonoids in defence response would be identified.

It has been reported that auxin transport regulation plays a role in the disease susceptibility of roots. In *Arabidopsis tt4* mutant that is deficient of flavonoids, the infection with *Fusarium oxysporum* is more extensive and damaging (Kidd et al., 2011). It was established in Chapter 3 that the flavonols and isoflavonoids play a role in the auxin transport balance as silencing of these groups prevents an inhibition of polar auxin transport. It was also observed there that silencing of all flavonoids in the *CHS*i roots increased the overall auxin responsive gene GH3 expression in the roots.

The results presented in this chapter point towards two possibilities - 1) auxin has direct effect on defence 2) auxin increases tolerance by enhancing root growth and lateral root formation.

5.4.1 Effect of auxin accumulation on defence

It was demonstrated in Chapter 3 that flavonoids had significant effects on synthesis, accumulation and transport of the plant hormone auxin. This could be important in the context of defence as auxin could mediate changes in plant growth responses during infection with pathogens described in this chapter. There are evidences showing that pathogens are able to enhance the synthesis of auxin. Auxin signalling in the host plant may be required for infection. Thilmony et al. (2006) demonstrated this in *Arabidopsis* that was infected with *Pseudomonas syringae.* Auxin sensitivity regulating genes also appeared to negatively control the induction of defence related genes such as *CEVI-1* in *Arabidopsis* that were infected with viral pathogens (Mayda et al., 2000). The external application of auxin also enhanced the pathogenicity symptoms such as those caused by *Pythium ultimatum* in tomato plants (Gravel et al., 2007). Furthermore, there is evidence that auxin signalling is required for certain R-gene mediated resistance mechanisms (Austin et al., 2002, Azevedo et al., 2002) and proteomic studies have demonstrated multiple defence-related genes as targets of auxin (van Noorden et al., 2007).

The increased concentrations of auxin as well as the failure to regulate auxin transport observed in the *CHS*i roots (Chapter 3) points to a likely link between flavonoid-regulated auxin synthesis, accumulation and transport with the susceptibility towards *R. solani* and *A. euteiches.* Since *FLS*i roots failed to regulate the auxin transport and flavonols were likely to be more important in nodulation-related auxin transport inhibition, it was interesting that these roots were more susceptible to *R. solani* (Figure 5.13). The *FLS*i expressing roots also showed a significant reduction in number of lateral roots emerging 14 dpi with *R. solani* (Figure 5.15), suggesting hormonal changes within the roots (discussed further below). This is further supported by the fact that the synthesis and action of several hormones including auxin, gibberellins, cytokinins and ethylene were also different in *CHS*i roots, as shown in Chapter 4.

5.4.2 *Flavonols and isoflavonoids may be important for lateral root formation when evading a pathogenic infection*

The uninoculated controls confirmed that the flavonol metabolic products were silenced in the *FLS*i roots. In these roots, the metabolic flux is altered to favour the synthesis of isoflavonoids such as prunetin/biochanin A. When *FLS*i roots were challenged by *R. solani*, these increased isoflavonoids were not sufficient to prevent an infection. On the contrary, there is evidence in pea that shows that prunetin acts as an attractant to *A. euteiches* zoospores (Yokosawa et al., 1986). This would suggest that the altering of flux towards isoflavonoids could even accelerate the infection process. However, in this study, the infection with both *A. euteiches* and *R. solani* was carried out by placing growing hyphae in contact with the root.

When *FLS* and *DFR* silenced roots were challenged with the nectroph *R. solani*, their growth was retarded. The plants ability to survive the infection with new lateral roots is also diminished in *FLS* silenced roots.

It should also be noted that flavonols have been implicated in the transport of auxin as shown in Chapter 3 and shown in previous studies e.g. Jacobs and Rubery (1988). The emergence of lateral roots may require an auxin accumulation in the meristems and it is likely dependent on the PIN mediated auxin transport (Benková et al., 2003). Therefore, reduced number of lateral roots emerging in *FLS*i could be a hormonal effect. It is suggested in the literature (Gaulin et al., 2007) and also observed during our experiments that one of the ways in which the roots overcame a pathogen challenge was through producing an increased number of lateral roots that could branch away from a decaying root apex. This would suggest that flavonols are required by plants to evade a pathogen through lateral root development.

When these flavonoid-silenced roots were challenged with the biotroph *A. euteiches*, the *FLS*i roots again showed the most severe growth retardation. In these roots, the number of lateral roots emerging were also lower than control,

although not significantly. The reduced regulation of auxin transport via the PIN transporter cycling could again be implicated in such interactions.

Isoflavonoid accumulation could lead to high tolerance against R. solani

The overexpression of different flavonoid synthesis enzymes was expected to improve the plant's ability to defend against the pathogenic challenges. The roots overexpressing the genes encoding enzymes CHS, FLS, IFS and DFR were challenged with *R. solani* and *A. euteiches*.

In uninoculated roots where *IFS* was overexpressed, the metabolic profile confirmed the significant increase of some of the isoflavonoids such as formononetin and its isomer. The flux also was altered to increase the synthesis of flavonols such as quercetin, although not significantly (Figure 2.9).

The change in these metabolites translated to an increased tolerance against *R. solani* infection in *IFS* overexpressing roots at both 7 and 14 dpi. The number of lateral roots emerging from below the point of inoculation was also significantly higher in *IFS* overexpressing roots. Isoflavonoids such as formononetin has previously been shown to significantly inhibit the PAT (Laffont et al., 2010), which could be important for lateral root formation.

Many of the isoflavonoids, including isoflavone derived coumestrol form pterocarpans that protect the plants from invading pathogens (Lyon and Wood, 1975) through non-specific mechanisms where they disrupt membrane activity (Weinstein and Albersheim, 1983) and/or through targeting specific enzymes such as ATPase or NADH-ubiquinone-oxidoreductase (Giannini et al., 1988, Parniske et al., 1991). The ability of isoflavonoids as well as flavonols to regulate auxin transport could also explain the increased number of lateral roots formed in these roots. This characteristic may allow roots to survive the nectrotrophic attack.

An increase in tolerance was not observed in flavonoid overexpressing roots against *A. euteiches*. The wild type A17 roots of *M. truncatula* already show a resistance to *A. euteiches*. Hence, the overexpression of the flavonoids did not have any significant effect on the root growth. In addition, as shown in Chapter 2, the

overexpression of only *IFS* led to any significant increase in accumulation of flavonoids.

5.4.3 Overall metabolic changes in flavonoid silenced roots indicate a difference in response to a nectrophic and a biotrophic pathogen

The changes in metabolites were remarkably different when roots expressing different RNAi constructs (silencing different genes encoding flavonoid biosynthesis enzymes), were challenged by a nectrotrophic or a biotrophic pathogen. The results showed that in tissues undergoing necrosis as a result of *R. solani* infections, a large amount of flavonoid metabolites accumulated. This was despite the reduction in transcription of genes encoding different flavonoid biosynthesis enzymes. It was shown in Chapter 2 that the RNAi silencing does not induce total reduction in transcript abundance.

The *M. truncatula* wild type A17 shows resistance to the oomycete *A. euteiches*. This resistance could be mediated through an increase in number of secondary roots via pericycle cell division and possibly through accumulation of defence phenolic compounds such as isoflavonoids (Djébali et al., 2009)

5.5 Conclusion

The studies presented in this chapter highlighted the importance of flavonols and isoflavonoids as metabolites that were critical in enhancing the *M. truncatula* roots' tolerance towards root pathogens. The isoflavonoids formononetin, one of its isomer and the flavonol quercetin were important for increasing this tolerance. The overexpression of *IFS* was most effective at accumulating isoflavonoid metabolites. Increasing the expression of *CHS*, which is higher in the flavonoid biosynthesis pathway, did not yield measurable differences in downstream flavonoid metabolite accumulation and it is likely that this enzyme was not rate limiting in the synthesis of downstream products.

The roots' tolerance to pathogens could also be related to the ability of flavonoids to regulate auxin transport in *M. truncatula*. It has been shown that an increase in lateral root density is an evasion technique utilized to increase the roots' tolerance to the pathogen and has been demonstrated in *A. euteiches* infection in *M. truncatula* (Djébali et al., 2009).

Chapter 6. General Discussion

6.1 Summary of the main results

The chapters presented in this thesis are concerned with the different functions of flavonoids during symbiotic interactions and attempts to improve plant health in pathogenic interactions with root-rot inducing fungi and oomycete. It was shown that flavonoid biosynthesis could be altered through manipulating its biosynthesis pathway. This was achieved through silencing or overexpression of the enzymes of the biosynthesis pathway.

In *Arabidopsis*, flavonoids have been suspected to regulate the cycling of auxin transporter proteins by altering protein and/or lipid phosphorylation (Peer et al., 2004), thus regulating the flow of auxin from its site of synthesis to site of action. The flavonols (such as quercetin) and isoflavonoids (such as formononetin) were shown to be likely candidates that control the flow of IAA during indeterminate nodule formation in *M. truncatula*. Whether similar mechanisms occur in determinate legumes will require further investigation although some reports indicate that auxin transport inhibition is not required in soybean (Subramanian et al., 2007).

It was also shown in Chapter 3 that application of synthetic auxin transport inhibitor, TIBA was insufficient to rescue nodule infection in flavonoid deficient roots. In these roots, cortical cell divisions were initiated, but they remained uninfected even in the presence of rhizobia on the root-surface. Therefore, this justified a whole transcriptome analysis of root-rhizobia interactions at 6 and 24 hpi in Control and *CHS*i roots.

The transcriptome analysis of flavonoid deficient roots showed that in addition to synthesis and response genes of auxin, the synthesis and response genes of other classical hormones such as cytokinin, ethylene and gibberellin were also differentially expressed. However, there was no significant difference found in the transcript levels of genes encoding auxin transport proteins PIN and LAX. It could

be hypothesised that the cycling or activity of these transporter proteins were regulated by flavonoids while their synthesis remained unchanged.

In addition to hormonal changes, the flavonoids also likely regulated key stages of infection thread formation through their antioxidative properties and alteration of expression of genes encoding enzymes involved in the regulation of ROS. It is possible that ROS induces specific cross-linking of proteins in the root hairs associated with infection thread formation (Ramu et al., 2002). This was supported by the observations where the wild-type plant showed increased accumulation of ROS in the root hairs during early stages of nodule formation.

The various antioxidative roles as well as increase in expression of transcripts synthesising pathogenesis related proteins in plant-rhizobia interaction was thought to increase a plant's ability to defend against pathogens. Using silencing and overexpression of genes encoding flavonoid synthesis enzymes, an increased tolerance to *R. solani* and *A. euteiches* was achieved.

Where roots expressed the *FLS*i constructs, an increased susceptibility to the fungal and oomycete root pathogen was observed. This could be attributed to the role of flavonol as crucial auxin regulator in the roots and potentially indicate an overlap in symbiotic and pathogenic interactions through auxin mediated changes in the root growth. Roots overexpressing *IFS* showed increased tolerance to the fungal pathogen *R. solani*.

6.2 Manipulation of the flavonoid biosynthesis pathway

The flavonoid synthesis pathway as shown in Figure 1.1 has evolved into multiple branches with isoflavonoids found almost exclusively in legumes. The manipulation of this biosynthesis pathway allowed a systematic study into the roles each of the flavonoid subgroups play in symbiotic and pathogenic interactions.

Gene silencing

I used RNAi to silence expression of genes encoding key flavonoid biosynthesis enzymes. I was successful in generation of transgenic hairy roots expressing all the silencing constructs and these roots also showed reduction in transcript abundance of the silenced genes. However, the metabolic profiling using LC-MS/MS showed some shortfalls.

The silencing was not complete. Even though the transcript abundance of gene encoding the biosynthesis enzyme showed reduction, it was also not complete. This is the drawback of RNAi-induced silencing where not every copy of the transcript is silenced. However, RNAi based technique allowed me to target multiple copies of the genes for silencing and thus justified its use. This is in contrast with *Arabidopsis* studies where a single gene can be targeted for complete knockouts. Generation of full transgenic plants of *M. truncatula* is also time-consuming, however, this model legume allowed the study of rhizobial interactions in hairy-root cultures.

Since the silencing of the genes encoding flavonoid biosynthesis enzymes was not complete, there was a reduction in metabolic end products but not complete absence. In addition, some flavonoid metabolites have been observed to be transported within the plants (Buer et al., 2007) and could be the reason for observing some variations in metabolite quantifications.

Manipulation of the biosynthesis pathway of the flavonoid metabolites also alters the metabolic flux in other branches of the synthesis. This is important as some of the observations made in this study could be related to accumulation of a flavonoid metabolite rather than the silencing of another.

Gene overexpression

Several of the genes targeted for silencing were also targeted for overexpression using a 35s promoter driven construct. The overexpression of the enzymes was not very successful with *CHS*ox showing no changes in its transcript abundance or metabolite changes. The overexpression of *FLS* and *IFS* showed an increase in its

transcript abundance. However, only roots expression *IFS*ox construct showed a significant increase in their respective metabolites. The overexpression of *DFR* in roots led to root-developmental defects with very few callus in *A. rhizogenes* infected seedlings developing any roots. This is the first report of *DFR* catalysed products as potential root-development regulators. Although as mentioned before, it is possible that changes in other metabolite concentrations could be responsible and this requires further confirmation.

Future strategies

The manipulation of flavonoid biosynthesis in *M. truncatula* hairy roots was a quick method to screen for potential metabolic flux changes induced in the transgenic roots. However, seedlings transformed with *A. rhizogenes* form composite plants where the shoot is not transformed. As it is likely that flavonoid compounds can be transported over long distances (Buer et al., 2007), it is important that the fully transformed plants using *A. tumifaciens* be generated for further evaluations.

Hairy roots also differ in their hormonal concentrations, thus fully stable plants would be better suited for developmental analysis during symbiotic and pathogenic interactions. In addition, the plants could be grown in soil and the effects in the rhizosphere could be further investigated.

Finally, it is also possible to manipulate flavonoid biosynthesis by targeting transcription factors involved in activating synthesis or conversion enzymes (Butelli et al., 2008) or transporter proteins to accumulate flavonoids in specific cells or its compartments (Zhao et al., 2011, Zhao and Dixon, 2009). As many flavonoids exist in glyco-conjugated forms, the enzymes involved in their specific conjugation could be targeted (Liu et al., 2006) for a more specific strategy to manipulate accumulation of a particular metabolite. Finally, cell-type specific promoters may also be utilized to alter flavonoids in a cell-specific manner (Baudry et al., 2006).

6.3 *Role of flavonoids in regulation of auxin transport and auxin accumulation during nodulation*

Auxin concentrations are modulated by the plants through synthesis, breakdown and transport to alter its local accumulation. Changes in the auxin and cytokinin ratio induce meristem development in shoot and root (Su et al., 2011) as well as nodules (Mathesius, 2008). Auxin is mainly synthesised in the shoot apex and meristematic regions and transported polarly through auxin transporters AUXIN RESISTANT1/LIKE AUX1 (AUX1/LAX) uptake permeases, ATP Binding Cassette subfamily B (ABCB) transporters, and PIN-FORMED (PIN) carrier proteins (Peer et al., 2011).

Flavonoids are the key to stimulation of a spatiotemporal change in auxin homeostasis in the roots during early stages of nodule formation. *In vitro* studies have shown that flavonoids alter auxin transport in non-legumes (Jacobs and Rubery, 1988). They affect the long-distance polar auxin transport (Murphy et al., 2000) by interfering with auxin transporters (Buer and Muday, 2004, Peer et al., 2004). However, flavonoids are not thought to be specific regulators of auxin, as they do not exhibit multiple targets for such an activity including affecting the trafficking machinery and kinases (Peer et al., 2011).

In this study, I have identified flavonols (such as quercetin) and isoflavonoids (such as formononetin) as potential candidates as auxin transport regulators in *M. truncatula.*

Flavonoids accumulate in regions of auxin accumulation where they inhibit activity of plant ABCBs. This is likely through the phosphorylation of the ATPase activity of the transporter or through allosteric binding (Szabó et al., 1997). Flavonoids may also affect folding of the ABCBs (Bailly et al., 2008). In *Arabidopsis* flavonoid mutant *tt4* where the CHS activity is knocked out, the PIN2 activity is reportedly slightly enhanced (Peer et al., 2004, Santelia et al., 2008). Effects of flavonoids on synthesis of genes encoding AUX1/LAX proteins have not been determined (Peer et al., 2011). However, transcript abundance of *PIN* genes was reported to be indirectly affected by flavonoids in *Arabidopsis* (Peer et al., 2004).

In this study, the expression of the different *PIN* and *LAX* genes were determined in flavonoid-silenced roots. These did not show any significant differences and supports the hypothesis that flavonoids affect the auxin transporters through post-translational modifications such as phosphorylation (Peer et al., 2011).

The data showed that auxin transport was inhibited in Control roots inoculated with rhizobia. However, there was some discrepancy in the amount of auxin that accumulated in comparison with *CHS*i roots. Hairy roots of *M. truncatula* A17 was shown to contain higher concentration of auxin and their conjugates compared to seedling roots and this high auxin concentration is a common feature of hairy roots (Shen et al., 1990, Shen et al., 1988). A decrease in IAA and its conjugates in Control hairy roots inoculated with rhizobia compared to mock inoculated roots suggested that the root attempted to reduce IAA concentrations to a biological "operating window" for successful nodulation. This could be due to IAA catabolism and flavonoids are critical to prevent oxidative damage from the ROS by-products. The inability of flavonoid-deficient roots to reduce concentrations of IAA or its conjugates in response to rhizobia inoculation could be due to its incapacity to protect roots from ROS damage.

The higher concentrations of auxin throughout the *CHS*i roots also suggested that the synthesis of auxin was high in these roots. Quantification of genes encoding auxin synthesis proteins YUCCA1/2/3 showed that *YUCCA1* abundance was significantly higher in *CHS*i roots that were inoculated with rhizobia. This agreed with the previous observations of higher auxin accumulation in *CHS*i roots.

Lower efficiency of nodulation was found to be common for hairy roots in my experiments. This suggested that although these roots are capable of forming nodules that are morphologically similar to seedling roots (Boisson-Dernier et al., 2001), their ability is reduced due to altered hormonal balance.

Flavonoids have been hypothesised to have primarily evolved to serve as ROS scavengers in plants. This activity is linked to their high reduction potential (Gill

and Tuteja, 2010). This activity is also important for protection during IAA catabolism and feed forward into further oxidizing auxin (Peer and Murphy, 2007).

Therefore, it could be hypothesised that flavonoids regulate auxin transport, synthesis and breakdown to alter auxin accumulation during nodule initiation in *M. truncatula*.

Figure 6.1 and Table 6.1 show the distribution of the flavonoid synthesis enzymes in various plant orders. The enzyme chalcone synthase was identified in all green plants and likely shows a common origin in all orders. This also supports the hypothesis that the plants evolved flavonoid synthesis to protect against ultraviolet radiation or as internal physiological regulators as they began colonising land (Stafford, 1991).

One of the functions of the flavonoids is its association with IAA synthesis and breakdown. Flavonoids such as 7,4'-dihydroxyflavone (DHF) inhibited auxin breakdown by peroxidases while the isoflavonoid Formononetin promoted peroxidase assisted IAA breakdown (Mathesius, 2001). The distribution of auxin synthesis enzymes in the green plants (Figure 6.1 and Table 6.1) showed some commonalities in the presence of FSII and IFS proteins in the plant orders that also had identified proteins similar to *Arabidopsis* CYP71A13 and CYP79B2/B3. Further studies exploring the evolution of these proteins in land plants could highlight if the evolution of flavonoid biosynthesis pathway was correlated with auxin synthesis since flavonoids have multiple regulatory effects on this hormone.

One limitation of the survey shown in Table 6.1 is the small number of organisms sequenced and collated in the NCBI database. However, this preliminary data could be used as a starting point to experimentally investigate the presence of various auxin synthesis enzymes in different plant orders.

It is important to recognise that the auxin homeostasis is maintained also through conversion and breakdown. These processes are mediated by other enzymes and their evolutionary network could be investigated in future to study if a relationship exists between the evolution of flavonoid synthesis and auxin.

To further specify the flavonoids responsible for maintenance of an auxin homeostasis, future experiments with application of specific flavonoid aglycone (such as quercetin and kaempferol) as well as their glycosides could be applied in a phenotypic rescue experiment for auxin transport and accumulation in *CHS*i roots. Another alternative method to identify these specific compounds could be through microspectrofluorometry assays coupled with laser capture microdissection to collect root flavonoids for identification using mass and structural analysis.

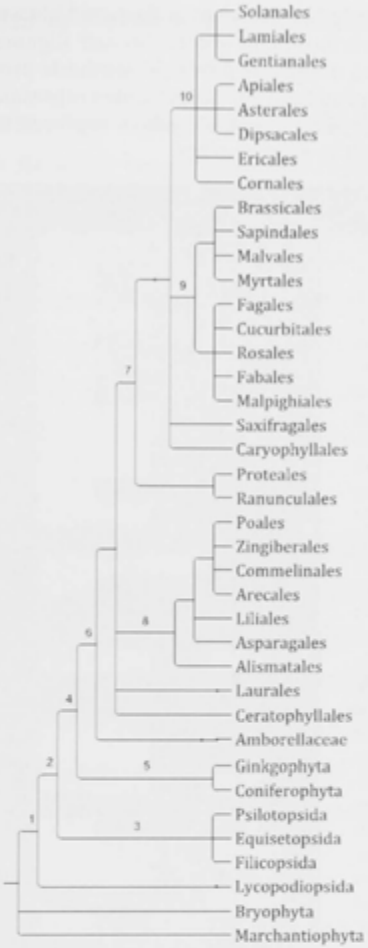

Figure 6.1 – A rectangular cladogram of the orders of green plants generated using the NCBI taxonomy data obtained through phyloT (www.phylot.biobyte.de) and visualized using TreeGraph 2 (Stöver and Müller, 2010). Vascular plants derived from Node 1 subdivide into Node 2 (Leafy plants), Node 3 (Ferns and Fern-like), Node 4 (Seed plants), Node 5 (Gymnosperm), Node 6 (Angiosperms), Node 7 (Eudicots), Node 8 (Monocots), Node 9 (Rosids) and Node 10 (Asterids). (Savolainen and Chase, 2003). Time scale is not reinforced.

Table 6.1 – A survey showing the presence of flavonoid biosynthesis enzymes and auxin synthesis enzymes across various plant orders through alignment search (NCBI BLASTP) with proteins of the Fabales order (for flavonoid synthesis proteins) and the Brassicales order (for auxin synthesis proteins). The colour codes represent percentage of alignment with green representing greater than 50 %, yellow representing greater than 30 % and red representing less than 20 % or no matches.

Order	Tax ID	CHS	FLS	DFR	FSII	IFS	AMI 1	AAO 1	YUC 1	CYP71A13	CYP79B2/B3	NIT1/2
Solanales (tomato, tobacco)	4069											
Lamiales (mint, Antirrhinum)	4143											
Gentianales (gentian)	4055											
Apiales (celery, carrot)	4036											
Asterales (sunflower, daisy)	4209											
Dipsacales (teasel)	4199											
Ericales (rhododendron)	41945											
Cornales (dogwood)	41934											
Brassicales (Arabidopsis)	3699											
Sapindales (maple)	41937											
Malvales (cotton)	41938											
Myrtales (myrtle)	41944											
Fagales (beech, oak)	3502											
Cucurbitales (cucumber)	71239											
Rosales (rose, apple)	3744											
Fabales (legumes)	72025											
Malpighiales (poplar, Hevea)	3646											
Saxifragales (saxifrage)	41946											
Caryophyllales (Spinacia)	3524											
Proteales (plane tree, lotus)	232378											
Ranunculales (buttercup)	41768											
Poales (grasses)	38820											
Zingiberales (bananas, gingers)	4618											
Commelinales (water hyacinths)	4739											
Arecales (palms)	40551											
Liliales (lilies)	4667											
Asparagales (orchids, onion, aloe)	73496											
Alismatales (water-weeds)	16360											
Laurales (laurel)	3432											
Ceratophyllales (Ceratophyllum)	91811											
Amborellaceae (Amborella)	22097											
Ginkgophyta (Ginkgo)	58021											
Coniferophyta (conifers)	3312											
Psilotopsida (whisk ferns)	3236											
Equisetophyta (horsetails)	3254											
Filicopsida (true ferns)	3290											
Lycopodiopsida (club mosses)	3248											
Bryophyta (mosses)	3208											
Marchantiophyta (liverworts)	3195											

6.4 *Additional roles of flavonoids in symbiotic interactions with rhizobia*

Flavonoids were shown to affect auxin transport inhibition during root-rhizobia interactions (Chapter 3). However, rescue experiments using synthetic ATI (TIBA), showed that flavonoids could complement the formation of infected nodules in *CHS*i but TIBA only rescued the organ formation and not infection. The *CHS* silenced roots did not form preceding infection threads as compared to Control roots. This suggested additional roles of flavonoids in root-rhizobia interactions and was investigated through a whole transcriptome analysis using microarrays (Chapter 4). So far, there has been no evidence of the involvement of flavonoids in rhizobial infection.

The results presented here suggested that flavonoids have a wider role in biosynthesis and responsive factors of multiple plant hormones such as ethylene, auxin, cytokinin and gibberellin. Additionally, the flavonoid-deficient roots showed changes in transcription of genes encoding ROS scavenging enzymes as well as defence related proteins. A gene ontology enrichment analysis also showed that the oxidoreductive pathway was highly represented in the transcriptome of flavonoid-deficient roots compared to control roots early in the interaction with rhizobia.

Figure 6.2 demonstrates an overall model of the changes in gene transcription in flavonoid-deficient roots compares to control roots during early (6 hpi) interaction with rhizobia. A majority of the genes were induced or repressed during this early interaction. It showed that the roots were only partially able to up-regulate the genes encoding proteins involved in nodule formation. Concurrently, the genes encoding proteins involved in defence against pathogens was also increased in flavonoid-deficient roots suggesting that these roots could not recognise the rhizobia as a symbiont. This could be due to its diminished potential to protect itself from abiotic and biotic stresses directed by flavonoids.

ROS accumulation activates a number of processes through the expression of enzymes notably peroxidases. The reduction in the transcription of a key enzyme

rhizobium induced peroxidase 1 (RIP1), suggested to be involved in detoxification of H_2O_2 to prevent a hypersensitive response (HR) induced cell death, cell-wall modification during infection thread progression, and regulation of plant signalling proteins (Ramu et al., 2002).

Interestingly, a number of genes encoding glutathione-S-transferases (GSTs) were increased in expression in flavonoid-deficient roots inoculated with rhizobia. This suggested that perhaps the roots compensated for the lack of flavonoids by increasing the accumulation of ROS scavenging GSTs. A functional assay where nodulation was attempted to be rescued by inhibition of ROS formation was unsuccessful. A staining for ROS showed its presence in the root hairs of control roots suggesting that flavonoids act via ROS to facilitate infection. This requires further testing in future to determine if a root-hair specific increase in ROS accumulation could be induced in *CHS*i roots to rescue infection with rhizobia.

Additionally, ROS accumulation in the root hairs could be quantified through other staining techniques. Although, NBT and DAB were also used in my studies to stain for other ROS species (NBT targeted superoxide anions and DAB targeted hydrogen peroxide), this was not successful in showing differences. These methods would require further optimization in future.

It would also be necessary to show if ROS staining and infection thread formation overlapped in the same root hair. Following this, different lines of flavonoid-profile altered roots or exogenous application of flavonoid compounds, could be used to narrow down specific metabolic candidates that regulated ROS accumulation in root-hairs.

The flavonoids also might regulate gene expression in the root hairs and transcriptomic studies of root hairs (similar to Libault et al., 2010) from *CHS*i plants could profile more specific flavonoid gene-targets involved in IT formation.

The Figure 6.3 shows a model of how flavonoids may alter ROS in the cell either directly via their ability to detoxify radicles or indirectly through activating peroxidases and other ROS scavenger proteins.

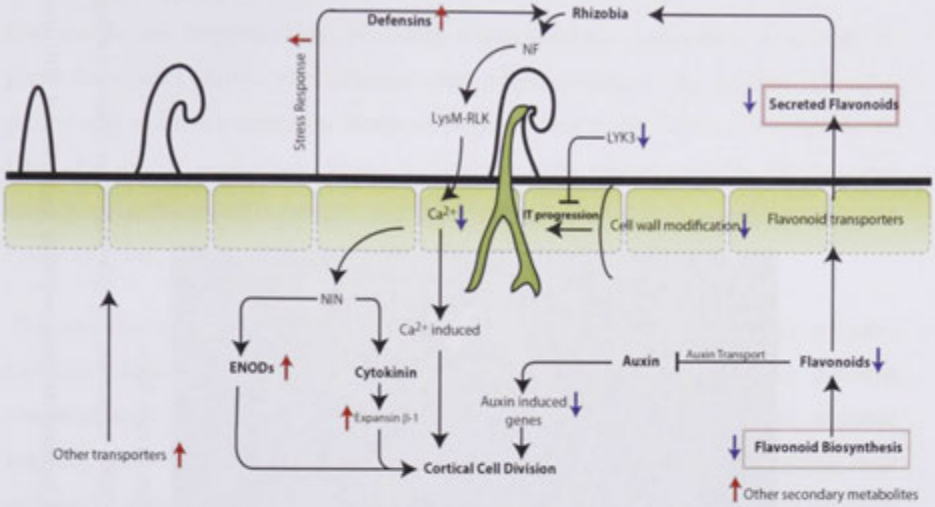

Figure 6.2 – The changes in transcript abundances of genes involved in the early rhizobia interaction (6 hpi) in flavonoid-deficient roots. The silencing of *CHS* is indicated by the reduction in a number of genes probes encoding flavonoid biosynthesis enzymes (including *CHS*). This was compensated by the plant to increase the gene expression of other secondary metabolite encoding enzymes. A reduction in flavonoid synthesis led to reduced flavonoid accumulation in the roots (confirmed with lack of auto-fluorescence under UV excitation). Since flavonoids were not synthesized, they could not be exuded into the rhizosphere to function as a signal to the rhizobia. Consequently, there was reduction in abundance of transcripts of calcium-induced genes, genes encoding cell wall modification enzymes, as well as auxin induced genes. However, there was an increase in abundance of some early nodulation gene transcripts (ENODs), but a larger number of stress-response and defense response genes were increased in their transcript abundances likely indicating a strong pathogenesis response to prevent infection.

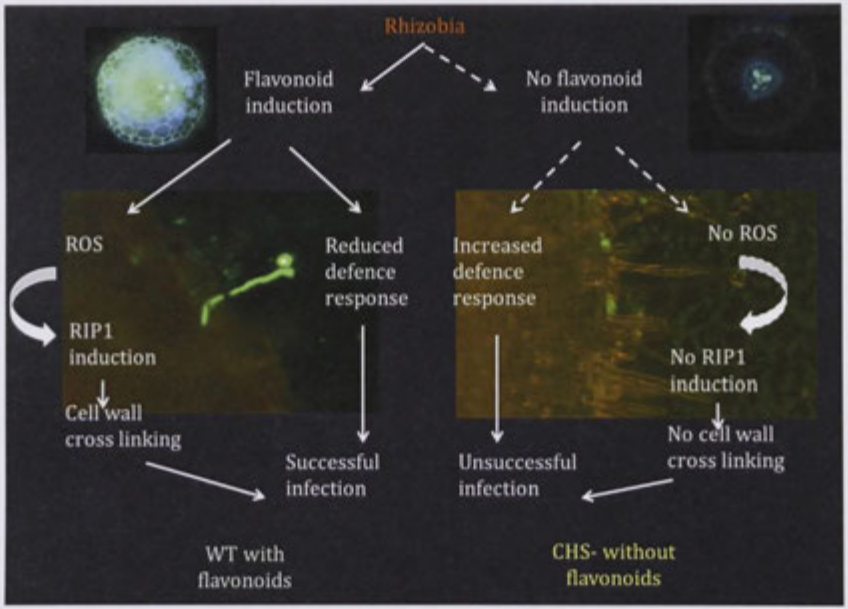

Figure 6.3 – Model for how the flavonoids may affect rhizobia-induced infection thread formation in root-hairs.

Flavonoids in WT roots (left) reduced defense response and altered ROS balance to induce *RIP1*, important for cell wall cross-linking during infection thread formation. Together this leads to successful infection.
Lack of flavonoids in *CHS*ì roots (right) shown with absence of root auto-fluorescence could increase defense response and reduced *RIP1* transcription leading to unsuccessful infection.

6.5 *Role of flavonoids in response to root-pathogens*

Flavonoids are important in defending plants against pathogens. A number of plant-flavonoids form phytoalexins and phytoanticipins to impart effective protection against pathogens. Many of these belong to the class of isoflavonoids that are almost exclusively found in legumes. The overexpression of the gene encoding isoflavonoid synthase led to increases in the isoflavonoid metabolite (such as Formononetin, see Chapter 2).

The mechanism of action of flavonoids against plant-fungal pathogens is wide-ranging. Skadhauge et al (1997) suggested that flavonoids in barley prevent crosslinking of pathogen's enzymes and chelate metals necessary for enzyme activity; inhibit cellulases, xylanases and pectinases required for degrading host cell wall during fungal penetration; and form a protective crystalline-like physical barrier against the attack. Several flavones in bittersweet orange (*Citrus aurantium*) show antifungal activity against *Cladosporium sphaerospermum* (Alcerito et al., 2002). Naringin (a flavanone) and tangertin (a polymethoxyflavone) showed activity against *Penicillium digitatum* (Arcas et al., 2000). In *Medicago*, the flavonoids medicarpin, vestitol, vestitone and sativan are produced in response to fungal attack (Jasiński et al., 2009, Naoumkina et al., 2007, Ahuja et al., 2012).

Flavonoids that show antifungal activities (naringenin and kaempferol) have so far not been effective in defence against *R. solani*. This fast-growing fungal pathogen was suggested to possess an ability to detoxify a variety of flavonoids (Padmavati et al., 1997), which influenced my selection of this pathogen in this study.

One of the flavonoid groups targeted for detoxification is the isoflavonoids. For instance, the fungus *Nectria haematococca* produces a cytochrome P450 pisatin demethylase (Pda) that inhibits the activity of the isoflavone pisatin in garden pea (Miao et al., 1991). This provides indirect evidence that isoflavonoids are involved in defence against pathogens.

One of the mechanisms through which roots show tolerance to pathogens is through outgrowing them before they cause extensive damage (Djébali et al., 2009). Therefore, I investigated root growth and lateral root numbers as indicative of disease progression in the transgenic *M. truncatula* hairy roots expressing RNAi or overexpression constructs.

Silencing of the gene encoding flavonol synthase led to a reduction in the levels of the flavonol quercetin which has been described as a potent antifungal compound (Lattanzio et al., 2006). It increased the susceptibility of the roots towards both *R. solani* and *A. euteiches*, the latter of which was determined to not cause infection in *M. truncatula* A17. This would suggest that flavonols formed an important defence mechanism for both fungal and oomycete attack. In addition, it was demonstrated that flavonols were important regulators of auxin transport (Chapter 3) and silencing of flavonols may have effects on auxin accumulation, which is also significant for pathogenesis (Gravel et al., 2007, Mayda et al., 2000). There are also significant overlaps in the plant-parasitic nematode induced gall formation, lateral root formation and nodules (Wasson et al., 2009). If these altered flavonoid profiles could be engineered in to crop plants, it could have an important impact on the agricultural productivity.

It was also found that the overexpression isoflavonoid biosynthesis increased the tolerance of the *M. truncatula* roots towards infection from *R. solani*. This would suggest that increasing the plant's arsenal of potent phytoalexin isoflavonoid deterred infection from this root-rot inducing pathogen. To identify the specific flavonoid end product is important for defence in *M. truncatula*, rescue experiments using exogenous application of flavonoid metabolites could be designed.

Finally, it would be important in future to further investigate if flavonoid overexpression led to effects on symbiotic interactions with rhizobia or mycorrhiza. It should be investigated if altered flavonoid profiles of the *M. truncatula* roots are capable of changing the root-interactions with other pathogenic organisms including bacteria and insects. Many flavonoids are also

deterrent to herbivory (Dixon and Steele, 1999) which could have a consequence to its application in pasture crops.

6.6 Conclusions

Flavonoids are versatile metabolites that perform a wide range of functions in plants. In this thesis, I have demonstrated that flavonols and isoflavonoids are capable of mediating auxin transport inhibition in *M. truncatula* roots infected with rhizobia. The inhibition of auxin transport creates a gradient in auxin accumulation, which precedes nodule organogenesis. However, the auxin transport inhibition was only one of the functions of flavonoids during nodulation as a synthetic auxin transport inhibitor was insufficient in restoring nodulation in flavonoid deficient roots. A whole transcriptome analysis showed that lack of flavonoids reduced the expression of a key RIP1 enzyme. The flavonoid-deficient roots also failed to show infection threads and lacked ROS accumulation in their root-hairs. In Figure 6.4, I have shown an overview of the roles flavonoids play in root-rhizobia symbioses. The findings highlighted in this thesis are coloured in red (boxes and text). Flavonoids were known to have *nod*-gene inducing and suspected to have quorum sensing mediating abilities (stage 1). My findings highlight that flavonoids also have roles in the infection process where it likely modulates redox control to affect infection thread formation (stage 2). As the nodule initiates (stage 3), the flavonols and isoflavonoids were demonstrated to be important for inhibition of polar auxin transport. Flavonoids in general were involved in accumulation of auxin through synthesis and breakdown in the presence of rhizobia. Flavonoids in the later stages of nodulation (stage 4) are believed to repress nod-gene activity and facilitate nodule differentiation.

Finally, I also demonstrated that by systematically silencing and overexpressing flavonoid biosynthesis enzymes in the roots of *M. truncatula* that increases in isoflavonoids led to an increase in tolerance towards the damaging *R. solani* AG8 fungal pathogen. Both flavonols and isoflavonoids were important for secondary root formation during a pathogen challenge.

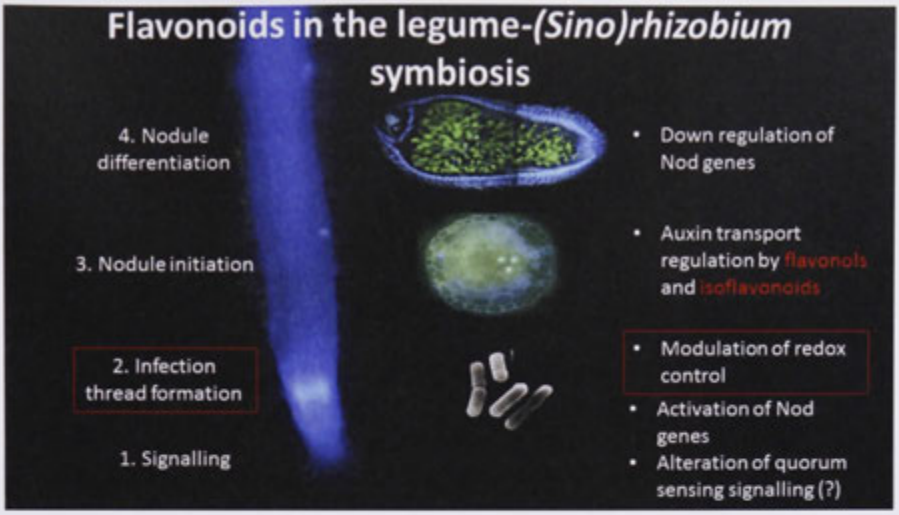

Figure 6.4 – Roles of flavonoids in legume-*rhizobium* symbioses. Text in red highlight the findings presented in this thesis. Flavonoids have been known to affect activation of *nod* genes and suspected to alter quorum-sensing signals in rhizobia. This thesis demonstrated that flavonoids also have roles in the infection thread formation, and this was likely through the modulation of redox state of the root-hairs. During nodule initiation, it was also shown that flavonols and isoflavonoids were likely candidates that inhibited PAT. Flavonoids are known to also down regulate *nod*-gene activation in later stages of nodule development to promote nodule differentiation.

Appendix

Table A2.1a – A list of the phenypropanoid standards that were run on the LC MS/MS for quantification sorted by retention times.

Compound	Rt (min)	Collission Energy (keV)	Parent ion [M-H]- (m/z)	Product ion(m/z)	Other Qualifiers(m/z)	Response factor (RF)	Standard curve	R^2	LOD (ppm)	LOQ (ppm)
Umbelliferone (Internal Standard)	*4.531*	*30*	*161.0244*	*77.04052*	*133.0305, 105.0349, 89.04*				*0.022*	*0.036*
Nicotinic Acid	1.07	10	122.0267	78.03504		3.205368	y = 1.5668x - 0.2123	0.9937	0.018	0.03
3,5-dihydroxybenzoic acid	1.339	15	153.0233	109.0298		0.376488	y = 5.4764x - 0.7811	0.9861	0.005	0.008
Puerarin (Daidzein-8-C-glucoside)	1.742	25	415.104	295.0618	267.0668	1.035965	y = 5.8712x - 1.3784	0.9753	0.017	0.028
p-hydroxy benzoic acid	1.743	15	137.0259	93.03564		0.301412	y = 4.9907x + 0.0186	0.9966	0.003	0.006
Esculetin	1.86	30	177.0182	89.0401	105.0342, 77.04002, 133.02959	1.260489	y = 1.9207x - 0.3471	0.9843	0.027	0.045
2,5-dihydroxybenzoic acid, (Gentisic Acid)	1.869	15	153.0233	108.0215		1.02412	y = 3.1755x - 0.4299	0.9887	0.008	0.013
4-hydroxy-3-methoxybenzoic acid	1.945	15	167.0365	152.0097	108.0202	10.54	y = 0.2489x + 0.0231	0.9653	0.08	0.133
Caffeic acid	2.01	15	179.0422	135.4573			Not quantifiable		2.05	3.416
Catechol	2.14	25	109.0305	108.0219	91.01955	1.312294	y = 1.473x - 0.0288	0.9978	0.014	0.024
2,4-dihydroxy benzoic acid	2.274	10	153.0233	109.0317	65.04088, 67.02143	0.270091	y = 9.9518x - 1.3538	0.9896	0.005	0.008
3-hydroxybenzoic acid	2.404	15	137.0259	93.03443		0.877753	y = 2.6933x - 0.2142	0.994	0.011	0.018
p-coumaric acid	3.609	12	163.027	119.0359			y = 32.969x - 15.081	0.992	0.002	0.003
4-hydroxycinnamic acid	3.733	12	163.027	119.0364			Not quantifiable			
aceto vanillone	4.67	10	165.0542	150.0319	122.0374	19.57058	y = 0.3x - 0.0749	0.9737	0.156	0.26
7-hydroxy-6-methoxy coumarin	4.67	15	191.035	176.0135	102.9488, 148.01707	0.529907	y = 9.0655x - 2.0547	0.9714	0.012	0.021
3',5'-dimethoxy-4'-hydroxyacetophenone	5.702	10	195.0662	180.0329	165.0139	32.76062	y = 0.0561x - 0.0242	0.9444	0.732	1.22
2',5'-dihydroxyacetophenone	6.002	25	151.0442	108.021	53.04111	1.005814	y = 1.4246x + 0.3085	0.9842	0.014	0.024
m-coumaric acid	6.665	12	163.027	119.0385			y = 10.888x - 10.594	0.9966		

Table A2.1a continued– A list of the phenypropanoid standards that were run on the LC MS/MS for quantification sorted by retention times.

Compound	Rt (min)	Collission Energy (keV)	Parent ion [M-H]- (m/z)	Product ion(m/z)	Other Qualifiers(m/z)	Response factor (RF)	Standard curve	R^2	LOD (ppm)	LOQ (ppm)
3,5,7,3',4'-pentahydroxyflavanone	6.928	20	303.052	125.0133	285.0284		Not quantifiable			
2',4'-dihydroxyacetophenone	8.4	25	151.0442	91.0204	65.04013	0.691792	y = 4.7898x - 0.8276	0.9846	0.013	0.021
Naringenin-7-O-glucoside	11.706	10	433.115	271.0609	151.0034	0.480101	y = 6.4956x - 1.0986	0.9874	0.006	0.009
7,3',4'-trihydroxyisoflavone	11.86	35	269.0511	213.0533	195.0423, 91.01792	2.243667	y = 1.5261x - 0.1417	0.9965	0.013	0.021
Genistin	11.964	32	431.098	268.0378		14.36351	y = 0.09x - 0.0065	0.9757	0.35	0.584
Naringin	11.988	35	579.173	271.0626	151.0043, 459.11546	2.669411	y = 2.8426x - 0.3412	0.9924	0.009	0.015
2',6'-dihydroxyacetophenone	11.993	25	151.0442	91.01861	109.0286, 83.01347, 135.0074, 65.03972	0.293406	y = 5.443x + 0.1585	0.9975	0.004	0.006
6,7,4'-trihydroxyisoflavone	12.395	35	269.0511	240.0405	195.0451, 95.142	1.554351	y = 0.8901x - 0.0805	0.9913	0.017	0.028
Resveratrol	12.628	27	227.0688	143.05	185.061	10.10361	y = 0.4391x - 0.0686	0.9918	0.069	0.116
7,4' Dihydroxyflavone	13.19	30	253.058	117.0344	135.0078, 91.019	0.22318	y = 7.3656x - 0.2485	0.994	0.002	0.003
Morin	13.319	25	301.0298	151.0033	65.00434	0.523837	y = 4.762x - 0.8103	0.9789	0.005	0.009
Daidzein	13.46	40	253.058	132.0217	91.01995, 223.04063	0.892693	y = 2.0693x - 0.0999	0.9948	0.01	0.017
Liquiritigenin	13.5	20	255.0547	119.0498	135.0083	1.813823	y = 0.6191x - 0.0299	0.9423	0.014	0.024
2-Mercaptobenzothiazole	13.732	30	165.9752	57.97622	134.0068	1.916747	y = 2.9644x - 0.0898	0.9917	0.005	0.008
Eriodictyol	13.798	15	287.0501	151.0003	135.0426	0.141985	y = 11.936x + 0.233	0.9929	0.001	0.002
Madecassoside	13.844	40	973.0501	674.586	101.4428		Not quantifiable			
Glycetein	13.851	25	283.0582	268.0381	240.0424	1.416528	y = 1.119x - 0.0517	0.9742	0.032	0.054
Luteolin	13.995	40	285.0415	133.0289		0.196809	y = 7.7621x - 0.0714	0.9505	0.001	0.002
trans-cinnamic acid	13.998	10	147.0381	102.9457	58.95883		Not quantifiable			
Quercetin	14.119	25	301.0298	151.0033	121.0287	0.184183	y = 5.0408x + 0.9412	0.9808	0.002	0.003

Table A2.1a continued– A list of the phenypropanoid standards that were run on the LC MS/MS for quantification sorted by retention times.

Compound	Rt (min)	Collission Energy (keV)	Parent ion [M-H]- (m/z)	Product ion(m/z)	Other Qualifiers(m/z)	Response factor (RF)	Standard curve	R^2	LOD (ppm)	LOQ (ppm)
Naringenin	14.656	20	271.0507	151.0008	119.0473	1.004125	y = 0.7829x + 0.0712	0.9675	0.017	0.028
Genistein	14.794	35	269.0511	133.0289	159.0457, 63.0243		Co-elutes with Apigenin			
Coumesterol	14.797	40	267.029	266.0203	211.0375, 91.01705, 167.04727	0.268063	y = 6.1164x - 0.3344	0.9916	0.002	0.004
Apigenin	14.797	35	269.0511	117.0354	107.0145, 151.00465	0.315596	y = 4.9548x - 0.1057	0.968	0.004	0.006
Kaempferol	14.917	40	285.0415	93.03446	117.0342, 65.00376	14.52931	y = 0.2114x - 0.0806	0.9262	0.154	0.257
Hesperetin	15.063	25	301.0597	164.0091	151.0013, 65.00416	1.690602	y = 0.5407x + 0.2034	0.9382	0.036	0.059
7-hydroxyflavone	15.182	40	237.0615	91.0191	208.0528	9.237254	y = 0.2582x - 0.0472	0.9706	0.342	0.569
3(3',4'-dimethoxyphenyl)-7-hydroxycoumarin	15.399	23	297.0659	267.0328	282.0565, 293.03745	0.193508	y = 11.68x - 0.7643	0.955	0.001	0.002
Isoliquiritigenin	15.5	20	255.0547	119.0498	135.0083	0.672722	y = 13.452x + 0.066	0.9896	0.001	0.001
6-hydroxyflavone	15.59	27	237.0615	193.0521	79.00821, 101.02747	2.436106	y = 0.6247x + 0.0109	0.9648	0.019	0.032
Formononetin	15.59	25	267.0554	252.0384	223.0376	0.058789	y = 29.639x - 3.5674	0.9816	0.0005	0.0008
5-hydroxy-7-methoxy flavone	15.59	25	267.0554	252.0293	223.0253, 195.0283		Not quantifiable			
5,7-dihydroxyflavone	16.518	35	253.058	63.02406	143.0484, 119.04851	4.909721	y = 0.5158x + 0.1486	0.9095	0.014	0.023
5,7'- dihydroxy-4-methoxyisoflavone (Biochanin A)	16.92	25	283.0582	268.0375	239.0346	0.347787	y = 11.133x + 1.0343	0.9175	0.004	0.007
5,4'-dihydroxy-7-methodyisoflavone	16.925	25	283.0582	268.0369	239.0334		Not quantifiable			

Table A2.1a continued– A list of the phenypropanoid standards that were run on the LC MS/MS for quantification sorted by retention times.

Compound	Rt (min)	Collission Energy (keV)	Parent ion [M-H]- (m/z)	Product ion(m/z)	Other Qualifiers(m/z)	Response factor (RF)	Standard curve	R^2	LOD (ppm)	LOQ (ppm)
3-Hydroxy-3',4'-Dimethoxyflavone	18.86	23	297.0659	267.0328			Not quantifiable			

Table A2.1b – List of compounds that were detected in root samples when parent and product ions for known standards were targeted.

Compound	Rt (min)	Parent ion [M-H]- (m/z)	Product ion(m/z)	Other Qualifiers(m/z)	Target compound
n-n-dihydroxyflavone-glucoside-like	2.377	433.108	253.0449		*Inferred from massbank profile*
p-hydroxy benzoic acid-like	9.6	137.0259	93.03564		p-hydroxy benzoic acid
3-hydroxybenzoic acid-like	10.616	137.0259	93.03443		p-hydroxy benzoic acid
Genistein, Isomer	11.89	269.0511	133.0289	159.0457, 63.0243	Genistein
Naringenin chalcone isomer	12.175	271.0507	151.0008	119.0473	Naringenin
Genistin, like	12.23	431.098	268.0378		Genistin
Formononetin-like	14.28	267.0554	252.0384	223.0376	Formononetin

A4.1 Microarray statistical analysis details as perfomed on Partek GS.

4-way ANOVA using REML (Thompson, 1960).

Input data was corrected using GCRMA background correction and normalised using Quantile Normalisation. The probe intensities were $\log_2$ transformed.

Model:

$$Y_{ijklm} = \mu + Genotype_i + Inoculation_j + Timepoint_k + Scan\ Date\ (Timepoint)_{kl} + Genotype * Inoculation_{ij} + Genotype * Inoculation * Timepoint_{ijk} + \varepsilon_{ijklm}$$

Where Y_{ijklm} represented the m^{th} observation on the i^{th} Genotype j^{th} Inoculation k^{th} Timepoint l^{th} Scan Date

μ was the common effect for the whole experiment.

ε_{ijklm} represented the random error present in the m^{th} observation on the i^{th} Genotype j^{th} Inoculation k^{th} Timepoint l^{th} Scan Date .The errors ε_{ijklm} were assumed to be normally and independently distributed with mean 0 and standard deviation δ for all measurements.

Scan Date was a random effect.

Contrast method: Fisher's Least Significant Difference (LSD)

The following contrast(s) (Dunlop and Tamhane, 2000) was performed to compare:

CHS vs. PH8
CHS * inoc+ vs. CHS * inoc-
CHS * inoc+ vs. PH8 * inoc+
CHS * inoc+ vs. PH8 * inoc-
CHS * inoc- vs. PH8 * inoc+
CHS * inoc- vs. PH8 * inoc-
PH8 * inoc+ vs. PH8 * inoc-
CHS * inoc+ * 24h vs. CHS * inoc+ * 6h
CHS * inoc+ * 24h vs. CHS * inoc- * 24h
CHS * inoc+ * 24h vs. CHS * inoc- * 6h
CHS * inoc+ * 24h vs. PH8 * inoc+ * 24h
CHS * inoc+ * 24h vs. PH8 * inoc+ * 6h
CHS * inoc+ * 24h vs. PH8 * inoc- * 24h
CHS * inoc+ * 24h vs. PH8 * inoc- * 6h
CHS * inoc+ * 6h vs. CHS * inoc- * 24h
CHS * inoc+ * 6h vs. CHS * inoc- * 6h
CHS * inoc+ * 6h vs. PH8 * inoc+ * 24h
CHS * inoc+ * 6h vs. PH8 * inoc+ * 6h
CHS * inoc+ * 6h vs. PH8 * inoc- * 24h
CHS * inoc+ * 6h vs. PH8 * inoc- * 6h

CHS * inoc- * 24h vs. CHS * inoc- * 6h
CHS * inoc- * 24h vs. PH8 * inoc+ * 24h
CHS * inoc- * 24h vs. PH8 * inoc+ * 6h
CHS * inoc- * 24h vs. PH8 * inoc- * 24h
CHS * inoc- * 24h vs. PH8 * inoc- * 6h
CHS * inoc- * 6h vs. PH8 * inoc+ * 24h
CHS * inoc- * 6h vs. PH8 * inoc+ * 6h
CHS * inoc- * 6h vs. PH8 * inoc- * 24h
CHS * inoc- * 6h vs. PH8 * inoc- * 6h
PH8 * inoc+ * 24h vs. PH8 * inoc+ * 6h
PH8 * inoc+ * 24h vs. PH8 * inoc- * 24h
PH8 * inoc+ * 24h vs. PH8 * inoc- * 6h
PH8 * inoc+ * 6h vs. PH8 * inoc- * 24h
PH8 * inoc+ * 6h vs. PH8 * inoc- * 6h
PH8 * inoc- * 24h vs. PH8 * inoc- * 6h

Sources of variation

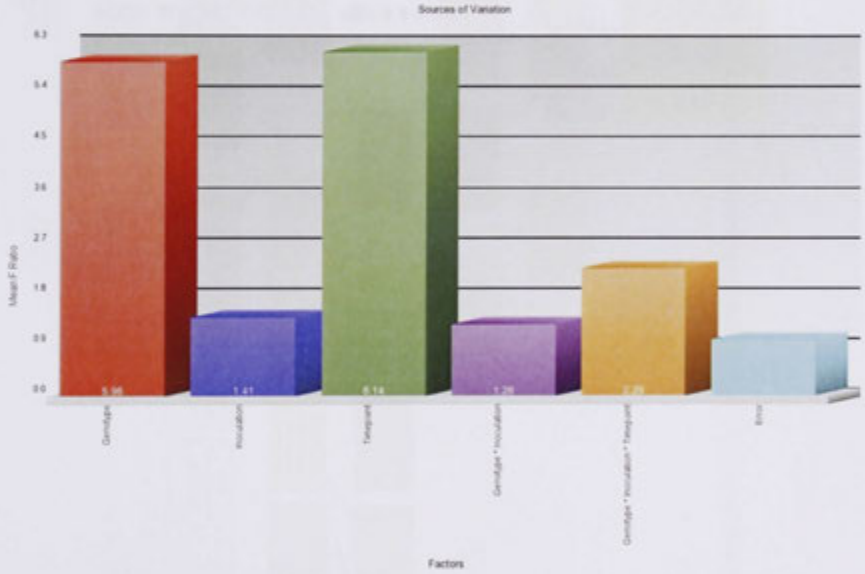

Figure A4.1- Sources of variations in 4-way ANOVA comparisons

Interpretation of statistics for Figures A4.2-4.8

Figures A4.2 – A4.8 shows the results of gene enrichment analysis. The statistical significance ranges from Level 1 (P<0.05) till Level 9 (P<5e-10) on the colour scale below –

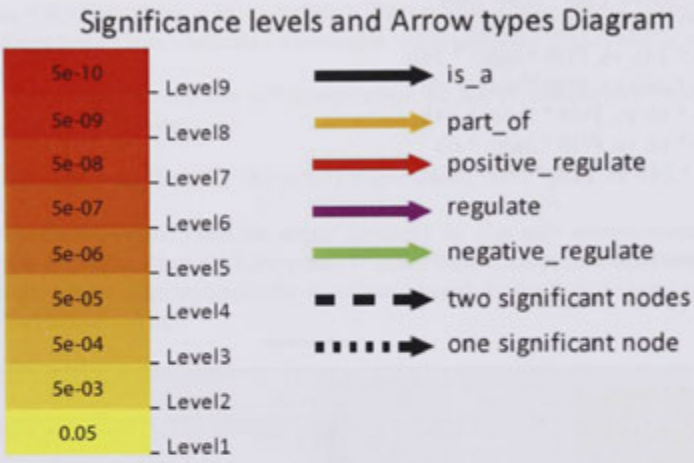

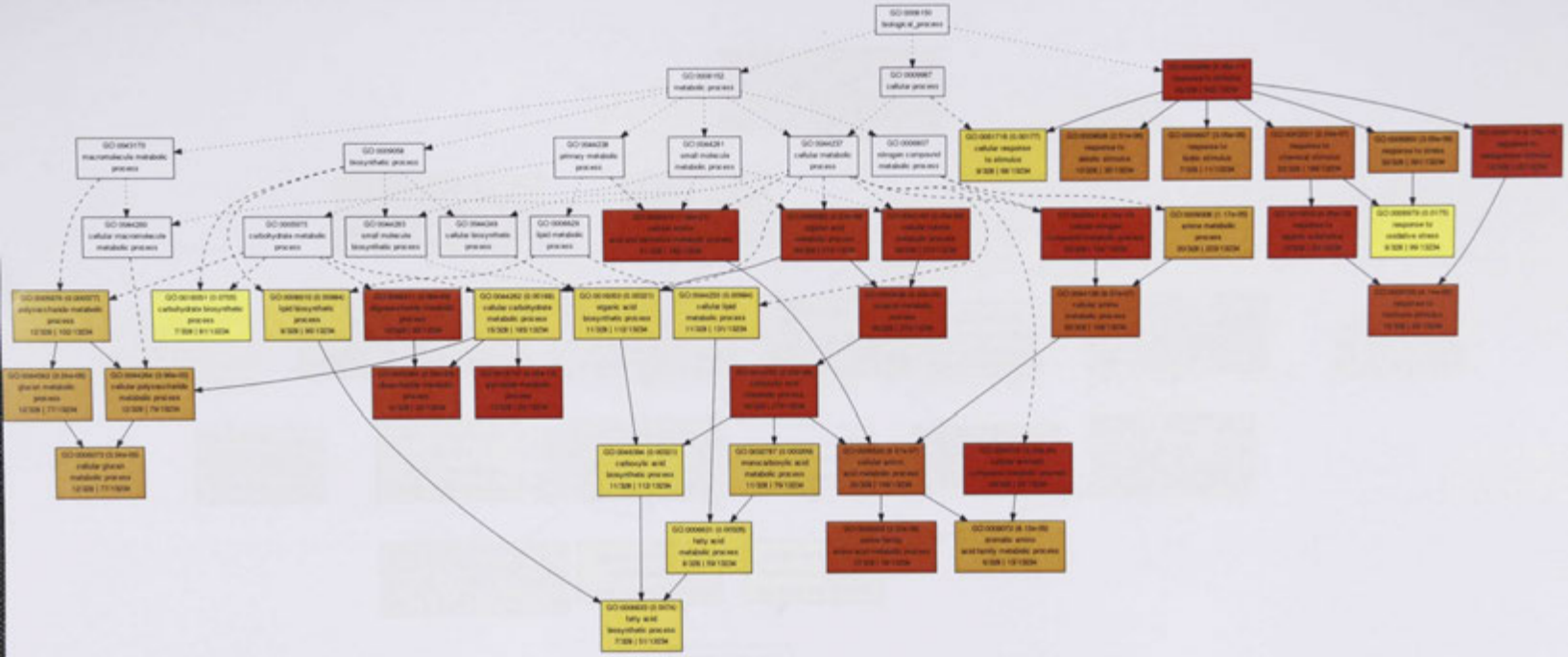

Figure A4.2 – CHSE6 vs CE6 Down-regulated genes showing enrichment of biological processes

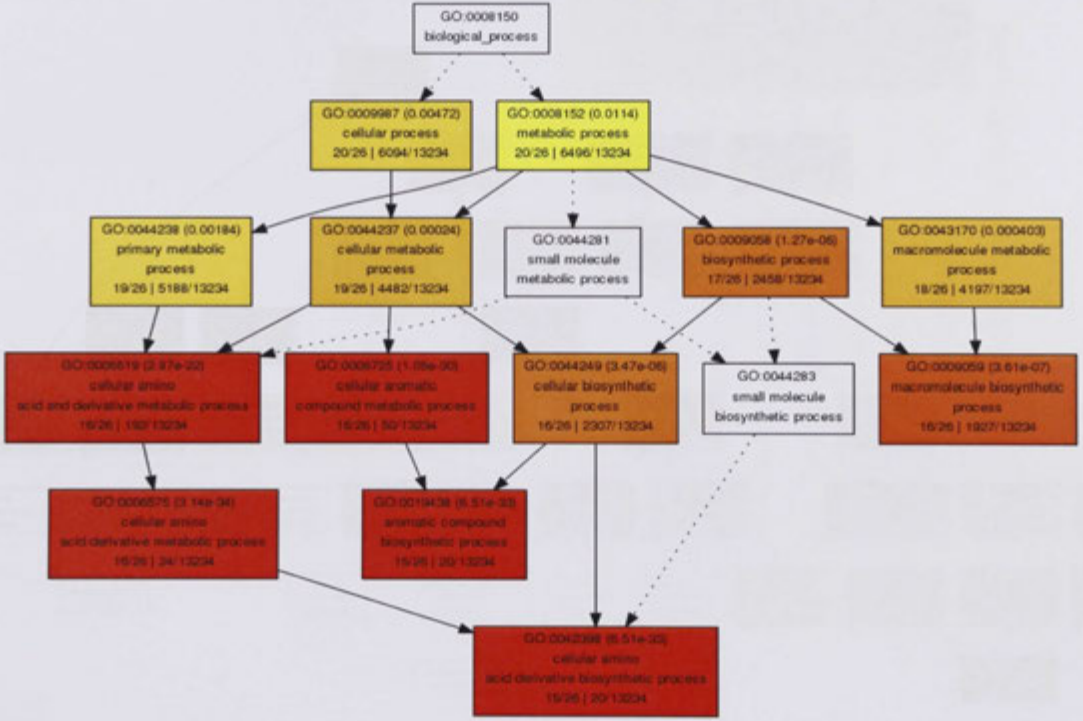

Figure A4.3 CHSE24 vs CE24 Down-regulated genes showing enrichment of biological processes

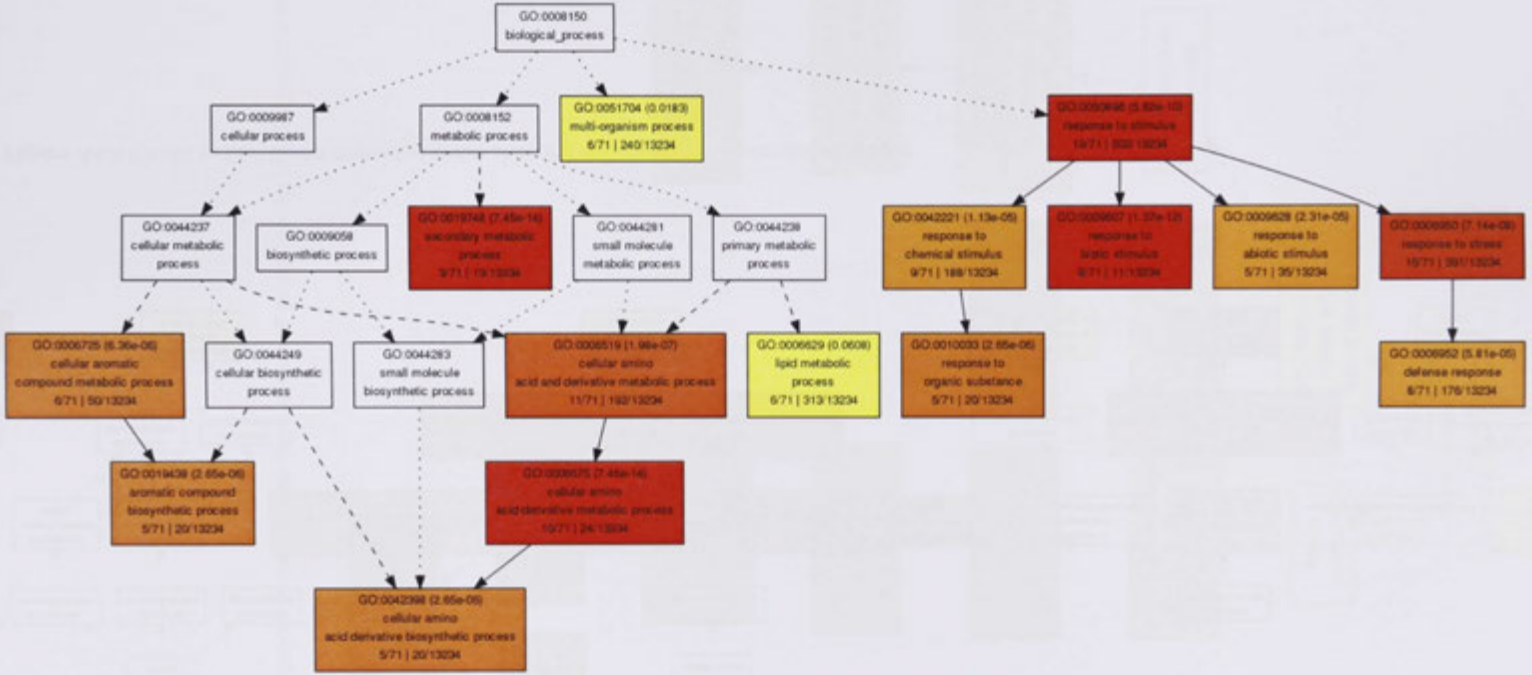

Figure A4.4 CHSE24 vs CE24 Up-regulated genes showing enrichment of biological processes

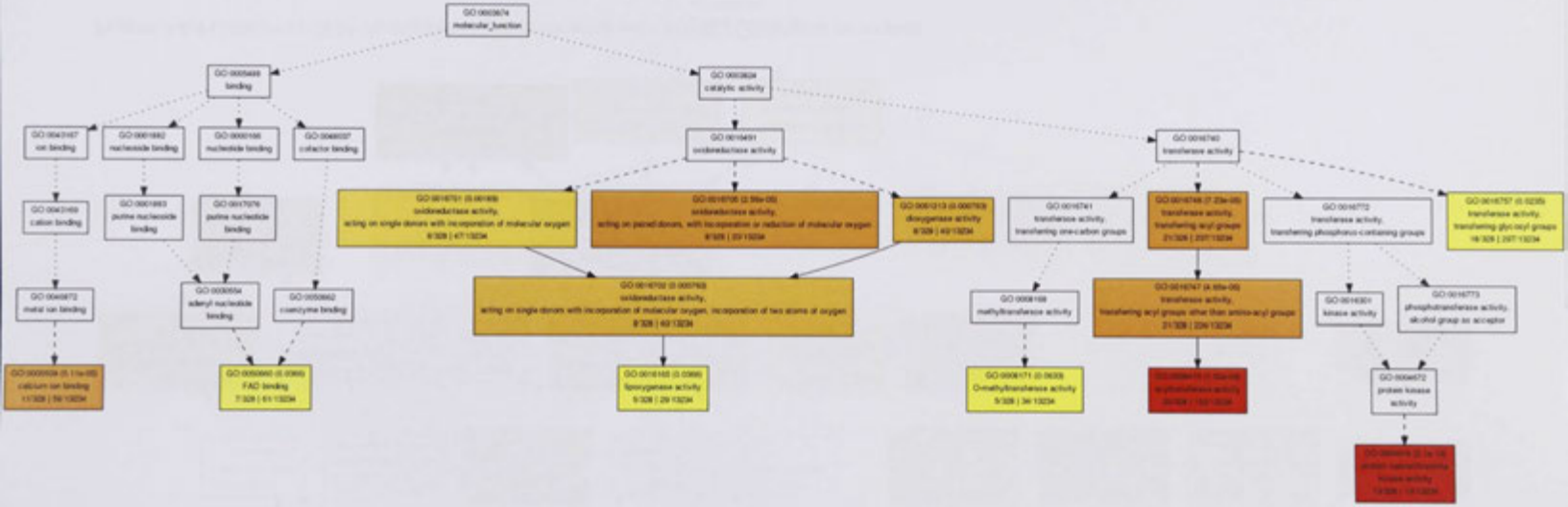

Figure A4.5 CHSE6 vs CE6 Down-regulated genes showing enrichment of molecular functions

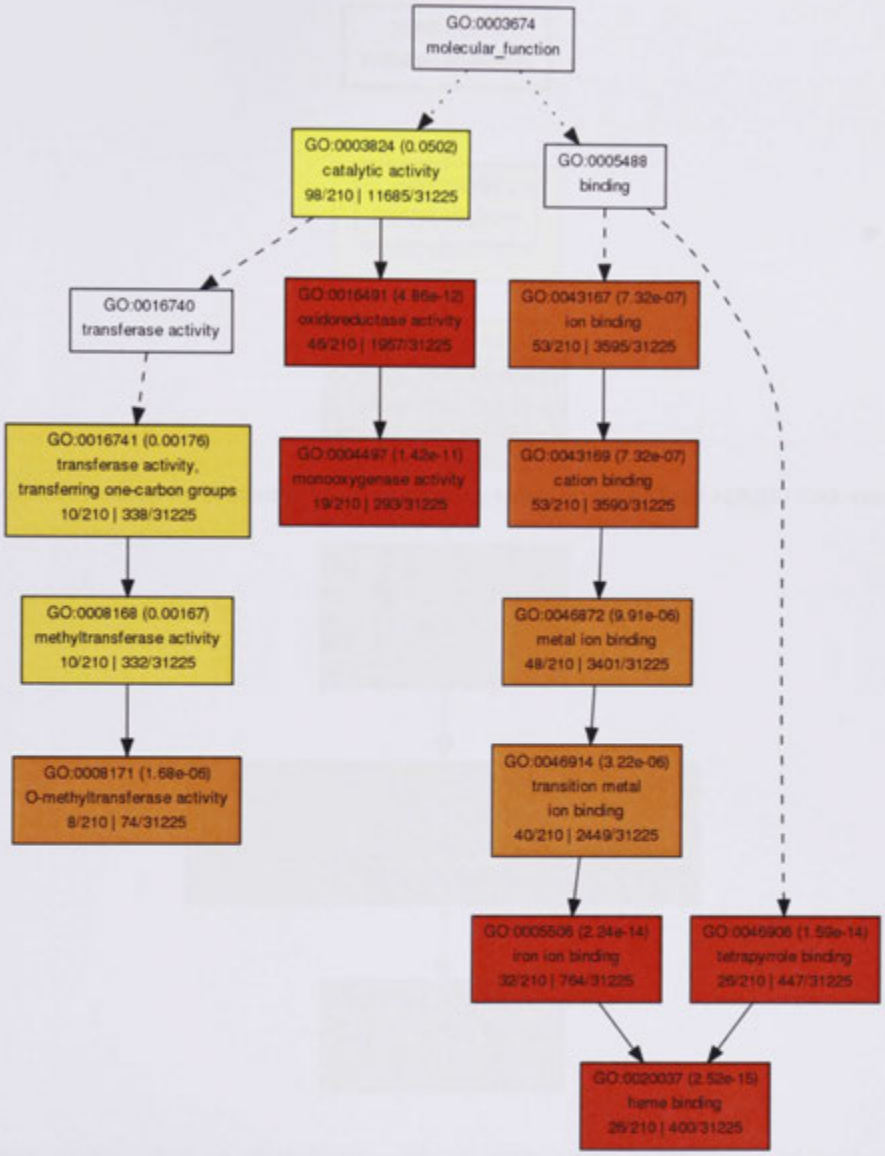

Figure A4.6 CHSE6 vs CE6 Up-regulated genes showing enrichment of molecular functions

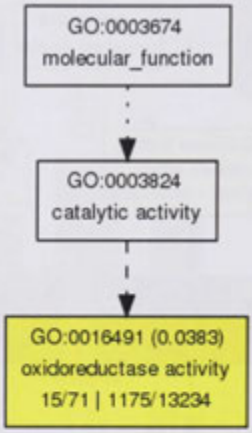

Figure A4.7 CHSE24 vs CE24 Up-regulated genes showing enrichment of molecular functions

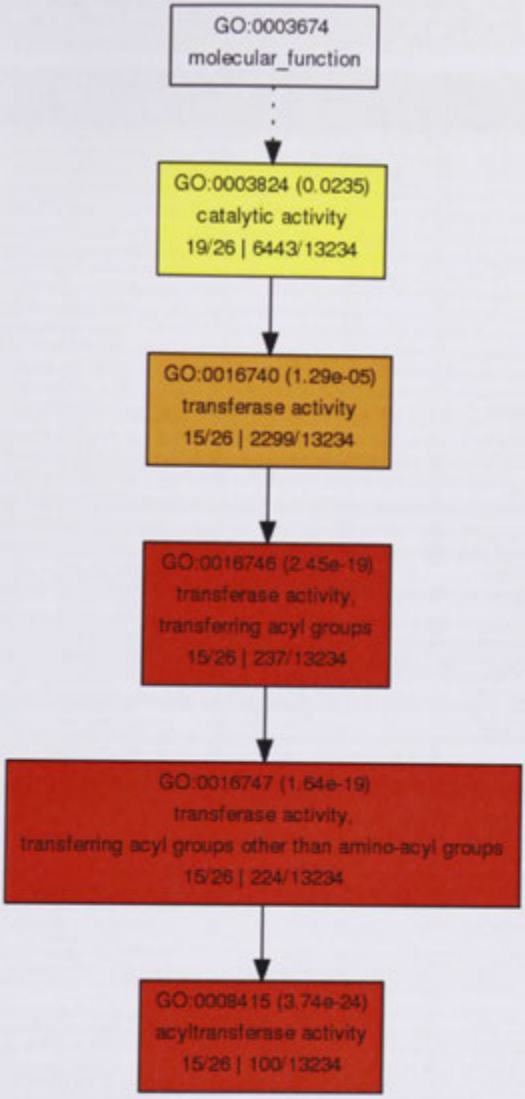

Figure A4.8 CHSE24 vs CE24 Down-regulated genes showing enrichment of molecular functions

Table A4.1 – Fold changes in transcripts across the ANOVA comparisons in CHS and Control (C) roots 6 and 24 hpi with E65 rhizobia (E) or Blank media (B). Table is sorted according to changes in first comparison column (CHSB6 vs CB6) followed by columns on the right. Please note that this table spans pages 252-267.

Probeset ID	Tentative Consensus	Gene	CHS B6 vs. CB6	CHS B24 vs. CB24	CHSE 6 vs. CE6	CHSE 24 vs. CHS B24	CHSE 24 vs. CHS E 6	CHSE 24 vs. CE24	CB24 vs. CB6	CE6 vs. CB6	CE24 vs. CB24	CE24 vs. CE6	CE vs. CB	CHS B vs.C B	CHSE vs. CHS B	CHSE vs. CE	CHS vs. C
Mtr.49572.1.S1_s_at	TC113999	chalcone synthase	-8.80	-5.92	-9.20			-6.41						-7.22		-7.68	-7.44
Mtr.43046.1.S1_at	TC123927	Enod12A precursor	-7.99		-6.72		15.55							5.92			-3.68
Msa.3134.1.S1_at	TC126033	chalcone synthase	-7.28	-4.68	-12.03			-4.58				-2.57		-5.84		-7.42	-6.58
Mtr.20187.1.S1_x_at	TC137455	chalcone synthase	-6.30	-4.89	-6.79			-5.54						-5.55		-6.13	-5.83
Mtr.17616.1.S1_x_at	TC120398	chalcone synthase	-6.25	-3.09	-5.49			-3.19						-4.39		-4.18	-4.29
Mtr.20187.1.S1_at	TC137455	chalcone synthase	-5.79	-4.60	-6.79			-4.94						-5.16		-5.79	-5.47
Mtr.17621.1.S1_x_at	TC118157	chalcone synthase	-5.19	-2.91	-5.80		2.03	-3.62						-3.89		-4.58	-4.22
Mtr.42071.1.S1_at	TC113204	GTP cyclohydrolase	-5.03		-5.04		2.41					-2.18		-3.00		-2.20	-2.57
Mtr.43118.1.S1_x_at	AW691409	Cytochrome P450 72A1	-4.98		-3.87												-2.35
Mtr.10369.1.S1_at	TC126033	chalcone synthase	-4.97	-3.54	-8.66			-3.64						-4.19		-5.62	-4.85
Mtr.1577.1.S1_x_at	AW560869	Potassium transporter 5	-4.57														
Mtr.45667.1.S1_x_at	TC116581	chalcone synthase	-4.31	-2.64	-4.44			-2.73						-3.38		-3.48	-3.43
Mtr.49572.1.S1_x_at	TC119999	chalcone synthase	-4.23	-2.77	-5.08			-2.79						-3.43		-3.76	-3.59
Mtr.40345.1.S1_at	TC114926	Putative uncharacterised protein	-3.86		-2.56											-2.01	
Mtr.28714.1.S1_at	TC122894	chalcone synthase	-3.74	-5.75	-5.90			-3.37						-4.64		-4.46	-4.55
Mtr.14428.1.S1_x_at	TC122894	chalcone synthase	-3.74	-3.36	-4.62			-2.96						-3.55		-3.70	-3.62
Mtr.45103.1.S1_at	TC136981	Putative uncharacterized protein	-3.72		-3.28		2.72							-2.53			-2.05
Mtr.20185.1.S1_x_at	TC119414	chalcone synthase	-3.66		-4.14			-2.13						-2.79		-2.97	-2.88
Mtr.27563.1.S1_at	BE205009	Pectinesterase 3 precursor	-3.65		-5.22							-6.25				-2.25	-2.02
Mtr.14428.1.S1_at	TC122894	chalcone synthase	-3.64	-2.31	-4.38			-2.81						-2.90		-3.51	-3.19
Mtr.10368.1.S1_at	TC139125	chalcone synthase	-3.61		-3.39									-3.24		-2.77	-3.00
Mtr.20567.1.S1_at	TC115732	chalcone synthase	-3.51	-4.03	-4.06			-4.55						-3.76		-4.30	-4.02
Mtr.32557.1.S1_at	AW695696	Cytochrome c oxidase subunit 1	-3.45														
Mtr.17612.1.S1_x_at	TC120398	chalcone synthase	-3.42	-2.30	-3.52			-2.51						-2.80		-2.97	-2.89
Mtr.38984.1.S1_at	TC121049	Putative uncharacterized protein	-3.42		-2.63				-2.63			-3.02					
Mtr.20185.1.S1_at	TC119414	chalcone synthase	-3.40		-4.16			-2.05						-2.62		-2.92	-2.77
Mtr.13272.1.S1_x_at	TC126523	Cytochrome P450	-3.40		-3.34							-3.79				-2.11	-2.02
Mtr.33191.1.S1_at	BF645909	Putative uncharacterized protein	-3.34														
Mtr.47587.1.S1_at	NP7272621	Wall-associated receptor kinase-like protein	-3.34		-6.33		3.62									-2.72	-2.24
Mtr.43143.1.S1_at	TC122330	Cytochrome P450, partial (45%)	-3.29														
Mtr.20464.1.S1_x_at	TC116581	chalcone synthase	-3.21		-2.52									-2.30		-2.18	-2.24
Mtr.5829.1.S1_at	TC138366	Putative uncharacterized protein	-3.17		-2.54							-2.67					
Mtr.29564.1.S1_at	TC120617	Putative uncharacterized protein	-3.17		-2.84							-2.59		-2.05			
Mtr.39363.1.S1_at	TC129071	Importin-7	-3.16														
Mtr.10373.1.S1_at	TC129282	Peroxidase	-3.10									2.72					
Mtr.35454.1.S1_at	TC131128	Transcription factor RF2b	-3.07									-3.67					
Mtr.48778.1.S1_x_at	TC123388	Cold and drought-regulated protein CORA	-3.01		-4.93				-5.00			-4.02				-2.13	
Mtr.43332.1.S1_at	TC116001	F-box family protein	-2.98		-3.27							-4.26					
Mtr.39896.1.S1_at	TC133663	Putative uncharacterized protein	-2.98		-3.10							-3.40				-2.11	
Mtr.17321.1.S1_x_at	TC120392	Cytochrome P450 monooxygenase	-2.95		-3.65		2.23							-2.29		-2.44	-2.36
Mtr.37287.1.S1_x_at	TC120763	Beta-glucosidase [Fragment]	-2.94		-3.69							-4.12		-2.24			-2.02
Mtr.50207.1.S1_s_at	NP7265452	UDP-N-acetylglucosamine/UDP-glucose/GDP-mannose transporter (MTR_1g012590)	-2.93		-2.24												
Mtr.12868.1.S1_at	TC131395	Cytochrome P450 71D11-like	-2.92		-2.69									-2.19			-2.01
Mtr.27484.1.S1_s_at	TC124388	probable protein arginine N-methyltransferase 6-like	-2.86														
Mtr.5884.1.S1_x_at	BG450986	Putative uncharacterized protein	-2.85														
Mtr.31521.1.S1_at	AL368579	lysine histidine transporter 1-like	-2.85														
Mtr.28556.1.S1_at	BG648602	Putative uncharacterized protein	-2.83									-2.37					
Mtr.33660.1.S1_x_at	BI262918	Cyclin-L1-1	-2.83														
Mtr.2664.1.S1_at	TC117558	weakly similar to Cyt P450 monooxygenase CYP93B12 / flavone synthase II	-2.80		-4.89							-3.90				-2.19	
Mtr.43706.1.S1_at	TC122761	Putative uncharacterized protein	-2.77		-2.30							-2.82					
Mtr.23567.1.S1_x_at	TC122142	Organ-specific protein S2 (MTR_3g034640)	-2.72														
Mtr.12016.1.S1_at	TC130919	Dolichyl-P-Man:Man(5)GlcNAc(2)-PP-dolichyl mannosyltransferase	-2.70														
Mtr.9079.1.S1_at	TC124783	Putative uncharacterized protein	-2.70											-2.50			
Mtr.1614.1.S1_at	AW586059	F-box family protein	-2.68									-2.47					
Mtr.16474.1.S1_at	TC129175	Putative narbonin	-2.66		-3.04			-2.38						-2.18		-2.69	-2.42
Mtr.6825.1.S1_at	CX526580	wall-associated receptor kinase 3-like	-2.65											-2.06			
Mtr.10900.1.S1_at	TC115147	probable receptor protein kinase TMK1-like	-2.64		-2.62							-2.79					
Mtr.12428.1.S1_at	TC180351	Albumin-2	-2.64											-2.46			
Mtr.38928.1.S1_at	TC131350	Choline transporter-like protein	-2.63		-2.14							-2.08					
Mtr.34918.1.S1_x_at	CX527996	Putative uncharacterised protein	-2.62														
Mtr.10183.1.S1_x_at	TC114079	Serine/threonine phosphatase-like	-2.60									-2.24					
Mtr.41019.1.S1_at	TC176902	Putative uncharacterised protein	-2.59		-3.07		4.47							-2.73			-2.25
Msa.3075.1.S1_at	TC114976	Alanine aminotransferase	-2.59														
Mtr.29567.1.S1_at	TC113607	CYCLOPS	-2.57		-2.28												
Mtr.9329.1.S1_x_at	TC127306	Cytochrome P450 71B9	-2.56		-2.57							-2.24					
Mtr.13079.1.S1_x_at	TC116336	Phosphoacetylglucosamine mutase	-2.55		-2.48							-2.17					
Mtr.28848.1.S1_a_at	BQ124307	Putative uncharacterised protein	-2.55		-2.13											-2.00	
Mtr.28133.1.S1_at	BG583562	WD repeat-containing protein, putative	-2.55		-2.64							-3.24					
Mtr.31090.1.S1_at	TC134545	Putative uncharacterised protein	-2.54		-2.81							-3.07					
Mtr.13614.1.S1_at	TC125315	Cytosolic 5'-nucleotidase III-like protein (MTR_1g090380)	-2.51														
Mtr.9175.1.S1_at	TC119433	UDP-glucosyltransferase	-2.48		-2.13												
Mtr.38681.1.S1_a_at	TC122102	Protoporphyrinogen oxidase	-2.47														
Mtr.10924.1.S1_at	TC123104	CAS1 domain-containing protein 1-like	-2.45		-3.04							-2.47				-2.01	
Mtr.5253.1.S1_at	AW694672	Serine carboxypeptidase family protein	-2.44		-2.78							-2.99					
Mtr.32730.1.S1_at	BE319726	Narbonin	-2.44														
Mtr.42323.1.S1_at	TC123345	Putative uncharacterised protein	-2.43									-2.11					
Mtr.32443.1.S1_at	TC131408	Putative uncharacterised protein	-2.40														
Mtr.33081.1.S1_at	BF641078	Putative uncharacterised protein	-2.39		-2.60							-3.19					
Mtr.34816.1.S1_a_at	CX525529	Putative uncharacterised protein	-2.38														
Mtr.28705.1.S1_at	BI310885	Putative uncharacterised protein	-2.37		-2.45											-2.11	
Mtr.13068.1.S1_at	TC125562	Amino acid transporter like protein	-2.37														
Mtr.11268.1.S1_at	TC122181	Receptor like protein kinase	-2.37														
Mtr.38441.1.S1_at	TC123974	RopGEF2	-2.35		-2.06							-2.18					
Mtr.44169.1.S1_at	TC125799	S-receptor kinase-like protein 3	-2.33									-2.23					
Mtr.33582.1.S1_at	TC191261	Ubiquitin carboxyl-terminal hydrolase	-2.32		-2.24			-2.35								-2.29	-2.14
Mtr.34409.1.S1_at	BQ147194	Putative uncharacterised protein	-2.31		-2.03												
Mtr.10286.1.S1_at	TC132957	S-receptor kinase-like protein 3	-2.30														
Mtr.49423.1.S1_at	NP7264210	chalcone synthase	-2.30	-2.14	-2.99			-2.47						-2.22		-2.72	-2.45
Mtr.43182.1.S1_at	TC128916	Beta-glucosidase (MTR_4g131810)	-2.30		-2.76												
Mtr.42664.1.S1_at	TC128711	Putative uncharacterised protein	-2.30														
Mtr.33706.1.S1_at	BI265271	Pentatricopeptide repeat-containing	-2.27														
Mtr.20427.1.S1_at	TC125063	Cc-nbs-lrr resistance protein	-2.27		-2.48				-2.53								
Mtr.28848.1.S1_at	BQ124307	Putative uncharacterised protein	-2.27														
Mtr.33402.1.S1_at	TC133428	Auxin-induced protein 5NG4	-2.26		-2.45							-2.32					
Mtr.37944.1.S1_at	TC115827	(iso)flavonoid glycosyltransferase	-2.25														
Mtr.12930.1.S1_at	TC115903	Putative uncharacterised protein	-2.25		-2.15							-2.02					
Mtr.33637.1.S1_at	TC121670	Putative uncharacterised protein	-2.24		-2.11												
Mtr.22278.1.S1_at	TC117284	Notum-like protein	-2.23		-2.54							-2.71					
Mtr.41781.1.S1_at	TC127479	UDP-N-acetylglucosamine/UDP-glucose/GDP-mannose transporter	-2.23														
Mtr.35739.1.S1_at	TC131346	Putative uncharacterised protein	-2.22		-2.40												
Mtr.1510.1.S1_s_at	TC124754	Putative uncharacterised protein	-2.22														
Mtr.32196.1.S1_at	TC112946	Putative uncharacterised protein	-2.20														
Mtr.33039.1.S1_s_at	BF639306	Putative uncharacterised protein	-2.19														
Mtr.14782.1.S1_at	TC119510	1-aminocyclopropane-1-carboxylate oxidase	-2.19											-2.11			
Mtr.9662.1.S1_at	TC125673	AP-4 complex subunit mu	-2.18		-2.14												
Mtr.11549.1.S1_at	TC125118	SCAI-like	-2.18		-2.22												
Mtr.37481.1.S1_at	TC118620	eukaryotic translation initiation factor 3 subunit E-like	-2.17														

Probeset ID	Tentative Consensus	Gene	CHSB 6 vs. CB6	CHSB 24 vs. CB24	CHSE6 vs. CE6	CHSE 24 vs. CHSB 24	CHSE 24 vs. CHS E 6	CHSE 24 vs. CE24	CB24 vs. CB6	CE6 vs. CB6	CE24 vs. CB24	CE24 vs. CE6	CE vs. CB	CHSB vs.CB	CHSE vs. CHSB	CHSE vs. CE	CHS vs.C
Mtr.38945.1.S1_at	TC128141	protein phosphatase 2C 52-like	-2.17														
Mtr.39466.1.S1_at	TC119549	WD-repeat protein-like protein	-2.16														
Msa.362.1.S1_at	TC122082	Putative uncharacterised protein	-2.15		-2.00							-2.04					
Mtr.42539.1.S1_at	TC130693	Putative uncharacterised protein	-2.15														
Mtr.41719.1.S1_s_at	TC138797	MAPKinase	-2.14														
Mtr.45185.1.S1_at	TC138918	chloroplastic outer envelope membrane protein TOC75	-2.12														
Mtr.22807.1.S1_at	NP7257713	Xylosyltransferase)	-2.12														
Mtr.27539.1.S1_at	BE204347	Reticuline oxidase-like protein	-2.12		-2.67							-2.70					
Mtr.7396.1.S1_at	TC121081	Putative uncharacterised protein	-2.11									-2.29					
Mtr.42234.1.S1_at	TC117649	Cytochrome P450, partial	-2.10														
Mtr.42977.1.S1_s_at	TC124621	S-adenosylmethionine decarboxylase (partial)	-2.10														
Mtr.9066.1.S1_at	TC133013	BURP-domain-containing protein	-2.10			2.02											
Mtr.29254.1.S1_s_at	TC115202	Putative uncharacterised protein	-2.10														
Mtr.31327.1.S1_s_at	TC113120	Protein kinase	-2.09														
Mtr.41573.1.S1_at	TC113857	Synaptotagmin-7	-2.09														
Mtr.6498.1.S1_at	BQ146800	Pentatricopeptide repeat-containing protein	-2.09														
Mtr.9982.1.S1_at	TC139571	CrcB-like protein	-2.09									-2.22					
Mtr.13566.1.S1_at	TC120695	Cytochrome P450 82A3	-2.09		-2.07	2.85											
Mtr.32820.1.S1_s_at	BE325200	Glucan 1,3-beta-glucosidase	-2.09														
Mtr.9162.1.S1_at	TC119633	serine carboxypeptidase-like 49-like	-2.09		-2.42							-2.01					
Mtr.12065.1.S1_at	TC125726	Putative uncharacterised protein	-2.08														
Mtr.10330.1.S1_s_at	TC126085	Putative uncharacterised protein	-2.08														
Mtr.44663.1.S1_s_at	TC113048	Protein kinase 2B	-2.07														
Mtr.37715.1.S1_at	TC122510	Putative uncharacterised protein	-2.07						-2.54								
Mtr.13054.1.S1_at	TC129546	Putative uncharacterised protein	-2.07														
Mtr.40106.1.S1_s_at	TC117553	MLP-like protein	-2.06		-5.58	2.51						-2.01		-2.18		-2.48	-2.33
Mtr.14639.1.S1_s_at	TC127976	Haem peroxidase	-2.05														
Mtr.35267.1.S1_at	CX540411	Putative uncharacterised protein	-2.03														
Mtr.22806.1.S1_at	NP7257712	Protein pxs1	-2.03														
Mtr.41172.1.S1_s_at	TC112919	Receptor-like protein kinase	-2.02		-3.40							-3.06				-2.06	
Mtr.18690.1.S1_at	NP7274161	Myosin-like protein	-2.02														
Mtr.9836.1.S1_at	TC128209	UDP-glucuronosyltransferase 3A1	-2.02														
Mtr.52092.1.S1_s_at	TC140439	Pectinesterase	-2.01		-3.99							-2.50					
Mtr.22423.1.S1_at	No TC	Harpin inducing protein 1 like protein	-2.01						-2.15								
Mtr.13466.1.S1_at	TC119598	trpH-like protein	-2.01														
Mtr.28009.1.S1_at	BF648773	Putative uncharacterised protein	-2.01														
Mtr.39781.1.S1_at	TC122207	Pectate lyase family protein	-2.00		-3.55							-4.04					
Mtr.37813.1.S1_s_at	TC128150	Putative uncharacterised protein	-2.00														
Mtr.4545.1.S1_s_at	TC135991	Symbiotic ammonium transporter7	-2.00		-2.38												
Mtr.47369.1.S1_s_at	NP7261349	Multidrug resistance protein ABC transporter family	-2.00														
Mtr.44325.1.S1_at	TC120439	Putative uncharacterised protein	-2.00														
Mtr.43714.1.S1_at	TC119509	Caesin kinase	2.00		2.13												
Mtr.43072.1.S1_at	TC113594	Fiber annexin	2.01														
Mtr.318.1.S1_at	TC129247	12-oxophytodienoate reductase	2.01														
Mtr.21272.1.S1_at	TC138677	heavy metal transport/detoxification protein	2.02		2.80												
Mtr.48895.1.S1_s_at	TC137471	Putative uncharacterised protein	2.03														
Mtr.35850.1.S1_at	TC132051	WRKY transcription factor	2.03		2.79												
Mtr.12656.1.S1_at	TC176766	NADPH quinone oxidoreductase	2.05	3.23	2.47			3.48						2.57		2.93	2.75
Mtr.10462.1.S1_at	TC178418	Non-symbiotic hemoglobin 1	2.05		3.15											2.11	
Mtr.44584.1.S1_at	TC121790	Myb family transcription factor APL	2.06		2.13												
Mtr.28017.1.S1_s_at	BF650436	Putative uncharacterised protein	2.08														
Mtr.48713.1.S1_at	TC116214	60S ribosomal protein L10	2.08														
Mtr.4063.1.S1_at	TC113350	Interferon-induced GTP-binding protein Mx	2.08		2.14							2.43					
Mtr.3229.1.S1_at	TC134153	F-box family protein	2.09		2.10												
Mtr.46708.1.S1_at	TC140965	Putative uncharacterised protein	2.11														
Mtr.35409.1.S1_at	TC133340	Partially similar to Cc-nbs-lrr resistance protein	2.11		2.16							2.36					
Mtr.25362.1.S1_s_at	TC114488	12-oxophytodienoate reductase	2.12														
Mtr.40564.1.S1_at	TC114052	Beta-glucosidase G1	2.13	2.77	2.61			3.71						2.43		3.11	2.75
Mtr.40252.1.S1_at	TC130180	Putative uncharacterised protein	2.13		2.41			2.14						2.37		2.27	2.32
Mtr.33914.1.S1_at	BI273162	gibberellin 2-oxidase	2.14														
Mtr.36679.1.S1_s_at	BQ145052	Putative uncharacterised protein	2.15														
Mtr.47992.1.S1_at	TC134986	Putative uncharacterised protein	2.16			2.03		2.75						2.35		2.18	2.26
Mtr.40252.1.S1_s_at	TC130180	Putative uncharacterised protein	2.16		2.34			2.00						2.28		2.17	2.22
Mtr.18771.1.S1_at	NP7253180	Putative uncharacterised protein	2.17		2.14							2.09					
Mtr.31015.1.S1_at	TC116903	Putative uncharacterised protein	2.17														
Mtr.43550.1.S1_at	TC118875	Tyrosine aminotransferase, partial	2.19		2.44			2.18						2.18		2.30	2.24
Mtr.33162.1.S1_at	BF644787	RZR3-MYB transcription factor	2.19	2.66										2.41			2.14
Mtr.29146.1.S1_at	CA990143	Putative uncharacterised protein	2.21														
Mtr.12327.1.S1_s_at	TC133807	Late embryogenesis abundant protein 1 (or 2)	2.24														
Mtr.42743.1.S1_at	TC134643	Putative uncharacterised protein	2.24														
Mtr.40555.1.S1_at	TC121925	Pathogenesis-related protein 5-1	2.25	3.62	3.41			3.53						2.85		3.47	3.14
Msa.878.1.S1_at	TC178418	Non-symbiotic hemoglobin 1	2.26		3.34											2.26	
Mtr.43621.1.S1_at	TC175901	Glutathione S-transferase	2.26		3.42			2.20						2.29		2.74	2.51
Mtr.20928.1.S1_at	NP7263914	Glucan endo-1,3-beta-glucosidase	2.27		2.08												
Mtr.41983.1.S1_at	TC117884	UDP-glucosyltransferase, putative	2.27		3.27							2.24		2.26		2.37	2.31
Mtr.11076.1.S1_at	TC121411	Putative uncharacterised protein	2.27		3.63											2.15	
Mtr.4438.1.S1_at	TC135478	Short-chain dehydrogenase Tic32	2.29		2.71							2.00		2.24		2.13	2.18
Mtr.8763.1.S1_at	TC177232	Thaumatin-like protein PR-5a	2.30		2.31									2.67		2.24	2.44
Mtr.17478.1.S1_at	TC114387	26S proteasome non-ATPase regulatory subunit	2.30														
Mtr.29072.1.S1_s_at	CA917321	Nonsymbiotic hemoglobin, partial	2.32		2.07												
Mtr.18067.1.S1_at	TC126789	Isoliquiritigenin 2'-O-methyltransferase	2.32	3.33	2.76	2.15		3.88						2.78		3.27	3.02
Mtr.6947.1.S1_at	CX531295	Putative uncharacterised protein	2.36														
Mtr.33927.1.S1_at	BQ079323	Putative uncharacterised protein	2.37		2.42	-2.03											
Msa.1965.1.S1_at	ES613827	Thaumatin-like protein PR-5a precursor, 081927	2.38		2.24			2.34						2.71		2.29	2.49
Mtr.29062.1.S1_at	CA917030	Putative uncharacterised protein	2.41		2.39												
Mtr.40878.1.S1_at	CA921921	Putative uncharacterised protein	2.41		2.14							2.76					
Mtr.24228.1.S1_at	TC173248	Isoflavone reductase-like protein (MTR_4g070340)	2.42		2.02											2.01	
Mtr.12322.1.S1_at	TC122421	MtN19-like protein	2.43		3.11									2.33		2.44	2.38
Mtr.17710.1.S1_at	TC124950	No apical meristem (NAM) protein	2.46		2.64												
Mtr.15791.1.S1_at	TC129410	Cytochrome P450	2.47		2.67									2.18		2.12	2.15
Mtr.37058.1.S1_at	TC140316	Putative uncharacterised protein	2.47														
Mtr.9355.1.S1_at	TC115729	Putative uncharacterised protein	2.51		2.69												
Mtr.2124.1.S1_s_at	TC127170	TMV resistance protein N	2.53		2.57							2.54					
Mtr.15981.1.S1_at	NP7273186	Disease resistance-like protein	2.54		3.10							2.40					
Mtr.35343.1.S1_at	CX550355	MtN19 protein precursor	2.54		4.91							2.34		2.18		2.88	2.50
Mtr.42231.1.S1_at	TC118839	Leucoanthocyanidin dioxygenase-like	2.57		2.10												
Mtr.39535.1.S1_at	CA922914	Hydroxycinnamoyl CoA shikimate -like	2.58		3.16							2.29		2.41		2.10	2.25
Mtr.37401.1.S1_at	TC183289	Nodule-specific cysteine-rich peptide 122	2.60														
Mtr.20618.1.S1_at	TC172944	Anthranilate N-benzoyltransferase protein	2.60		2.87									2.65		2.41	2.53
Mtr.37609.1.S1_at	TC126611	Putative uncharacterised protein	2.62		2.31												
Mtr.44349.1.S1_at	TC123356	MTR_2g097580	Zinc transporter	2.63		5.30		-2.88									2.32	2.08
Mtr.13544.1.S1_at	TC136915	MORC family CW-type zinc finger protein	2.66		2.09				2.94								
Msa.509.1.S1_at	TC136240	Putative uncharacterised protein	2.68														
Mtr.40531.1.S1_at	TC117506	weakly similar to Isoliquiritigenin 2'-O-methyltransferase	2.69		3.90			2.39						2.81		3.05	2.93
Mtr.34958.1.S1_at	TC137575	Putative uncharacterised protein	2.71				2.71	2.66						2.62			2.19
Mtr.32076.1.S1_at	TC132452	Putative uncharacterised protein	2.72		2.76												
Mtr.34081.1.S1_at	BQ137674	Cytochrome P450 monooxygenase CYP72A59	2.74		2.91									2.89		2.13	2.48
Mtr.20618.1.S1_s_at	TC172944	Anthranilate N-benzoyltransferase protein	2.75		3.68			2.48						2.90		3.02	2.96
Mtr.19752.1.S1_at	TC120586	Isoflavonoid malonyl transferase	2.77		2.26									2.33			2.08
Mtr.42154.1.S1_at	TC121650	Eukaryotic translation initiation factor 1A	2.79		3.12							2.15		2.20			2.08
Mtr.43877.1.S1_at	TC96232	Copper transport protein	2.84		2.15												
Mtr.32629.1.S1_s_at	AW777075	weakly similar to Thaumatin-like protein PR-5a	2.87		2.83			2.50						3.43		2.66	3.02

Probeset ID	Tentative Consensus	Gene	CHSB 6 vs. CB6	CHSB 24 vs. CB24	CHSE6 vs. CE6	CHSE 24 vs. CHSB 24	CHSE 24 vs. CHS E6	CHSE 24 vs. CE24	CB24 vs. CB6	CE6 vs. CB6	CE24 vs. CB24	CE24 vs. CE6	CE vs. CB	CHSB vs.CB	CHSE vs. CHSB	CHSE vs. CE	CHS vs. C
Mtr.34371.1.S1_at	TC131983	Putative uncharacterised protein	2.92		2.51												
Mtr.8466.1.S1_at	TC127896	partially similar to aquaporin (aqp1 gene)/ Probable aquaporin TIP-type	2.94		3.96							2.82		2.09		2.46	2.27
Mtr.37455.1.S1_at	TC174236	Hydroquinone glucosyltransferase	2.96		3.44									2.82		2.90	2.86
Mtr.21701.1.S1_s_at	TC125229	(Iso)flavonoid glycosyltransferase	3.03	3.16	4.43		2.02	3.22				2.78		3.09		3.78	3.42
Mtr.39358.1.S1_at	TC125229	(Iso)flavonoid glycosyltransferase	3.06		5.53		2.16	3.60				3.32		3.12		4.46	3.73
Mtr.42876.1.S1_at	TC126852	Pathogenesis-related protein 4A,	3.13														
Mtr.12316.1.S1_at	TC121824	Glutathione S-transferase GST	3.24		2.60											2.12	
Mtr.8574.1.S1_at	TC120567	Pectate lyase	3.28		9.30							6.83		2.57		2.81	2.69
Mtr.39734.1.S1_at	TC124916	Glutathione S-transferase GST	3.47				-2.56					-2.31					
Mtr.43254.1.S1_at	TC118645	Putative uncharacterized protein	3.51		5.39			3.34				3.09		3.47		4.24	3.84
Mtr.46540.1.S1_at	TC120912	Calvin cycle protein CP12	3.63		3.05		-2.21							2.02			
Mtr.43158.1.S1_s_at	TC138508	Alternative oxidase	3.86		3.92		-2.75							2.03			
Mtr.35486.1.S1_at	TC132544	Fasciclin-like arabinogalactan protein	3.87		7.14							3.75				3.55	2.97
Mtr.43157.1.S1_at	TC119443	Alternative oxidase	3.89		4.00							2.54		2.30			2.05
Mtr.40420.1.S1_at	TC115093	Putative uncharacterised protein	4.05		5.97		-2.01					2.96		2.23		2.45	2.34
Mtr.10662.1.S1_at	TC114690	Heat shock protein hsp23	4.06		2.50												
Mtr.40379.1.S1_at	TC183336	Irucoanthocyanidin dioxygenase-like	4.09		5.27		-2.93							2.54		2.32	2.43
Mtr.4639.1.S1_at	TC130731	Nodule-specific protein Nlj70	4.17		6.75			2.10	2.00			2.76		2.78		3.76	3.23
Mtr.10498.1.S1_at	TC124437	wound-inducible putative cytosolic terpene synthase 2	4.49											3.08			2.00
Mtr.16277.1.S1_at	TC132463	Proteinase inhibitor I12, Bowman-Birk	4.55	5.52	4.16		2.07	4.47						5.01		4.31	4.65
Mtr.44792.1.S1_at	TC116843	wound-inducible putative cytosolic terpene synthase 2 mRNA	4.60											2.15			
Mtr.28796.1.S1_at	BM814294	Cytochrome P450 monooxygenase	4.60		4.63									3.17		3.11	3.14
Mtr.32965.1.S1_at	BF635325	Cytochrome B5	4.66	3.75	3.85			4.78						4.18		4.29	4.23
Mtr.33281.1.S1_s_at	BF649143	Putative uncharacterised protein	4.71											3.22			
Mtr.28729.1.S1_at	BI311944	Subtilisin-like serine protease	4.75														
Mtr.19575.1.S1_at	TC181965	Putative uncharacterised protein	5.16		13.37			3.15				4.19		5.21		6.49	5.82
Mtr.38954.1.S1_at	TC125263	NADPH oxidase	5.23		8.68		-2.64		2.27			2.22		2.56		3.59	3.03
Mtr.5107.1.S1_s_at	AW687337	Partially similar to wound-inducible putative cytosolic terpene synthase 2 mRNA	5.43											3.11			2.06
Mtr.12433.1.S1_at	TC114809	(+)-delta-cadinene synthase isozyme A	6.04		8.79							4.80		3.83		3.33	3.57
Mtr.24231.1.S1_at	TC113385	Pterocarpan reductase	6.63	11.8 9	8.16			8.45						8.88		8.30	8.59
Mtr.10220.1.S1_s_at	TC126789	Isoliquiritigenin 2'-O-methyltransferase	7.59	10.6 7	15.17			8.75				3.06		9.00		11.5 2	10.18
Mtr.1191.1.S1_at	NP7270414	Elongation factor G	7.64		2.63									2.76			2.26
Mtr.12321.1.S1_at		MtN19-like protein	9.88		9.02									7.52		4.30	5.69
Mtr.8568.1.S1_at	TC100672	Ferredoxin-nitrite reductase	15.6 5		17.08		-8.49							4.55		3.63	4.07
Mtr.5486.1.S1_s_at	BF632529	Protein SRG1		2.39			2.05	3.16								2.29	
Mtr.9913.1.S1_s_at	TC172660	Peptide transporter PTR1		2.53													
Mtr.42023.1.S1_at	TC119489	GDSL esterase/lipase		2.71				2.47								2.02	
Mtr.12477.1.S1_at	TC126253	Quinone-oxidoreductase QR1		2.71	2.16									2.26			2.04
Msa.2622.1.S1_at	TC121925	Pathogenesis-related protein 5-1		3.10	2.48			3.31						2.49		2.87	2.67
Mtr.10958.1.S1_at	TC118129	Peroxidase 52 precursor		3.55			2.21										
Mtr.9478.1.S1_at	TC139541	Laccase-7 precursor		4.40	3.78			5.02						3.08		4.35	3.66
Mtr.40970.1.S1_at	TC129031	weakly similar to Glycine max cationic peroxidase 1-like, transcript variant 1		6.25			3.08							2.84			2.23
Mtr.40263.1.S1_at	**TC125691**	**Auxin-responsive GH3 product**		**6.53**	**3.21**									**2.80**			**2.15**
Mtr.43572.1.S1_at	TC124578	Germin-like protein subfamily 1 member		7.08			5.06	3.69						3.44		2.18	2.74
Mtr.43713.1.S1_at	TC177640	chalcone synthase			-8.97											-8.25	-6.55
Mtr.21912.1.S1_at	TC174279	Kunitz-type trypsin inhibitor-like 1 protein			-7.48		3.68					-4.13					
Mtr.15215.1.S1_at	TC129565	Putative uncharacterised protein			-6.31		5.39										-2.39
Mtr.42299.1.S1_s_at	AP74693	Latex cysteine-rich beta glucosidase			-5.29											-2.55	-2.37
Mtr.40946.1.S1_at	TC114666	GDSL esterase/lipase CPRD49-like			-4.82		3.01							-2.41		-2.13	-2.27
Mtr.46868.1.S1_s_at	TC122215	Lipoxygenase			-4.81		4.90							-2.89			-2.40
Mtr.25885.1.S1_s_at	TC130379	Transcription factor bHLH120			-4.58		2.16					-2.53					
Mtr.23965.1.S1_s_at	TC136043	Wound-induced protein			-4.58							-4.56					
Mtr.46870.1.S1_at	TC118775	Lipoxygenase			-4.39		4.16							-3.19			-2.48
Mtr.47022.1.S1_s_at	TC123476	Wound-induced protein			-4.36							-4.44					
Mtr.19030.1.S1_at	TC113366	Flavonol sulfotransferase-like protein			-4.21		2.42					-2.37					
Mtr.15490.1.S1_at	NP7263869	Phosphatidylinositol transfer-like protein II			-4.12							-2.46				-2.16	
Mtr.2844.1.S1_at	BQ154020	Putative uncharacterised protein			-4.12							-2.59					
Mtr.12361.1.S1_at	TC137391	N8 protein			-3.91							-2.45					
Mtr.42466.1.S1_at	TC114087	Inorganic phosphate transporter 1-4			-3.76							-6.24					
Mtr.22590.1.S1_at	No TC	Putative uncharacterised protein			-3.66							-2.38					
Mtr.12041.1.S1_s_at	TC130859	Sec14 cytosolic factor			-3.65							-3.86					
Mtr.28691.1.S1_at	BI310480	Nine-cis-epoxycarotenoid dioxygenase3			-3.60												
Mtr.1205.1.S1_at	NP7260240	Actin depolymerizing factor			-3.59							-2.67					
Mtr.27822.1.S1_at	BF003758	Amino acid permease AAP4			-3.58							-3.57				-2.53	-2.24
Mtr.29577.1.S1_at	TC138301	Flavonol sulfotransferase-like protein			-3.52		2.42										
Mtr.39333.1.S1_at	TC129996	Hypothetical protein			-3.50		6.02										
Mtr.14323.1.S1_at	NP7265495	Reticulon family protein			-3.47							-2.91					
Mtr.34114.1.S1_s_at	TC141769	Pathogenesis related protein			-3.46							-3.70					
Mtr.37368.1.S1_at	TC120049	Anthocyanidin 3-O-glucosyltransferase			-3.37							-2.47					
Mtr.44456.1.S1_at	TC129834	Pectinesterase			-3.33							-3.22				-2.08	
Mtr.41405.1.S1_at	TC190235	Isomerase, putative			-3.31		3.46										
Mtr.45409.1.S1_at	TC128516	Cytochrome P450			-3.29												
Mtr.13370.1.S1_at	TC123648	Gibberellin 3-beta-hydroxylase			-3.28		2.46										
Mtr.37050.1.S1_at	TC135239	Putative uncharacterised protein			-3.24		2.60										
Mtr.14184.1.S1_s_at	TC115097	Annexin type V			-3.23							-2.38					
Mtr.5263.1.S1_at	AW694985	Transcription factor BEE			-3.22							-2.34					
Mtr.35725.1.S1_at	TC130380	Transcription factor bHLH120			-3.21		2.18										
Mtr.26489.1.S1_at	TC136552	Pectolytic enzyme, Pectin lyase fold			-3.18											-2.18	
Mtr.31772.1.S1_s_at	TC134052	Sulfotransferase			-3.16												
Mtr.8478.1.S1_s_at	TC136134	Beta-glucosidase			-3.14							-2.82					
Mtr.16275.1.S1_at	TC130630	Proteinase inhibitor I12, Bowman-Birk			-3.09		2.39										
Mtr.35064.1.S1_at	CX531990	Cucumisin-like serine protease subtilisin-like protease			-3.07							-3.70					
Mtr.31189.1.S1_at	TC119403	Trehalose-phosphate phosphatase			-3.06							-2.22					
Mtr.28564.1.S1_at	TC128951	Lysine/histidine transporter			-3.05												
Mtr.37912.1.S1_at	TC122080	Putative uncharacterised protein			-3.03	7.39	6.79				7.24		5.17				
Mtr.17321.1.S1_at	TC180185	Cytochrome P450			-3.03									-2.29		-2.11	-2.20
Mtr.7344.1.S1_at	TC136234	Anthocyanidin 3-O-glucosyltransferase			-2.99		2.33										
Mtr.45376.1.S1_at	TC131096	Peptide transporter PTR5			-2.95							-3.17					
Mtr.25759.1.S1_at	TC125735	Albumin-2			-2.94							-2.64					
Mtr.50093.1.S1_s_at	TC133152	Glucose-6-phosphate isomerase			-2.94							-3.60					
Mtr.36069.1.S1_s_at	AJ845941	Glucosyltransferase			-2.94												
Mtr.11344.1.S1_s_at	TC113104	Beta-galactoside alpha-2,6-sialyltransferase			-2.94							-2.95					
Mtr.21341.1.S1_at	TC114436	Glutamyl-tRNA reductase			-2.90												
Mtr.38330.1.S1_at	TC118024	Putative uncharacterised protein			-2.88							-4.61					
Mtr.23516.1.S1_at	NP7257575	hypothetical protein (80 similarity with Metal transporter CNNM4			-2.87					5.97	4.67		5.28		2.81	-2.12	
Mtr.9953.1.S1_at	TC136483	Putative uncharacterised protein			-2.87		2.37										
Mtr.27468.1.S1_at	TC138094	Nitrate transporter			-2.87							-3.50					
Mtr.8427.1.S1_at	TC122096	Lipoxygenase			-2.85			2.22				-6.01					
Mtr.1511.1.S1_at	AW256912	Putative uncharacterised protein			-2.84												
Mtr.8507.1.S1_at	TC123318	Pathogenesis related protein			-2.83		2.74					-2.77					
Mtr.12690.1.S1_at	TC133363	Putative uncharacterized protein			-2.83							-3.46					
Mtr.9895.1.S1_at	TC127423	Putative uncharacterised protein			-2.82												
Mtr.44789.1.S1_at	**TC112920**	**Nodulation-signaling pathway 2 protein**			**-2.81**												
Mtr.32193.1.S1_s_at	AW684440	Em3-binding f-box protein			**-2.81**							-3.08				-2.14	

Probeset ID	Tentative Consensus	Gene	CHSB 6 vs. CB6	CHSB 24 vs. CB24	CHSE6 vs. CE6	CHSE 24 vs. CHSB 24	CHSE 24 vs. CHS E6	CHSE 24 vs. CE24	CB24 vs. CB6	CE6 vs. CB6	CE24 vs. CB24	CE24 vs. CE6	CE vs. CB	CHSB vs.CB	CHSE vs. CHSB	CHSE vs. CE	CHS vs. C
Mtr.45228.1.S1_at	TC140738	putative pectinesterase/pectinesterase inhibitor 24-like			-2.80							-2.78					
Mtr.39005.1.S1_at	TC125584	Nitrate transporter			-2.78												
Mtr.26731.1.S1_x_at	TC138253	Annexin			-2.77												
Mtr.17359.1.S1_at	TC126550	Pectinesterase/pectinesterase inhibitor			-2.76							-2.16					
Mtr.40684.1.S1_at	TC120671	isoflavonoid malonyl transferase 3 (MAT3)			-2.76												
Mtr.22308.1.S1_at	NP7260612	Protein kinase			-2.75							-2.31					
Mtr.605.1.S1_x_at	NP7260612	Sulfotransferase			-2.74							-2.25					
Mtr.26881.1.S1_x_at	AL365936	Putative uncharacterised protein			-2.74							-3.14					
Mtr.25211.1.S1_x_at	**TC113389**	**Rhizobium induced Peroxidase**			-2.72							-2.02					
Mtr.31772.1.S1_at	TC134052	Sulfotransferase			-2.72												
Mtr.10954.1.S1_at	TC133063	CBL-interacting protein kinase 1			-2.71							-2.49					
Mtr.17053.1.S1_at	TC132885	Protein kinase-like; Calcium-binding EF-hand			-2.70							-2.13					
Mtr.1154.1.S1_at	TC134767	Putative uncharacterized protein			-2.68							-2.04					
Mtr.34393.1.S1_x_at	BQ146796	probable polygalacturonase-like			-2.67							-4.15					
Mtr.13070.1.S1_at	TC178144	Putative uncharacterized protein			-2.66												
Mtr.37724.1.S1_x_at	TC114591	S-adenosyl-L-methionine: 2`7`4`-trihydroxyisoflavanone 4`-O-methyltransferase			-2.64												
Mtr.15323.1.S1_x_at	TC112865	Phosphate transporter 3			-2.63												
Mtr.42370.1.S1_x_at	TC138675	Flavonol synthase/flavanone 3-hydroxylase			-2.62		2.11										
Mtr.41977.1.S1_at	TC131040	Glucose-6-phosphate/phosphate translocator			-2.61												
Mtr.51214.1.S1_at	TC129069	O-methyltransferase			-2.61												
Mtr.16954.1.S1_at	TC127344	Auxin-induced protein 6B			-2.60												
Mtr.11507.1.S1_at	TC131018	Taxane 13-alpha-hydroxylase			-2.59	2.70	2.42						2.04				
Mtr.40820.1.S1_at	TC141262	Glutathione peroxidase			-2.59							-2.58					
Mtr.99.1.S1_at	**TC172631**	**LysM domain-containing receptor-like kinase 3**			**-2.58**						**-3.23**	**-3.68**					
Mtr.11311.1.S1_at	TC133668	Sugar transporter ERD6, putative			-2.58												
Mtr.40861.1.S1_at	TC115545	cytochrome P450 monooxygenase CYP93B12			-2.57												
Mtr.35127.1.S1_x_at	CX533620	Flavonol synthase/flavanone 3-hydroxylase			-2.57		2.12										
Mtr.45474.1.S1_at	TC129835	Putative uncharacterised protein			-2.57							-2.00					
Mtr.45023.1.S1_at	TC124345	Xylosyltransferase			-2.56							-2.51					
Mtr.10905.1.S1_at	TC122483	polygalacturonase At1g48100-like			-2.56												
Mtr.9377.1.S1_at	TC133904	Putative uncharacterised protein			-2.55							-2.34					
Mtr.13049.1.S1_at	TC126705	Putative uncharacterised protein			-2.55							-3.07					
Mtr.12753.1.S1_at	TC124433	Putative uncharacterised protein			-2.55												
Mtr.27178.1.S1_at	AW585836	Putative uncharacterised protein			-2.55		2.20										
Mtr.21903.1.S1_at	TC124661	Putative uncharacterised protein			-2.54												
Mtr.10395.1.S1_at	TC127526	Partially similar to cellulose synthase			-2.54												
Mtr.43727.1.S1_x_at	TC124159	Squalene epoxidase			-2.54							3.54					
Mtr.12517.1.S1_at	TC117913	Lipase			-2.54												
Mtr.17057.1.S1_at	TC130859	Sec14 cytosolic factor			-2.53							-2.24					
Mtr.16730.1.S1_at	TC113834	Lectin			-2.53												
Mtr.31952.1.S1_at	TC132572	Serine/threonine protein kinase			-2.53												
Mtr.20206.1.S1_x_at	TC125192	Retinol dehydrogenase			-2.52												
Mtr.25211.1.S1_at	**TC113389**	**Rhizobium induced Peroxidase**			**-2.50**												
Mtr.11938.1.S1_at	TC115989	Auxin-induced protein 5NG4			-2.50							-2.36					
Mtr.26083.1.S1_x_at	TC139634	Putative small molecule transporter			-2.49												
Mtr.42405.1.S1_at	TC141062	Putative uncharacterised protein			-2.48		2.20										
Mtr.31502.1.S1_at	TC136090	Putative uncharacterised protein			-2.48							-2.23					
Mtr.32131.1.S1_at	AW584649	Type I inositol-1,4,5-trisphosphate 5-phosphatase			-2.48												
Mtr.44741.1.S1_at	TC116447	Putative uncharacterised protein			-2.47		2.18										
Mtr.17938.1.S1_at	TC112741	WD repeat-containing protein			-2.46							-2.40					
Mtr.35968.1.S1_at	AI974832	Putative uncharacterised protein			-2.45												
Mtr.38043.1.S1_at	TC115341	Cytokinin-O-glucosyltransferase			-2.45							-2.42					
Mtr.45897.1.S1_at	CB891950	Flavonol synthase/flavanone 3-hydroxylase			-2.45		2.35										
Mtr.8467.1.S1_at	TC131245	Putative uncharacterised protein			-2.45												
Mtr.33475.1.S1_x_at	BG451611	GDSL esterase/lipase APG			-2.44							-3.40					
Msa.3038.1.S1_at	TC117623	high-affinity phosphate transporter (PT1) gene			-2.44												
Mtr.40400.1.S1_at	TC136467	Reticuline oxidase-like protein			-2.43												
Mtr.24223.1.S1_at	NP7255616	IQ domain-containing protein			-2.43							-2.39					
Mtr.28860.1.S1_at	BQ124937	cytochrome P450 monooxygenase CYP72A67			-2.42												
Mtr.13532.1.S1_at	TC116537	Cytochrome P450 81D1			-2.42							-2.20					
Mtr.45553.1.S1_at	TC123725	Protein HOTHEAD			-2.42												
Mtr.8895.1.S1_at	TC140968	Putative uncharacterised protein			-2.41							-2.01					
Mtr.37288.1.S1_at	TC120763	Beta-glucosidase			-2.40							-2.46					
Mtr.11704.1.S1_at	TC125674	Putative uncharacterised protein			-2.39							-2.79					
Mtr.7556.1.S1_at	TC131277	Pathogenesis-related transcriptional factor and ERF			-2.39		2.04										
Mtr.20234.1.S1_at	TC119108	1-aminocyclopropane-1-carboxylate synthase			-2.39							-2.43					
Mtr.41958.1.S1_at	TC122371	Putative uncharacterised protein			-2.39												
Mtr.34762.1.S1_x_at	CX523832	Putative uncharacterised protein			-2.38												
Mtr.46203.1.S1_at	TC122728	Putative uncharacterised protein			-2.38							-3.34					
Mtr.50426.1.S1_at	TC122728	Putative uncharacterised protein			-2.38							-2.38					
Mtr.24980.1.S1_at	NP7259660	RNA polymerase sigma factor			-2.38												
Mtr.9492.1.S1_at	TC129949	expansin gene			-2.37							-2.36					
Mtr.39594.1.S1_at	TC139023	Putative uncharacterised protein			-2.37												
Mtr.15281.1.S1_at	NP7258554	Anthocyanin 5-aromatic acyltransferase			-2.37												
Mtr.14732.1.S1_at	NP7268304	FAD linked oxidase, N-terminal			-2.37												
Mtr.32717.1.S1_at	BE319374	equilibrative nucleoside transporter 2-like			-2.36							-2.16					
Mtr.8523.1.S1_at	TC117480	Protease inhibitor (MTR_3g106580)			-2.36		2.02										
Mtr.26736.1.S1_x_at	TC120185	Annexin D4 (MTR_8g038170)			-2.36							-2.15					
Mtr.30678.1.S1_at	CA917457	Putative uncharacterised protein			-2.36		2.18										
Mtr.27178.1.S1_x_at	AW585836	Putative uncharacterised protein			-2.35		2.17										
Mtr.28096.1.S1_at	TC131714	Nodule inception protein (NIN)			-2.35	6.10	3.57				5.25		4.89		3.44		
Mtr.31634.1.S1_at	AL373275	Putative uncharacterised protein			-2.34												
Mtr.4723.1.S1_at	AL378019	Putative uncharacterised protein			-2.34							-2.14					
Mtr.11288.1.S1_at	TC132637	Ripening-related protein-like			-2.34								2.03				
Mtr.15717.1.S1_at	TC126503	Chlorophyll a/b-binding protein			-2.34		2.41										
Mtr.9278.1.S1_at	TC121413	pleckstrin homology domain-containing family A member 8-like			-2.33												
Mtr.37810.1.S1_x_at	TC130171	Serine/threonine protein phosphatase 2A 57 kDa regulatory subunit B` iota isoform			-2.33							-2.92					
Mtr.15789.1.S1_at	**TC119454**	**LysM-domain containing receptor-like kinase NFP**			**-2.33**												
Mtr.43503.1.S1_at	TC119454	Putative uncharacterised protein			-2.33							-2.37					
Mtr.35965.1.S1_at	AI974746	Exocyst complex component EXO70			-2.33							-2.38					
Mtr.13661.1.S1_at	TC124565	Glycerophosphodiesterase-like protein			-2.33							-2.18					
Mtr.11490.1.S1_at	TC138347	Putative uncharacterised protein			-2.32							-2.16					
Mtr.37286.1.S1_at	TC118793	Beta-glucosidase			-2.32							-2.04					
Mtr.30517.1.S1_at	TC119133	RZR3-MYB transcription factor			-2.31												
Mtr.1797.1.S1_at	BE124666	MYB-related transcription factor			-2.31												
Mtr.33467.1.S1_at	BG451415	Putative uncharacterised protein			-2.31												
Mtr.27956.1.S1_x_at	BF632518	Putative uncharacterised protein			-2.31							-2.40					
Mtr.4415.1.S1_x_at	TC140004	Putative uncharacterised protein			-2.31		2.28										
Mtr.17272.1.S1_at	TC128588	Tubulin beta chain			-2.31								3.16				
Mtr.35480.1.S1_at	TC114240	Ser/Thr protein kinase (PRK); exostosin-like protein (EXO);			-2.31												
Mtr.50675.1.S1_at	TC113019	Leucine-rich repeat receptor-like protein kinase			-2.29												
Mtr.2382.1.S1_at	BG588537	Putative uncharacterised protein			-2.29							-2.24					
Mtr.45131.1.S1_at	TC136284	Putative uncharacterised protein			-2.29												
Mtr.5253.1.S1_x_at	AW694672	Serine carboxypeptidase family protein			-2.29							-2.99					
Mtr.28783.1.S1_x_at	BM813232	Putative uncharacterised protein			-2.29												
Mtr.41285.1.S1_at	TC116165	Laccase-like multicopper oxidase			-2.28							-2.61					

Probeset ID	Tentative Consensus	Gene	CHSB 6 vs. CB6	CHSB 24 vs. CB24	CHSE6 vs. CE6	CHSE 24 vs. CHSB 24	CHSE 24 vs. CHS E6	CHSE 24 vs. CE24	CB24 vs. CB6	CE6 vs. CB6	CE24 vs. CB24	CE24 vs. CE6	CE vs. CB	CHSB vs.CB	CHSE vs. CHSB	CHSE vs. CE	CHS vs. C
Mtr.5232.1.S1_at	AW693631	Beta-glucosidase			-2.28												
Mtr.41850.1.S1_at	TC126001	UDS1			-2.28												
Mtr.40400.1.S1_x_at	TC136467	Reticuline oxidase-like protein			-2.27												
Mtr.46628.1.S1_x_at	TC127622	Peroxidase			-2.27												
Mtr.32796.1.S1_at	BE323856	Putative uncharacterised protein			-2.27												
Mtr.14762.1.S1_at	TC124159	Squalene epoxidase			-2.27							-2.62					
Mtr.28283.1.S1_at	BG587472	Respiratory burst oxidase-like protein			-2.26							-2.72					
Mtr.45303.1.S1_at	TC137851	Putative uncharacterised protein			-2.26												
Mtr.46863.1.S1_x_at	TC119040	Lipoxygenase			-2.26												
Mtr.32240.1.S1_at	AW685718	pleiotropic drug resistance protein 1-like			-2.26							-3.04					
Mtr.12041.1.S1_at	TC130859	Sec14 cytosolic factor			-2.26												
Mtr.27895.1.S1_at	TC129300	phosphatase 2c-like protein			-2.26												
Mtr.5284.1.S1_at	AW696367	son of sevenless homolog 1			-2.26							-2.57					
Mtr.33813.1.S1_at	BI270502	Receptor protein kinase			-2.26							-2.08					
Mtr.428.1.S1_x_at	TC112919	Receptor-like protein kinase			-2.26												
Mtr.25183.1.S1_x_at	TC141731	Putative uncharacterised protein			-2.25												
Mtr.41085.1.S1_at	TC121596	Glycosyltransferase, putative			-2.25							-2.19					
Mtr.49789.1.S1_at	TC136137	Auxin-induced protein-like protein			-2.25							-2.07					
Mtr.9933.1.S1_at	TC134660	CTD small phosphatase-like protein			-2.25							-3.03					
Mtr.16214.1.S1_at	TC113229	Receptor-like kinase			-2.24	4.95	2.39			5.27			5.27		3.27		
Mtr.1511.1.S1_x_at	AW256912	Putative uncharacterized protein			-2.24												
Mtr.5356.1.S1_x_at	BE316821	Beta-glucosidase			-2.24												
Mtr.37384.1.S1_at	TC136130	Similar to granule-bound starch synthase			-2.23												
Mtr.9514.1.S1_at	TC133063	Putative uncharacterised protein			-2.23												
Mtr.39250.1.S1_at	TC115333	NBS-containing resistance-like protein			-2.22							-2.23					
Mtr.42366.1.S1_at	TC141262	Putative uncharacterised protein			-2.22							-2.18					
Mtr.4595.1.S1_at	AL368659	Pectinesterase			-2.22							-2.30					
Mtr.39465.1.S1_at	TC129614	Putative uncharacterised protein			-2.21							-2.46					
Mtr.4367.1.S1_at	AJ498552	Putative uncharacterised protein			-2.21												
Mtr.11000.1.S1_at	TC118640	GDSL-esterase/lipase			-2.21												
Mtr.8757.1.S1_at	TC120340	S-adenosyl-L-methionine: 2`7 4`-trihydroxyisoflavanone 4`-O-methyltransferase			-2.21												
Mtr.5571.1.S1_x_at	BF635996	Agenet and bromo-adjacent homology (BAH) domain-containing protein-like protein			-2.20							-3.04					
Mtr.44959.1.S1_at	TC126765	Fiber expressed protein			-2.20							-2.71					
Mtr.40666.1.S1_at	TC119349	thioredoxin s2			-2.20												
Mtr.15577.1.S1_at	TC122383	Peptidase A1, putative			-2.20												
Mtr.6541.1.S1_at	BQ148704	Rop guanine nucleotide exchange factor			-2.20							-2.19					
Mtr.7219.1.S1_at	TC114247	BURP domain-containing protein			-2.19												
Mtr.19945.1.S1_at	TC114710	malonyl CoA flavonoid malonyltransferase 5 (MaT5)			-2.19												
Mtr.45170.1.S1_at	TC139280	Lotus japonicus LYS7 mRNA for LysM type receptor kinase			-2.19												
Mtr.39566.1.S1_at	TC139308	Putative uncharacterised protein			-2.19							-2.64					
Mtr.16941.1.S1_at	TC119063	UDP-glycosyltransferase 73B3-like			-2.19												
Mtr.42673.1.S1_at	TC129226	Receptor protein kinase-like protein			-2.19							-2.41					
Mtr.9665.1.S1_at	TC125576	RING finger protein			-2.19							-2.31					
Mtr.40067.1.S1_x_at	TC126424	hydroxyproline-rich glycoprotein precursor gene			-2.18		3.96										
Mtr.39899.1.S1_at	TC134019	Putative uncharacterised protein			-2.18		3.64										
Mtr.16010.1.S1_at	NP7258368	Putative uncharacterised protein			-2.18												
Mtr.30687.1.S1_at	CA919111	Glycosyltransferase, putative			-2.17												
Mtr.26885.1.S1_at	AL366325	Putative uncharacterised protein			-2.17							-2.14					
Mtr.5840.1.S1_at	BG448659	Putative uncharacterised protein			-2.17												
Mtr.32228.1.S1_at	AW685311	Patatin-like protein			-2.17												
Mtr.31160.1.S1_at	TC137528	Guanine nucleotide-binding protein G(I)/G(S)/G(T) subunit beta-2			-2.17												
Mtr.36889.1.S1_x_at	TC133390	Aquaporin NIP6-1 (Nodulin-like intrinsic)			-2.16												
Mtr.10375.1.S1_at	TC119042	Putative uncharacterised protein			-2.16							-2.33					
Mtr.20368.1.S1_at	TC120185	Annexin D4			-2.16												
Mtr.42828.1.S1_at	TC132783	Vapyrin			-2.16	3.51	2.71			4.46	4.87		4.66		2.90		
Mtr.10358.1.S1_at	TC123730	Putative uncharacterised protein			-2.16							-2.98					
Mtr.31383.1.S1_x_at	TC135126	Putative uncharacterised protein			-2.16												
Mtr.11457.1.S1_at	TC131795	Weakly similar to Receptor-like protein kinase			-2.16												
Mtr.37228.1.S1_at	TC122462	UDP-glucuronosyltransferase 2B5			-2.16												
Mtr.51660.1.S1_at	TC117161	Acetyltransferase, putative			-2.15												
Mtr.10364.1.S1_at	TC129369	MLP-like protein			-2.15							-2.05					
Mtr.10331.1.S1_at	TC134327	Weakly similar to O-methyltransferase			-2.15		3.53					2.00					
Mtr.8347.1.S1_at	TC128916	Partially similar to Beta-glucosidase			-2.15												
Mtr.41911.1.S1_s_at	TC120726	Scarecrow-like transcription factor PAT1			-2.15							-2.88					
Mtr.38344.1.S1_at	TC124970	Weakly similar to Limonoid UDP-glucosyltransferase			-2.15							-2.34					
Mtr.26963.1.S1_at	AL383157	Putative uncharacterised protein			-2.15							-2.23					
Mtr.42541.1.S1_s_at	TC132558	Palmitoyltransferase AKR1			-2.15							-2.28					
Mtr.44970.1.S1_at	TC114723	Putative uncharacterised protein			-2.14												
Mtr.2439.1.S1_at	BG644996	Respiratory burst oxidase-like protein			-2.14							-2.33					
Mtr.48557.1.S1_at	TC124318	Putative uncharacterised protein			-2.14							-2.84					
Mtr.38220.1.S1_at	TC115891	Peroxidase			-2.14												
Mtr.42944.1.S1_x_at	TC137319	Putative uncharacterised protein			-2.14		4.16										
Msa.3151.1.S1_at	TC125584	Nitrate transporter			-2.14												
Mtr.12285.1.S1_at	TC119693	Putative uncharacterised protein			-2.14												
Mtr.44060.1.S1_at	TC120998	two-component response-regulator-like APRR2-like			-2.14							-2.13					
Mtr.24407.1.S1_at	TC123039	Glycogenin glucosyltransferase			-2.13												
Mtr.45254.1.S1_at	TC137649	Putative uncharacterised protein			-2.12												
Mtr.2951.1.S1_at	TC117136	Putative uncharacterised protein			-2.12							-2.08					
Msa.2805.1.S1_at	TC117480	Protease inhibitor (MTR_3g106580)			-2.12												
Mtr.39172.1.S1_at	TC123700	Magnesium transporter NIPA2			-2.12							-2.20					
Mtr.46484.1.S1_at	TC119609	Receptor-like protein kinase			-2.12												
Mtr.4583.1.S1_at	TC136090	Putative uncharacterised protein			-2.12												
Mtr.13431.1.S1_at	TC120594	serine/threonine-protein kinase Nek2-like			-2.12							-2.77					
Mtr.43203.1.S1_at	TC131158	Putative uncharacterised protein			-2.12							-2.07					
Mtr.39860.1.S1_at	TC125978	Putative uncharacterised protein			-2.12												
Mtr.10837.1.S1_at	TC118374	Putative uncharacterised protein			-2.11							-2.22					
Mtr.31694.1.S1_at	AL375661	Similar to myosin-J heavy chain-like			-2.11												
Mtr.11138.1.S1_at	TC113480	Nitrate/chlorate transporter			-2.11												
Mtr.45199.1.S1_at	TC139158	Auxin-induced protein 5NG4			-2.11							-2.01					
Mtr.4658.1.S1_at	AL373405	Putative uncharacterised protein			-2.11							-2.18					
Mtr.42488.1.S1_at	TC138565	Putative uncharacterised protein			-2.11												
Mtr.1550.1.S1_at	AW559311	Isoflavonoid glucosyltransferase			-2.11												
Mtr.46426.1.S1_s_at	TC129798	Cellulose synthase-like protein G1			-2.11												
Mtr.41920.1.S1_at	TC123150	Glyoxylate reductase			-2.10							-2.05					
Mtr.35927.1.S1_at	TC131185	Putative uncharacterised protein			-2.10												
Mtr.42422.1.S1_at	TC140757	Putative uncharacterised protein			-2.09		2.24										
Mtr.32723.1.S1_at	TC117730	Similar to formimidoyltransferase-cyclodeaminase-like			-2.09												
Mtr.13923.1.S1_at	TC126949	Nudix hydrolase			-2.09												
Mtr.11011.1.S1_at	TC113592	Nitrate/chlorate transporter			-2.09		2.16										
Mtr.42492.1.S1_at	TC140955	Neutral cholesterol ester hydrolase			-2.09												
Mtr.41244.1.S1_at	TC119194	Putative uncharacterised protein			-2.08												
Mtr.25935.1.S1_x_at	TC128097	Auxin-induced SAUR-like protein			-2.08												
Mtr.6532.1.S1_x_at	BQ148400	3-oxoacyl-ACP synthase			-2.08							-3.32					
Mtr.36367.1.S1_at	BF633501	Putative uncharacterised protein			-2.08		3.94										
Msa.1593.1.S1_at	TC126503	Chlorophyll a/b-binding protein			-2.07		2.32										
Mtr.44509.1.S1_at	TC123362	Partially similar to probable aquaporin PIP1-2-like			-2.07												

Probeset ID	Tentative Consensus	Gene	CHSB 6 vs. CB6	CHSB 24 vs. CB24	CHSE6 vs. CE6	CHSE 24 vs. CHSB 24	CHSE 24 vs. CHS E 6	CHSE 24 vs. CE24	CB24 vs. CB6	CE6 vs. CB6	CE24 vs. CB24	CE24 vs. CE6	CE vs. CB	CHSB vs.CB	CHSE vs. CHSB	CHSE vs. CE	CHS vs. C
Mtr.7629.1.S1_at	TC138217	Partially similar to Beta glucosidase D2			-2.07												
Mtr.10730.1.S1_at	TC137478	Partially similar to probable polygalacturonase-like			-2.07							-2.30					
Mtr.42496.1.S1_at	TC117436	Putative uncharacterised protein			-2.07												
Mtr.7376.1.S1_at	TC130859	Sec14 cytosolic factor [			-2.07												
Mtr.25132.1.S1_at	CX542123	Ovarian cancer-associated gene 2 protein-like protein			-2.07												
Mtr.14976.1.S1_at	AW774268	Carboxymethylenebutenolidase-like protein			-2.07												
Mtr.22988.1.S1_at	TC184901	Transcription factor bHLH19			-2.07												
Mtr.14460.1.S1_at	TC138613	WD repeat-containing protein			-2.07												
Mtr.35364.1.S1_at	CX550698	G-type lectin receptor-like tyrosine-protein kinase At1g52310-like			-2.06												
Mtr.6709.1.S1_at	CX518272	Putative uncharacterised protein			-2.06												
Mtr.281.1.S1_at	TC140871	Trehalose-phosphate phosphatase			-2.06												
Mtr.174.1.S1_at	TC127591	Two-component response regulator ARR8			-2.05												
Mtr.24929.1.S1_at	TC113479	Nodulin-like intrinsic protein NIP1-1			-2.05												
Mtr.33362.1.S1_at	TC127378	Weakly similar to probable serine/threonine-protein kinase At5g41260-like			-2.05												
Mtr.6644.1.S1_at	BQ152864	Putative uncharacterised protein			-2.05												
Mtr.18834.1.S1_at	TC123582	Calcium-binding protein CML42			-2.05												
Mtr.40109.1.S1_at	TC131626	MLP-like protein			-2.05												
Mtr.49372.1.S1_at	TC141388	Putative uncharacterised protein			-2.04												
Mtr.13392.1.S1_at	TC125023	Weakly similar to proline-rich receptor-like protein kinase PERK13-like			-2.03							-2.72					
Mtr.40319.1.S1_at	TC115931	Putative uncharacterised protein			-2.03	2.08											
Mtr.32384.1.S1_at	AW689929	Putative uncharacterised protein			-2.03												
Mtr.29220.1.S1_at	CB891334	Putative uncharacterised protein			-2.03												
Mtr.32493.1.S1_at	AW693918	Ankyrin repeat-rich protein			-2.03							-2.28					
Mtr.11212.1.S1_s_at	TC139480	Weakly similar to Isoflavonoid glucosyltransferase			-2.03												
Mtr.19723.1.S1_at	NP7265818	MAP kinase kinase kinase SSK2			-2.03												
Mtr.47758.1.S1_at	TC131763	Transcription factor bHLH25			-2.03												
Mtr.13113.1.S1_at	TC121750	Serine/threonine protein phosphatase 2A 55 kDa regulatory subunit B beta isoform			-2.03							-2.39					
Mtr.38768.1.S1_at	TC125204	Putative uncharacterised protein			-2.02	2.42											
Mtr.38138.1.S1_at	TC129076	Putative uncharacterised protein			-2.02												
Mtr.25935.1.S1_at	TC128097	Auxin-induced SAUR-like protein			-2.02												
Mtr.40444.1.S1_at	TC121652	Serine carboxypeptidase-like protein			-2.02							-2.12					
Mtr.32384.1.S1_x_at	AW689929	Putative uncharacterised protein			-2.02												
Mtr.39065.1.S1_at	TC187067	Putative uncharacterised protein			-2.02												
Mtr.5159.1.S1_at	AW689715	Putative uncharacterised protein			-2.02							-2.50					
Mtr.51909.1.S1_at	TC113709	Phenylalanine ammonia-lyase			-2.02												
Mtr.19988.1.S1_at	TC114810	Similar to probable methyltransferase PMT4-like			-2.02							-2.61					
Mtr.32213.1.S1_at	AW684979	Peptide transporter PTR5 (MTR_7g088790)			-2.01												
Mtr.11556.1.S1_at	TC120652	Putative uncharacterised protein			-2.01							-2.18					
Mtr.11670.1.S1_x_at	TC116391	O-acyltransferase WSD1			-2.01							-2.11					
Mtr.46207.1.S1_at	NP7274094	Putative uncharacterised protein			-2.01							-2.05					
Mtr.50427.1.S1_at	TC132688	Seed lipoxygenase			-2.01												
Mtr.14771.1.S1_at	TC119590	Phosphoglycolate phosphatase			-2.01												
Msa.1574.1.S1_at	TC117699	Putative uncharacterised protein			-2.01												
Mtr.48351.1.S1_at	TC121286	Kunitz-type trypsin inhibitor-like 2 protein			-2.01												
Mtr.1812.1.S1_at	BE202825	Secondary cell wall-related glycosyltransferase family			-2.01							-2.20					
Mtr.40932.1.S1_at	TC114255	Cyclin-D1-1			-2.01												
Mtr.20048.1.S1_at	NP7266812	Putative uncharacterised protein			-2.01	2.48											
Mtr.5824.1.S1_at	BG447918	Putative uncharacterised protein			-2.01												
Mtr.50163.1.S1_at	NP7253201	Transcription factor bHLH85			-2.00							-2.17					
Mtr.42503.1.S1_at	TC137942	Putative uncharacterised protein			-2.00												
Mtr.9031.1.S1_at	TC123378	Aspartic proteinase-like protein			-2.00							-2.21					
Mtr.5800.1.S1_at	BF650255	probable LRR receptor-like serine/threonine-protein kinase At5g16900-like			-2.00												
Mtr.28421.1.S1_at	BG645363	Isoflavonoid glucosyltransferase			-2.00							-2.11					
Mtr.13919.1.S1_s_at	TC127436	Putative uncharacterised protein			-2.00												
Mtr.27937.1.S1_at	BF520859	Putative uncharacterised protein			-2.00												
Mtr.13237.1.S1_at	TC123960	Putative uncharacterised protein			-2.00							-2.02					
Mtr.41168.1.S1_at	TC128632	Multidrug resistance protein ABC transporter family			-2.01												
Mtr.11245.1.S1_at	TC122990	Weakly similar to CLAVATA3/ESR (CLE)-related protein TDIF-like			-2.01												
Mtr.11933.1.S1_at	TC130414	Disease resistance-like protein (MTR_6g074650)			-2.01												
Mtr.23865.1.S1_at	TC113600	Receptor-like protein kinase			-2.01												
Mtr.3149.1.S1_at	TC124030	Putative uncharacterised protein			-2.01												
Mtr.27606.1.S1_at	BE240339	Putative uncharacterised protein			-2.01												
Mtr.11345.1.S1_at	TC116121	Putative uncharacterised protein			-2.01												
Mtr.9580.1.S1_at	TC134859	Putative uncharacterised protein			-2.02												
Mtr.2288.1.S1_at	BG584771	Beta-glucosidase			-2.02							-2.09					
Mtr.46061.1.S1_s_at	TC113350	Interferon-induced GTP-binding protein Mx			-2.02												
Msa.945.1.S1_at	TC115387	Caffeic acid 3-O-methyltransferase			-2.03												
Mtr.27080.1.S1_at	AW257437	40S ribosomal protein S3			-2.03												
Mtr.41053.1.S1_at	TC127496	Putative uncharacterised protein			-2.03												
Mtr.8934.1.S1_at	TC134157	Alternative oxidase			-2.03		2.09									2.06	2.01
Mtr.41561.1.S1_at	TC114480	Expansin			-2.03							2.46					
Mtr.27561.1.S1_x_at	BE204930	Putative uncharacterised protein			-2.03												
Mtr.42268.1.S1_at	TC117027	Similar to inositol oxygenase 1-like			-2.04												
Mtr.41655.1.S1_at	TC124289	Putative uncharacterised protein			-2.04										2.31		2.04
Mtr.10732.1.S1_at	TC130640	Putative uncharacterised protein			-2.04												
Mtr.41503.1.S1_at	TC133382	Putative uncharacterised protein			-2.04												
Mtr.21000.1.S1_at	TC115453	Universal stress protein A-like protein			-2.04												
Mtr.5689.1.S1_at	BF644345	Putative uncharacterised protein			-2.05												
Mtr.9160.1.S1_at	CX550357	Putative uncharacterised protein			-2.05												
Mtr.41060.1.S1_at	TC114875	Isochorismatase family protein pncA, putative			-2.06												
Mtr.41137.1.S1_at	TC179440	Peroxidase 11 precursor			-2.06	2.11						-2.94					
Mtr.44416.1.S1_at	TC119978	WRKY53, n=1, Glycine max			-2.06	2.25	3.51								2.02	2.69	2.33
Mtr.43127.1.S1_at	TC113540	Putative uncharacterised protein			-2.06												
Mtr.41077.1.S1_at	TC120986	Zinc finger protein			-2.07												
Mtr.26920.1.S1_at	AL374251	Putative uncharacterised protein			-2.08												
Mtr.10760.1.S1_at	TC121010	N-hydroxycinnamoyl /benzoyltransferase			-2.09												
Mtr.23679.1.S1_x_at	TC127565	ABC transporter B family member			-2.09												
Mtr.42205.1.S1_at	TC125757	Cysteine-rich receptor-like protein kinase			-2.09												
Mtr.9270.1.S1_at	TC122192	Putative uncharacterised protein (possible metal binding protein)			-2.10							-2.23					
Mtr.18549.1.S1_x_at	NP7275355	Weakly similar to TRANSPARENT TESTA 1-like			-2.10												
Mtr.9381.1.S1_at	TC123061	Weakly similar ro cytochrome P450 71A6-like			-2.10												
Mtr.11641.1.S1_at	TC114747	Putative uncharacterised protein			-2.10												
Mtr.1796.1.S1_at	TC134133	Serine rich protein			-2.10												
Mtr.40363.1.S1_at	TC115081	Universal stress protein			-2.11												
Mtr.29449.1.S1_at	CX537847	Putative uncharacterised protein			-2.11												
Mtr.20710.1.S1_at	TC112916	Ferulate 5-hydroxylase			-2.11							2.51					
Mtr.16694.1.S1_at	TC136529	Putative uncharacterised protein			-2.12												
Mtr.43508.1.S1_at	TC114131	Putative uncharacterised protein			-2.12												
Mtr.45497.1.S1_s_at	TC172695	Myrcene synthase			-2.12												
Mtr.9846.1.S1_at	TC122506	Glycine max probable purine permease 11-like			-2.12												
Msa.1665.1.S1_at	TC114001	Thiazole biosynthetic enzyme			-2.13							2.58					
Mtr.42257.1.S1_at	CX538358	Putative uncharacterised protein			-2.13												

Probeset ID	Tentative Consensus	Gene	CHSB 6 vs. CB6	CHSB 24 vs. CB24	CHSE6 vs. CE6	CHSE 24 vs. CHSB 24	CHSE 24 vs. CHS E 6	CHSE 24 vs. CE24	CB24 vs. CB6	CE6 vs. CB6	CE24 vs. CB24	CE24 vs. CE6	CE vs. CB	CHSB vs.CB	CHSE vs. CHSB	CHSE vs. CE	CHS vs. C
Mtr.39979.1.S1_x_at	TC133299	Putative uncharacterised protein			2.14							2.04					
Mtr.39979.1.S1_at	TC133299	Putative uncharacterised protein			2.14							2.00					
Mtr.43393.1.S1_at	TC121698	Putative uncharacterised protein]			2.14												
Mtr.41025.1.S1_at	TC132055	Putative uncharacterised protein			2.15												
Mtr.30102.1.S1_at	TC140591	Putative uncharacterised protein			2.15				2.06			2.06					
Mtr.12569.1.S1_at	TC122795	Putative uncharacterised protein			2.15												
Mtr.15053.1.S1_at	TC133697	Thaumatin-like protein			2.16		-2.09										
Mtr.48599.1.S1_at	TC129531	Terminal Flower Like TFL1			2.17							2.94					
Mtr.42124.1.S1_at	TC133695	Putative uncharacterised protein			2.19												
Mtr.46435.1.S1_x_at	TC192310	Putative uncharacterised protein			2.19												
Mtr.29602.1.S1_at	TC135018	Putative uncharacterised protein			2.19												
Mtr.12447.1.S1_at	TC118176	Weakly similar to lysine histidine transporter 2-like			2.20							2.41					
Mtr.13551.1.S1_at	TC129481	Putative uncharacterised protein			2.20		-2.11										
Mtr.10393.1.S1_at	TC114001	Thiazole biosynthetic enzyme			2.21							3.30					
Mtr.18649.1.S1_s_at	TC113264	Glucan endo-1,3-beta-glucosidase			2.21			2.46								2.33	
Msa.1202.1.S1_at	TC128547	Isoflavone synthase			2.22			2.11								2.16	
Mtr.15199.1.S1_at	TC121346	Putative uncharacterised protein			2.24												
Mtr.37429.1.S1_at	TC123347	Aldehyde dehydrogenase			2.24							2.14					
Mtr.27713.1.S1_at	BE943181	Putative uncharacterised protein			2.25												
Mtr.50730.1.S1_at	TC141275	Putative uncharacterised protein			2.26												
Mtr.29026.1.S1_at	BQ156165	Putative uncharacterised protein			2.26												
Mtr.5765.1.S1_at	BF648162	Receptor-like protein kinase HAIKU2			2.27												
Mtr.43942.1.S1_x_at	TC133377	Putative uncharacterised protein			2.27												
Mtr.49558.1.S1_at	NP7263365	Putative uncharacterised protein			2.27												
Mtr.38931.1.S1_at	TC133192	Putative uncharacterised protein			2.27												
Mtr.15443.1.S1_at	TC136306	Putative uncharacterised protein			2.28												
Mtr.50786.1.S1_at	TC137843	Weakly similar to TRANSPARENT TESTA 1-like			2.28												
Mtr.5109.1.S1_at	TC122000	Cytochrome P450			2.28												
Mtr.771.1.S1_at	TC115387	Caffeic acid 3-O-methyltransferase			2.30												
Mtr.20947.1.S1_s_at	TC139036	Kinase R-like protein			2.30							2.32					
Mtr.29585.1.S1_at	TC130830	Quinohaemoprotein ethanol dehydrogenase type-1			2.31												
Mtr.27711.1.S1_at	BE943060	Putative uncharacterised protein			2.31												
Mtr.32325.1.S1_at	AW688239	Weakly similar to probable pectate lyase 12-like			2.32												
Mtr.33655.1.S1_at	TC133240	Putative uncharacterised protein, weakly similar to Cytochrome P450			2.32									2.02		2.01	2.02
Mtr.44720.1.S1_at	TC117683	Putative uncharacterised protein			2.32												
Mtr.39199.1.S1_at	TC115756	Cytochrome P450			2.32												
Mtr.37420.1.S1_at	TC120646	Putative uncharacterised protein			2.32												
Mtr.40890.1.S1_at	TC190654	Putative uncharacterised protein			2.33		2.14	2.64								2.48	2.11
Mtr.35677.1.S1_at	TC129237	Zinc finger protein family-like			2.34		2.36	2.86								2.59	2.10
Mtr.9504.1.S1_at	TC123305	class I KNOX homeobox transcription factor(KNOX2)			2.34												
Mtr.13357.1.S1_at	TC124756	Putative uncharacterised protein			2.34												
Mtr.11130.1.S1_at	TC134870	Putative uncharacterised protein			2.34							2.37					
Mtr.45373.1.S1_at	TC130945	2-aminoethanethiol dioxygenase			2.35												
Mtr.50897.1.S1_at	TC184104	Fasciclin-like arabinogalactan protein			2.35												
Mtr.28199.1.S1_at	BG586132	Putative uncharacterised protein			2.36												
Mtr.48649.1.S1_at	TC121930	Cellulose synthase			2.37							3.38					
Mtr.5709.1.S1_at	BF643395	Putative uncharacterised protein			2.37							2.20					
Mtr.11678.1.S1_at	TC127345	Tetratricopeptide repeat protein 7B			2.37							2.78					
Mtr.7267.1.S1_at	TC140443	Transcriptional repressor NF-X1			2.38												
Mtr.7637.1.S1_at	AJ548187	Putative uncharacterised protein			2.38												
Mtr.12073.1.S1_at	TC129415	Cytochrome P450 monooxygenase			2.39			3.10								2.72	2.33
Mtr.31248.1.S1_s_at	AJ501185	Putative uncharacterised protein			2.39												
Mtr.20947.1.S1_at	TC139036	Kinase R-like protein			2.39							2.53					
Mtr.35145.1.S1_at	TC138103	Putative uncharacterised protein			2.41												
Mtr.8948.1.S1_at	TC113806	Cytochrome P450 82A1			2.41												
Mtr.41581.1.S1_at	**TC131878**	**Ethylene response factor required for nodulation(EFD)**			2.42												
Mtr.32925.1.S1_at	BF633960	Putative uncharacterised protein			2.43												
Mtr.13171.1.S1_at	TC129980	Putative uncharacterised protein			2.44												
Mtr.29716.1.S1_at	TC135387	Caffeic acid 3-O-methyltransferase			2.45			2.10								2.27	
Mtr.37300.1.S1_at	TC117452	Cytochrome P450 monooxygenase CYP72A59			2.45									2.06		2.20	2.13
Mtr.49862.1.S1_at	TC113293	Isoflavone-7-O-methyltransferase			2.45												
Mtr.24731.1.S1_at	TC129924	Plant disease resistance response protein			2.47			2.15								2.30	
Mtr.20227.1.S1_at	TC114214	UDP-glucose flavonoid 7-O-glucosyltransferase			2.47												
Mtr.18579.1.S1_at	TC140071	Myb-like transcription factor			2.49												
Mtr.41235.1.S1_at	TC127478	UDP-glucose 6-dehydrogenase, partial			2.49											2.01	
Msa.1089.1.S1_at	EX528368	Flavonol synthase			2.50												
Mtr.21374.1.S1_at	TC125443	Zinc finger protein CONSTANS-like protein			2.51							2.22					
Mtr.11021.1.S1_at	TC117855	Putative uncharacterised protein			2.57											2.07	
Mtr.5947.1.S1_at	BG453618	Putative uncharacterised protein			2.58											2.16	
Mtr.15516.1.S1_at	TC121765	Putative uncharacterised protein			2.59												
Mtr.24396.1.S1_at	TC125643	Non-specific lipid-transfer protein			2.59							3.85					
Mtr.42256.1.S1_at	TC134529	ZINC INDUCED FACILITATOR-LIKE 1-like			2.59												
Mtr.51976.1.S1_at	TC128579	Putative uncharacterised protein			2.59											2.01	
Mtr.244.1.S1_at	TC116103	Chaperone protein dnaJ			2.60											2.19	
Mtr.8987.1.S1_at	TC117656	cytochrome P450 monooxygenase CYP76X3			2.61							2.17					
MtrAffx.53599.1.S1_s_at	TC119615	18S-25/28S ribosomal RNA intergenic spacer			2.62												
Mtr.40276.1.S1_at	TC128547	Isoflavone synthase			2.63			2.45						2.24		2.54	2.38
Mtr.26370.1.S1_at	TC125626	GASA5-like protein			2.64		-2.14										
Mtr.10283.1.S1_at	TC131163	Epoxide hydrolase			2.64							2.58					
Mtr.42933.1.S1_s_at	TC124791	Non-specific lipid-transfer protein			2.66							2.37					
Msa.1018.1.S1_at		Putative uncharacterised protein			2.67							2.84					
Mtr.48743.1.S1_at	NP7272446	Ribonuclease T2			2.68		-2.33										
Mtr.11595.1.S1_at	TC126346	Putative uncharacterised protein			2.71											2.24	
Mtr.13503.1.S1_at	TC114707	Cytochrome P450			2.72							2.05					
Mtr.15545.1.S1_at	TC114707	5'-methylthioadenosine/S-adenosylhomocysteine nucleosidase			2.73							4.09					
Mtr.42692.1.S1_at	TC126223	Putative uncharacterised protein			2.73											2.05	2.08
Mtr.35665.1.S1_at	TC123580	Putative uncharacterised protein			2.74											2.14	
Mtr.4250.1.S1_at	TC119153	Acetolactate synthase			2.75												
Mtr.3549.1.S1_at	BE202932	cytochrome P450 monooxygenase CYP72A59			2.76												
Mtr.29340.1.S1_at	CB894445	Flavonoid 3'5' hydroxylase			2.79			2.48						2.24		2.63	2.43
Mtr.37415.1.S1_x_at	TC174561	Copper transport protein ATOX1			2.85												
Mtr.43862.1.S1_at	TC188842	Putative uncharacterised protein			2.85											2.28	
Mtr.51040.1.S1_x_at	TC130824	Ferric-chelate reductase			2.88											2.03	
Mtr.33148.1.S1_at	BF644261	Putative uncharacterised protein			2.88												
Mtr.10063.1.S1_at	TC137279	Putative uncharacterised protein			2.92												
Mtr.10494.1.S1_x_at	TC123031	Glutathione S-transferase GST			2.92							2.14				2.21	
Mtr.31647.1.S1_at	TC122794	NAC domain protein [No Apical Meristem NAM protein]			2.92									2.42		2.08	2.24
Mtr.48952.1.S1_s_at	BE999763	Thiosulfate sulfurtransferase			2.93											2.50	
Mtr.10604.1.S1_at	TC130773	Nitrate reductase			2.93												
Mtr.11377.1.S1_at	TC179462	Hypothetical protein similar to Glutathione S-transferase			2.98							2.23				2.14	
Mtr.12601.1.S1_at	TC183217	Peroxidase 5			3.00											2.08	
Mtr.33824.1.S1_at	BI270742	Pathogenesis-related protein			3.03											2.93	2.00
Mtr.47734.1.S1_at	TC199126	Ubiquitin carboxyl-terminal hydrolase			3.07							2.29					
Mtr.13183.1.S1_at	TC132433	Putative uncharacterised protein			3.08											2.07	2.04
Mtr.2486.1.S1_at	TC139119	Putative uncharacterised protein			3.13											2.15	
Mtr.43150.1.S1_at	TC126442	Beta-galactosidase			3.19											2.32	
Mtr.8517.1.S1_at	TC120282	Putative uncharacterised protein			3.20												
Mtr.21416.1.S1_at	TC113722	Ribonuclease T2			3.22		-2.27										
Mtr.31645.1.S1_at	AL373660	Putative uncharacterised protein			3.22												
Mtr.50900.1.S1_at	TC185768	Beta-lg-H3/fasciclin			3.23											2.16	

Probeset ID	Tentative Consensus	Gene	CHSB 6 vs. CB6	CHSB 24 vs. CB24	CHSE6 vs. CE6	CHSE 24 vs. CHSB 24	CHSE 24 vs. CHSE 6	CHSE 24 vs. CE24	CB24 vs. CB6	CE6 vs. CB6	CE24 vs. CB24	CE24 vs. CE6	CE vs. CB	CHSB vs.CB	CHSE vs. CHSB	CHSE vs. CE	CHS vs.C
Msa.1741.1.S1_at	TC129924	Plant disease resistance response protein			3.25			2.06				2.25				2.58	
Mtr.6484.1.S1_at	BQ145041	Phosphate transporter 2			3.26									2.30		2.69	2.49
Mtr.15141.1.S1_at	TC192679	Transparent testa 12 protein			3.26							2.90				2.24	
Mtr.36333.1.S1_at	TC122566	Putative uncharacterised protein			3.30		-2.41										
Mtr.166.1.S1_at	NP7259676	Auxin-induced protein 6B			3.31		-2.42										
Mtr.9679.1.S1_at	TC125417	Thioredoxin H2			3.34							2.76					
Mtr.48952.1.S1_at	BE999763	Thiosulfate sulfurtransferase			3.36											2.75	
Sme.4889.1.S1_s_at	---	hypothetical protein (Sinorhizobium meliloti 1021)			3.37												
Mtr.45568.1.S1_at	TC131155	Phosphate transporter			3.45									2.29		2.62	2.45
Mtr.51360.1.S1_at	TC131140	Plant lipid transfer protein/Par allergen			3.46							3.36				2.24	2.01
Mtr.31923.1.S1_at	AL385713	Isoflavone conjugate-specific beta-glucosidase (partially similar)			3.49							3.56					
Mtr.43507.1.S1_at	TC182277	Seed coat peroxidase precursor			3.51							2.80		2.28		2.83	2.54
Mtr.50038.1.S1_at	TC126219	NAC domain transcription factor			3.53		-2.06									2.01	
Mtr.13186.1.S1_at	TC115361	Putative uncharacterised protein			3.58												2.10
Mtr.43492.1.S1_at	TC118975	Peptide transporter PTR1			3.60							3.09				2.38	2.03
Mtr.44908.1.S1_at	TC132283	Putative uncharacterised protein			3.69												
Mtr.12256.1.S1_at	TC195681	Non-specific lipid-transfer protein			3.69												
Mtr.39853.1.S1_at	TC126337	Pathogenesis-related protein			3.82											2.13	
Mtr.40293.1.S1_at	TC119881	weakly similar to Glutathione S transferase			3.82							3.47		2.95		2.80	2.87
Msa.2966.1.S1_a_at	TC124791	Non-specific lipid-transfer protein			3.83												
Mtr.42933.1.S1_x_at	TC124791	Non-specific lipid-transfer protein			4.06												
Mtr.9411.1.S1_at	TC126153	SRG-1 [predicted]			4.12		3.05	4.00				3.15		3.02		4.06	3.50
Mtr.27355.1.S1_s_at	AW774638	(+)-delta-cadinene synthase isozyme A			4.26											2.44	2.26
Mtr.35335.1.S1_x_at	CX550152	Glutathione S-transferase 12			4.37			2.56						2.58		3.35	2.94
Mtr.11101.1.S1_at	TC121688	Partially similar to Endo-1 4-beta-glucanase			4.38							5.45					
Mtr.49921.1.S1_at	TC180661	Cytochrome P450			4.40											2.38	2.17
Mtr.1633.1.S1_x_at	TC168199	2,4-D inducible glutathione-S-transferase			4.50			5.31						4.40		4.89	4.64
Mtr.13136.1.S1_at	TC114658	Fasciclin-like AGP			4.51											2.74	2.06
Mtr.17361.1.S1_at	TC174571	Beta-Ig-H3/fasciclin			4.54											2.68	2.10
Mtr.46735.1.S1_x_at	TC130389	EG45-like domain containing protein (Expansin)			4.63											2.47	
Mtr.51607.1.S1_at	TC174969	Beta-Ig-H3/fasciclin			4.74											2.76	2.20
Mtr.38111.1.S1_at	TC123357	Glutathione S-transferase 19			4.74			2.46				3.17		2.52		3.42	2.93
Mtr.24717.1.S1_s_at	TC199873	Beta-Ig-H3/fasciclin			4.80											2.74	2.20
Mtr.30779.1.S1_s_at	CA923050	Putative uncharacterised protein			4.83							3.52				2.26	
Mtr.10992.1.S1_at	TC131494	Fasciclin-like arabinogalactan protein 12 precursor			4.87							3.78				2.58	2.40
Mtr.46435.1.S1_at	TC192310	Putative uncharacterised protein			4.95							4.22				2.24	2.10
Mtr.46735.1.S1_x_at	TC130389	EG45-like domain containing protein (Expansin)			5.11											2.46	
Mtr.49920.1.S1_s_at	TC180661	Cytochrome P450			5.19							3.48				2.52	2.41
Mtr.41020.1.S1_at	TC115064	IOMT 1			5.38												2.91
Mtr.4076.1.S1_s_at	CA921764	partially similar to Isoflavone-7-O-methyltransferase			5.48												2.81
Mtr.44047.1.S1_at	TC120336	Putative uncharacterised protein			5.61							2.84		2.35		3.37	2.82
Mtr.18380.1.S1_at	TC113489	Beta-Ig-H3/fasciclin			5.63							3.24				2.97	2.61
Mtr.38034.1.S1_at	TC131421	1-aminocyclopropane-1-carboxylate oxidase-like			5.64							3.07		2.93		3.26	3.09
Mtr.50819.1.S1_x_at	TC132811	Putative uncharacterised protein			5.65											2.87	2.55
Mtr.47490.1.S1_s_at	TC119363	Cytochrome P450 71D9 - Glycine max			6.01							3.50		2.95		3.23	3.09
Mtr.47490.1.S1_x_at	TC119363	Cytochrome P450 71D9 - Glycine max			6.38							3.69		2.64		3.27	2.94
Mtr.12833.1.S1_at	TC117324	Putative uncharacterised protein			10.28												2.61
Mtr.43680.1.S1_at	TC120583	RD22-like protein			18.24							10.81		4.57		5.59	5.06
Mtr.42519.1.S1_at	TC138218	Putative uncharacterised protein				2.39											
Mtr.47095.1.S1_x_at	NP7260213	ABC transporter, Pleiotropic drug resistance protein				2.72	3.10						2.32				
Mtr.15436.1.S1_at	TC113415	Gibberellin 20 oxidase				2.80	3.19	2.21	2.25								
Mtr.45719.1.S1_at	TC124041	Helix-loop-helix DNA-binding				2.97	2.41						3.15				
Mtr.8157.1.S1_at	TC124041	Helix-loop-helix DNA-binding				3.21					3.32		3.27		2.44		
Mtr.32254.1.S1_at	AW686309	Zinc finger protein , C2H2 family				3.27	2.95										
Mtr.40868.1.S1_at	TC130349	isoliquiritigenin 2'-O-methyltransferase				3.49									2.70		
Msa.2558.1.S1_at	TC179864	Isoliquiritigenin 2'-O-methyltransferase				3.56									2.73		
Mtr.4797.1.S1_s_at	AL383715	**Mt Dwarf 27**				**4.26**	**2.65**						**3.12**		**2.96**		
Mtr.13473.1.S1_at	**TC123589**	**enod11 gene for putative repetitive proline-rich protein**				**9.14**	**10.8 1**				**12.2 6**	**10.3 8**					
Mtr.27058.1.S1_at	AW256857	DNA (cytosine-5)-methyltransferase					-3.93										
Mtr.26833.1.S1_at	TC140809	Putative uncharacterised protein					-3.57										
Mtr.35231.1.S1_s_at	TC133697	Thaumatin-like protein					-3.02										
Mtr.11293.1.S1_at	TC122708	Polygalacturonase inhibitor-like protein (Fragment), partial (43%)					-2.83										
Mtr.32118.1.S1_at	TC137526	Putative uncharacterised protein					-2.75										
Mtr.35947.1.S1_at	TC135173	Putative uncharacterised protein					-2.69		-2.76								
Mtr.27554.1.S1_at	BE204824	Anthranilate N-hydroxycinnamoyl/benzoyltransferase					-2.68					-2.16					
Mtr.32118.1.S1_x_at	TC137526	Putative uncharacterised protein					-2.66										
Mtr.12482.1.S1_at	CB892616	Putative uncharacterised protein					-2.57					-2.30					
Mtr.5715.1.S1_at	TC118018	beta-glucan binding protein 2 (GBP2)					-2.50					-2.60					
Mtr.50397.1.S1_at	TC126230	Putative uncharacterised protein					-2.50										
Mtr.5638.1.S1_at	BF640272	Cytokinin O-glucosyltransferase					-2.47										
Mtr.31354.1.S1_at	TC127698	Putative uncharacterised protein					-2.44										
Mtr.13465.1.S1_s_at	TC116464	Pectate lyase					-2.43										
Mtr.694.1.S1_s_at	TC115539	High-affinity nickel-transport family protein, putative					-2.39										
Mtr.39803.1.S1_at	TC126685	Putative uncharacterised protein					-2.35	-2.05									
Mtr.43747.1.S1_at	TC135082	TRANSPORT INHIBITOR RESPONSE 1-like					-2.35										
Mtr.31622.1.S1_at	AL372561	Glutathione peroxidase					-2.33										
Mtr.38949.1.S1_x_at	TC128211	Putative uncharacterised protein					-2.33										
Mtr.43774.1.S1_at	TC123390	probable exocyst complex component 6-like					-2.31										
Mtr.34024.1.S1_at	BQ137035	AP2 domain-containing transcription factor					-2.31										
Mtr.39237.1.S1_at	TC137677	RNA-binding protein with multiple splicing					-2.30										
Mtr.38809.1.S1_at	TC131134	Similar to P. sativum glutathione reductase, P27456					-2.30										
Msa.1479.1.S1_at	TC118155	YTH domain family protein					-2.30										
Mtr.44762.1.S1_s_at	TC127103	Glucan endo-1,3-beta-glucosidase					-2.29										
Mtr.12808.1.S1_at	TC128022	Putative uncharacterised protein					-2.28										
Mtr.44006.1.S1_x_at	TC114045	DNA-3-methyladenine glycosylase					-2.27										
Mtr.14824.1.S1_at	TC114176	NAC domain-containing protein					-2.20										
Mtr.39228.1.S1_at	TC125133	Rho guanine nucleotide exchange factor					-2.19										
Mtr.6512.1.S1_at	BQ147616	Putative uncharacterised protein					-2.19					-2.55					
Mtr.27586.1.S1_at	BE203481	Beta-D-glucosidase					-2.18										
Mtr.5728.1.S1_at	BF646288	Cellulose synthase-like protein G1					-2.17					-2.32					
Mtr.7122.1.S1_at	TC134738	Solute carrier family 35 member G2					-2.16										
Mtr.10279.1.S1_s_at	AW695244	Peptide transporter PTR2					-2.16					-2.21					
Mtr.1951.1.S1_s_at	TC128191	Zinc finger protein CONSTANS-LIKE protein					-2.15		-2.12			-2.36					
Mtr.6337.1.S1_at	BQ139859	Heterogeneous nuclear ribonucleoprotein A3-like protein					-2.14										
Mtr.39868.1.S1_at	TC134344	insulin-degrading enzyme-like					-2.14										
Mtr.11942.1.S1_at	TC129203	Two-component response regulator ARR1					-2.12										
Mtr.40643.1.S1_s_at	TC134655	Dolichyl-diphosphooligosaccharide-protein glycosyltransferase subunit					-2.12										
Mtr.9830.1.S1_at	TC121218	expansin-A1-like protein					-2.12										

Probeset ID	Tentative Consensus	Gene	CHSB 6 vs. CB6	CHSB 24 vs. CB24	CHSE6 vs. CE6	CHSE 24 vs. CHSB 24	CHSE 24 vs. CHS E6	CHSE 24 vs. CE24	CB24 vs. CB6	CE6 vs. CB6	CE24 vs. CB24	CE24 vs. CE6	CE vs. CB	CHSB vsCB	CHSE vs. CHSB	CHSE vs. CE	CHS vs C
Mtr.10157.1.S1_at	TC130517	Putative uncharacterised protein					-2.10					-2.10					
Mtr.9739.1.S1_at	TC114460	Putative uncharacterised protein					-2.10										
Mtr.6126.1.S1_at	BI270652	Putative uncharacterised protein					-2.10										
Mtr.4744.1.S1_at	AL379799	Putative uncharacterised protein					-2.09										
Mtr.31726.1.S1_at	AL377152	Glycosyl transferase protein A					-2.08										
Mtr.4541.1.S1_s_at	AL365534	Putative uncharacterised protein					-2.08										
Mtr.12540.1.S1_s_at	TC119553	Nucleoredoxin					-2.06										
Mtr.32869.1.S1_at	BF632020	pre-mRNA-splicing factor CWC22 homolog					-2.06										
Mtr.9908.1.S1_at	TC130708	IQ domain-containing protein					-2.05										
Mtr.8920.1.S1_at	TC122821	2-oxoglutarate/malate translocator					-2.05										
Mtr.41989.1.S1_at	TC127149	tRNA-dihydrouridine synthase A					-2.05										
Mtr.39461.1.S1_at	TC130217	UDP-glucuronosyltransferase 1-1					-2.04										
Mtr.38949.1.S1_at	TC128211	Putative uncharacterised protein					-2.04										
Mtr.23398.1.S1_at	NP7257493	1-acyl-sn-glycerol-3-phosphate acyltransferase					-2.03										
Mtr.27605.1.S1_at	BE240245	Putative uncharacterised protein					-2.03										
Mtr.19235.1.S1_at	TC126690	Early flowering					-2.02					-2.23					
Mtr.15708.1.S1_at	NP7262602	Cotton fiber expressed protein					-2.00										
Mtr.9802.1.S1_at	TC119888	Putative uncharacterised protein					-2.00										
Mtr.4411.1.S1_at	AJ501851	Vesicle-associated membrane protein					-2.00										
Mtr.44600.1.S1_at	TC119384	Putative uncharacterised protein					2.00					2.79					
Mtr.43320.1.S1_at	TC121408	Putative uncharacterised protein					2.00					2.78					
Mtr.25557.1.S1_at	TC113766	1-aminocyclopropane-1-carboxylate oxidase					2.01										
Mtr.50580.1.S1_s_at	TC134852	ATP4-like protein					2.01										
Msa.2816.1.S1_at	TC138619	Glycerol-3-phosphate dehydrogenase					2.01					2.02					
Mtr.4414.1.S1_at	AJ501907	Cysteine-rich receptor-like protein kinase					2.01										
Mtr.35269.1.S1_at	TC135354	Unc-13-like protein					2.01	2.03									
Mtr.36073.1.S1_s_at	AJ845987	Putative uncharacterised protein					2.01										
Mtr.24465.1.S1_at	BF646763	Cysteine-rich receptor-like protein kinase					2.02										
Mtr.9637.1.S1_at	TC134167	Putative uncharacterised protein					2.02										
Mtr.29849.1.S1_at	AW287889	Putative uncharacterised protein					2.02										
Mtr.49375.1.S1_at	EV257591	Tir-nbs resistance protein					2.02										
Mtr.46391.1.S1_at	TC117549	Putative uncharacterised protein					2.02										
Mtr.22836.1.S1_s_at	TC138474	Putative uncharacterised protein					2.03										
Mtr.39431.1.S1_at	TC139283	Dihydroflavonol-4-reductase					2.03	2.01									
Mtr.18354.1.S1_at	TC117179	Ring-H2 zinc finger protein					2.03										
Mtr.13539.1.S1_at	TC133521	Putative uncharacterised protein					2.03										
Mtr.4095.1.S1_at	TC134802	Putative uncharacterised protein					2.03		2.81			2.24					
Mtr.33792.1.S1_at	TC138412	Putative uncharacterised protein					2.04					2.63					
Mtr.28066.1.S1_s_at	BG580463	Zinc transporter (MTR_3g082050)					2.04										
Mtr.13746.1.S1_at	TC130161	Cytochrome P450 (MTR_7g092600)					2.05										
Mtr.37263.1.S1_at	TC125822	Putative uncharacterised protein					2.05		2.31			2.08					
Mtr.49039.1.S1_s_at	AJ846730	Putative uncharacterised protein					2.05		3.21								
Mtr.40765.1.S1_at	TC123942	Putative uncharacterised protein					2.06										
Mtr.45615.1.S1_s_at	CA990893	ATP-dependent Clp protease proteolytic subunit					2.06					2.48					
Mtr.32159.1.S1_at	TC176233	Type-A response regulator					2.06										
Mtr.22543.1.S1_s_at	TC133430	Putative uncharacterised protein					2.06										
Mtr.37335.1.S1_at	TC125401	Putative uncharacterised protein					2.06										
Mtr.9372.1.S1_at	TC122621	Putative uncharacterised protein					2.06										
Mtr.28297.1.S1_at	BG588104	Putative uncharacterised protein					2.07										
Mtr.16234.1.S1_at	TC123271	Cysteine-rich secretory protein LCCL domain-containing					2.07										
Mtr.43009.1.S1_at	TC178471	Isoflavone 2'-hydroxylase					2.07										
Mtr.40553.1.S1_at	TC123521	Disease resistance response protein					2.07										
Mtr.43284.1.S1_at	TC118792	Putative uncharacterised protein					2.08										
Mtr.10995.1.S1_at	TC122890	transcription activator GLK1-like					2.08										
Mtr.10927.1.S1_at	TC134620	Putative uncharacterised protein					2.08					2.04					
Mtr.28435.1.S1_at	BG645710	Putative uncharacterised protein					2.08										
Mtr.6102.1.S1_at	BI268885	Putative uncharacterised protein					2.08					2.04					
Mtr.24490.1.S1_at	TC132479	Putative uncharacterised protein					2.09		3.49								
Mtr.40399.1.S1_at	TC141558	Putative uncharacterised protein					2.09										
Mtr.37369.1.S1_at	TC120528	Putative uncharacterised protein					2.09										
Mtr.46949.1.S1_at	TC127637	Auxin-induced protein 5NG4					2.09										
Mtr.45963.1.S1_at	TC134699	O-methyltransferase					2.09										
Msa.2945.1.S1_at	TC125102	Putative uncharacterised protein					2.09		2.11								
Msa.2484.1.S1_at	TC132479	Putative uncharacterised protein					2.09		3.33								
Mtr.10071.1.S1_at	TC138496	WRKY transcription factor					2.10										
Mtr.13293.1.S1_at	TC123828	Putative uncharacterised protein					2.10										
Mtr.3442.1.S1_at	AW560639	Putative uncharacterised protein					2.10										
Mtr.41814.1.S1_at	TC140096	Putative uncharacterised protein					2.11										
Mtr.10071.1.S1_s_at	TC138496	WRKY transcription factor					2.11										
Mtr.32745.1.S1_at	TC138389	WRKY transcription factor					2.11										
Mtr.9516.1.S1_at	TC128619	Disease resistance response protein					2.12										
Mtr.5380.1.S1_s_at	BE319602	O-methyltransferase					2.13										
Mtr.5990.1.S1_s_at	BG455728	Putative uncharacterised protein					2.13										
Mtr.45600.1.S1_s_at	AI847421	Ycf68 protein					2.13										
Mtr.9254.1.S1_at	TC118596	Phenylalanine ammonia-lyase					2.14	2.43									
Mtr.49680.1.S1_at	TC138130	Putative uncharacterised protein					2.14										
Mtr.18700.1.S1_at	TC126395	177 protein					2.14										
Mtr.43233.1.S1_at	TC123096	Putative uncharacterised protein					2.14										
Mtr.8363.1.S1_at	TC130545	Putative uncharacterised protein					2.14					2.67					
Mtr.31998.1.S1_at	AL388370	Putative uncharacterised protein					2.15										
Mtr.52241.1.S1_at	TC126833	Putative uncharacterised protein					2.15					2.63					
Mtr.25945.1.S1_at	TC120741	Putative uncharacterised protein					2.15										
Mtr.43296.1.S1_at	TC123068	Putative uncharacterised protein					2.15					3.21					
Mtr.13629.1.S1_at	TC139790	Putative uncharacterised protein					2.16										
Mtr.5343.1.S1_s_at	TC134893	Type-A response regulator					2.16										
Mtr.3205.1.S1_at	TC132562	Putative uncharacterised protein					2.16										
Mtr.4716.1.S1_at	AL377378	Peptide transporter PTR5					2.16										
Mtr.20782.1.S1_at	NP7265578	Putative uncharacterised protein					2.16										
Mtr.40925.1.S1_at	TC126816	Leucine-rich repeat protein-like					2.17										
Mtr.40941.1.S1_at	TC125828	proline-rich protein (PRP2) mRNA					2.17					2.95					
Mtr.8420.1.S1_at	TC132773	Putative uncharacterised protein					2.18										
Mtr.46651.1.S1_s_at	TC141469	Ycf68 protein					2.18										
Mtr.41859.1.S1_at	TC114359	Putative uncharacterised protein					2.18					2.19					
Mtr.31779.1.S1_at	AL379888	Putative uncharacterised protein					2.18					2.74					
Mtr.31405.1.S1_at	AJ847134	Aspartic proteinase nepenthesin-1					2.19										
Msa.1237.1.S1_at	TC121408	Beta-ketoacyl-CoA synthase					2.19					2.04					
Mtr.24683.1.S1_s_at	TC131304	Putative uncharacterised protein					2.19										
Mtr.45601.1.S1_s_at	AJ847421	Putative uncharacterised protein					2.20										
Mtr.30762.1.S1_at	CA922263	Weakly similar to Anthocyanin 5-aromatic acyltransferase					2.20										
Mtr.51829.1.S1_s_at	TC134893	Type-A response regulator					2.20										
Mtr.4372.1.S1_at	AJ498954	Putative uncharacterised protein					2.20										
Msa.2953.1.S1_at	TC121008	Chlorophyll a/b binding protein					2.20										
Mtr.26850.1.S1_at	AJ846050	Ethylene-responsive transcription factor TINY					2.21										
Mtr.32877.1.S1_at	TC141511	Putative uncharacterised protein					2.21										
Mtr.45319.1.S1_at	TC126112	Putative uncharacterised protein					2.21	2.05									
Mtr.24523.1.S1_at	NP7252022	Receptor-like kinase					2.23										
Mtr.4037.1.S1_at	CA919900	polygalacturonase precursor (PG7)					2.23										
Mtr.45637.1.S1_s_at	NP7269476	NAD(P)H-quinone oxidoreductase subunit K					2.23										
Mtr.26850.1.S1_x_at	AJ846050	Ethylene-responsive transcription factor TINY					2.23										
Mtr.37245.1.S1_s_at	TC124479	Chlorophyll a/b binding protein					2.23										
Mtr.11343.1.S1_at	TC128669	Mt Dwarf 27					2.23						2.96				
Mtr.12950.1.S1_at	TC179984	partially similar to EPIDERMAL PATTERNING FACTOR-like protein					2.24										
Mtr.1494.1.S1_at	AW126348	Putative uncharacterised protein					2.25										
Mtr.11386.1.S1_at	TC124101	Putative uncharacterised protein					2.25					2.61					
Mtr.18570.1.S1_at	NP7267887	Peroxidase					2.26					3.39					
Mtr.32312.1.S1_at	AW687900	WRKY transcription factor					2.26										
Mtr.38599.1.S1_at	TC120510	MtN5 protein					2.26										
Mtr.4300.1.S1_s_at	AI974744	NAC domain protein					2.26										

Probeset ID	Tentative Consensus	Gene	CHSB 6 vs. CB6	CHSB 24 vs. CB24	CHSE6 vs. CE6	CHSE 24 vs. CHSB 24	CHSE 24 vs. CHS E6	CHSE 24 vs. CE24	CB24 vs. CB6	CB6 vs. CB6	CE24 vs. CB24	CE24 vs. CE6	CE vs. CB	CHSB vsCB	CHSE vs. CHSB	CHSE vs. CE	CHS vs. C
Mtr.37210.1.S1_at	TC121008	Chlorophyll a/b binding protein					2.26										
Mtr.38422.1.S1_at	TC130173	Putative uncharacterised protein					2.26					3.01					
Msa.1320.1.S1_at	BF647189	Zinc finger protein CONSTANS-like protein					2.27										
Mtr.39861.1.S1_at	TC117960	Putative uncharacterised protein					2.27										
Mtr.1858.1.S1_at	BE204703	Cytochrome P450					2.27										
Mtr.1926.1.S1_at	BE940909	Putative uncharacterised protein					2.28	2.21									
Mtr.10898.1.S1_at	TC117292	Putative uncharacterised protein					2.28	2.38									
Mtr.44039.1.S1_at	TC134687	Primary amine oxidase					2.29										
Mtr.35816.1.S1_at	TC138356	Putative uncharacterised protein					2.29										
Mtr.7449.1.S1_at	TC119489	GDSL esterase/lipase					2.30	2.49								2.02	
Mtr.44649.1.S1_at	TC124370	ABC transporter G family member					2.30					2.87					
Mtr.14599.1.S1_at	TC135980	Putative uncharacterised protein					2.31		3.93			2.71					
Mtr.38836.1.S1_at	TC123758	Putative uncharacterised protein					2.31										
Mtr.8526.1.S1_at	TC117681	Putative uncharacterised protein					2.31										
Mtr.33157.1.S1_at	BF644611	Putative uncharacterised protein					2.32					2.09					
Mtr.14599.1.S1_x_at	TC135980	Putative uncharacterised protein					2.32		4.02			2.46					
Mtr.992.1.S1_at	TC134078	GDSL esterase/lipase					2.33					2.13					
Mtr.51761.1.S1_at	TC112653	Galactinol-sucrose galactosyltransferase					2.34					2.85					
Mtr.29741.1.S1_at	AL373144	Putative uncharacterised protein					2.34					2.56					
Mtr.29662.1.S1_at	AJ548058	Putative uncharacterised protein					2.34					3.34					
Mtr.16356.1.S1_s_at	TC112884	ER glycerol-phosphate acyltransferase					2.34					2.53					
Mtr.14000.1.S1_at	TC125684	Pectinesterase inhibitor					2.35										
Mtr.25148.1.S1_at	**BF633905**	Wall-associated receptor kinase-like protein					2.35										
Mtr.4526.1.S1_at	TC141582	16S ribosomal RNA gene					2.35										
Mtr.31435.1.S1_at	AJ847835	Putative uncharacterised protein					2.37		5.60			3.40					
Mtr.49783.1.S1_at	TC136026	Endo-beta-1,3-glucanase					2.38										
Mtr.16372.1.S1_x_at	TC121769	Resistance protein PLTR					2.38										
Mtr.27103.1.S1_at	TC131157	Putative uncharacterised protein					2.39					2.05					
Mtr.7638.1.S1_at	TC123539	glucan endo-beta-1,3-glucosidase, acidic isoform					2.39										
Mtr.38421.1.S1_at	TC135915	Putative uncharacterised protein					2.40					2.71					
Mtr.9818.1.S1_at	TC137099	Zinc finger protein CONSTANS-like protein					2.40					2.36					
Mtr.22454.1.S1_at	NP7257659	diacylglycerol O-acyltransferase 2-like					2.41					2.08					
Mtr.29365.1.S1_at	CB895040	Putative uncharacterised protein					2.42										
Mtr.14834.1.S1_at	TC112884	ER glycerol-phosphate acyltransferase					2.43					3.11					
Mtr.33794.1.S1_at	TC126480	Putative uncharacterised protein					2.44										
Mtr.42979.1.S1_at	TC119971	Putative uncharacterised protein					2.45										
Mtr.42525.1.S1_x_at	TC141053	Putative uncharacterised protein					2.45										
Mtr.18508.1.S1_at	TC118445	LOB domain-containing protein					2.45										
Mtr.32088.1.S1_x_at	TC190597	GDSL esterase/lipase At2g23540-like					2.46					2.94					
Mtr.32982.1.S1_at	BF636044	Nudix hydrolase					2.46	2.44									
Mtr.40165.1.S1_at	TC134712	MsRSY-SP5501 16S ribosomal RNA gene					2.46		2.18								
Mtr.13167.1.S1_at	TC135352	long-chain acyl-CoA synthetase 2-like					2.48					2.91					
Mtr.41147.1.S1_at	TC123515	Putative uncharacterised protein					2.48										
Mtr.15769.1.S1_at	NP7258795	Putative uncharacterised protein					2.49					3.38					
Mtr.40733.1.S1_at	TC118885	Putative uncharacterised protein					2.49					2.22					
Mtr.18605.1.S1_at	TC122217	Putative uncharacterised protein					2.52										
Mtr.37882.1.S1_at	TC128595	Putative uncharacterised protein					2.52										
Mtr.7670.1.S1_at	TC133037	Albumin					2.52					2.21					
Mtr.50309.1.S1_s_at	TC126419	ATP-dependent Clp protease proteolytic subunit					2.55					3.44					
Mtr.9311.1.S1_at	TC136239	Putative uncharacterised protein					2.55					2.56					
Mtr.46524.1.S1_at	TC126222	Cyclic peptide transporter					2.55						2.13				
Mtr.19871.1.S1_at	TC124584	Calcium-binding EF-hand					2.56	2.51									
Mtr.36986.1.S1_s_at	TC127716	NAD(P)H-quinone oxidoreductase					2.57										
Mtr.13185.1.S1_at	TC115244	Putative uncharacterised protein					2.57					2.38					
Mtr.18041.1.S1_at	TC120378	ABC transporter G family member					2.60					2.86					
Msa.3135.1.S1_at	TC121008	Chlorophyll a/b binding protein					2.60										
Mtr.26036.1.S1_s_at	TC113573	3-ketoacyl-CoA synthase					2.60					2.99					
Mtr.13397.1.S1_at	BG645569	Putative uncharacterised protein					2.60					2.64					
Mtr.10968.1.S1_at	TC180277	Pathogenesis-related protein 5-1 (partial)					2.61	2.61									
Mtr.44922.1.S1_at	TC132990	Putative uncharacterised protein					2.61					4.41					
Mtr.18605.1.S1_x_at	TC122217	Putative uncharacterised protein					2.63					2.77					
Mtr.43797.1.S1_at	TC190597	GDSL esterase/lipase At2g23540-like					2.65					3.98					
Mtr.38036.1.S1_at	TC135089	partially similar to Zinc transporter					2.67										
Mtr.25019.1.S1_at	TC129589	NAD-dependent epimerase/dehydratase, Dihydroflavonol-4-reductase					2.67					2.56					
Mtr.43917.1.S1_at	TC131275	RING-H2 finger protein ATL1E					2.69										
Mtr.24395.1.S1_at	TC127965	Non-specific lipid-transfer protein					2.69					3.51					
Mtr.50760.1.S1_at	TC132757	Putative uncharacterised protein					2.70					2.40					
Mtr.38253.1.S1_at	TC115015	GDSL esterase/lipase					2.71					3.39					
Mtr.40695.1.S1_at	TC135886	2-succinylbenzoate-CoA ligase					2.74					2.32					
Mtr.35856.1.S1_at	TC119831	16s Ribosomal proteins S12, S7					2.76		3.31			3.03					
Mtr.1751.1.S1_at	AW776248	Partially similar to MsRSY-SP8401 16S ribosomal RNA gene					2.76										
Mtr.42072.1.S1_at	TC133140	Flotillin-like protein					2.78										
Mtr.11271.1.S1_at	TC120324	Putative uncharacterised protein					2.80										
Mtr.47425.1.S1_s_at	TC113203	Beta-glucosidase					2.80					2.58					
Mtr.40695.1.S1_x_at	TC135886	2-succinylbenzoate-CoA ligase					2.81										
Mtr.1751.1.S1_s_at	AW776248	Putative uncharacterised protein					2.82										
Mtr.12155.1.S1_at	TC121807	Putative uncharacterised protein					2.84										
Mtr.5174.1.S1_at	AW690414	Putative uncharacterised protein					2.85										
Mtr.50035.1.S1_at	TC114448	Putative uncharacterised protein					2.85					3.69					
Mtr.45603.1.S1_s_at	TC137458	RegenSY-T2 16S ribosomal RNA and tRNA-Val (trnV-GAC)					2.89					3.05					
Mtr.35830.1.S1_at	TC133707	Putative uncharacterised protein					2.99										
Msa.1765.1.S1_at	TC118656	partially similar to Thaumatin-like protein precursor (pathogenesis related 5)					2.89										
Mtr.24211.1.S1_at	TC127827	Putative uncharacterised protein					2.94										
Mtr.13150.1.S1_at	TC127030	Putative uncharacterised protein					2.95										
Msa.3085.1.S1_at	TC132341	Putative uncharacterised protein					2.97										
Mtr.50959.1.S1_at	TC134802	Putative uncharacterised protein					2.98					2.90					
Mtr.43750.1.S1_at	**TC117738**	**MtHAP2-1 (CCAAT-binding TF)**					**2.99**					**2.76**					
Mtr.36039.1.S1_at	TC118607	Putative uncharacterised protein					3.00					2.51					
Mtr.4513.1.S1_x_at	AJ847424	Putative uncharacterised protein					3.06										
Mtr.37688.1.S1_at	TC119539	Putative uncharacterised protein					3.10										
Msa.2509.1.S1_at	NP7268179	Putative uncharacterised protein					3.22		7.72			5.46					
Mtr.9894.1.S1_at	TC120505	(+)-neomenthol dehydrogenase					3.24										
Mtr.42967.1.S1_at	TC120550	Albumin					3.29										
Mtr.10332.1.S1_at	TC174282	Endochitinase)					3.31										
Mtr.12519.1.S1_at	TC116151	Beta-ketoacyl-CoA synthase					3.38					2.63					
Mtr.40778.1.S1_at	TC116500	Putative uncharacterised protein					3.38										
Mtr.20201.1.S1_at	TC119784	K(+)/H(+) antiporter					3.43										
Mtr.18822.1.S1_at	TC135049	ATFP4-like protein					3.46										
Mtr.42944.1.S1_s_at	TC137219	Putative uncharacterised protein					3.48										
Mtr.45638.1.S1_s_at	TC131652	ATP synthase epsilon chain					3.56					3.63					
Mtr.6197.1.S1_s_at	TC132130	partially similar to PsEXT5.11 root nodule extensin					3.60										
Mtr.29366.1.S1_at	TC137876	Cysteine-rich receptor-like protein kinase					3.61										
Mtr.14668.1.S1_at	TC178473	Apyrase-like protein					3.68										
Mtr.45639.1.S1_s_at	TC113878	H+-transporting two-sector ATPase					3.72					3.72					
Mtr.37500.1.S1_at	TC193510	MtN1 protein precursor					3.72					3.26					
Mtr.51803.1.S1_s_at	BQ150498	ATP synthase epsilon chain					3.73					3.79					
Mtr.45564.1.S1_at	TC134810	Putative uncharacterised protein					3.74										
Mtr.1356.1.S1_s_at	AJ504152	Putative uncharacterised protein					3.82	3.28									
Mtr.42966.1.S1_at	TC184946	Pathogenesis-related protein PR10					3.90	3.85									
Mtr.42912.1.S1_at	TC137319	Putative uncharacterised protein					3.91										
Mtr.41028.1.S1_at	TC177692	Putative uncharacterised protein					3.99					2.53	3.53				
Mtr.407.1.S1_at	TC123494	Jasmonate O-methyltransferase					4.23										
Mtr.7380.1.S1_at	TC135403	Putative uncharacterised protein					4.48										

Probeset ID	Tentative Consensus	Gene	CHSB 6 vs. CB6	CHSB 24 vs. CB24	CHSE6 vs. CE6	CHSE 24 vs. CHSB 24	CHSE 24 vs. CHS E6	CHSE 24 vs. CE24	CB24 vs. CB6	CE6 vs. CB6	CE24 vs. CB24	CE24 vs. CE6	CE vs. CB	CHSB vs.CB	CHSE vs. CHSB	CHSE vs. CE	CHS vs. C
Mtr.40047.1.S1_s_at	TC126984	Putative uncharacterised protein					4.52										
Mtr.1973.1.S1_at	TC134134	Putative uncharacterised protein					5.11		8.68			6.28					
Mtr.35185.1.S1_at	CX535175	Putative uncharacterised protein					5.51					2.09					
Mtr.36378.1.S1_at	TC178473	Apyrase-like protein					5.51	4.05									
Mtr.689.1.S1_at	TC139937	Reticuline oxidase-like protein					5.53										
Mtr.15627.1.S1_x_at	TC139394	Blue (type 1) copper domain					5.60					3.95					
Mtr.36076.1.S1_at	AJ846072	Putative uncharacterised protein					5.80										
Mtr.45710.1.S1_s_at	TC113283	Beta-glucosidase					6.05					5.11					
Mtr.37585.1.S1_a_at	TC118594	Putative uncharacterised protein					6.12										
Mtr.35511.1.S1_at	TC135762	Trypsin inhibitor					6.27						7.28				
Mtr.35815.1.S1_at	TC132710	Germin-like protein subfamily 1 member					7.83	7.34									3.68
Mtr.50075.1.S1_s_at	TC179870	Germin-like protein subfamily 1 member					8.58	8.72								3.18	3.49
Mtr.8572.1.S1_at	TC113538	Thaumatin-like protein 1a precursor					12.39	9.92						2.81		3.14	2.97
Mtr.50074.1.S1_at	TC179869	Germin-like protein subfamily 1 member					13.72	11.3 7								2.99	2.81
Mtr.11247.1.S1_at	TC183764	Ubiquitin carboxyl-terminal hydrolase						-2.18									
Mtr.6915.1.S1_at	CX529979	DNA-directed RNA polymerase subunit beta						-2.17									
Mtr.22448.1.S1_s_at	NP7275080	Transcription factor bZIP106						-2.12									
Mtr.11591.1.S1_at	TC127248	E3 ubiquitin-protein ligase COP1						-2.06									
Mtr.4636.1.S1_at	AL371575	Putative uncharacterised protein						-2.05									
Mtr.47993.1.S1_at	TC126750	Putative uncharacterised protein						-2.01									
Mtr.43023.1.S1_at	TC116025	Aldo/keto reductase						-2.01									
Mtr.51826.1.S1_at	TC117611	Putative uncharacterised protein						2.01									
Mtr.43138.1.S1_at	TC174541	Putative basic PR1 (Pisum sativum)						2.02									
Msa.2530.1.S1_at	TC188731	Isoflavone reductase						2.06									
Mtr.42141.1.S1_at	TC128539	Peroxidase						2.07									
Mtr.42263.1.S1_at	TC136182	Putative uncharacterised protein						2.07									
Msa.1774.1.S1_at	TC115650	Receptor-like protein kinase						2.08									
Mtr.41653.1.S1_at	TC194453	partially similar to phosphate carrier protein, mitochondrial-like						2.08									
Mtr.10896.1.S1_s_at	TC190654	Putative uncharacterised protein						2.10									
Msa.3030.1.S1_at	TC173566	Esterase PIR7B						2.10									
Mtr.37984.1.S1_at	TC119293	Putative uncharacterised protein						2.12									
Mtr.12511.1.S1_at	TC129962	Heat stress transcription factor B-3						2.12									
Mtr.37708.1.S1_at	TC185195	Sulfate transporter 3.1						2.12									
Mtr.19471.1.S1_at	NP7263850	Putative uncharacterised protein						2.16									
Mtr.6352.1.S1_a_at	BQ140458	Alternative oxidase						2.19									
Mtr.11055.1.S1_at	TC138759	Protein SRG1						2.21									
Mtr.33372.1.S1_at	TC128780	Putative uncharacterised protein						2.22									
Mtr.9569.1.S1_at	TC126941	Putative uncharacterised protein						2.25									
Mtr.34199.1.S1_at	TC126191	Gibberellin 20 oxidase						2.32									
Mtr.10325.1.S1_at	EX528833	Chitinase-related agglutinin (partial)						2.40						2.06			
Mtr.6811.1.S1_s_at	CX525743	Putative uncharacterised protein						2.41									
Mtr.27985.1.S1_at	BF641475	Putative uncharacterised protein						2.56									
Mtr.42416.1.S1_at	TC140411	Putative uncharacterised protein						2.63									
Mtr.10628.1.S1_at	TC113871	Ferulate 5-hydroxylase						2.67						2.26		2.41	2.33
Mtr.33212.1.S1_x_at	BF646621	Putative uncharacterised protein						2.67						2.21		2.22	2.22
Mtr.41938.1.S1_at	TC126157	Flowering promoting factor-like protein						2.77								2.02	
Mtr.34584.1.S1_at	TC137363	Bowman-Birk type proteinase inhibitor D-II precursor						2.83									
Mtr.6489.1.S1_at	TC123131	Glutathione S-transferase, C-terminal; Thioredoxin-like						3.61						2.14		2.77	2.44
Mtr.43627.1.S1_at	TC123545	Progesterone 5-beta-reductase putative						5.13								3.13	3.30
Mtr.40504.1.S1_at	TC174347	Caffeoyl-CoA O-methyltransferase						6.37								4.18	3.35
Mtr.12303.1.S1_at	TC118402	Putative uncharacterised protein							-3.46								
Mtr.13865.1.S1_at	TC129842	Putative uncharacterised protein							-3.03								
Msa.1282.1.S1_at	TC122307	Lactoylglutathione lyase							-2.64								
Mtr.40028.1.S1_at	TC117107	Endochitinase							-2.59								
Mtr.6928.1.S1_x_at	TC121284	Putative uncharacterised protein							-2.47			-2.46					
Mtr.5209.1.S1_at	AW692531	Putative uncharacterised protein							-2.45								
Mtr.46900.1.S1_at	TC122307	Lactoylglutathione lyase							-2.43			-2.01					
Mtr.44872.1.S1_at	TC117125	Weakly similar to Cytochrome P450 monooxygenase							-2.27								
Mtr.50821.1.S1_at	TC128895	Putative uncharacterised protein							-2.21								
Mtr.31306.1.S1_at	AJ502802	Chitinase domain-containing protein							-2.13								
Mtr.2189.1.S1_at	BG452132	F-box/LRR-repeat protein							-2.07			-2.23					
Mtr.37825.1.S1_at	TC123256	Putative uncharacterised protein							-2.06			-2.02					
Mtr.38704.1.S1_at	TC120326	Putative uncharacterised protein							2.01								
Mtr.25524.1.S1_s_at	TC113656	Eukaryotic translation initiation factor 3 subunit G							2.03								
Mtr.6304.1.S1_at	TC127533	Putative uncharacterised protein							2.07								
Mtr.11701.1.S1_at	TC131954	Putative uncharacterised protein							2.09								
Msa.845.1.S1_at	TC128809	Plasma membrane calcium-transporting ATPase							2.09								
Mtr.16843.1.S1_s_at	NP7264754	NAD(P)H-quinone oxidoreductase subunit H							2.11								
Mtr.30644.1.S1_at	TC126176	Putative uncharacterised protein							2.13			2.12					
Msa.2860.1.S1_at	TC117569	Putative uncharacterised protein							2.13			2.01					
Mtr.32329.1.S1_at	TC118729	Lysine-specific demethylase 3B							2.19								
Msa.1170.1.S1_at		Cactin (SS5)							2.19								
Mtr.3154.1.S1_s_at	TC137708	Putative uncharacterised protein							2.38								
Mtr.31240.1.S1_s_at	AJ501082	Putative uncharacterised protein							2.47								
Mtr.11717.1.S1_at	TC119939	Auxin-induced protein 5NG4							2.48			2.47					
Msa.3141.1.S1_at	EX532877	DNA-directed RNA polymerase subunit beta							2.51								
Mtr.37096.1.S1_a_at	TC121136	Putative uncharacterised protein							2.60								
Mtr.31595.1.S1_at	AL371524	F-box-like/WD repeat-containing protein TBL1XR1							2.62								
Mtr.14064.1.S1_s_at	TC134704	NAD(P)H-quinone oxidoreductase subunit							2.63								
Mtr.45390.1.S1_at	TC131127	Putative uncharacterised protein							2.66								
Mtr.52094.1.S1_at	TC123380	50S ribosomal protein L14 (MTR_2g087550)							2.86			2.36					
Mtr.39331.1.S1_at	TC129036	Putative uncharacterised protein							2.89								
Mtr.34824.1.S1_at	CX525690	Partially similar to ABC transporter D family member							2.94								
Mtr.27259.1.S1_at	AW688673	Putative uncharacterised protein							2.95								
Mtr.9794.1.S1_at	TC132732	Weakly similar to Glycine max filament-like plant protein 7-like							2.97								
Msa.1055.1.S1_at	TC141197	Lotus japonicus strain MG-20 mitochondrion							3.02								
Mtr.1861.1.S1_at	BE204901	Putative uncharacterised protein							3.05			2.75					
Mtr.45598.1.S1_s_at	TC122147	NAD(P)H-quinone oxidoreductase subunit H							3.08								
Mtr.32166.1.S1_at	AW683656	Putative uncharacterised protein							3.13			2.50					
Mtr.6778.1.S1_at	CX524340	Putative uncharacterised protein							3.22								
Mtr.13971.1.S1_at	TC133585	Putative uncharacterised protein							3.53								
Mtr.40299.1.S1_at	TC181172	Putative uncharacterised protein							3.53			2.68					
Mtr.41656.1.S1_at	TC117569	Weakly similar to Glycine max pre-rRNA-processing protein TSR1 homolog							3.61			3.60					
Mtr.4460.1.S1_at	AJ348112	Putative uncharacterised protein							3.79			2.31					
Mtr.45599.1.S1_s_at	TC122147	30S ribosomal protein S15							4.04			2.96					
Mtr.8298.1.S1_at	TC136822	NADH dehydrogenase subunit 4							4.18								
Mtr.6492.1.S1_at	TC127716	Putative uncharacterised protein							4.28								
Mtr.39312.1.S1_at	TC129182	Cell division cycle and apoptosis regulator protein							4.82			3.21					
Mtr.49038.1.S1_s_at		Ribosomal protein S7							6.35			4.24					
Mtr.45595.1.S1_s_at	TC128940	50S ribosomal protein L32							7.41			4.26					
Mtr.28784.1.S1_at	BM813243	Partially similar to LOB domain-containing protein									2.41		2.08				
Mtr.43055.1.S1_s_at	TC124224	SUT1-1 mRNA										-5.93					
Mtr.37562.1.S1_at	TC123477	Succinate dehydrogenase										-5.55					
Mtr.49123.1.S1_at	TC114192	**Aquaporin**										-5.36					
Mtr.32192.1.S1_at	AW684429	LATD/NIP										-5.26					
Mtr.5656.1.S1_s_at	TC123032	Vacuolar H+-ATPase B subunit										-5.23					

Probeset ID	Tentative Consensus	Gene	CHSB 6 vs. CB6	CHSB 24 vs. CB24	CHSE6 vs. CE6	CHSE 24 vs. CHSB 24	CHSE 24 vs. CHS E 6	CHSE 24 vs. CE24	CB24 vs. CB6	CE6 vs. CB6	CE24 vs. CB24	CE24 vs. CE6	CE vs. CB	CHSB vs.CB	CHSE vs. CHSB	CHSE vs. CE	CHS vs.C
Mtr.32250.1.S1_s_at	AW686208	Partially similar to RNA-binding protein, putative										-5.02					
Mtr.35713.1.S1_at	TC139996	Protein disulfide isomerase L-2										-4.92					
Mtr.6806.1.S1_s_at	TC117226	Protein kinase										-4.46					
Mtr.5143.1.S1_s_at	AW689093	Glucomannan 4-beta-mannosyltransferase										-4.45					
Mtr.44626.1.S1_at	TC135799	Partially similar to F-box protein										-4.36					
Mtr.45369.1.S1_at	TC122182	Na+/H+ antiporter										-4.36					
Mtr.9063.1.S1_at	TC114333	Hedgehog-interacting protein										-4.22					
Mtr.37471.1.S1_s_at	TC124266	probable methyltransferase PMT2-like										-4.20					
Mtr.41162.1.S1_at	TC120356	Similar to Anthocyanidin 3-O-glucosyltransferase										-4.14					
Mtr.37539.1.S1_s_at	TC115877	Putative uncharacterised protein										-4.12					
Mtr.50430.1.S1_at	TC112628	Lipoxygenase										-4.11					
Mtr.11536.1.S1_at	TC122934	Weakly similar to Glycine max CBL-interacting protein kinase 18-like										-4.08					
Mtr.29213.1.S1_s_at	CB891084	Partially similar to Vacuolar-processing enzyme										-4.06					
Mtr.8495.1.S1_s_at	TC114930	Similar to Glycine max BiP isoform C										-4.06					
Mtr.28586.1.S1_s_at	TC141122	Putative uncharacterised protein										-3.95					
Mtr.28242.1.S1_at	TC117459	Beta-glucan-binding protein										-3.90					
Mtr.43633.1.S1_at	TC121308	Putative uncharacterised protein										-3.89					
Mtr.4682.1.S1_x_at	AL375366	Monocopper oxidase-like protein SKU5										-3.88					
Mtr.43970.1.S1_at	TC121611	Calcium dependent protein kinase										-3.81					
Mtr.39450.1.S1_at	TC113982	Putative uncharacterised protein										-3.78					
Mtr.12370.1.S1_s_at	TC139076	putative AP2/EREBP transcription factor (WXP2) mRNA/ Ethylene-responsive transcription factor RAP2-4										-3.67					
Mtr.43653.1.S1_at	TC117598	Putative uncharacterised protein										-3.50					
Mtr.48411.1.S1_s_at	TC127375	Beta-galactosidase										-3.45					
Mtr.39169.1.S1_at	TC119317	Transmembrane protein										-3.41					
Msa.2605.1.S1_at	TC123415	Partially similar to V-type proton ATPase subunit H										-3.39					
Mtr.29267.1.S1_at	TC127200	Endoplasmic reticulum-type calcium-transporting ATPase										-3.33					
Mtr.10625.1.S1_at	TC124902	Putative uncharacterised protein										-3.31					
Msa.1242.1.S1_at	TC112880	Alanine aminotransferase										-3.22					
Msa.2835.1.S1_at	TC121348	Weakly similar to Nucleobase ascorbate transporter										-3.16					
Mtr.48899.1.S1_at	TC117803	Ferritin-3										-3.16					
Msa.2865.1.S1_at	TC120104	Citrate synthase										-3.15					
Mtr.40566.1.S1_s_at	TC120838	Weakly similar to BONZAI 1-like										-3.08					
Mtr.12018.1.S1_at	TC128301	Putative uncharacterised protein										-2.95					
Mtr.13455.1.S1_at	TC127628	Membrane protein, putative										-2.93					
Mtr.40439.1.S1_at	TC137081	Multidrug resistance protein ABC transporter family										-2.91					
Mtr.40198.1.S1_at	TC137081	Putative uncharacterised protein										-2.90					
Mtr.12850.1.S1_at	TC128416	Putative uncharacterised protein										-2.87					
Mtr.35334.1.S1_s_at	CX550105	Similar to Glycerophosphodiester phosphodiesterase										-2.86					
Mtr.9474.1.S1_at	TC126159	MLO1 (Barley mildew resistance locus o , calmodulin binding)										-2.86					
Mtr.11230.1.S1_at	TC119708	Laccase										-2.85					
Mtr.8443.1.S1_at	TC116497	Putative uncharacterised protein										-2.84					
Mtr.17849.1.S1_s_at	BG648475	Partially similar to Long-chain-fatty-acid-CoA ligase										-2.83					
Msa.942.1.S1_at	TC132398	Similar to 2,3-bisphosphoglycerate-independent phosphoglycerate mutase										-2.82					
Msa.1025.1.S1_at	TC115969	Dihydropyrimidinase										-2.82					
Mtr.37400.1.S1_at	TC117182	Weakly similar to transcription factor bHLH62-like										-2.81					
Mtr.38644.1.S1_at	TC117595	Beta-galactosidase										-2.77					
Mtr.38633.1.S1_at	TC131702	Ent-kaurene oxidase										-2.77					
Mtr.32221.1.S1_at	AW685164	Calmodulin-binding protein										-2.77					
Mtr.5170.1.S1_at	AW690340	Cellulose synthase-like protein										-2.77					
Mtr.4738.1.S1_s_at	AL379211	Putative uncharacterised protein										-2.75					
Mtr.41347.1.S1_at	TC127095	Putative uncharacterised protein										-2.75					
Mtr.11644.1.S1_at	TC128271	Partially similar to casein kinase I isoform delta-like, transcript variant 3										-2.75					
Mtr.9486.1.S1_at	TC122596	Zinc finger protein CONSTANS-LIKE protein										-2.74					
Mtr.40343.1.S1_s_at	TC121199	Dihydrofolate reductase-thymidylate synthase										-2.71					
Mtr.37250.1.S1_at	TC117345	Putative uncharacterised protein										-2.70					
Mtr.37895.1.S1_at	TC118569	NPR1-1 protein (Nonexpressor of PR genes)										-2.69					
Mtr.27296.1.S1_at	AW736221	Villin-2										-2.69					
Mtr.49527.1.S1_at	TC126401	GDSL esterase/lipase APG										-2.68					
Mtr.4297.1.S1_s_at	TC133906	Importin subunit alpha-1										-2.68					
Mtr.13320.1.S1_at	TC129193	Vascular protein										-2.66					
Mtr.11811.1.S1_s_at	TC116470	Putative uncharacterised protein										-2.65					
Mtr.9755.1.S1_at	TC122836	U5 small nuclear ribonucleoprotein 200 kDa helicase										-2.65					
Mtr.6853.1.S1_s_at	TC120414	Sec14 cytosolic factor										-2.65					
Mtr.38575.1.S1_at	TC117543	Solute carrier family 35 member G2										-2.64					
Mtr.12536.1.S1_at	TC120444	Glutamyl-tRNA reductase										-2.64					
Mtr.14419.1.S1_s_at	TC114198	Purple acid phosphatase										-2.64					
Mtr.31597.1.S1_at	AL371560	**Expansin-A7**										-2.62					
Mtr.26623.1.S1_at	TC115926	Tubulin beta chain										-2.62					
Mtr.39660.1.S1_at	TC137157	Xyloglucan glycosyltransferase										-2.61					
Mtr.9669.1.S1_at	TC120816	Anthranilate N-hydroxycinnamoyl/benzoyltransferase										-2.60					
Mtr.39289.1.S1_at	TC136682	Anthocyanidin 3-O-glucosyltransferase										-2.59					
Mtr.11075.1.S1_s_at	TC130664	Protein disulfide-isomerase										-2.57					
Mtr.43280.1.S1_x_at	TC120308	beta-glucosidase G2										-2.57					
Mtr.7014.1.S1_at	TC123371	peptide transporter 1 (PTR1)										-2.56					
Mtr.27526.1.S1_at	BE203998	Putative uncharacterised protein										-2.56					
Mtr.9480.1.S1_at	TC122743	Atypical receptor-like kinase MARK										-2.55					
Mtr.38185.1.S1_at	TC123629	Protein tolB										-2.55					
Mtr.37207.1.S1_at	TC132969	Thymus-specific serine protease										-2.54					
Mtr.7066.1.S1_at	TC114329	Laccase-11										-2.53					
Mtr.43874.1.S1_s_at	TC115874	Putative uncharacterised protein										-2.53					
Mtr.34120.1.S1_s_at	TC126216	Similar to Glycine max peptide transporter PTR1-like										-2.53					
Mtr.12562.1.S1_s_at	TC115327	Acyl-CoA-binding domain-containing protein										-2.52					
Mtr.7384.1.S1_s_at	TC117245	Receptor-like protein kinase										-2.52					
Mtr.29334.1.S1_s_at	CB894188	Putative uncharacterised protein										-2.50					
Mtr.41924.1.S1_at	TC121977	Hexose transporter										-2.50					
Mtr.44837.1.S1_at	TC122648	Putative uncharacterised protein										-2.50					
Mtr.28549.1.S1_at	BG648419	Peptide transporter PTR3-A										-2.50					
Mtr.43759.1.S1_at	TC124063	Similar to Glycine max probable beta-1,3-galactosyltransferase 2-like										-2.49					
Mtr.9031.1.S1_s_at	TC123378	Aspartic proteinase-like protein										-2.49					
Mtr.12177.1.S1_s_at	TC131573	Partially similar to GTPase activating-like protein										-2.49					
Mtr.31246.1.S1_s_at	TC131927	Putative uncharacterised protein										-2.48					
Mtr.43258.1.S1_s_at	TC126577	Putative uncharacterised protein										-2.48					
Mtr.42340.1.S1_at	TC136295	Importin subunit alpha-1										-2.48					
Mtr.42215.1.S1_at	TC135810	Spinster-like protein										-2.48					
Mtr.29239.1.S1_at	CB892013	Phosphoinositide phospholipase C										-2.47					
Mtr.43717.1.S1_at	TC125907	Putative uncharacterised protein										-2.47					

Probeset ID	Tentative Consensus	Gene	CHSB 6 vs. CB6	CHSB 24 vs. CB24	CHSE6 vs. CE6	CHSE 24 vs. CHSB 24	CHSE 24 vs. CHS E 6	CHSE 24 vs. CE24	CB24 vs. CB6	CE6 vs. CB6	CE24 vs. CB24	CE24 vs. CE6	CE vs. CB	CHSB vs.CB	CHSE vs. CHSB	CHSE vs. CE	CHS vs C
Mtr.12738.1.S1_at	TC117341	Serine/threonine protein phosphatase 2A 59 kDa regulatory subunit B' eta isoform										-2.47					
Mtr.5628.1.S1_x_at	BF640256	Partially similar to Seed lipoxygenase										-2.47					
Mtr.45394.1.S1_at	TC131215	Wall-associated receptor kinase-like protein										-2.46					
Mtr.22601.1.S1_at	TC121700	Xyloglucan endotransglucosylase										-2.46					
Mtr.43657.1.S1_at	TC115818	Putative uncharacterised protein										-2.46					
Mtr.42094.1.S1_at	TC121141	Callose synthase										-2.45					
Mtr.39084.1.S1_at	TC121076	Similar to Glycine max zinc finger CCCH domain-containing protein 37-like										-2.44					
Mtr.33334.1.S1_at	BF650594	Putative uncharacterised protein										-2.44					
Mtr.38371.1.S1_at	TC119866	Calcium-binding protein, putative										-2.44					
Mtr.42578.1.S1_at	TC122833	Putative uncharacterised protein										-2.43					
Mtr.9367.1.S1_at	TC121302	Conserved oligomeric Golgi complex subunit										-2.42					
Mtr.11984.1.S1_x_at	TC124208	Peptide transporter PTR1										-2.41					
Mtr.43280.1.S1_at	TC120308	beta-glucosidase G2										-2.41					
Mtr.34428.1.S1_x_at	TC141575	Partially (78%) similar to Glyceraldehyde-3-phosphate dehydrogenase										-2.39					
Mtr.46047.1.S1_at	BG585312	Peroxidase										-2.39					
Mtr.42190.1.S1_at	TC129153	Putative uncharacterised protein										-2.38					
Mtr.40794.1.S1_at	TC120686	Putative uncharacterised protein										-2.38					
Mtr.41639.1.S1_at	TC130110	Putative uncharacterised protein										-2.38					
Msa.1670.1.S1_at	TC117803	ferritin										-2.37					
Msa.432.1.S1_at	TC119131	Putative uncharacterised protein										-2.37					
Mtr.38623.1.S1_at	TC134154	Partially similar (89%) to N-terminal kinase-like protein										-2.37					
Mtr.44035.1.S1_at	TC125367	Putative uncharacterised protein										-2.37					
Mtr.32635.1.S1_at	BE247944	Auxin-induced protein 5NG4										-2.36					
Mtr.34929.1.S1_at	TC138319	Partially (58%) similar to Zinc finger protein CONSTANS-like protein										-2.35					
Mtr.39156.1.S1_at	TC115638	Glycine max exocyst complex component 2-like										-2.35					
Mtr.10990.1.S1_at	TC116417	Glycine max peptide transporter PTR2-like										-2.34					
Mtr.39976.1.S1_x_at	TC125736	Mitochondrial chaperone										-2.34					
Mtr.12609.1.S1_at	TC124534	Similar (87%) to Glycine max acyl-coenzyme A oxidase 2, peroxisomal-like										-2.34					
Mtr.9555.1.S1_at	TC130491	Partially (88%) similar to Medicago sativa mesa acidic cell wall invertase 5										-2.33					
Mtr.3453.1.S1_x_at	**AW574263**	**CYCLOPS**										**-2.33**					
Mtr.5831.1.S1_x_at	TC116043	RCC1 and BTB domain-containing protein (MTR_7g016640)										-2.33					
Mtr.3030.1.S1_at	CB892424	Ubiquitin-activating enzyme E1										-2.32					
Mtr.41567.1.S1_x_at	TC112661	Dolichyl-diphosphooligosaccharide-protein glycosyltransferase subunit STT3A										-2.32					
Mtr.33354.1.S1_at	BF651172	GH3 family protein										-2.32					
Mtr.44730.1.S1_at	TC122670	Nitrate transporter										-2.32					
Mtr.40746.1.S1_at	TC118604	Kinesin-like protein										-2.32					
Mtr.27374.1.S1_at	AW774989	Isoflavonoid glucosyltransferase										-2.32					
Mtr.51429.1.S1_at	TC118844	Receptor-like protein kinase										-2.31					
Mtr.45573.1.S1_at	TC126687	ABC transporter C family member										-2.31					
Mtr.40958.1.S1_at	TC128093	Putative uncharacterised protein										-2.31					
Mtr.48412.1.S1_x_at	TC127375	Beta-galactosidase										-2.31					
Mtr.9619.1.S1_at	TC119752	Conserved oligomeric Golgi complex subunit										-2.30					
Mtr.38103.1.S1_x_at	TC124796	Kinesin-like protein KIF2A										-2.30					
Mtr.5307.1.S1_x_at	TC134718	Fasciclin-like arabinogalactan protein										-2.30					
Mtr.1625.1.S1_x_at	AW586364	Partiall (83%) similar to Dual specificity protein kinase pyk2										-2.30					
Mtr.38983.1.S1_at	TC119351	Protein tolB										-2.29					
Mtr.38994.1.S1_at	TC119378	Putative uncharacterised protein										-2.29					
Mtr.37837.1.S1_x_at	TC119937	Putative uncharacterised protein										-2.29					
Mtr.31088.1.S1_at	AW974514	Putative uncharacterised protein										-2.29					
Mtr.5503.1.S1_at	BF633197	Putative uncharacterised protein										-2.29					
Mtr.47143.1.S1_x_at	CB892920	Xyloglucan endotransglycosylase/hydrolase XTH-21										-2.29					
Mtr.41566.1.S1_at	TC127007	PGPS/D10- Petunia germination pollen specific D10										-2.29					
Mtr.32768.1.S1_x_at	TC119998	E3 ubiquitin-protein ligase synovolin										-2.28					
Mtr.13089.1.S1_at	TC118036	Putative uncharacterised protein										-2.28					
Mtr.41688.1.S1_at	TC115226	1-phosphatidylinositol-3-phosphate 5-kinase-like protein										-2.27					
Mtr.41298.1.S1_at	TC115250	Putative uncharacterised protein										-2.27					
Mtr.10277.1.S1_at	TC133317	Putative uncharacterised protein										-2.27					
Mtr.28423.1.S1_at	TC115088	Putative uncharacterised protein										-2.26					
Mtr.41462.1.S1_at	TC123090	Phosphatidylserine decarboxylase										-2.26					
Mtr.12879.1.S1_at	TC123841	E3 ubiquitin-protein ligase synovolin										-2.26					
Mtr.27059.1.S1_at	AW256897	Similar (89%) to Glycine max alpha-xylosidase-like										-2.26					
Mtr.35017.1.S1_at	CX530834	Phosphoglucosamine mutase										-2.25					
Mtr.12699.1.S1_x_at	TC120415	Phosphoglucosamine mutase										-2.25					
Mtr.8558.1.S1_at	TC114530	Putative uncharacterised protein										-2.25					
Mtr.13740.1.S1_at	TC139469	Brefeldin A-inhibited guanine nucleotide-exchange										-2.25					
Msa.1032.1.S1_at	TC128301	U-box domain-containing protein										-2.23					
Mtr.31511.1.S1_at	AL368361	F-box/kelch-repeat protein										-2.23					
Mtr.6527.1.S1_at	TC117606	Partially similar to Acid beta-fructofuranosidase										-2.23					
Mtr.41029.1.S1_x_at	TC114250	Palmitoyltransferase										-2.23					
Mtr.2376.1.S1_at	TC126666	Blue copper protein										-2.22					
Mtr.26042.1.S1_at	TC118239	Thylakoid membrane phosphoprotein 14 kDa										-2.22					
Mtr.43458.1.S1_x_at	TC127598	Putative uncharacterised protein										-2.22					
Mtr.40874.1.S1_at	TC124999	Phosphomevalonate kinase										-2.22					
Mtr.41870.1.S1_at	TC119913	Similar to (86%) Glycine max E3 ubiquitin protein ligase UPL4-like										-2.22					
Mtr.15646.1.S1_at	BQ151465	cold-acclimation specific protein 15 gene/Dehydrin										-2.22					
Mtr.31825.1.S1_at	AL382068	Pleiotropic drug resistance ABC transporter family protein										-2.22					
Mtr.38218.1.S1_at	TC131226	Glycine max probable serine/threonine-protein kinase At5g41260-like										-2.22					
Mtr.51543.1.S1_x_at	TC112825	Heat shock protein Hsp70										-2.21					
Mtr.44886.1.S1_at	TC132165	Putative uncharacterised protein										-2.21					
Mtr.38092.1.S1_at	TC125129	Putative uncharacterised protein										-2.21					
Mtr.11730.1.S1_at	TC124405	Putative uncharacterised protein										-2.21					
Mtr.13318.1.S1_at	TC128610	Wall-associated receptor kinase-like protein										-2.20					
Mtr.44046.1.S1_at	TC127328	Similar (91%) to Glycine max ABC transporter B family member 25-like										-2.20					
Mtr.39041.1.S1_at	TC119735	Similar (89%) Glycine max probable protein phosphatase 2C 15-like										-2.20					
Mtr.11289.1.S1_at	TC132503	Two-component response regulator ARR14										-2.19					
Mtr.31619.1.S1_at	AL372490	Putative uncharacterised protein										-2.19					
Mtr.41297.1.S1_at	TC119626	Ethylene-responsive transcription factor ERF061										-2.19					
Mtr.39141.1.S1_at	TC118954	Calcium-dependent protein kinase										-2.19					
Mtr.13489.1.S1_at	TC140637	Similar (90%) to Glycine max callose synthase 1-like, transcript variant 2										-2.18					

Probeset ID	Tentative Consensus	Gene	CHSB 6 vs. CB6	CHSB 24 vs. CB24	CHSE6 vs. CE6	CHSE 24 vs. CHSB 24	CHSE 24 vs. CHS E 6	CHSE 24 vs. CE24	CB24 vs. CB6	CE6 vs. CB6	CE24 vs. CB24	CE24 vs. CE6	CE vs. CB	CHSB vs.CB	CHSE vs. CHSB	CHSE vs. CE	CHS vs. C
Mtr.5058.1.S1_at	AW684811	Putative uncharacterised protein										-2.18					
Mtr.33677.1.S1_x_at	BI264097	Nucleotide pyrophosphatase/phosphodiester ase										-2.18					
Mtr.2249.1.S1_at	BG583023	Putative uncharacterised protein										-2.18					
Mtr.48023.1.S1_x_at	TC129518	3-hydroxy-3-methylglutaryl coenzyme A reductase										-2.17					
Mtr.46961.1.S1_at	TC112733	Similar (86%) to Glycine max probable methyltransferase PMT15-like										-2.17					
Mtr.41750.1.S1_at	TC128965	Putative uncharacterised protein										-2.16					
Mtr.31746.1.S1_at	AL378146	Putative uncharacterised protein										-2.16					
Mtr.31693.1.S1_at	TC129869	Similar (86%) to GRAS family transcription factor										-2.16					
Mtr.50501.1.S1_at	TC113742	Aquaporin TIP2-1										-2.16					
Mtr.4738.1.S1_at	AL379211	Putative uncharacterised protein										-2.15					
Mtr.13011.1.S1_at	TC118132	Putative uncharacterised protein										-2.14					
Mtr.37656.1.S1_at	TC130729	Pectinesterase										-2.14					
Mtr.8861.1.S1_at	TC124832	Partially (35%) similar to Patatin-T5										-2.14					
Mtr.5115.1.S1_x_at	TC112886	Glucan endo-1,3-beta-glucosidase										-2.14					
Mtr.44246.1.S1_at	TC120060	Cytokinin-O-glucosyltransferase										-2.13					
Mtr.13682.1.S1_at	TC136792	Lysosomal alpha-mannosidase										-2.13					
Mtr.37937.1.S1_at	TC132535	Aspartic proteinase nepenthesin-2										-2.13					
Mtr.41027.1.S1_at	TC125035	Putative uncharacterised protein										-2.13					
Mtr.3501.1.S1_x_at	TC140535	Aquaporin TIP2-3										-2.12					
Msa.1125.1.S1_at	TC138182	Zinc finger CCCH domain-containing protein										-2.12					
Mtr.3060.1.S1_x_at	CB893306	Putative uncharacterised protein										-2.12					
Mtr.48133.1.S1_s_at	TC117284	Notum-like protein										-2.12					
Mtr.13193.1.S1_a_at	TC114913	Putative uncharacterised protein										-2.11					
Mtr.11865.1.S1_x_at	TC126005	Signal peptide peptidase-like 2B										-2.11					
Mtr.7208.1.S1_s_at	TC133520	Dolichyl pyrophosphate Glc1Man9GlcNAc2 alpha-1,3-glucosyltransferase										-2.11					
Mtr.11232.1.S1_at	TC118208	Partially (77%) similar (87%) to Glycine max serine/threonine protein kinase-like protein										-2.11					
Mtr.45293.1.S1_at	TC132345	PQ-loop repeat-containing protein										-2.10					
Mtr.3083.1.S1_at	NP7257292	Multidrug resistance protein ABC transporter family (MTR_1g099280)										-2.10					
Mtr.42822.1.S1_at	TC132989	Pectate lyase 1-27										-2.10					
Mtr.43690.1.S1_s_at	TC114193	Zinc finger protein										-2.10					
Msa.1414.1.S1_at	TC115980	Putative uncharacterised protein										-2.10					
Mtr.34830.1.S1_at	TC134123	Putative uncharacterised protein										-2.10					
Mtr.33519.1.S1_at	TC135660	cold-acclimation specific protein 15 gene.										-2.09					
Mtr.12226.1.S1_at	TC124419	Putative uncharacterised protein										-2.09					
Mtr.38882.1.S1_s_at	TC127521	Cell division protein ftsZ										-2.08					
Mtr.11344.1.S1_at	TC113104	Beta-galactoside alpha-2,6-sialyltransferase										-2.08					
Msa.1760.1.S1_at	TC113984	Partially (89%) similar (83%) to Glycine max probable glutathione S-transferase-like										-2.08					
Mtr.35160.1.S1_at	CX534540	Aspartic proteinase-like protein										-2.08					
Msa.1883.1.S1_at	TC118179	Putative uncharacterised protein										-2.07					
Mtr.29832.1.S1_s_at	AW256676	Cytochrome P450										-2.07					
Mtr.12132.1.S1_at	TC135084	WD-repeat protein-like protein										-2.07					
Mtr.31598.1.S1_at	TC130775	Expansin-A7 (MTR_5g011210)										-2.07					
Mtr.41848.1.S1_at	TC126201	Peroxisomal acyl-CoA oxidase 1A										-2.06					
Mtr.35813.1.S1_at	TC122542	Protein kinase 2B										-2.06					
Mtr.5557.1.S1_at	BF635270	Xylan 1,4-beta-xylosidase										-2.06					
Mtr.43603.1.S1_at	TC120785	Similar (85%) to Glycine max receptor-like protein kinase 3-like										-2.06					
Mtr.37630.1.S1_at	TC114026	Membrane related protein-like protein										-2.06					
Mtr.44751.1.S1_at	TC125314	RING finger protein										-2.06					
Mtr.39098.1.S1_at	TC126821	Putative uncharacterised protein										-2.05					
Mtr.33379.1.S1_x_at	TC116186	LysM domain-containing receptor-like kinase 6										-2.05					
Mtr.9892.1.S1_x_at	TC118359	RING finger protein										-2.05					
Mtr.44281.1.S1_at	TC119360	Similar (86%) to Glycine max purple acid phosphatase 8-like										-2.05					
Mtr.7521.1.S1_at	TC125891	Putative uncharacterised protein										-2.05					
Mtr.27945.1.S1_x_at	TC129444	Putative uncharacterised protein										-2.05					
Mtr.42660.1.S1_at	TC128765	Putative uncharacterised protein										-2.05					
Mtr.32344.1.S1_at	AW688950	Serine/threonine protein kinase cdk9										-2.04					
Mtr.37409.1.S1_x_at	TC121952	Putative uncharacterised protein										-2.04					
Mtr.50857.1.S1_at	TC114160	Serine carboxypeptidase family protein										-2.04					
Mtr.40881.1.S1_x_at	TC140966	CBL-interacting protein kinase										-2.04					
Mtr.12349.1.S1_at	TC115017	Putative uncharacterised protein										-2.04					
Mtr.9682.1.S1_at	TC117512	Putative uncharacterised protein										-2.04					
Mtr.3522.1.S1_at	TC124860	Putative uncharacterised protein										-2.04					
Mtr.35915.1.S1_at	TC130593	Putative uncharacterised protein										-2.04					
Mtr.9213.1.S1_at	TC127005	Similar (89%) to Glycine max serine/threonine-protein kinase Nek4-like										-2.03					
Mtr.9194.1.S1_x_at	TC121583	Similar (91%) to Glycine max probable protein phosphatase 2C 5-like										-2.03					
Mtr.24640.1.S1_at	TC125029	Putative uncharacterised protein										-2.03					
Mtr.12240.1.S1_at	TC132383	Putative uncharacterised protein										-2.03					
Mtr.22026.1.S1_at	TC136112	Partially (75%) similar to Polyphosphoinositide phosphatase										-2.03					
Mtr.27382.1.S1_at	TC140976	Similar (90%) to Glycine max conserved oligomeric Golgi complex subunit 1-like										-2.03					
Mtr.44767.1.S1_at	TC123405	Putative uncharacterised protein										-2.02					
Mtr.42537.1.S1_s_at	TC125266	GDP-fucose protein-O-fucosyltransferase										-2.02					
Mtr.40408.1.S1_at	TC137221	Photosystem II 5 kDa protein										-2.02					
Mtr.37250.1.S1_x_at	TC117345	Putative uncharacterised protein										-2.02					
Msa.2565.1.S1_at	TC114644	Zinc finger CCCH domain-containing protein										-2.02					
Mtr.11672.1.S1_at	TC119002	Putative uncharacterised protein										-2.02					
Mtr.42564.1.S1_at	TC129947	Similar (84%) to Glycine max galactoside 2-alpha-L-fucosyltransferase-like										-2.01					
Mtr.9838.1.S1_at	TC121250	Putative uncharacterised protein										-2.01					
Mtr.15379.1.S1_at	TC113407	Peroxidase										-2.01					
Mtr.43151.1.S1_at	TC122903	Putative uncharacterised protein										-2.01					
Mtr.50857.1.S1_x_at	TC114160	Serine carboxypeptidase family protein										-2.01					
Mtr.37876.1.S1_at	TC118691	Putative uncharacterised protein										-2.01					
Mtr.43613.1.S1_at	TC137225	Poly(A) polymerase										-2.01					
Mtr.2218.1.S1_at	BG681284	Putative uncharacterised protein										-2.00					
Mtr.11414.1.S1_at	TC129795	ABC transporter G family member										-2.00					
Mtr.4709.1.S1_at	AL376760	Putative uncharacterised protein										2.01					
Mtr.7856.1.S1_at	TC138517	Putative uncharacterised protein										2.01					
Mtr.9796.1.S1_at	TC132648	Putative uncharacterised protein										2.02					
Mtr.13375.1.S1_at	TC122368	Putative uncharacterised protein										2.02					
Mtr.30958.1.S1_at	CX541923	Chaperone protein clpB										2.02					
Mtr.21136.1.S1_at	NP7266314	**Nodule-specific glycine-rich protein 3C**										2.03					
Mtr.8651.1.S1_at	TC115437	cold-acclimation specific protein 31 gene (Dehydrin-like)										2.03					
Mtr.39379.1.S1_s_at	TC127399	Amino acid permease										2.03					
Mtr.6706.1.S1_at	CX517792	Putative uncharacterised protein										2.03					
Mtr.42955.1.S1_at	TC124608	Transparent testa 12 protein) (membrane protein, MATE transporter family)										2.05					

Probeset ID	Tentative Consensus	Gene	CHSB 6 vs. CB6	CHSB 24 vs. CB24	CHSE6 vs. CE6	CHSE 24 vs. CHSB 24	CHSE 24 vs. CHS E 6	CHSE 24 vs. CE24	CB24 vs. CB6	CE6 vs. CB6	CE24 vs. CB24	CE24 vs. CE6	CE vs. CB	CHSB vs.CB	CHSE vs. CHSB	CHSE vs. CE	CHS vs. C
Mtr.25454.1.S1_at	TC135052	Macrophage migration inhibitory factor-like protein										2.06					
Mtr.12557.1.S1_at	TC130088	Weakly similar to L-ascorbate oxidase homolog										2.06					
Mtr.13933.1.S1_at	TC125850	Putative uncharacterised protein										2.06					
Mtr.31148.1.S1_at	AJ497224	Putative uncharacterised protein										2.06					
Mtr.24165.1.S1_at	No TC	Putative uncharacterised protein										2.09					
Mtr.6458.1.S1_at	BQ144272	Partially similar to Sulfate transporter										2.10					
Mtr.7990.1.S1_at	BI266955	Putative uncharacterised protein										2.10					
Mtr.43988.1.S1_at	TC115946	metal transport protein (ZIP1)										2.10					
Mtr.37252.1.S1_at	TC118510	Salt-tolerance protein										2.11					
Mtr.40237.1.S1_at	TC114145	Phosphoethanolamine/phosphocholine phosphatase										2.11					
Mtr.46090.1.S1_at	NP7272280	Putative uncharacterised protein										2.11					
Mtr.37092.1.S1_at	TC116777	Putative uncharacterised chloroplast protein										2.12					
Mtr.9814.1.S1_at	TC127045	Putative uncharacterised protein										2.12					
Mtr.8651.1.S1_a_at	TC115437	cold-acclimation specific protein 31 gene , Dehydrin-like										2.12					
Mtr.9728.1.S1_at	TC122809	Putative uncharacterised protein										2.12					
Mtr.32811.1.S1_at	BE324764	Partially (56%) to RXT3-like protein										2.13					
Mtr.35596.1.S1_at	TC129569	Putative uncharacterised protein										2.14					
Msa.1835.1.S1_at	TC135352	long chain acyl-CoA synthetase 2-like										2.14					
Mtr.45630.1.S1_s_at	TC116777	Photosystem II reaction center protein M										2.14					
Mtr.2344.1.S1_at	BG587062	Actin depolymerizing factor										2.15					
Mtr.15867.1.S1_at	TC139307	AP2 domain-containing transcription factor										2.15					
Msa.1730.1.S1_at	TC127154	Similar (93%) to 30S ribosomal protein S3 chloroplastic										2.15					
Mtr.5570.1.S1_at	TC138588	Partially (83%) similar (77%) to Glycine max probable sulfate transporter 3.4-like										2.15					
Mtr.9730.1.S1_at	AW686322	NBS/LRR resistance protein-like protein										2.15					
Mtr.2473.1.S1_s_at	TC118319	Putative uncharacterised protein										2.16					
Mtr.50502.1.S1_at	TC127764	Cysteine-rich receptor-like protein kinase										2.16					
Mtr.19994.1.S1_at	TC118319	Putative uncharacterised protein										2.16					
Mtr.14042.1.S1_s_at	NP7251561	Photosystem II CP47 chlorophyll apoprotein (MTR_4g051370)										2.17					
Mtr.12968.1.S1_at	TC135168	Putative uncharacterised protein										2.17					
Mtr.33999.1.S1_at	TC136905	Partially (80%) similar to Proteasome subunit alpha type										2.18					
Mtr.37103.1.S1_at	TC129334	Putative uncharacterised protein										2.19					
Mtr.40306.1.S1_at	TC121912	Putative uncharacterised protein										2.20					
Mtr.28296.1.S1_at	TC137053	Putative uncharacterised protein										2.21					
Mtr.11740.1.S1_at	TC129621	Putative uncharacterised protein										2.22					
Mtr.45051.1.S1_at	TC128687	Kelch-like protein										2.22					
Mtr.14421.1.S1_at	TC132702	Putative uncharacterised protein										2.24					
Mtr.4253.1.S1_at	TC138487	Putative uncharacterised protein										2.24					
Mtr.44316.1.S1_at	TC128680	Interstitial collagenase										2.25					
Mtr.6131.1.S1_at	BI270698	Putative uncharacterised protein										2.27					
Mtr.975.1.S1_at	TC117599	Putative uncharacterised protein										2.28					
Mtr.29718.1.S1_at	AL367162	FACT complex subunit SPT16										2.28					
Mtr.39379.1.S1_at	TC127199	Amino acid permease										2.30					
Mtr.8924.1.S1_at	TC127504	Early nodulin 12 precursor										2.30					
Mtr.52155.1.S1_at	TC187845	177 protein										2.30					
Mtr.8510.1.S1_at	TC113188	Early nodulin										2.31					
Mtr.41396.1.S1_at	TC115379	Partially (45%) similar to Cell wall protein Exp5 (Expansin)										2.33					
Mtr.28740.1.S1_at	TC128990	Testis-specific Y-encoded protein										2.35					
Mtr.44840.1.S1_at	TC131578	Partially (46%) similar to Protein kinase like protein										2.35					
Mtr.37166.1.S1_at	TC132239	Partially (45%) similar to UDP-glucose glucosyltransferase										2.36					
Mtr.42011.1.S1_at	TC134249	Cytochrome P450 monooxygenase CYP72A59										2.37					
Mtr.14037.1.S1_s_at	TC127154	30S ribosomal protein S3 chloroplastic										2.38					
Mtr.14054.1.S1_s_at	TC134802	ATP synthase subunit a chloroplastic										2.39					
Mtr.19977.1.S1_at	NP7271727	Putative uncharacterised protein										2.39					
Mtr.773.1.S1_s_at	TC114048	Circadian clock-associated protein 1a										2.40					
Mtr.27722.1.S1_at	TC125825	ABC transporter G family member										2.41					
Mtr.12921.1.S1_at	TC134285	N-hydroxythioamide S-beta-glucosyltransferase										2.41					
Msa.2287.1.S1_at	BG449311	Putative uncharacterised protein										2.41					
Mtr.49936.1.S1_at	TC133493	Cytochrome P450										2.53					
Mtr.31123.1.S1_at	AJ388912	U5 small nuclear ribonucleoprotein 200 kDa helicase										2.56					
Mtr.52006.1.S1_s_at	TC117706	Argininosuccinate synthase										2.57					
Mtr.49764.1.S1_at	TC113258	Auxin Efflux Carrier										2.57					
Mtr.45640.1.S1_s_at	TC126834	Maturase K										2.60					
Mtr.42909.1.S1_at	TC133573	Putative uncharacterised protein										2.61					
Mtr.20751.1.S1_at	NP7266746	BZIP transcription factor bZIP73A										2.64					
Mtr.16114.1.S1_at	TC140026	Putative uncharacterised protein										2.66					
Mtr.30034.1.S1_at	BE203732	Partially (72%) similar (91%) to LRR receptor-like serine/threonine-protein kinase EFR										2.69					
Mtr.8505.1.S1_at	TC124906	Embryonic abundant protein USP92										2.69					
Mtr.11085.1.S1_at	TC114048	Circadian clock-associated protein 1a										2.71					
Mtr.27961.1.S1_s_at	BF633770	Putative uncharacterised protein										2.78					
Mtr.23461.1.S1_at	AJ974744	NAC domain protein										2.79					
Mtr.13685.1.S1_at	TC125178	Putative uncharacterised protein										2.80					
Mtr.17183.1.S1_at	TC174437	O-acyltransferase WSD1										2.80					
Mtr.27499.1.S1_at	TC138045	Putative uncharacterised protein										2.80					
Mtr.40380.1.S1_at	TC175943	Protein SRG1										2.80					
Mtr.37751.1.S1_at	TC113277	Isoflavone-7-O-methyltransferase										2.82					
Mtr.9308.1.S1_at	TC126904	PAR-1a (photoassimilate responsive) protein										2.82					
Mtr.44216.1.S1_at	TC125046	Putative uncharacterised protein										2.84					
Mtr.1920.1.S1_at	BE325818	Putative uncharacterised protein										2.88					
Mtr.34720.1.S1_at	CX520171	Putative uncharacterised protein										2.89					
Mtr.7337.1.S1_at	TC125982	Putative uncharacterised protein										2.90					
Mtr.1889.1.S1_at	BE240538	Putative uncharacterised protein										2.91					
Msa.3142.1.S1_at	CA990893	Putative uncharacterised chloroplast protein										2.96					
Mtr.45617.1.S1_s_at	TC125178	30S ribosomal protein S12										2.99					
Mtr.36084.1.S1_at	TC190767	Ribosomal protein L20										3.09					
Mtr.11734.1.S1_at	TC130158	Sulfate/bicarbonate/oxalate exchanger and transporter sat-1										3.11					
Mtr.39593.1.S1_at	TC138969	Cytochrome P450										3.14					
Mtr.35078.1.S1_at	TC113081	Mitochondrial chaperone BCS1										3.18					
Mtr.20282.1.S1_s_at	TC136106	DNA-directed RNA polymerase										3.29					
Mtr.14592.1.S1_at	TC114005	Peroxidase										3.37					
Mtr.12199.1.S1_at	TC133143	Putative uncharacterised protein										3.61					
Mtr.27594.1.S1_at	BE239595	Putative uncharacterised protein										3.82					
Mtr.39772.1.S1_at	TC122345	Putative uncharacterised protein										3.97					
Mtr.7546.1.S1_at	TC137903	weakly similar to MtN15 protein precursor										4.03					
Mtr.14057.1.S1_s_at	TC131688	DNA-directed RNA polymerase										4.14					
Mtr.13963.1.S1_at	TC134627	Putative uncharacterised protein											3.69				
Mtr.20144.1.S1_at	TC121454	Multi antimicrobial extrusion protein MatE											3.81				
Mtr.14237.1.S1_at	NP7261865	Sieve element-occluding protein															-4.69
Msa.1573.1.S1_at	TC116655	Tubulin beta chain															-2.08
Mtr.31637.1.S1_at	AL373292	Partially similar to Peroxidase															-2.05

Probeset ID	Tentative Consensus	Gene	CHSB 6 vs. CB6	CHSB 24 vs. CB24	CHSE6 vs. CE6	CHSE 24 vs. CHSB 24	CHSE 24 vs. CHS E 6	CHSE 24 vs. CE24	CB24 vs. CB6	CB6 vs. CB6	CE24 vs. CB24	CE24 vs. CE6	CE vs. CB	CHSB vs.CB	CHSE vs. CHSB	CHSE vs. CE	CHS vs. C
Mtr.42039.1.S1_at	TC120072	Putative uncharacterised protein														2.05	2.05
Mtr.30765.1.S1_at	TC175803	Isoflavone synthase 1														2.05	2.10
Mtr.1299.1.S1_s_at	TC112893	Licodione synthase														2.23	2.11
Mtr.43770.1.S1_at	TC119741	Pathogenesis-related protein												2.27			2.12
Mtr.23266.1.S1_at	TC137543	Protease inhibitor															2.27
Mtr.44529.1.S1_at	TC134347	Isoliquiritigenin 2'-O-methyltransferase														2.71	2.37
Mtr.10438.1.S1_at	TC122640	Kunitz proteinase inhibitor															2.47
Mtr.27695.1.S1_at	TC126547	Blue (type 1) copper domain														3.94	2.60
Msa.2861.1.S1_at	TC125088	Pathogenesis-related protein 4A;														4.28	4.18
Mtr.8884.1.S1_at	TC125088	Pathogenesis-related protein 4A;														4.86	5.05
Mtr.14224.1.S1_at	TC193299	Inhibitor of trypsin and hagerman factor												2.05			
Mtr.16497.1.S1_at	TC123964	Calcium-binding EF-hand												2.09			
Mtr.45092.1.S1_at	TC126232	Endoglucanase														2.27	
Mtr.40277.1.S1_at	TC135754	putative isoflavone synthase														2.01	
Mtr.40277.1.S1_x_at	TC135755	putative isoflavone synthase														2.02	
Mtr.10382.1.S1_at	TC134956	B12D-like protein, weakly similar														2.05	
Mtr.38067.1.S1_at	TC184993	Putative uncharacterised protein														2.10	
Mtr.4531.1.S1_x_at	AJ847976	B12D-like protein														2.57	
Mtr.43047.1.S1_at	TC187336	Early nodulin 12ff precursor														3.26	

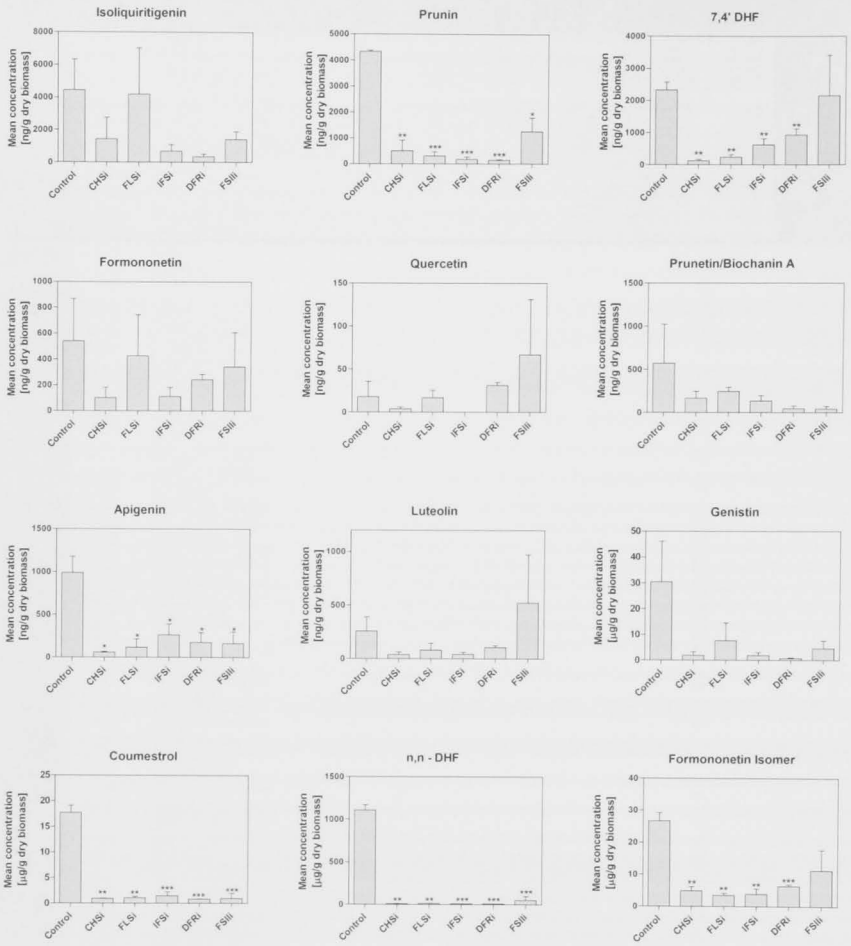

Figure A5.1 – Flavonoid content of roots expressing RNAi construct 14 dpi A. euteiches. Mean ±SEM of five replicates with 70-80 roots each. 1-way ANOVA shows significant difference as marked with asterisks.

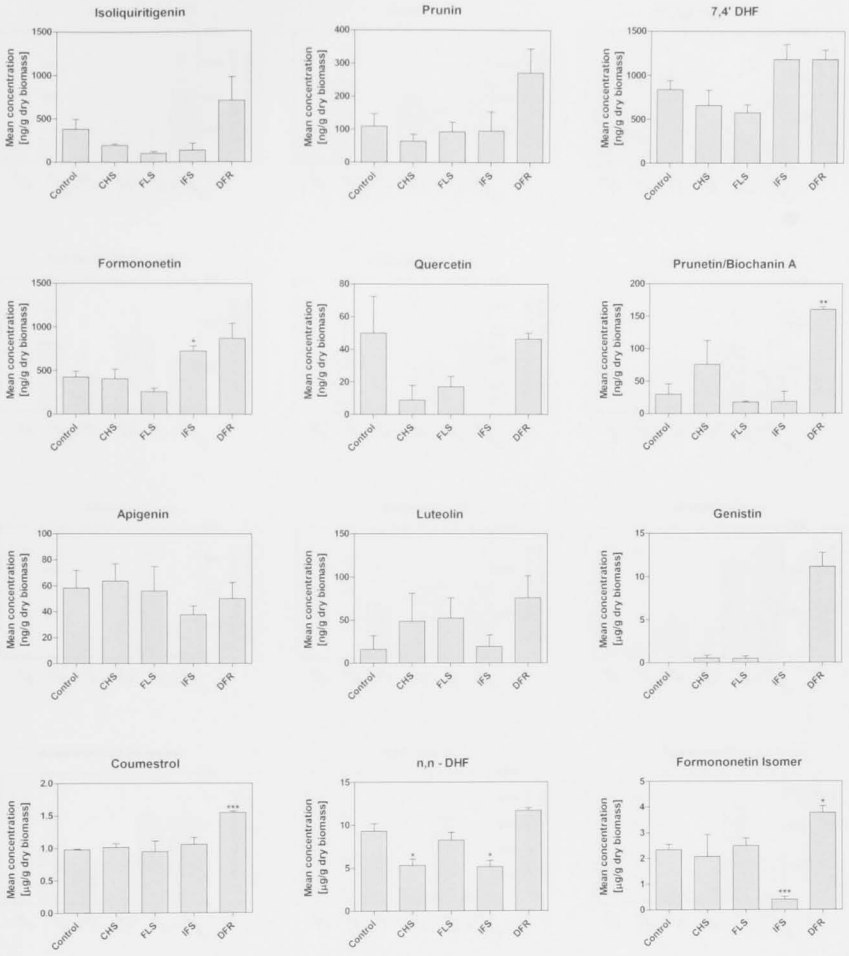

Figure A5.2 – Flavonoid content of roots expressing overexpression construct 14 dpi *A. euteiches.* Mean ±SEM of five replicates with 70-80 roots each. 1-way ANOVA shows significant difference as marked with asterisks.

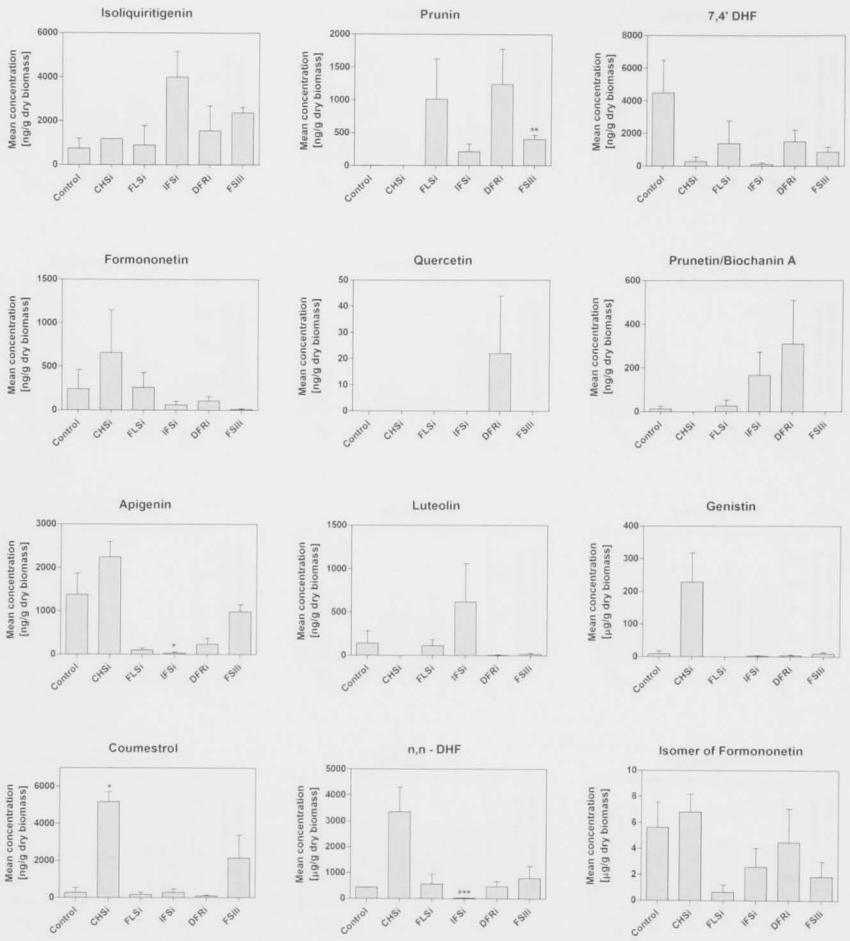

Figure A5.3 – Flavonoid content of roots expressing RNAi construct 14 dpi *R. solani* AG8. Mean ±SEM of five replicates with 70-80 roots each. 1-way ANOVA shows significant difference as marked with asterisks.

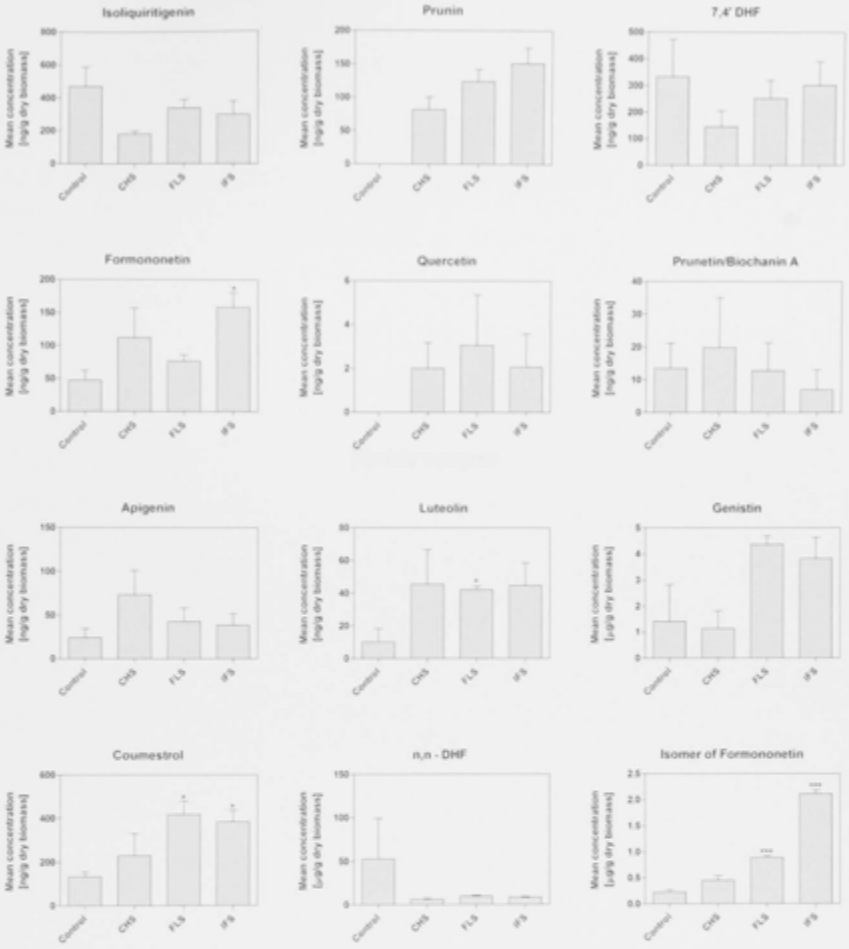

Figure A5.4 – Flavonoid content of roots expressing overexpression construct 14 dpi *R. solani* AG8. Mean ±SEM of five replicates with 70-80 roots each. 1-way ANOVA shows significant difference as marked with asterisks.

References

AGUILAR, J. M. M., ASHBY, A. M., RICHARDS, A. J. M., LOAKE, G. J., WATSON, M. D. & SHAW, C. H. 1988. Chemotaxis of *Rhizobium leguminosarum* Biovar *phaseoli* towards flavonoid inducers of the symbiotic nodulation genes. *Journal of general microbiology,* 134, 2741-2746.

AHUJA, I., KISSEN, R. & BONES, A. M. 2012. Phytoalexins in defense against pathogens. *Trends in Plant Science,* 17, 73-90.

AKIYAMA, K., MATSUOKA, H. & HAYASHI, H. 2002. Isolation and identification of a phosphate deficiency-induced C-glycosylflavonoid that stimulates arbuscular mycorrhiza formation in melon roots. *Molecular Plant-Microbe Interactions,* 15, 334-340.

AKIYAMA, K., TANIGAWA, F., KASHIHARA, T. & HAYASHI, H. 2010. Lupin pyranoisoflavones inhibiting hyphal development in arbuscular mycorrhizal fungi. *Phytochemistry,* 71, 1865-1871.

ALCERITO, T., BARBO, F. E., NEGRI, G., SANTOS, D. Y., MEDA, C. I., YOUNG, M. C. M., CHÁVEZ, D. & BLATT, C. L. T. 2002. Foliar epicuticular wax of *Arrabidaea brachypoda*: flavonoids and antifungal activity. *Biochemical Systematics and Ecology,* 30, 677-683.

ALFORD, E. R., VIVANCO, J. M. & PASCHKE, M. W. 2009. The effects of flavonoid allelochemicals from knapweeds on legume-rhizobia candidates for restoration. *Restoration Ecology,* 17, 506-514.

ALKHALFIOUI, F., RENARD, M., FRENDO, P., KEICHINGER, C., MEYER, Y., GELHAYE, E., HIRASAWA, M., KNAFF, D. B., RITZENTHALER, C. & MONTRICHARD, F. 2008. A novel type of thioredoxin dedicated to symbiosis in legumes. *Plant Physiology,* 148, 424-435.

ANDRIANKAJA, A., BOISSON-DERNIER, A., FRANCES, L., SAUVIAC, L., JAUNEAU, A., BARKER, D. G. & DE CARVALHO-NIEBEL, F. 2007. AP2-ERF transcription factors mediate Nod factor dependent Mt *ENOD11* activation in root hairs via a novel cis-regulatory motif. *Plant Cell,* 19, 2866-85.

ANTUNES, P. M., RAJCAN, I. & GOSS, M. J. 2006. Specific flavonoids as interconnecting signals in the tripartite symbiosis formed by arbuscular mycorrhizal fungi, *Bradyrhizobium japonicum* (Kirchner) Jordan and soybean (*Glycine max* (L.) Merr.). *Soil Biology & Biochemistry,* 38, 533-543.

AOKI, T., AKASHI, T. & AYABE, S. 2000. Flavonoids of leguminous plants: Structure, biological activity, and biosynthesis. *Journal of Plant Research,* 113, 475-488.

ARCAS, M. C., BOTIA, J. M., ORTUNO, A. M. & DEL RIO, J. A. 2000. UV irradiation alters the levels of flavonoids involved in the defence mechanism of *Citrus aurantium* fruits against *Penicillium digitatum*. *European Journal of Plant Pathology,* 106, 617-622.

ARMBRUSTER, D. A. & PRY, T. 2008. Limit of blank, limit of detection and limit of quantitation. *Clinical Biochemists Review,* 29 Suppl 1, S49-52.

ARMERO, J., REQUEJO, R., JORRIN, J., LOPEZ-VALBUENA, R. & TENA, M. 2001. Release of phytoalexins and related isoflavonoids from intact chickpea seedlings elicited with reduced glutathione at root level. *Plant Physiology and Biochemistry,* 39, 785-795.

ARRIGHI, J.-F., GODFROY, O., DE BILLY, F., SAURAT, O., JAUNEAU, A. & GOUGH, C. 2008. The RPG gene of *Medicago truncatula* controls *Rhizobium*-directed polar growth during infection. *Proceedings of the National Academy of Sciences of the United States of America,* 105, 9817-9822.

AUSTIN, M. J., MUSKETT, P., KAHN, K., FEYS, B. J., JONES, J. D. & PARKER, J. E. 2002. Regulatory role of SGT1 in early R gene-mediated plant defenses. *Science,* 295, 2077-2080.

AZEVEDO, C., SADANANDOM, A., KITAGAWA, K., FREIALDENHOVEN, A., SHIRASU, K. & SCHULZE-LEFERT, P. 2002. The RAR1 interactor SGT1, an essential component of R gene-triggered disease resistance. *Science,* 295, 2073-2076.

BADRI, D. V., LOYOLA-VARGAS, V. M., BROECKLING, C. D., DE-LA-PENA, C., JASINSKI, M., SANTELIA, D., MARTINOIA, E., SUMNER, L. W., BANTA, L. M., STERMITZ, F. & VIVANCO, J. M. 2008. Altered profile of secondary metabolites in the root exudates of *Arabidopsis* ATP-binding cassette transporter mutants. *Plant Physiology,* 146, 762-771.

BADRI, D. V., QUINTANA, N., EL KASSIS, E. G., KIM, H. K., CHOI, Y. H., SUGIYAMA, A., VERPOORTE, R., MARTINOIA, E., MANTER, D. K. & VIVANCO, J. M. 2009. An ABC transporter mutation alters root exudation of phytochemicals that provoke an overhaul of natural soil microbiota. *Plant Physiology,* 151, 2006-2017.

BAILLY, A., SOVERO, V., VINCENZETTI, V., SANTELIA, D., BARTNIK, D., KOENIG, B. W., MANCUSO, S., MARTINOIA, E. & GEISLER, M. 2008. Modulation of P-glycoproteins by auxin transport inhibitors is mediated by interaction with immunophilins. *Journal of Biological Chemistry,* 283, 21817-21826.

BAIS, H. P., VEPACHEDU, R., GILROY, S., CALLAWAY, R. M. & VIVANCO, J. M. 2003. Allelopathy and exotic plant invasion: From molecules and genes to species interactions. *Science,* 301, 1377-1380.

BAJGUZ, A. & PIOTROWSKA, A. 2009. Conjugates of auxin and cytokinin. *Phytochemistry,* 70, 957-969.

BANASIAK, J., BIALA, W., STASZKOW, A., SWARCEWICZ, B., KEPCZYNSKA, E., FIGLEROWICZ, M. & JASINSKI, M. 2013. A *Medicago truncatula* ABC transporter belonging to subfamily G modulates the level of isoflavonoids. *Journal of Experimental Botany,* 64, 1005-15.

BANDURSKI, R. S. & SCHULZE, A. 1977. Concentration of indole-3-acetic acid and its derivatives in plants. *Plant Physiology,* 60, 211-3.

BARNETT, M. J., TOMAN, C. J., FISHER, R. F. & LONG, S. R. 2004. A dual-genome Symbiosis Chip for coordinate study of signal exchange and development in a prokaryote–host interaction. *Proceedings of the National Academy of Sciences of the United States of America,* 101, 16636-16641.

BAUDRY, A., CABOCHE, M. & LEPINIEC, L. 2006. TT8 controls its own expression in a feedback regulation involving TTG1 and homologous MYB and bHLH factors, allowing a strong and cell-specific accumulation of flavonoids in *Arabidopsis thaliana*. *The Plant Journal,* 46, 768-779.

BECANA, M., DALTON, D. A., MORAN, J. F., ITURBE-ORMAETXE, I., MATAMOROS, M. A. & C RUBIO, M. 2000. Reactive oxygen species and antioxidants in legume nodules. *Physiologia Plantarum,* 109, 372-381.

BÉCARD, G., TAYLOR, L. P., DOUDS, D., PFEFFER, P. E. & DONER, L. W. 1995. Flavonoids are not necessary plant signal compounds in arbuscular mycorrhizal symbioses. *Molecular Plant-Microbe Interactions,* 8, 252-258.

BECKMAN, C. H. 2000. Phenolic-storing cells: keys to programmed cell death and periderm formation in wilt disease resistance and in general defence responses in plants? *Physiological and Molecular Plant Pathology,* 57, 101-110.

BEGUM, A. A., LEIBOVITCH, S., MIGNER, P. & ZHANG, F. 2001. Specific flavonoids induced *nod* gene expression and pre-activated *nod* genes of *Rhizobium leguminosarum* increased pea (*Pisum sativum* L.) and lentil (*Lens culinaris* L.) nodulation in controlled growth chamber environments. *Journal of Experimental Botany,* 52, 1537-1543.

BENJAMINI, Y. & YEKUTIELI, D. 2001. The control of the false discovery rate in multiple testing under dependency. *Annals of Statistics,* 29, 1165-1188.

BENKOVÁ, E., MICHNIEWICZ, M., SAUER, M., TEICHMANN, T., SEIFERTOVÁ, D., JÜRGENS, G. & FRIML, J. 2003. Local, efflux-dependent auxin gradients as a common module for plant organ formation. *Cell,* 115, 591-602.

BENOIT, L. F. & BERRY, A. M. 1997. Flavonoid-like compounds from seeds of red alder (*Alnus rubra*) influence host nodulation by *Frankia* (Actinomycetales). *Physiologia Plantarum,* 99, 588-593.

BESSEAU, S., HOFFMANN, L., GEOFFROY, P., LAPIERRE, C., POLLET, B. & LEGRAND, M. 2007. Flavonoid accumulation in *Arabidopsis* repressed in lignin synthesis affects auxin transport and plant growth. *Plant Cell,* 19, 148-162.

BHALERAO, R. P., EKLÖF, J., LJUNG, K., MARCHANT, A., BENNETT, M. & SANDBERG, G. 2002. Shoot-derived auxin is essential for early lateral root emergence in *Arabidopsis* seedlings. *The Plant Journal,* 29, 325-332.

BIMBOIM, H. C. & DOLY, J. 1979. A rapid alkaline extraction procedure for screening recombinant plasmid DNA. *Nucleic Acids Research,* 7, 1513-1523.

BLAIR, A. C., HANSON, B. D., BRUNK, G. R., MARRS, R. A., WESTRA, P., NISSEN, S. J. & HUFBAUER, R. A. 2005. New techniques and findings in the study of a candidate allelochemical implicated in invasion success. *Ecology Letters,* 8, 1039-1047.

BLANC, G. & WOLFE, K. H. 2004. Widespread paleopolyploidy in model plant species inferred from age distributions of duplicate genes. *Plant Cell,* 16, 1667-78.

BLOUNT, J. W., DIXON, R. A. & PAIVA, N. L. 1992. Stress responses in alfalfa (*Medicago sativa* L) XVI. Antifungal activity of medicarpin and its biosynthetic precursors - implications for the genetic manipulation of stress metabolites. *Physiological and Molecular Plant Pathology,* 41, 333-349.

BODINI, S. F., MANFREDINI, S., EPP, M., VALENTINI, S. & SANTORI, F. 2009. Quorum sensing inhibition activity of garlic extract and p-coumaric acid. *Letters in Applied Microbiology,* 49, 551-555.

BOISSON-DERNIER, A., CHABAUD, M., GARCIA, F., BÉCARD, G., ROSENBERG, C. & BARKER, D. G. 2001. *Agrobacterium rhizogenes*-transformed roots of Medicago truncatula for the study of nitrogen-fixing and endomycorrhizal symbiotic associations. *Molecular Plant-Microbe Interactions,* 14, 695-700.

BOLANOS-VASQUEZ, M. C. & WARNER, D. 1997. Effects of *Rhizobium tropici*, *R. etli*, and *R. leguminosarum* bv *phaseoli* on *nod* gene-inducing flavonoids in root exudates of *Phaseolus vulgaris*. *Molecular Plant-Microbe Interactions,* 10, 339-346.

BOOT, K. J. M., VAN BRUSSEL, A. A. N., TAK, T., SPAINK, H. P. & KIJNE, J. W. 1999. Lipochitin oligosaccharides from *Rhizobium leguminosarum* bv. viciae reduce auxin transport capacity in *Vicia sativa* subsp *nigra* roots. *Molecular Plant-Microbe Interactions,* 12, 839-844.

BOROWICZ, V. A. 2001. Do arbuscular mycorrhizal fungi alter plant-pathogen relations? *Ecology,* 82, 3057-3068.

BOUCHÉ, N. & BOUCHEZ, D. 2001. *Arabidopsis* gene knockout: phenotypes wanted. *Current Opinion in Plant Biology,* 4, 111-117.

BROWN, D. E., RASHOTTE, A. M., MURPHY, A. S., NORMANLY, J., TAGUE, B. W., PEER, W. A., TAIZ, L. & MUDAY, G. K. 2001. Flavonoids act as negative regulators of auxin transport in vivo in *Arabidopsis. Plant Physiology,* 126, 524-535.

BUER, C. S. & DJORDJEVIC, M. A. 2009. Architectural phenotypes in the *transparent testa* mutants of *Arabidopsis thaliana. Journal of Experimental Botany,* 60, 751-763.

BUER, C. S. & MUDAY, G. K. 2004. The *transparent testa4* mutation prevents flavonoid synthesis and alters auxin transport and the response of *Arabidopsis* roots to gravity and light. *Plant Cell,* 16, 1191-1205.

BUER, C. S., MUDAY, G. K. & DJORDJEVIC, M. A. 2007. Flavonoids are differentially taken up and transported long distances in *Arabidopsis. Plant Physiology,* 145, 478-490.

BUTELLI, E., TITTA, L., GIORGIO, M., MOCK, H. P., MATROS, A., PETEREK, S., SCHIJLEN, E. G. W. M., HALL, R. D., BOVY, A. G., LUO, J. & MARTIN, C. 2008. Enrichment of tomato fruit with health-promoting anthocyanins by expression of select transcription factors. *Nature Biotechnology,* 26, 1301-1308.

CABALLERO, P., SMITH, C. M., FRONCZEK, F. R. & FISCHER, N. H. 1986. Isoflavones from an insect-resistant variety of soybean and the molecular structure of afrormosin. *Journal of Natural Products,* 49, 1126-1129.

CANNON, S. B., STERCK, L., ROMBAUTS, S., SATO, S., CHEUNG, F., GOUZY, J., WANG, X., MUDGE, J., VASDEWANI, J. & SCHIEX, T. 2006. Legume genome evolution viewed through the *Medicago truncatula* and *Lotus japonicus* genomes. *Proceedings of the National Academy of Sciences of the United States of America,* 103, 14959-14964.

CAO, G., SOFIC, E. & PRIOR, R. L. 1997. Antioxidant and prooxidant behavior of flavonoids: structure-activity relationships. *Free Radical Biology and Medicine,* 22, 749-760.

CÁRDENAS, L., MARTÍNEZ, A., SÁNCHEZ, F. & QUINTO, C. 2008. Fast, transient and specific intracellular ROS changes in living root hair cells responding to Nod factors (NFs). *The Plant Journal,* 56, 802-813.

CÁRDENAS, L., VIDALI, L., DOMíNGUEZ, J., PÉREZ, H., SÁNCHEZ, F., HEPLER, P. K. & QUINTO, C. 1998. Rearrangement of actin microfilaments in plant root hairs responding to *Rhizobium etli* nodulation signals. *Plant Physiology,* 116, 871-877.

CARLING, D. & SUMNER, D. 1992. *Rhizoctonia. In:* SINGLETON, L. L., MIHAIL, J. D. & RUSH, C. M. (eds.) *Methods for research on soilborne phytopathogenic fungi.* Minnesota: APS Press.

CARLSEN, S. C. K., UNDERSTRUP, A., FOMSGAARD, I. S., MORTENSEN, A. G. & RAVNSKOV, S. 2008. Flavonoids in roots of white clover: interaction of arbuscular mycorrhizal fungi and a pathogenic fungus. *Plant and Soil,* 302, 33-43.

CATFORD, J. G., STAEHELIN, C., LAROSE, G., PICHE, Y. & VIERHEILIG, H. 2006. Systemically suppressed isoflavonoids and their stimulating effects on nodulation and mycorrhization in alfalfa split-root systems. *Plant and Soil,* 285, 257-266.

CESCO, S., NEUMANN, G., TOMASI, N., PINTON, R. & WEISSKOPF, L. 2010. Release of plant-borne flavonoids into the rhizosphere and their role in plant nutrition. *Plant and Soil,* 329, 1-25.

CHENG, H. P. & WALKER, G. C. 1998. Succinoglycan is required for initiation and elongation of infection threads during nodulation of alfalfa by *Rhizobium meliloti*. *Journal of Bacteriology,* 180, 5183-91.

COELHO, S. M., TAYLOR, A. R., RYAN, K. P., SOUSA-PINTO, I., BROWN, M. T. & BROWNLEE, C. 2002. Spatiotemporal patterning of reactive oxygen production and Ca^{2+} wave propagation in fucus rhizoid cells. *Plant Cell,* 14, 2369-2381.

COMBIER, J.-P., FRUGIER, F., DE BILLY, F., BOUALEM, A., EL-YAHYAOUI, F., MOREAU, S., VERNIÉ, T., OTT, T., GAMAS, P., CRESPI, M. & NIEBEL, A. 2006. *MtHAP2-1* is a key transcriptional regulator of symbiotic nodule development regulated by microRNA169 in *Medicago truncatula*. *Genes & Development,* 20, 3084-3088.

COOK, D., DREYER, D., BONNET, D., HOWELL, M., NONY, E. & VANDENBOSCH, K. 1995. Transient induction of a peroxidase gene in *Medicago truncatula* precedes infection by *Rhizobium meliloti*. *Plant Cell,* 7, 43-55.

COOPER, J. B. & LONG, S. R. 1994. Morphogenetic rescue of *Rhizobium meliloti* nodulation mutants by trans-zeatin secretion. *Plant Cell,* 6, 215-225.

COOPER, J. E. 2004. Multiple responses of rhizobia to flavonoids during legume root infection. *In:* CALLOW, J. A. (ed.) *Advances in Botanical Research.* Academic Press.

CORDIER, C., POZO, M. J., BAREA, J. M., GIANINAZZI, S. & GIANINAZZI-PEARSON, V. 1998. Cell defense responses associated with localized and systemic resistance to *Phytophthora parasitica* induced in tomato by an arbuscular mycorrhizal fungus. *Molecular Plant-Microbe Interactions,* 11, 1017-1028.

CORONADO, C., ZUANAZZI, J. A. S., SALLAUD, C., QUIRION, J.-C., ESNAULT, R., HUSSON, H.-P., KONDOROSI, A. & RATET, P. 1995. Alfalfa root flavonoid production is nitrogen regulated. *Plant Physiology,* 108, 533-542.

CURIR, P., DOLCI, M. & GALEOTTI, F. 2005. A phytoalexin-like flavonol involved in the carnation (*Dianthus caryophyllus*)-*Fusarium oxysporum* f. sp *dianthi* pathosystem. *Journal of Phytopathology,* 153, 65-67.

CUSHNIE, T. P. T. & LAMB, A. J. 2005. Antimicrobial activity of flavonoids. *International Journal of Antimicrobial Agents,* 26, 343-356.

CUSHNIE, T. P. T. & LAMB, A. J. 2011. Recent advances in understanding the antibacterial properties of flavonoids. *International Journal of Antimicrobial Agents,* 38, 99-107.

DAKORA, F. D. 1995. Plant flavonoids - Biological molecules for useful exploitation. *Australian Journal of Plant Physiology,* 22, 87-99.

DAKORA, F. D., JOSEPH, C. M. & PHILLIPS, D. A. 1993. Common bean root exudates contain elevated levels of daidzein and coumestrol in response to *Rhizobium* inoculation. *Molecular Plant-Microbe Interactions,* 6, 665-668.

DEBEAUJON, I., LÉON-KLOOSTERZIEL, K. M. & KOORNNEEF, M. 2000. Influence of the testa on seed dormancy, germination, and longevity in *Arabidopsis*. *Plant Physiology,* 122, 403-414.

DEHNE, H. 1979. The influence of endotrophic mycorrhiza on plant diseases. II. Phenol metabolism and lignification. *Journal of Phytopathology,* 95, 210-216.

DEINUM, E. E., GEURTS, R., BISSELING, T. & MULDER, B. M. 2012. Modeling a cortical auxin maximum for nodulation: different signatures of potential strategies. *Frontiers in plant science,* 3, 96.

DENNY, T. P. & VANETTEN, H. D. 1981. Tolerance by *Nectria haematococca* MP-VI of the chickpea (*Cicer-Arietinum*) phytoalexins medicarpin and maackiain. *Physiological Plant Pathology,* 19, 419-437.

DENNY, T. P. & VANETTEN, H. D. 1982. Metabolism of the phytoalexins medicarpin and maackiain by *Fusarium solani. Phytochemistry,* 21, 1023-1028.

DESBROSSES, G. J. & STOUGAARD, J. 2011. Root nodulation: a paradigm for how plant-microbe symbiosis influences host developmental pathways. *Cell host & microbe,* 10, 348-358.

DHARMATILAKE, A. J. & BAUER, W. D. 1992. Chemotaxis of *Rhizobium meliloti* towards nodulation gene-inducing compounds from alfalfa roots. *Applied and Environmental Microbiology,* 58, 1153-1158.

DING, Y. L., KALO, P., YENDREK, C., SUN, J. H., LIANG, Y., MARSH, J. F., HARRIS, J. M. & OLDROYD, G. E. D. 2008. Abscisic acid coordinates Nod factor and cytokinin signaling during the regulation of nodulation in *Medicago truncatula. Plant Cell,* 20, 2681-2695.

DIXON, R. A. 2001. Natural products and plant disease resistance. *Nature,* 411, 843-7.

DIXON, R. A. & PAIVA, N. L. 1995. Stress-induced phenylpropanoid metabolism. *Plant Cell,* 7, 1085-1097.

DIXON, R. A. & STEELE, C. L. 1999. Flavonoids and isoflavonoids - a gold mine for metabolic engineering. *Trends in Plant Science,* 4, 394-400.

DJÉBALI, N., ARIBI, S., TAAMALLI, W., ARRAOUADI, S., AOUANI, M. & BADRI, M. 2013. Natural variation of *Medicago truncatula* resistance to *Aphanomyces euteiches. European Journal of Plant Pathology,* 135, 831-843.

DJÉBALI, N., JAUNEAU, A., AMELINE-TORREGROSA, C., CHARDON, F., JAULNEAU, V., MATHÉ, C., BOTTIN, A., CAZAUX, M., PILET-NAYEL, M.-L. & BARANGER, A. 2009. Partial resistance of *Medicago truncatula* to *Aphanomyces euteiches* is associated with protection of the root stele and is controlled by a major QTL rich in proteasome-related genes. *Molecular Plant-Microbe Interactions,* 22, 1043-1055.

DJORDJEVIC, M. A., MATHESIUS, U., SCHLAMAN, H. R. M., SPAINK, H. P., SAUTTER, C. & ROLFE, B. G. 1998. Auxin transport inhibition precedes root nodule formation in white clover roots and is regulated by flavonoids and derivatives of chitin oligosaccharides. *The Plant Journal,* 14, 23-34.

DJORDJEVIC, M. A., REDMOND, J. W., BATLEY, M. & ROLFE, B. G. 1987. Clovers secrete specific phenolic-compounds which either stimulate or repress *nod* gene expression in *Rhizobium trifolii. EMBO Journal,* 6, 1173-1179.

DU, Z., ZHOU, X., LING, Y., ZHANG, Z. & SU, Z. 2010. agriGO: a GO analysis toolkit for the agricultural community. *Nucleic Acids Research,* 38, W64-70.

DUKE, S. O., BLAIR, A. C., DAYAN, F. E., JOHNSON, R. D., MEEPAGALA, K. M., COOK, D. & BAJSA, J. 2009. Is (-)-catechin a novel weapon of spotted knapweed (*Centaurea stoebe*)? *Journal of Chemical Ecology,* 35, 141-153.

DUNN, M. F., PUEPPKE, S. G. & KRISHNAN, H. B. 1992. The *nod* gene inducer genistein alters the composition and molecular mass distribution of extracellular polysaccharides produced by *Rhizobium fredii* USDA193. *FEMS microbiology letters,* 97, 107-112.

ERLEJMAN, A. G., VERSTRAETEN, S. V., FRAGA, C. G. & OTEIZA, P. I. 2004. The interaction of flavonoids with membranes: Potential determinant of flavonoid antioxidant effects. *Free Radical Research,* 38, 1311-1320.

FÅHRAEUS, G. 1957. The infection of clover root hairs by nodule bacteria studied by a simple glass slide technique. *Journal of general microbiology,* 16, 374-381.

FARAG, M. A., HUHMAN, D. V., DIXON, R. A. & SUMNER, L. W. 2008. Metabolomics reveals novel pathways and differential mechanistic and elicitor-specific responses in phenylpropanoid and isoflavonoid biosynthesis in *Medicago truncatula* cell cultures. *Plant Physiology,* 146, 387-402.

FERGUSON, B. J., FOO, E., ROSS, J. J. & REID, J. B. 2011. Relationship between gibberellin, ethylene and nodulation in *Pisum sativum*. *New Phytologist,* 189, 829-842.

FERGUSON, B. J., INDRASUMUNAR, A., HAYASHI, S., LIN, M. H., LIN, Y. H., REID, D. E. & GRESSHOFF, P. M. 2010. Molecular analysis of legume nodule development and autoregulation. *Journal of Integrative Plant Biology,* 52, 61-76.

FERGUSON, B. J. & MATHESIUS, U. 2014. Phytohormone regulation of legume-rhizobia interactions. *Journal of Chemical Ecology,* 40, 770-90.

FERRER, J. L., AUSTIN, M. B., STEWART, C. & NOE, J. P. 2008. Structure and function of enzymes involved in the biosynthesis of phenylpropanoids. *Plant Physiology and Biochemistry,* 46, 356-370.

FOO, E. & DAVIES, N. 2011. Strigolactones promote nodulation in pea. *Planta,* 234, 1073-1081.

FOREMAN, J., DEMIDCHIK, V., BOTHWELL, J. H., MYLONA, P., MIEDEMA, H., TORRES, M. A., LINSTEAD, P., COSTA, S., BROWNLEE, C., JONES, J. D., DAVIES, J. M. & DOLAN, L. 2003. Reactive oxygen species produced by NADPH oxidase regulate plant cell growth. *Nature,* 422, 442-6.

FOWLER, Z. L. & KOFFAS, M. A. G. 2009. Biosynthesis and biotechnological production of flavanones: current state and perspectives. *Applied Microbiology and Biotechnology,* 83, 799-808.

FRIEDERICH, S., RUEFFER, M., ASAKAWA, Y. & ZENK, M. H. 1999. Cytochromes P-450 catalyze the formation of marchantins A and C in *Marchantia polymorpha*. *Phytochemistry,* 52, 1195-1202.

FRUGIER, F., KOSUTA, S., MURRAY, J. D., CRESPI, M. & SZCZYGLOWSKI, K. 2008. Cytokinin: secret agent of symbiosis. *Trends in Plant Science,* 13, 115-120.

FUQUA, C., PARSEK, M. R. & GREENBERG, E. P. 2001. Regulation of gene expression by cell-to-cell communication: Acyl-homoserine lactone quorum sensing. *Annual Review of Genetics,* 35, 439-468.

FUQUA, W. C., WINANS, S. C. & GREENBERG, E. P. 1994. Quorum sensing in bacteria: the LuxR-LuxI family of cell density-responsive transcriptional regulators. *Journal of bacteriology,* 176, 269-75.

GAO, M. S., TEPLITSKI, M., ROBINSON, J. B. & BAUER, W. D. 2003. Production of substances by *Medicago truncatula* that affect bacterial quorum sensing. *Molecular Plant-Microbe Interactions,* 16, 827-834.

GAULIN, E., JACQUET, C., BOTTIN, A. & DUMAS, B. 2007. Root rot disease of legumes caused by *Aphanomyces euteiches*. *Molecular Plant Pathology,* 8, 539-548.

GELDNER, N., FRIML, J., STIERHOF, Y.-D., JUÈRGENS, G. & PALME, K. 2001. Auxin transport inhibitors block PIN1 cycling and vesicle trafficking. *Nature,* 413, 425-428.

GHEYSEN, G. & MITCHUM, M. G. 2011. How nematodes manipulate plant development pathways for infection. *Current Opinion in Plant Biology,* 14, 415-421.

GIANNINI, J. L., BRISKIN, D. P., HOLT, J. S. & PAXTON, J. D. 1988. Inhibition of plasma membrane and tonoplast H+-transporting ATPases by glyceollin. *Phytopathology,* 78, 1000-1003.

GILL, S. S. & TUTEJA, N. 2010. Reactive oxygen species and antioxidant machinery in abiotic stress tolerance in crop plants. *Plant Physiology and Biochemistry,* 48, 909-930.

GLYAN'KO, A. & VASIL'EVA, G. 2010. Reactive oxygen and nitrogen species in legume-rhizobial symbiosis: a review. *Applied biochemistry and microbiology,* 46, 15-22.

GNANAMANICKAM, S. S. 1979. Isolation of isoflavonoid phytoalexins from seeds of *Phaseolus vulgaris* L. *Experientia,* 35, 323-323.

GOMEZ-ROLDAN, V., FERMAS, S., BREWER, P. B., PUECH-PAGES, V., DUN, E. A., PILLOT, J. P., LETISSE, F., MATUSOVA, R., DANOUN, S., PORTAIS, J. C., BOUWMEESTER, H., BECARD, G., BEVERIDGE, C. A., RAMEAU, C. & ROCHANGE, S. F. 2008. Strigolactone inhibition of shoot branching. *Nature,* 455, 189-94.

GONZÁLEZ-GUERRERO, M., MATTHIADIS, A., SÁEZ, Á. & LONG, T. A. 2014. Fixating on metals: new insights into the role of metals in nodulation and symbiotic nitrogen fixation. *Frontiers in plant science,* 5, 45.

GONZALEZ-RIZZO, S., CRESPI, M. & FRUGIER, F. 2006. The *Medicago truncatula* CRE1 cytokinin receptor regulates lateral root development and early symbiotic interaction with *Sinorhizobium meliloti*. *Plant Cell,* 18, 2680-2693.

GONZALEZ, J. E. & MARKETON, M. M. 2003. Quorum sensing in nitrogen-fixing rhizobia. *Microbiology and Molecular Biology Reviews,* 67, 574-+.

GOODMAN, C. D., CASATI, P. & WALBOT, V. 2004. A multidrug resistance-associated protein involved in anthocyanin transport in *Zea mays*. *Plant Cell,* 16, 1812-26.

GOVERSE, A., ENGLER, J. D., VERHEES, J., VAN DER KROL, S., HELDER, J. & GHEYSEN, G. 2000. Cell cycle activation by plant parasitic nematodes. *Plant Molecular Biology,* 43, 747-761.

GRAHAM, T. L. 1991. Flavonoid and isoflavonoid distribution in developing soybean seedling tissues and in seed and root exudates. *Plant Physiology,* 95, 594-603.

GRAHAM, T. L., GRAHAM, M. Y., SUBRAMANIAN, S. & YU, O. 2007. RNAi silencing of genes for elicitation or biosynthesis of 5-deoxyisoflavonoids suppresses race-specific resistance and hypersensitive cell death in *Pytophthora sojae* infected tissues. *Plant Physiology,* 144, 728-740.

GRAVEL, V., ANTOUN, H. & TWEDDELL, R. J. 2007. Effect of indole-acetic acid (IAA) on the development of symptoms caused by *Pythium ultimum* on tomato plants. *European journal of plant pathology,* 119, 457-462.

GRAYER, R. J. & HARBORNE, J. B. 1994. A survey of antifungal compounds from higher plants, 1982–1993. *Phytochemistry,* 37, 19-42.

GRESSEL, J., HANAFI, A., HEAD, G., MARASAS, W., OBILANA, B., OCHANDA, J., SOUISSI, T. & TZOTZOS, G. 2004. Major heretofore intractable biotic constraints to African food security that may be amenable to novel biotechnological solutions. *Crop Protection,* 23, 661-689.

GROTEWOLD, E. 2006. *The science of flavonoids,* New York, Springer.

GROTEWOLD, E. 2008. Transcription factors for predictive plant metabolic engineering: are we there yet? *Current opinion in biotechnology,* 19, 138-144.

GRUNEWALD, W., VAN NOORDEN, G., VAN ISTERDAEL, G., BEECKMAN, T., GHEYSEN, G. & MATHESIUS, U. 2009. Manipulation of auxin transport in plant roots during *Rhizobium* symbiosis and nematode parasitism. *Plant Cell,* 21, 2553-2562.

GUENOUNE, D., GALILI, S., PHILLIPS, D. A., VOLPIN, H., CHET, I., OKON, Y. & KAPULNIK, Y. 2001. The defense response elicited by the pathogen *Rhizoctonia solani* is suppressed by colonization of the AM-fungus *Glomus intraradices. Plant Science,* 160, 925-932.

GUERREIRO, N., REDMOND, J. W., ROLFE, B. G. & DJORDJEVIC, M. A. 1997. New *Rhizobium leguminosarum* flavonoid-induced proteins revealed by proteome analysis of differentially displayed proteins. *Molecular Plant-Microbe Interactions,* 10, 506-516.

HAGEN, G., MARTIN, G., LI, Y. & GUILFOYLE, T. J. 1991. Auxin-induced expression of the soybean GH3 promoter in transgenic tobacco plants. *Plant Molecular Biology,* 17, 567-579.

HAIN, R., REIF, H. J., KRAUSE, E., LANGEBARTELS, R., KINDL, H., VORNAM, B., WIESE, W., SCHMELZER, E., SCHREIER, P. H., STOCKER, R. H. & STENZEL, K. 1993. Disease resistance results from foreign phytoalexin expression in a novel plant. *Nature,* 361, 153-156.

HANAHAN, D. & GLOVER, D. M. 1985. DNA cloning: a practical approach. *DNA cloning: a practical approach,* 1, 109-135.

HANE, J. K., ANDERSON, J. P., WILLIAMS, A. H., SPERSCHNEIDER, J. & SINGH, K. B. 2014. Genome sequencing and comparative genomics of the broad host-range pathogen *Rhizoctonia solani* AG8. *PLoS Genetics,* 10, e1004281.

HARRISON, M. J. 2005. Signaling in the arbuscular mycorrhizal symbiosis. *Annual review of microbiology,* 59, 19-42.

HARRISON, M. J. & DIXON, R. A. 1993. Isoflavonoid accumulation and expression of defense gene transcripts during the establishment of vesicular-arbuscular mycorrhizal associations in roots of *Medicago truncatula. Molecular Plant-Microbe Interactions,* 6, 643-654.

HARRISON, M. J. & DIXON, R. A. 1994. Spatial patterns of expression of flavonoid/isoflavonoid pathway genes during interactions between roots of *Medicago truncatula* and the mycorrhizal fungus *Glomus versiforme. The Plant Journal,* 6, 9-20.

HAWES, M. C., BRIGHAM, L. A., WEN, F., WOO, H. H. & ZHU, Z. 1998. Function of root border cells in plant health: Pioneers in the rhizosphere. *Annual Review of Phytopathology,* 36, 311-327.

HAYASHI, S., GRESSHOFF, P. M. & FERGUSON, B. J. 2014. Mechanistic action of gibberellins in legume nodulation. *Journal of Integrative Plant Biology.*

HAYASHI, S., REID, D. E., LORENC, M. T., STILLER, J., EDWARDS, D., GRESSHOFF, P. M. & FERGUSON, B. J. 2012. Transient Nod factor-dependent gene expression in the nodulation-competent zone of soybean (*Glycine max* [L.] *Merr.*) roots. *Plant biotechnology journal,* 10, 995-1010.

HAYASHI, T., BANBA, M., SHIMODA, Y., KOUCHI, H., HAYASHI, M. & IMAIZUMI-ANRAKU, H. 2010. A dominant function of CCaMK in intracellular accommodation of bacterial and fungal endosymbionts. *The Plant Journal,* 63, 141-154.

HEATH, M. C. 2000. Hypersensitive response-related death. *Plant Molecular Biology,* 44, 321-321-34.

HEIM, K. E., TAGLIAFERRO, A. R. & BOBILYA, D. J. 2002. Flavonoid antioxidants: chemistry, metabolism and structure-activity relationships. *Journal of Nutritional Biochemistry,* 13, 572-584.

HELLIWELL, C. A., WESLEY, S. V., WIELOPOLSKA, A. J. & WATERHOUSE, P. M. 2002. High-throughput vectors for efficient gene silencing in plants. *Functional Plant Biology,* 29, 1217-1225.

HERNÁNDEZ, I., ALEGRE, L., VAN BREUSEGEM, F. & MUNNÉ-BOSCH, S. 2009. How relevant are flavonoids as antioxidants in plants? *Trends in Plant Science,* 14, 125-132.

HERNÁNDEZ, I. & VAN BREUSEGEM, F. 2010. Opinion on the possible role of flavonoids as energy escape valves: Novel tools for nature's Swiss army knife? *Plant Science,* 179, 297-301.

HÉROUART, D., BAUDOUIN, E., FRENDO, P., HARRISON, J., SANTOS, R., JAMET, A., VAN DE SYPE, G., TOUATI, D. & PUPPO, A. 2002. Reactive oxygen species, nitric oxide and glutathione: a key role in the establishment of the legume– *Rhizobium* symbiosis? *Plant Physiology and Biochemistry,* 40, 619-624.

HICHRI, I., BARRIEU, F., BOGS, J., KAPPEL, C., DELROT, S. & LAUVERGEAT, V. 2011. Recent advances in the transcriptional regulation of the flavonoid biosynthetic pathway. *Journal of Experimental Botany,* 62, erq442.

HIGGINS, V. J. 1978. The effect of some pterocarpanoid phytoalexins on germ tube elongation of *Stemphylium botryosum*. *Phytopathology,* 68, 339-345.

HIPSKIND, J. D. & PAIVA, N. L. 2000. Constitutive accumulation of a resveratrol-glucoside in transgenic alfalfa increases resistance to *Phoma medicaginis*. *Molecular Plant-Microbe Interactions,* 13, 551-562.

HIRATA, Y., FUNATO, Y., TAKANO, Y. & MIKI, H. 2014. Mg^{2+}-dependent Interactions of ATP with the cystathionine-β-synthase (CBS) domains of a magnesium transporter. *Journal of Biological Chemistry,* 289, 14731-14739.

HIRSCH, A. M., BHUVANESWARI, T. V., TORREY, J. G. & BISSELING, T. 1989. Early nodulin genes are induced in alfalfa root outgrowths elicited by auxin transport inhibitors. *Proceedings of the National Academy of Sciences of the United States of America,* 86, 1244-8.

HIRSCH, S., KIM, J., MUNOZ, A., HECKMANN, A. B., DOWNIE, J. A. & OLDROYD, G. E. D. 2009. GRAS proteins form a DNA binding complex to induce gene expression during nodulation signaling in *Medicago truncatula*. *Plant Cell,* 21, 545-557.

HOLSTERS, M., DEWAELE, D., DEPICKER, A., MESSENS, E., VANMONTAGU, M. & SCHELL, J. 1978. Transfection and transformation of *Agrobacterium tumefaciens*. *Molecular and General Genetics,* 163, 181-187.

HOOPER, A. M., HASSANALI, A., CHAMBERLAIN, K., KHAN, Z. & PICKETT, J. A. 2009. New genetic opportunities from legume intercrops for controlling *Striga* spp. parasitic weeds. *Pest Management Science,* 65, 546-552.

HOOPER, A. M., TSANUO, M. K., CHAMBERLAIN, K., TITTCOMB, K., SCHOLES, J., HASSANALI, A., KHAN, Z. R. & PICKETT, J. A. 2010. Isoschaftoside, a C-glycosylflavonoid from *Desmodium uncinatum* root exudate, is an allelochemical against the development of *Striga*. *Phytochemistry,* 71, 904-908.

HÜBERLI, D., CONNOR, M., MIYAN, S., MACLEOD, W., DESBIOLLES, J., BOGACKI, P. & MCKAY, A. 2013. Integrated disease management options to control rhizoctonia

bare-patch in cereals. *2013 Agribusiness Crop Updates.* Perth, Australia: Department of Agriculture and Food.

HUNGRIA, M., JOSEPH, C. M. & PHILLIPS, D. A. 1991. Anthocyanidins and flavonols, major *nod* gene inducers from seeds of a black-seeded common bean (*Phaseolus vulgaris* L.). *Plant Physiology,* 97, 751-758.

HUNTER, W. J. 1993. Ethylene production by root-nodules and effect of ethylene on nodulation in *Glycine Max*. *Applied and Environmental Microbiology,* 59, 1947-1950.

HUTANGURA, P., MATHESIUS, U., JONES, M. G. K. & ROLFE, B. G. 1999. Auxin induction is a trigger for root gall formation caused by root-knot nematodes in white clover and is associated with the activation of the flavonoid pathway. *Australian Journal of Plant Physiology,* 26, 221-231.

HUTZLER, P., FISCHBACH, R., HELLER, W., JUNGBLUT, T. P., REUBER, S., SCHMITZ, R., VEIT, M., WEISSENBOCK, G. & SCHNITZLER, J. P. 1998. Tissue localization of phenolic compounds in plants by confocal laser scanning microscopy. *Journal of Experimental Botany,* 49, 953-965.

INGHAM, J. L. 1976. Fungal modification of pterocarpan phytoalexins from *Melilotus alba* and *Trifolium pratense*. *Phytochemistry,* 15, 1489-1495.

IVASHUTA, S., LIU, J., LIU, J., LOHAR, D. P., HARIDAS, S., BUCCIARELLI, B., VANDENBOSCH, K. A., VANCE, C. P., HARRISON, M. J. & GANTT, J. S. 2005. RNA interference identifies a calcium-dependent protein kinase involved in *Medicago truncatula* root development. *Plant Cell,* 17, 2911-21.

JACOBS, M. & RUBERY, P. H. 1988. Naturally-occurring auxin transport regulators. *Science,* 241, 346-349.

JASIŃSKI, M., KACHLICKI, P., RODZIEWICZ, P., FIGLEROWICZ, M. & STOBIECKI, M. 2009. Changes in the profile of flavonoid accumulation in *Medicago truncatula* leaves during infection with fungal pathogen *Phoma medicaginis*. *Plant Physiology and Biochemistry,* 47, 847-853.

JEZ, J. M., BOWMAN, M. E. & NOEL, J. P. 2002. Expanding the biosynthetic repertoire of plant type III polyketide synthases by altering starter molecule specificity. *Proceedings of the National Academy of Sciences of the United States of America,* 99, 5319-5324.

JIA, Z., ZOU, B., WANG, X., QIU, J., MA, H., GOU, Z., SONG, S. & DONG, H. 2010. Quercetin-induced H_2O_2 mediates the pathogen resistance against *Pseudomonas syringae* pv. Tomato DC3000 in *Arabidopsis thaliana*. *Biochemical and biophysical research communications,* 396, 522-527.

JIANG, K. & FELDMAN, L. J. 2005. Regulation of root apical meristem development. *Annual Review of Cell and Developmental Biology,* 21, 485-509.

JIANG, K., MENG, Y. L. & FELDMAN, L. J. 2003. Quiescent center formation in maize roots is associated with an auxin-regulated oxidizing environment. *Development,* 130, 1429-1438.

JIMÉNEZ-GONZÁLEZ, L., ÁLVAREZ-CORRAL, M., MUÑOZ-DORADO, M. & RODRÍGUEZ-GARCÍA, I. 2008. Pterocarpans: interesting natural products with antifungal activity and other biological properties. *Phytochemistry Reviews,* 7, 125-154.

JONES, J. T., FURLANETTO, C. & PHILLIPS, M. S. 2007. The role of flavonoids produced in response to cyst nematode infection of *Arabidopsis thaliana*. *Nematology,* 9, 671-677.

JOO, J. H., BAE, Y. S. & LEE, J. S. 2001. Role of auxin-induced reactive oxygen species in root gravitropism. *Plant Physiology,* 126, 1055-1060.

JORGENSEN, K., RASMUSSEN, A. V., MORANT, M., NIELSEN, A. H., BJARNHOLT, N., ZAGROBELNY, M., BAK, S. & MOLLER, B. L. 2005. Metabolon formation and metabolic channeling in the biosynthesis of plant natural products. *Current Opinion in Plant Biology,* 8, 280-291.

JUSZCZUK, I. M., WIKTOROWSKA, A., MALUSA, E. & RYCHTER, A. M. 2004. Changes in the concentration of phenolic compounds and exudation induced by phosphate deficiency in bean plants (*Phaseolus vulgaris* L.). *Plant and Soil,* 267, 41-49.

KAKAR, K., WANDREY, M., CZECHOWSKI, T., GAERTNER, T., SCHEIBLE, W. R., STITT, M., TORRES-JEREZ, I., XIAO, Y., REDMAN, J. C., WU, H. C., CHEUNG, F., TOWN, C. D. & UDVARDI, M. K. 2008. A community resource for high-throughput quantitative RT-PCR analysis of transcription factor gene expression in *Medicago truncatula*. *Plant Methods,* 4, 18.

KARIMI, M., INZÉ, D. & DEPICKER, A. 2002. GATEWAY vectors for *Agrobacterium*-mediated plant transformation. *Trends in Plant Science,* 7, 193-195.

KATSUMOTO, Y., FUKUCHI-MIZUTANI, M., FUKUI, Y., BRUGLIERA, F., HOLTON, T. A., KARAN, M., NAKAMURA, N., YONEKURA-SAKAKIBARA, K., TOGAMI, J., PIGEAIRE, A., TAO, G. Q., NEHRA, N. S., LU, C. Y., DYSON, B. K., TSUDA, S., ASHIKARI, T., KUSUMI, T., MASON, J. G. & TANAKA, Y. 2007. Engineering of the rose flavonoid biosynthetic pathway successfully generated blue-hued flowers accumulating delphinidin. *Plant and Cell Physiology,* 48, 1589-600.

KAWANO, T. 2003. Roles of the reactive oxygen species-generating peroxidase reactions in plant defense and growth induction. *Plant Cell Reports,* 21, 829-837.

KERESZT, A., LI, D., INDRASUMUNAR, A., NGUYEN, C. D., NONTACHAIYAPOOM, S., KINKEMA, M. & GRESSHOFF, P. M. 2007. *Agrobacterium rhizogenes*-mediated transformation of soybean to study root biology. *Nature protocols,* 2, 948-952.

KERK, N. M. & FELDMAN, N. 1995. A biochemical model for the initiation and maintenance of the quiescent center: implications for organization of root meristems. *Development,* 121, 2825-2833.

KEVEI, Z., LOUGNON, G., MERGAERT, P., HORVÁTH, G. V., KERESZT, A., JAYARAMAN, D., ZAMAN, N., MARCEL, F., REGULSKI, K., KISS, G. B., KONDOROSI, A., ENDRE, G., KONDOROSI, E. & ANÉ, J.-M. 2007. 3-hydroxy-3-methylglutaryl coenzyme A reductase1 interacts with NORK and is crucial for nodulation in *Medicago truncatula*. *Plant Cell,* 19, 3974-3989.

KHAN, Z. R., MIDEGA, C. A. O., BRUCE, T. J. A., HOOPER, A. M. & PICKETT, J. A. 2010. Exploiting phytochemicals for developing a 'push-pull' crop protection strategy for cereal farmers in Africa. *Journal of Experimental Botany,* 61, 4185-4196.

KHAN, Z. R., PICKETT, J. A., WADHAMS, L. J., HASSANALI, A. & MIDEGA, C. A. O. 2006. Combined control of *Striga hermonthica* and stemborers by maize-*Desmodium* spp. intercrops. *Crop Protection,* 25, 989-995.

KIDD, B. N., KADOO, N. Y., DOMBRECHT, B., TEKEOGLU, M., GARDINER, D. M., THATCHER, L. F., AITKEN, E. A., SCHENK, P. M., MANNERS, J. M. & KAZAN, K. 2011. Auxin signaling and transport promote susceptibility to the root-infecting fungal pathogen *Fusarium oxysporum* in *Arabidopsis*. *Molecular Plant-Microbe Interactions,* 24, 733-748.

KIELISZEWSKI, M. J. & LAMPORT, D. T. A. 1994. Extensin - repetitive motifs, functional sites, post-translational codes, and phylogeny. *The Plant Journal,* 5, 157-172.

KIJNE, J. W., SMIT, G., DIAZ, C. L. & LUGTENBERG, B. J. 1988. Lectin-enhanced accumulation of manganese-limited *Rhizobium leguminosarum* cells on pea root hair tips. *Journal of bacteriology,* 170, 2994-3000.

KIKUCHI, K., MATSUSHITA, N., SUZUKI, K. & HOGETSU, T. 2007. Flavonoids induce germination of basidiospores of the ectomycorrhizal fungus *Suillus bovinus*. *Mycorrhiza,* 17, 563-570.

KISU, Y., HARADA, Y., GOTO, M. & ESAKA, M. 1997. Cloning of the pumpkin ascorbate oxidase gene and analysis of a cis-acting region involved in induction by auxin. *Plant and cell physiology,* 38, 631-637.

KJOLLER, R. & ROSENDAHL, S. 1998. Enzymatic activity of the mycelium compared with oospore development during infection of pea roots by *Aphanomyces euteiches*. *Phytopathology,* 88, 992-6.

KOES, R., VERWEIJ, W. & QUATTROCCHIO, F. 2005. Flavonoids: a colorful model for the regulation and evolution of biochemical pathways. *Trends in Plant Science,* 10, 236-242.

KORASICK, D. A., ENDERS, T. A. & STRADER, L. C. 2013. Auxin biosynthesis and storage forms. *Journal of Experimental Botany,* 64, 2541-55.

KOSSLAK, R. M., BOOKLAND, R., BARKEI, J., PAAREN, H. E. & APPELBAUM, E. R. 1987. Induction of *Bradyrhizobium japonicum* common *nod g*enes by isoflavones isolated from *Glycine max*. *Proceedings of the National Academy of Sciences of the United States of America,* 84, 7428-7432.

KRISHNAN, H. B., LORIO, J., KIM, W. S., JIANG, G. Q., KIM, K. Y., DEBOER, M. & PUEPPKE, S. G. 2003. Extracellular proteins involved in soybean cultivar-specific nodulation are associated with pilus-like surface appendages and exported by a type III protein secretion system in *Sinorhizobium fredii* USDA257. *Molecular Plant-Microbe Interactions,* 16, 617-625.

KWAK, J. M., NGUYEN, V. & SCHROEDER, J. I. 2006. The role of reactive oxygen species in hormonal responses. *Plant Physiology,* 141, 323-329.

LAFFONT, C., BLANCHET, S., LAPIERRE, C., BROCARD, L., RATET, P., CRESPI, M., MATHESIUS, U. & FRUGIER, F. 2010. The *compact root architecture1* gene regulates lignification, flavonoid production, and polar auxin transport in *Medicago truncatula*. *Plant Physiology,* 153, 1597-1607.

LAGRANGE, H., JAY-ALLGMAND, C. & LAPEYRIE, F. 2001. Rutin, the phenolglycoside from eucalyptus root exudates, stimulates *Pisolithus* hyphal growth at picomolar concentrations. *New Phytologist,* 149, 349-355.

LANGCAKE, P. & PRYCE, R. 1976. The production of resveratrol by *Vitis vinifera* and other members of the Vitaceae as a response to infection or injury. *Physiological Plant Pathology,* 9, 77-86.

LAPLAZE, L., GHERBI, H., FRUTZ, T., PAWLOWSKI, K., FRANCHE, C., MACHEIX, J. J., AUGUY, F., BOGUSZ, D. & DUHOUX, E. 1999. Flavan-containing cells delimit *Frankia*-infected compartments in *Casuarina glauca* nodules. *Plant Physiology,* 121, 113-122.

LAROSE, G., CHÊNEVERT, R., MOUTOGLIS, P., GAGNÉ, S., PICHÉ, Y. & VIERHEILIG, H. 2002. Flavonoid levels in roots of *Medicago sativa* are modulated by the

developmental stage of the symbiosis and the root colonizing arbuscular mycorrhizal fungus. *Journal of Plant Physiology,* 159, 1329-1339.

LATTANZIO, V., LATTANZIO, V. M. T. & CARDINALI, A. 2006. Role of phenolics in the resistance mechanism of plants against fungal pathogens and insects. *In:* IMPERATO, F. (ed.) *Phytochemistry: Advances in Research.* Trivandrum, Kerala, India: Research Signpost.

LEE, K. H. & LARUE, T. A. 1992. Ethylene as a possible mediator of light-induced and nitrate-induced inhibition of nodulation of *Pisum sativum* L. cv Sparkle. *Plant Physiology,* 100, 1334-1338.

LEÓN-BARRIOS, M., DAKORA, F. D., JOSEPH, C. M. & PHILLIPS, D. A. 1993. Isolation of Rhizobium meliloti *nod* gene inducers from alfalfa rhizosphere soil. *Applied and environmental microbiology,* 59, 636-639.

LI, F. Q., HOU, B. H., CHEN, L., YAO, Z. J. & HONG, G. F. 2008. *In vitro* observation of the molecular interaction between NodD and its inducer naringenin as monitored by fluorescence resonance energy transfer. *Acta Biochimica Et Biophysica Sinica,* 40, 783-789.

LI, J., OU-LEE, T.-M., RABA, R., AMUNDSON, R. G. & LAST, R. L. 1993. *Arabidopsis* flavonoid mutants are hypersensitive to UV-B irradiation. *Plant Cell,* 5, 171-179.

LI, X., BONAWITZ, N. D., WENG, J.-K. & CHAPPLE, C. 2010. The growth reduction associated with repressed lignin biosynthesis in *Arabidopsis thaliana* is independent of flavonoids. *Plant Cell,* 22, 1620-1632.

LIBAULT, M., FARMER, A., BRECHENMACHER, L., DRNEVICH, J., LANGLEY, R. J., BILGIN, D. D., RADWAN, O., NEECE, D. J., CLOUGH, S. J. & MAY, G. D. 2010. Complete transcriptome of the soybean root hair cell, a single-cell model, and its alteration in response to *Bradyrhizobium japonicum* infection. *Plant Physiology,* 152, 541-552.

LIEVENS, S., GOORMACHTIG, S., DEN HERDER, J., CAPOEN, W., MATHIS, R., HEDDEN, P. & HOLSTERS, M. 2005. Gibberellins are involved in nodulation of *Sesbania rostrata. Plant Physiology,* 139, 1366-1379.

LIMPENS, E., FRANKEN, C., SMIT, P., WILLEMSE, J., BISSELING, T. & GEURTS, R. 2003. LysM domain receptor kinases regulating rhizobial Nod factor-induced infection. *Science,* 302, 630-633.

LIU, C. J., BLOUNT, J. W., STEELE, C. L. & DIXON, R. A. 2002. Bottlenecks for metabolic engineering of isoflavone glycoconjugates in *Arabidopsis. Proceedings of the National Academy of Sciences of the United States of America,* 99, 14578-14583.

LIU, C. J., DEAVOURS, B. E., RICHARD, S. B., FERRER, J. L., BLOUNT, J. W., HUHMAN, D., DIXON, R. A. & NOEL, J. P. 2006. Structural basis for dual functionality of isoflavonoid *O*-methyltransferases in the evolution of plant defense responses. *Plant Cell,* 18, 3656-3669.

LIU, W., KOHLEN, W., LILLO, A., OP DEN CAMP, R., IVANOV, S., HARTOG, M., LIMPENS, E., JAMIL, M., SMACZNIAK, C., KAUFMANN, K., YANG, W. C., HOOIVELD, G. J. E. J., CHARNIKHOVA, T., BOUWMEESTER, H. J., BISSELING, T. & GEURTS, R. 2011. Strigolactone biosynthesis in *Medicago truncatula* and rice requires the symbiotic GRAS-type transcription factors NSP1 and NSP2. *Plant Cell,* 23, 3853-3865.

LJUNG, K. 2013. Auxin metabolism and homeostasis during plant development. *Development,* 140, 943-50.

LJUNG, K., HULL, A. K., CELENZA, J., YAMADA, M., ESTELLE, M., NORMANLY, J. & SANDBERG, G. 2005. Sites and regulation of auxin biosynthesis in Arabidopsis roots. *Plant Cell,* 17, 1090-104.

LORENC-KUKUŁA, K., WRÓBEL-KWIATKOWSKA, M., STARZYCKI, M. & SZOPA, J. 2007. Engineering flax with increased flavonoid content and thus *Fusarium* resistance. *Physiological and Molecular Plant Pathology,* 70, 38-48.

LUDWIG-MÜLLER, J. 2011. Auxin conjugates: their role for plant development and in the evolution of land plants. *Journal of Experimental Botany,* 62, 1757-73.

LYNCH, D. V. & THOMPSON, J. E. 1984. Lipoxygenase-mediated production of superoxide anion in senescing plant tissue. *FEBS letters,* 173, 251-254.

LYON, F. M. & WOOD, R. 1975. Production of phaseollin, coumestrol and related compounds in bean leaves inoculated with *Pseudomonas* spp. *Physiological Plant Pathology,* 6, 117-124.

MACE, M., BELL, A. & STIPANOVIC, R. 1978. Histochemistry and identification of flavanols in *Verticillium* wilt-resistant and-susceptible cottons. *Physiological Plant Pathology,* 13, 143-149.

MAKOI, J. H. J. R. & NDAKIDEMI, P. A. 2007. Biological, ecological and agronomic significance of plant phenolic compounds in rhizosphere of the symbiotic legumes. *African Journal of Biotechnology,* 6, 1358-1368.

MANEFIELD, M., DE NYS, R., KUMAR, N., READ, R., GIVSKOV, M., STEINBERG, P. & KJELLEBERG, S. A. 1999. Evidence that halogenated furanones from *Delisea pulchra* inhibit acylated homoserine lactone (AHL)-mediated gene expression by displacing the AHL signal from its receptor protein. *Microbiology,* 145, 283-291.

MANO, Y. & NEMOTO, K. 2012. The pathway of auxin biosynthesis in plants. *Journal of Experimental Botany,* 63, 2853-72.

MANTHEY, K., KRAJINSKI, F., HOHNJEC, N., FIRNHABER, C., PÜHLER, A., PERLICK, A. M. & KÜSTER, H. 2004. Transcriptome profiling in root nodules and arbuscular mycorrhiza identifies a collection of novel genes induced during Medicago truncatula root endosymbioses. *Molecular Plant-Microbe Interactions,* 17, 1063-1077.

MARINO, D., PUCCIARIELLO, C., PUPPO, A. & FRENDO, P. 2009. The redox state, a referee of the legume–*Rhizobia* symbiotic game. *Advances in Botanical research,* 52, 115-151.

MARRS, K. A. 1996. The functions and regulation of glutathione S-transferases in plants. *Annual Review of Plant Physiology and Plant Molecular Biology,* 47, 127-158.

MARRS, K. A., ALFENITO, M. R., LLOYD, A. M. & WALBOT, V. 1995. A glutathione-S-transferase Involved in vacuolar transfer encoded by the maize gene *Bronze-2*. *Nature,* 375, 397-400.

MARSH, J. F., RAKOCEVIC, A., MITRA, R. M., BROCARD, L., SUN, J., ESCHSTRUTH, A., LONG, S. R., SCHULTZE, M., RATET, P. & OLDROYD, G. E. D. 2007. *Medicago truncatula NIN* is essential for rhizobial-independent nodule organogenesis induced by autoactive calcium/calmodulin-dependent protein kinase. *Plant Physiology,* 144, 324-335.

MASAOKA, Y., KOJIMA, M., SUGIHARA, S., YOSHIHARA, T., KOSHINO, M. & ICHIHARA, A. 1993. Dissolution of ferric phosphate by alfalfa (*Medicago sativa* L.) root exudates. *Plant and Soil,* 155-156, 75-78.

MASHIGUCHI, K., TANAKA, K., SAKAI, T., SUGAWARA, S., KAWAIDE, H., NATSUME, M., HANADA, A., YAENO, T., SHIRASU, K., YAO, H., MCSTEEN, P., ZHAO, Y., HAYASHI, K., KAMIYA, Y. & KASAHARA, H. 2011. The main auxin biosynthesis pathway in *Arabidopsis*. *Proceedings of the National Academy of Sciences of the United States of America,* 108, 18512-7.

MATHESIUS, U. 2001. Flavonoids induced in cells undergoing nodule organogenesis in white clover are regulators of auxin breakdown by peroxidase. *Journal of Experimental Botany,* 52, 419-426.

MATHESIUS, U. 2008. Auxin: at the root of nodule development? *Functional Plant Biology,* 35, 651-668.

MATHESIUS, U., BAYLISS, C., WEINMAN, J. J., SCHLAMAN, H. R. M., SPAINK, H. P., ROLFE, B. G., MCCULLY, M. E. & DJORDJEVIC, M. A. 1998a. Flavonoids synthesized in cortical cells during nodule initiation are early developmental markers in white clover. *Molecular Plant-Microbe Interactions,* 11, 1223-1232.

MATHESIUS, U., DJORDJEVIC, M. A., OAKES, M., GOFFARD, N., HAERIZADEH, F., WEILLER, G. F., SINGH, M. B. & BHALLA, P. L. 2011. Comparative proteomic profiles of the soybean (*Glycine max*) root apex and differentiated root zone. *Proteomics,* 11, 1707-1719.

MATHESIUS, U., MULDERS, S., GAO, M., TEPLITSKI, M., CAETANO-ANOLLES, G., ROLFE, B. G. & BAUER, W. D. 2003. Extensive and specific responses of a eukaryote to bacterial quorum-sensing signals. *Proceedings of the National Academy of Sciences of the United States of America,* 100, 1444-9.

MATHESIUS, U., SCHLAMAN, H. R. M., SPAINK, H. P., SAUTTER, C., ROLFE, B. G. & DJORDJEVIC, M. A. 1998b. Auxin transport inhibition precedes root nodule formation in white clover roots and is regulated by flavonoids and derivatives of chitin oligosaccharides. *The Plant Journal,* 14, 23-34.

MAXWELL, C. A., HARTWIG, U. A., JOSEPH, C. M. & PHILLIPS, D. A. 1989. A chalcone and two related flavonoids released from alfalfa roots induce *nod* genes of *Rhizobium meliloti*. *Plant Physiology,* 91, 842-847.

MAYDA, E., MARQUÉS, C., CONEJERO, V. & VERA, P. 2000. Expression of a pathogen-induced gene can be mimicked by auxin insensitivity. *Molecular Plant-Microbe Interactions,* 13, 23-31.

MEADE, H. M., LONG, S. R., RUVKUN, G. B., BROWN, S. E. & AUSUBEL, F. M. 1982. Physical and genetic characterization of symbiotic and auxotrophic mutants of *Rhizobium meliloti* induced by transposon Tn*5* mutagenesis. *Journal of bacteriology,* 149, 114-22.

MIAO, V. P., MATTHEWS, D. E. & VANETTEN, H. D. 1991. Identification and chromosomal locations of a family of cytochrome P-450 genes for pisatin detoxification in the fungus *Nectria haematococca*. *Molecular and General Genetics,* 226, 214-223.

MIDDLETON, A. M., ÚBEDA-TOMÁS, S., GRIFFITHS, J., HOLMAN, T., HEDDEN, P., THOMAS, S. G., PHILLIPS, A. L., HOLDSWORTH, M. J., BENNETT, M. J. & KING, J. R. 2012. Mathematical modeling elucidates the role of transcriptional feedback in gibberellin signaling. *Proceedings of the National Academy of Sciences of the United States of America,* 109, 7571-7576.

MIDDLETON, P. H., JAKAB, J., PENMETSA, R. V., STARKER, C. G., DOLL, J., KALO, P., PRABHU, R., MARSH, J. F., MITRA, R. M., KERESZT, A., DUDAS, B., VANDENBOSCH,

K., LONG, S. R., COOK, D. R., KISS, G. B. & OLDROYD, G. E. D. 2007. An ERF transcription factor in *Medicago truncatula* that is essential for Nod factor signal transduction. *Plant Cell,* 19, 1221-1234.

MIWA, H., SUN, J., OLDROYD, G. E. D. & DOWNIE, J. A. 2006. Analysis of calcium spiking using a cameleon calcium sensor reveals that nodulation gene expression is regulated by calcium spike number and the developmental status of the cell. *The Plant Journal,* 48, 883-894.

MOHNEY, B. K., MATZ, T., LAMOREAUX, J., WILCOX, D. S., GIMSING, A. L., MAYER, P. & WEIDENHAMER, J. D. 2009. *In situ* silicone tube microextraction: a new method for undisturbed sampling of root-exuded thiophenes from Marigold (*Tagetes erecta* L.) in soil. *Journal of Chemical Ecology,* 35, 1279-87.

MORANDI, D. 1996. Occurrence of phytoalexins and phenolic compounds in endomycorrhizal interactions, and their potential role in biological control. *Plant and Soil,* 185, 241-251.

MORANDI, D., BAILEY, J. A. & GIANINAZZIPEARSON, V. 1984. Isoflavonoid accumulation in soybean roots infected with vesicular arbuscular mycorrhizal fungi. *Physiological Plant Pathology,* 24, 357-364.

MORANDI, D., LE SIGNOR, C., GIANINAZZI-PEARSON, V. & DUC, G. 2009. A *Medicago truncatula* mutant hyper-responsive to mycorrhiza and defective for nodulation. *Mycorrhiza,* 19, 435-441.

MORRIS, P. F., BONE, E. & TYLER, B. M. 1998. Chemotropic and contact responses of *Phytophthora sojae* hyphae to soybean isoflavonoids and artificial substrates. *Plant Physiology,* 117, 1171-1178.

MORRIS, P. F. & WARD, E. W. B. 1992. Chemoattraction of zoospores of the soybean pathogen, *Phytophthora sojae,* by isoflavones. *Physiological and Molecular Plant Pathology,* 40, 17-22.

MORTIER, V., WASSON, A., JAWOREK, P., DE KEYSER, A., DECROOS, M., HOLSTERS, M., TARKOWSKI, P., MATHESIUS, U. & GOORMACHTIG, S. 2014. Role of LONELY GUY genes in indeterminate nodulation on *Medicago truncatula*. *New Phytologist,* 202, 582-593.

MOSCATIELLO, R., SQUARTINI, A., MARIANI, P. & NAVAZIO, L. 2010. Flavonoid-induced calcium signalling in *Rhizobium leguminosarum* bv. *viciae*. *New Phytologist,* 188, 814-823.

MUELLER, L. A., GOODMAN, C. D., SILADY, R. A. & WALBOT, V. 2000. AN9, a petunia glutathione S-transferase required for anthocyanin sequestration, is a flavonoid-binding protein. *Plant Physiology,* 123, 1561-1570.

MUIR, S. R., COLLINS, G. J., ROBINSON, S., HUGHES, S., BOVY, A., DE VOS, C. R., VAN TUNEN, A. J. & VERHOEYEN, M. E. 2001. Overexpression of petunia chalcone isomerase in tomato results in fruit containing increased levels of flavonols. *Nature Biotechnology,* 19, 470-474.

MÜLLER, M. & MUNNÉ-BOSCH, S. 2011. Rapid and sensitive hormonal profiling of complex plant samples by liquid chromatography coupled to electrospray ionization tandem mass spectrometry. *Plant Methods,* 7, 37.

MURPHY, A., PEER, W. A. & TAIZ, L. 2000. Regulation of auxin transport by aminopeptidases and endogenous flavonoids. *Planta,* 211, 315-24.

MURRAY, J. D., KARAS, B. J., SATO, S., TABATA, S., AMYOT, L. & SZCZYGLOWSKI, K. 2007. A cytokinin perception mutant colonized by *Rhizobium* in the absence of nodule organogenesis. *Science,* 315, 101-104.

MURRAY, J. D., MUNI, R. R., TORRES-JEREZ, I., TANG, Y., ALLEN, S., ANDRIANKAJA, M., LI, G., LAXMI, A., CHENG, X., WEN, J., VAUGHAN, D., SCHULTZE, M., SUN, J., CHARPENTIER, M., OLDROYD, G., TADEGE, M., RATET, P., MYSORE, K. S., CHEN, R. & UDVARDI, M. K. 2011. *Vapyrin,* a gene essential for intracellular progression of arbuscular mycorrhizal symbiosis, is also essential for infection by rhizobia in the nodule symbiosis of *Medicago truncatula*. *The Plant Journal,* 65, 244-52.

NANDA, A. K., ANDRIO, E., MARINO, D., PAULY, N. & DUNAND, C. 2010. Reactive oxygen species during plant-microorganism early interactions. *Journal of Integrative Plant Biology,* 52, 195-204.

NAOUMKINA, M. & DIXON, R. A. 2008. Subcellular localization of flavonoid natural products: A signaling function? *Plant Signaling & Behavior,* 3, 573-575.

NAOUMKINA, M., FARAG, M. A., SUMNER, L. W., TANG, Y., LIU, C.-J. & DIXON, R. A. 2007. Different mechanisms for phytoalexin induction by pathogen and wound signals in *Medicago truncatula*. *Proceedings of the National Academy of Sciences of the United States of America,* 104, 17909-17915.

NAOUMKINA, M. A., ZHAO, Q. A., GALLEGO-GIRALDO, L., DAI, X. B., ZHAO, P. X. & DIXON, R. A. 2010. Genome-wide analysis of phenylpropanoid defence pathways. *Molecular Plant Pathology,* 11, 829-846.

NIU, Y., CHAI, R., LIU, L., JIN, G., LIU, M., TANG, C. & ZHANG, Y. 2014. Magnesium availability regulates the development of root hairs in *Arabidopsis thaliana* (L.) Heynh. *Plant, Cell & Environment,* 37, 2795-2813.

NORMAND, P., LAPIERRE, P., TISA, L. S., GOGARTEN, J. P., ALLOISIO, N., BAGNAROL, E., BASSI, C. A., BERRY, A. M., BICKHART, D. M., CHOISNE, N., COULOUX, A., COURNOYER, B., CRUVEILLER, S., DAUBIN, V., DEMANGE, N., FRANCINO, M. P., GOLTSMAN, E., HUANG, Y., KOPP, O. R., LABARRE, L., LAPIDUS, A., LAVIRE, C., MARECHAL, J., MARTINEZ, M., MASTRONUNZIO, J. E., MULLIN, B. C., NIEMANN, J., PUJIC, P., RAWNSLEY, T., ROUY, Z., SCHENOWITZ, C., SELLSTEDT, A., TAVARES, F., TOMKINS, J. P., VALLENET, D., VALVERDE, C., WALL, L. G., WANG, Y., MEDIGUE, C. & BENSON, D. R. 2007. Genome characteristics of facultatively symbiotic *Frankia* sp strains reflect host range and host plant biogeography. *Genome Research,* 17, 7-15.

NOVAK, K., CHOVANEC, P., SKRDLETA, V., KROPACOVA, M., LISA, L. & NEMCOVA, M. 2002. Effect of exogenous flavonoids on nodulation of pea (*Pisum sativum* L.). *Journal of Experimental Botany,* 53, 1735-1745.

NYAMSUREN, O., COLDITZ, F., ROSENDAHL, S., TAMASLOUKHT, M., BEKEL, T., MEYER, F., KUESTER, H., FRANKEN, P. & KRAJINSKI, F. 2003. Transcriptional profiling of Medicago truncatula roots after infection with *Aphanomyces euteiches* (oomycota) identifies novel genes upregulated during this pathogenic interaction. *Physiological and Molecular Plant Pathology,* 63, 17-26.

ODELL, J. T., NAGY, F. & CHUA, N. H. 1985. Identification of DNA sequences required for activity of the cauliflower mosaic virus 35S promoter. *Nature,* 313, 810-2.

OGAWA, M., HANADA, A., YAMAUCHI, Y., KUWAHARA, A., KAMIYA, Y. & YAMAGUCHI, S. 2003. Gibberellin biosynthesis and response during *Arabidopsis* seed germination. *Plant Cell,* 15, 1591-604.

OGOSHI, A., COOK, R. & BASSETT, E. 1990. *Rhizoctonia* species and anastomosis groups causing root rot of wheat and barley in the Pacific Northwest. *Phytopathology,* 80, 784-788.

OLDROYD, G. E., ENGSTROM, E. M. & LONG, S. R. 2001. Ethylene inhibits the Nod factor signal transduction pathway of *Medicago truncatula*. *Plant Cell,* 13, 1835-49.

OLDROYD, G. E. D. 2007. Nodules and hormones. *Science,* 315, 52-53.

OLDROYD, G. E. D. & DOWNIE, J. M. 2008. Coordinating nodule morphogenesis with rhizobial infection in legumes. *Annual Review of Plant Biology,* 59, 519-546.

OSAKABE, Y., MIYATA, S., URAO, T., SEKI, M., SHINOZAKI, K. & YAMAGUCHI-SHINOZAKI, K. 2002. Overexpression of *Arabidopsis* response regulators, ARR4/ATRR1/IBC7 and ARR8/ATRR3, alters cytokinin responses differentially in the shoot and in callus formation. *Biochemical and Biophysical Research Communications,* 293, 806-815.

OSTROUMOVA, O., EFIMOVA, S., MALEV, V. & SCHAGINA, L. 2013. Plant flavonoids affect membrane activity of antimicrobial agents. *FEBS Journal,* 280, 191-192.

PADMAVATI, M., SAKTHIVEL, N., THARA, K. V. & REDDY, A. R. 1997. Differential sensitivity of rice pathogens to growth inhibition by flavonoids. *Phytochemistry,* 46, 499-502.

PANG, Y., PEEL, G. J., SHARMA, S. B., TANG, Y. & DIXON, R. A. 2008. A transcript profiling approach reveals an epicatechin-specific glucosyltransferase expressed in the seed coat of Medicago truncatula. *Proceedings of the National Academy of Sciences of the United States of America,* 105, 14210-14215.

PANKHURST, C. E. & BIGGS, D. R. 1980. Sensitivity of *Rhizobium* to selected isoflavonoids. *Canadian Journal of Microbiology,* 26, 542-5.

PARNISKE, M., AHLBORN, B. & WERNER, D. 1991. Isoflavonoid-inducible resistance to the phytoalexin glyceollin in soybean rhizobia. *Journal of Bacteriology,* 173, 3432-9.

PARVEZ, M. M., TOMITA-YOKOTANI, K., FUJII, Y., KONISHI, T. & IWASHINA, T. 2004. Effects of quercetin and its seven derivatives on the growth of *Arabidopsis thaliana* and *Neurospora crassa*. *Biochemical Systematics and Ecology,* 32, 631-635.

PASSARDI, F., COSIO, C., PENEL, C. & DUNAND, C. 2005. Peroxidases have more functions than a Swiss army knife. *Plant Cell Reports,* 24, 255-265.

PECK, M. C., FISHER, R. F. & LONG, S. R. 2006. Diverse flavonoids stimulate NodD1 binding to *nod* gene promoters in *Sinorhizobium meliloti*. *Journal of Bacteriology,* 188, 5417-5427.

PEDRAS, M. S. C. & AHIAHONU, P. W. K. 2005. Metabolism and detoxification of phytoalexins and analogs by phytopathogenic fungi. *Phytochemistry,* 66, 391-411.

PEER, W. & MURPHY, A. S. 2006. Flavonoids as signal molecules: targets of flavonoid action. *In:* GROTEWOLD, E. (ed.) *The science of flavonoids.* Springer.

PEER, W. A., BANDYOPADHYAY, A., BLAKESLEE, J. J., MAKAM, S. I., CHEN, R. J., MASSON, P. H. & MURPHY, A. S. 2004. Variation in expression and protein localization of the PIN family of auxin efflux facilitator proteins in flavonoid mutants with altered auxin transport in *Arabidopsis thaliana*. *Plant Cell,* 16, 1898-1911.

PEER, W. A., BLAKESLEE, J. J., YANG, H. & MURPHY, A. S. 2011. Seven things we think we know about auxin transport. *Molecular Plant,* 4, 487-504.

PEER, W. A., BROWN, D. E., TAGUE, B. W., MUDAY, G. K., TAIZ, L. & MURPHY, A. S. 2001. Flavonoid accumulation patterns of transparent testa mutants of *Arabidopsis*. *Plant Physiology,* 126, 536-548.

PEER, W. A. & MURPHY, A. S. 2007. Flavonoids and auxin transport: modulators or regulators? *Trends in Plant Science,* 12, 556-563.

PENMETSA, R. V. & COOK, D. R. 1997. A legume ethylene-insensitive mutant hyperinfected by its rhizobial symbiont. *Science,* 275, 527-530.

PENMETSA, R. V., FRUGOLI, J. A., SMITH, L. S., LONG, S. R. & COOK, D. R. 2003. Dual genetic pathways controlling nodule number in *Medicago truncatula*. *Plant Physiology,* 131, 998-1008.

PENMETSA, R. V., URIBE, P., ANDERSON, J., LICHTENZVEIG, J., GISH, J. C., NAM, Y. W., ENGSTROM, E., XU, K., SCKISEL, G., PEREIRA, M., BAEK, J. M., LOPEZ-MEYER, M., LONG, S. R., HARRISON, M. J., SINGH, K. B., KISS, G. B. & COOK, D. R. 2008. The *Medicago truncatula* ortholog of Arabidopsis EIN2, *sickle*, is a negative regulator of symbiotic and pathogenic microbial associations. *The Plant Journal,* 55, 580-595.

PEREZ-MONTANO, F., GUASCH-VIDAL, B., GONZALEZ-BARROSO, S., LOPEZ-BAENA, F. J., CUBO, T., OLLERO, F. J., GIL-SERRANO, A. M., RODRIGUEZ-CARVAJAL, M. A., BELLOGIN, R. A. & ESPUNY, M. R. 2011. Nodulation-gene-inducing flavonoids increase overall production of autoinducers and expression of *N*-acyl homoserine lactone synthesis genes in rhizobia. *Research in microbiology,* 162, 715-723.

PETERS, D. J. & CONSTABEL, C. P. 2002. Molecular analysis of herbivore-induced condensed tannin synthesis: cloning and expression of dihydroflavonol reductase from trembling aspen (*Populus tremuloides*). *The Plant Journal,* 32, 701-712.

PETERS, N. K. & CRIST-ESTES, D. K. 1989. Nodule formation is stimulated by the ethylene inhibitor aminoethoxyvinylglycine. *Plant physiology,* 91, 690-693.

PETERS, N. K., FROST, J. W. & LONG, S. R. 1986. A plant flavone, Luteolin, induces expression of *Rhizobium meliloti* nodulation genes. *Science,* 233, 977-980.

PFAFFL, M. W. 2001. A new mathematical model for relative quantification in real-time RT-PCR. *Nucleic Acids Research,* 29, e45.

PFEIFFER, W. & HÖFTBERGER, M. 2001. Oxidative burst in *Chenopodium rubrum* suspension cells: Induction by auxin and osmotic changes. *Physiologia Plantarum,* 111, 144-150.

PIGNOCCHI, C. & FOYER, C. H. 2003. Apoplastic ascorbate metabolism and its role in the regulation of cell signalling. *Current Opinion in Plant Biology,* 6, 379-389.

PLAPER, A., GOLOB, M., HAFNER, I., OBLAK, M., SOLMAJER, T. & JERALA, R. 2003. Characterization of quercetin binding site on DNA gyrase. *Biochemical and Biophysical Research Communications,* 306, 530-536.

POPOVICI, J., COMTE, G., BAGNAROL, E., ALLOISIO, N., FOURNIER, P., BELLVERT, F., BERTRAND, C. & FERNANDEZ, M. P. 2010. Differential effects of rare specific flavonoids on compatible and incompatible strains in the *Myrica gale-Frankia* actinorhizal symbiosis. *Applied and Environmental Microbiology,* 76, 2451-60.

PRAYITNO, J., ROLFE, B. G. & MATHESIUS, U. 2006. The ethylene-insensitive *sickle* mutant of *Medicago truncatula* shows altered auxin transport regulation during nodulation. *Plant Physiology,* 142, 168-180.

PUEPPKE, S. G. & VANETTEN, H. D. 1974. Pisatin accumulation and lesion development in peas infected with *Aphanomyces euteiches*, *Fusarium solani* f. sp. pisi, or *Rhizoctonia solani*. *Phytopathology,* 64, 1433-1440.

QUATTROCCHIO, F., BAUDRY, A., LEPINIEC, L. & GROTEWOLD, E. 2006. The regulation of flavonoid biosynthesis. *In:* GROTEWOLD, E. (ed.) *The science of flavonoids.* Columbus OH, USA: Springer.

QUITTENDEN, L. J., DAVIES, N. W., SMITH, J. A., MOLESWORTH, P. P., TIVENDALE, N. D. & ROSS, J. J. 2009. Auxin biosynthesis in pea: Characterization of the tryptamine pathway. *Plant Physiology,* 151, 1130-1138.

RAJAMANI, S., BAUER, W. D., ROBINSON, J. B., FARROW, J. M., PESCI, E. C., TEPLITSKI, M., GAO, M. S., SAYRE, R. T. & PHILLIPS, D. A. 2008. The vitamin riboflavin and its derivative lumichrome activate the LasR bacterial quorum-sensing receptor. *Molecular Plant-Microbe Interactions,* 21, 1184-1192.

RAMU, S. K., PENG, H. M. & COOK, D. R. 2002. Nod factor induction of reactive oxygen species production is correlated with expression of the early nodulin gene *rip1* in *Medicago truncatula*. *Molecular Plant-Microbe Interactions,* 15, 522-528.

RAO, J. R. & COOPER, J. E. 1994. Rhizobia catabolize *nod* gene-inducing flavonoids via C-ring fission mechanisms. *Journal of Bacteriology,* 176, 5409-5413.

RAO, J. R. & COOPER, J. E. 1995. Soybean nodulating rhizobia modify *nod* gene inducers daidzein and genistein to yield aromatic products that can influence gene-inducing activity. *Molecular Plant-Microbe Interactions,* 8, 855-862.

RATHBUN, E. A., NALDRETT, M. J. & BREWIN, N. J. 2002. Identification of a family of extensin-like glycoproteins in the lumen of *Rhizobium*-induced infection threads in pea root nodules. *Molecular Plant Microbe Interactions,* 15, 350-9.

RAVNSKOV, S., CARLSEN, S. C. K., UNDERSTRUP, A., FOMSGAARD, I. S. & MORTENSEN, A. G. 2008. Flavonoids in roots of white clover: interaction of arbuscular mycorrhizal fungi and a pathogenic fungus. *Plant and Soil,* 302, 33-43.

RAY, H., YU, M., AUSER, P., BLAHUT-BEATTY, L., MCKERSIE, B., BOWLEY, S., WESTCOTT, N., COULMAN, B., LLOYD, A. & GRUBER, M. Y. 2003. Expression of anthocyanins and proanthocyanidins after transformation of alfalfa with maize *Lc*. *Plant Physiology,* 132, 1448-1463.

REDMOND, J. W., BATLEY, M., DJORDJEVIC, M. A., INNES, R. W., KUEMPEL, P. L. & ROLFE, B. G. 1986. Flavones induce expression of nodulation genes in *Rhizobium*. *Nature,* 323, 632-635.

RICE-EVANS, C. A., MILLER, N. J. & PAGANGA, G. 1996. Structure-antioxidant activity relationships of flavonoids and phenolic acids. *Free Radical Biology and Medicine,* 20, 933-956.

RIECHMANN, J. L. & MEYEROWITZ, E. M. 1998. The AP2/EREBP family of plant transcription factors. *Biological Chemistry,* 379, 633-46.

RIGHTMYER, A. P. & LONG, S. R. 2011. Pseudonodule formation by wild-type and symbiotic mutant *Medicago truncatula* in response to auxin transport inhibitors. *Molecular Plant-Microbe Interactions,* 24, 1372-1384.

RINGLI, C., BIGLER, L., KUHN, B. M., LEIBER, R. M., DIET, A., SANTELIA, D., FREY, B., POLLMANN, S. & KLEIN, M. 2008. The modified flavonol glycosylation profile in the *Arabidopsis rol1* mutants results in alterations in plant growth and cell shape formation. *Plant Cell,* 20, 1470-1481.

ROLFE, B., GRESSHOFF, P. & SHINE, J. 1980. Rapid screening for symbiotic mutants of *Rhizobium* and white clover. *Plant Science Letters,* 19, 277-284.

ROSQUETE, M. R., BARBEZ, E. & KLEINE-VEHN, J. 2012. Cellular auxin homeostasis: Gatekeeping is housekeeping. *Molecular Plant,* 5, 772-786.

RUAN, Y. J., KOTRAIAH, V. & STRANEY, D. C. 1995. Flavonoids stimulate spore germination in *Fusarium solani* pathogenic on legumes in a manner sensitive to inhibitors of cAMP-dependent protein kinase. *Molecular Plant-Microbe Interactions,* 8, 929-938.

RUBERY, P. & SHELDRAKE, A. 1974. Carrier-mediated auxin transport. *Planta,* 118, 101-121.

RUYTER-SPIRA, C., AL-BABILI, S., VAN DER KROL, S. & BOUWMEESTER, H. 2013. The biology of strigolactones. *Trends in Plant Science,* 18, 72-83.

SAKAKIBARA, H. 2006. Cytokinins: activity, biosynthesis, and translocation. *Annual Review of Plant Biolgy,* 57, 431-49.

SALZWEDEL, J. L. & DAZZO, F. B. 1993. pSym *nod* gene influence on elicitation of peroxidase-activity from white clover and pea roots by *Rhizobia* and their cell-free supernatants. *Molecular Plant-Microbe Interactions,* 6, 127-134.

SAMBROOK, J., RUSSELL, D. W. & RUSSELL, D. W. 2001. *Molecular cloning: a laboratory manual,* Cold spring harbor laboratory press Cold Spring Harbor, New York:.

SANTELIA, D., HENRICHS, S., VINCENZETTI, V., SAUER, M., BIGLER, L., KLEIN, M., BAILLY, A., LEE, Y., FRIML, J., GEISLER, M. & MARTINOIA, E. 2008. Flavonoids redirect PIN-mediated polar auxin fluxes during root gravitropic responses. *Journal of Biological Chemistry,* 283, 31218-31226.

SASLOWSKY, D. E., WAREK, U. & WINKEL, B. S. J. 2005. Nuclear localization of flavonoid enzymes in *Arabidopsis*. *Journal of Biological Chemistry,* 280, 23735-23740.

SAVOLAINEN, V. & CHASE, M. W. 2003. A decade of progress in plant molecular phylogenetics. *Trends in Genetics,* 19, 717-724.

SAVOURÉ, A., SALLAUD, C., EL-TURK, J., ZUANAZZI, J., RATET, P., SCHULTZE, M., KONDOROSI, A., ESNAULT, R. & KONDOROSI, E. 1997. Distinct response of *Medicago* suspension cultures and roots to Nod factors and chitin oligomers in the elicitation of defense-related responses. *The Plant Journal,* 11, 277-287.

SCERVINO, J. M., PONCE, M. A., ERRA-BASSELLS, R., BORNPADRE, J., VIERHEILIG, H., OCAMPO, J. A. & GODEAS, A. 2007. The effect of flavones and flavonols on colonization of tomato plants by arbuscular mycorrhizal fungi of the genera *Gigaspora* and *Glomus*. *Canadian Journal of Microbiology,* 53, 702-709.

SCERVINO, J. M., PONCE, M. A., ERRA-BASSELLS, R., VIERHEILIG, H., OCAMPO, J. A. & GODEAS, A. 2005. Flavonoids exhibit fungal species and genus specific effects on the presymbiotic growth of *Gigaspora* and *Glomus*. *Mycological Research,* 109, 789-794.

SCHAEFER, A. L., GREENBERG, E. P., OLIVER, C. M., ODA, Y., HUANG, J. J., BITTAN-BANIN, G., PERES, C. M., SCHMIDT, S., JUHASZOVA, K., SUFRIN, J. R. & HARWOOD, C. S. 2008. A new class of homoserine lactone quorum-sensing signals. *Nature,* 454, 595-U6.

SCHEIDT, H. A., PAMPEL, A., NISSLER, L., GEBHARDT, R. & HUSTER, D. 2004. Investigation of the membrane localization and distribution of flavonoids by high-resolution magic angle spinning NMR spectroscopy. *Biochimica et Biophysica Acta (BBA)-Biomembranes,* 1663, 97-107.

SCHMIDT, P. E., BROUGHTON, W. J. & WERNER, D. 1994. Nod-factors of *Bradyrhizobium japonicum* and *Rhizobium* Sp NGR234 induce flavonoid accumulation in soybean root exudate. *Molecular Plant-Microbe Interactions,* 7, 384-390.

SCHMITTGEN, T. D. & LIVAK, K. J. 2008. Analyzing real-time PCR data by the comparative CT method. *Nature protocols,* 3, 1101-1108.

SCHNABEL, E. L. & FRUGOLI, J. 2004. The PIN and LAX families of auxin transport genes in *Medicago truncatula*. *Molecular Genetics and Genomics,* 272, 420-32.

SCHNEEBELI, K., MATHESIUS, U. & WATT, M. 2014. *Brachypodium distachyon* is a pathosystem model for the study of the wheat disease rhizoctonia root rot. *Plant Pathology*.

SCHOPFER, P. 2001. Hydroxyl radical-induced cell-wall loosening in vitro and in vivo: implications for the control of elongation growth. *The Plant Journal,* 28, 679-688.

SCHOPFER, P., LISZKAY, A., BECHTOLD, M., FRAHRY, G. & WAGNER, A. 2002. Evidence that hydroxyl radicals mediate auxin-induced extension growth. *Planta,* 214, 821-828.

SEKIZAKI, H. & YOKOSAWA, R. 1988. Studies on zoospore-attracting Activity. I.: Synthesis of isoflavones and their attracting activity to *Aphanomyces euteiches* zoospore. *Chemical & pharmaceutical bulletin,* 36, 4876-4880.

SHAW, L. J. & HOOKER, J. E. 2008. The fate and toxicity of the flavonoids naringenin and formononetin in soil. *Soil Biology & Biochemistry,* 40, 528-536.

SHAW, L. J., MORRIS, P. & HOOKER, J. E. 2006. Perception and modification of plant flavonoid signals by rhizosphere microorganisms. *Environmental Microbiology,* 8, 1867-1880.

SHEN, W. H., DAVIOUD, E., DAVID, C., BARBIERBRYGOO, H., TEMPE, J. & GUERN, J. 1990. High sensitivity to auxin is a common feature of hairy root. *Plant Physiology,* 94, 554-560.

SHEN, W. H., PETIT, A., GUERN, J. & TEMPE, J. 1988. Hairy roots are more sensitive to auxin than normal roots. *Proceedings of the National Academy of Sciences of the United States of America,* 85, 3417-3421.

SHIU, S.-H. & BLEECKER, A. B. 2001. Plant receptor-like kinase gene family: diversity, function, and signaling. *Science Signaling,* 2001, re22.

SINGH, S. & PARNISKE, M. 2012. Activation of calcium- and calmodulin-dependent protein kinase (CCaMK), the central regulator of plant root endosymbiosis. *Current Opinion in Plant Biology,* 15, 444-453.

SIQUEIRA, J. O., SAFIR, G. R. & NAIR, M. G. 1991. Stimulation of vesicular-arbuscular mycorrhiza formation and growth of white clover by flavonoid compounds. *New Phytologist,* 118, 87-93.

SKADHAUGE, B., THOMSEN, K. K. & VON WETTSTEIN, D. 1997. The role of the barley testa layer and its flavonoid content in resistance to *Fusarium* infections. *Hereditas,* 126, 147-160.

SOMASEGARAN, P. & HOBEN, H. J. 1994. *Handbook for rhizobia : methods in legume-Rhizobium technology,* New York, Springer-Verlag.

SOYANO, T., KOUCHI, H., HIROTA, A. & HAYASHI, M. 2013. NODULE INCEPTION directly targets *NF-Y* subunit genes to regulate essential processes of root nodule development in *Lotus japonicus*. *PLoS Genetics,* 9, e1003352.

SPAINK, H. P. 1995. The molecular basis of infection and nodulation by rhizobia: the ins and outs of sympathogenesis. *Annual Review of Phytopathology,* 33, 345-68.

STAFFORD, H. A. 1990. *Flavonoid metabolism*, CRC press.
STAFFORD, H. A. 1991. Flavonoid evolution: An enzymic approach. *Plant Physiology*, 96, 680-685.
STASZKÓW, A., SWARCEWICZ, B., BANASIAK, J., MUTH, D., JASIŃSKI, M. & STOBIECKI, M. 2011. LC/MS profiling of flavonoid glycoconjugates isolated from hairy roots, suspension root cell cultures and seedling roots of Medicago truncatula. *Metabolomics*, 7, 604-613.
STEINKELLNER, S., LENDZEMO, V., LANGER, I., SCHWEIGER, P., KHAOSAAD, T., TOUSSAINT, J. P. & VIERHEILIG, H. 2007. Flavonoids and strigolactones in root exudates as signals in symbiotic and pathogenic plant-fungus interactions. *Molecules*, 12, 1290-1306.
STEPANOVA, A. N., YUN, J., ROBLES, L. M., NOVAK, O., HE, W., GUO, H., LJUNG, K. & ALONSO, J. M. 2011. The *Arabidopsis* YUCCA1 flavin monooxygenase functions in the indole-3-pyruvic acid branch of auxin biosynthesis. *Plant Cell*, 23, 3961-73.
STEVE ROZEN & SKALETSKY, H. J. 1998. Primer3. Code available at http://www-genome.wi.mit.edu/genome_software/other/primer3.html.
STÖVER, B. C. & MÜLLER, K. F. 2010. TreeGraph 2: Combining and visualizing evidence from different phylogenetic analyses. *BMC Bioinformatics*, 11, 7.
STREETER, T. C., RENGEL, Z., NEATE, S. M. & GRAHAM, R. D. 2001. Zinc fertilisation increases tolerance to *Rhizoctonia solani* (AG 8) in *Medicago truncatula*. *Plant and soil*, 228, 233-242.
SU, Y. H., LIU, Y. B. & ZHANG, X. S. 2011. Auxin-cytokinin interaction regulates meristem development. *Molecular Plant*, 4, 616-625.
SUBRAMANIAN, S., GRAHAM, M. Y., YU, O. & GRAHAM, T. L. 2005. RNA interference of soybean isoflavone synthase genes leads to silencing in tissues distal to the transformation site and to enhanced susceptibility to *Phytophthora sojae*. *Plant Physiology*, 137, 1345-1353.
SUBRAMANIAN, S., HU, X., LU, G. H., ODELL, J. T. & YU, O. 2004. The promoters of two isoflavone synthase genes respond differentially to nodulation and defense signals in transgenic soybean roots. *Plant Molecular Biology*, 54, 623-639.
SUBRAMANIAN, S., STACEY, G. & YU, O. 2006. Endogenous isoflavones are essential for the establishment of symbiosis between soybean and *Bradyrhizobium japonicum*. *The Plant Journal*, 48, 261-273.
SUBRAMANIAN, S., STACEY, G. & YU, O. 2007. Distinct, crucial roles of flavonoids during legume nodulation. *Trends in Plant Science*, 12, 282-285.
SUGIYAMA, A., SHITAN, N. & YAZAKI, K. 2007. Involvement of a soybean ATP-binding cassette-type transporter in the secretion of genistein, a signal flavonoid in legume-*Rhizobium* symbiosis. *Plant Physiology*, 144, 2000-2008.
SUZUKI, H., TAKAHASHI, S., WATANABE, R., FUKUSHIMA, Y., FUJITA, N., NOGUCHI, A., YOKOYAMA, R., NISHITANI, K., NISHINO, T. & NAKAYAMA, T. 2006. An isoflavone conjugate-hydrolyzing β-glucosidase from the roots of soybean (*Glycine max*) seedlings. *Journal of Biological Chemistry*, 281, 30251-30259.
SZABÓ, K., BAKOS, É., WELKER, E., MÜLLER, M., GOODFELLOW, H. R., HIGGINS, C. F., VÁRADI, A. & SARKADI, B. 1997. Phosphorylation site mutations in the human multidrug transporter modulate its drug-stimulated ATPase activity. *Journal of Biological Chemistry*, 272, 23165-23171.

TAYLOR, L. P. & GROTEWOLD, E. 2005. Flavonoids as developmental regulators. *Current Opinion in Plant Biology,* 8, 317-323.

TEPLITSKI, M., ROBINSON, J. B. & BAUER, W. D. 2000. Plants secrete substances that mimic bacterial *N*-acyl homoserine lactone signal activities and affect population density-dependent behaviors in associated bacteria. *Molecular Plant-Microbe Interactions,* 13, 637-648.

TERASAKA, K., BLAKESLEE, J. J., TITAPIWATANAKUN, B., PEER, W. A., BANDYOPADHYAY, A., MAKAM, S. N., LEE, O. R., RICHARDS, E. L., MURPHY, A. S., SATO, F. & YAZAKI, K. 2005. PGP4, an ATP binding cassette P-glycoprotein, catalyzes auxin transport in *Arabidopsis thaliana* roots. *Plant Cell,* 17, 2922-39.

THEUNIS, M., KOBAYASHI, H., BROUGHTON, W. J. & PRINSEN, E. 2004. Flavonoids, NodD1, NodD2, and *nod*-box NB15 modulate expression of the y4wEFG locus that is required for indole-3-acetic acid synthesis in *Rhizobium* sp strain NGR234. *Molecular Plant-Microbe Interactions,* 17, 1153-1161.

THILMONY, R., UNDERWOOD, W. & HE, S. Y. 2006. Genome-wide transcriptional analysis of the *Arabidopsis thaliana* interaction with the plant pathogen *Pseudomonas syringae* pv. tomato DC3000 and the human pathogen *Escherichia coli* O157: H7. *The Plant Journal,* 46, 34-53.

TO, J. P. C. & KIEBER, J. J. 2008. Cytokinin signaling: two-components and more. *Trends in Plant Science,* 13, 85-92.

TOGNETTI, V. B., MÜHLENBOCK, P. E. R. & VAN BREUSEGEM, F. 2012. Stress homeostasis–the redox and auxin perspective. *Plant, Cell & Environment,* 35, 321-333.

TOMASI, N., WEISSKOPF, L., RENELLA, G., LANDI, L., PINTON, R., VARANINI, Z., NANNIPIERI, P., TORRENT, J., MARTINOIA, E. & CESCO, S. 2008. Flavonoids of white lupin roots participate in phosphorus mobilization from soil. *Soil Biology & Biochemistry,* 40, 1971-1974.

TREUTTER, D. 2005. Significance of flavonoids in plant resistance and enhancement of their biosynthesis. *Plant Biology,* 7, 581-591.

TSAI, S. M. & PHILLIPS, D. A. 1991. Flavonoids released naturally from alfalfa promote development of symbiotic *Glomus* spores *in vitro*. *Applied and Environmental Microbiology,* 57, 1485-1488.

UNTERGASSER, A., CUTCUTACHE, I., KORESSAAR, T., YE, J., FAIRCLOTH, B. C., REMM, M. & ROZEN, S. G. 2012. Primer3-new capabilities and interfaces. *Nucleic Acids Research,* 40.

UPPALAPATI, S. R., MAREK, S. M., LEE, H. K., NAKASHIMA, J., TANG, Y., SLEDGE, M. K., DIXON, R. A. & MYSORE, K. S. 2009. Global gene expression profiling during *Medicago truncatula-Phymatotrichopsis omnivora* interaction reveals a role for jasmonic acid, ethylene, and the flavonoid pathway in disease development. *Molecular Plant-Microbe Interactions,* 22, 7-17.

VAN BRUSSEL, A. A., BAKHUIZEN, R., VAN SPRONSEN, P. C., SPAINK, H. P., TAK, T., LUGTENBERG, B. J. & KIJNE, J. W. 1992. Induction of pre-infection thread structures in the leguminous host plant by mitogenic lipo-oligosaccharides of *Rhizobium*. *Science,* 257, 70-72.

VAN NOORDEN, G. E., KERIM, T., GOFFARD, N., WIBLIN, R., PELLERONE, F. I., ROLFE, B. G. & MATHESIUS, U. 2007. Overlap of proteome changes in *Medicago truncatula*

in response to auxin and *Sinorhizobium meliloti*. *Plant Physiology,* 144, 1115-1131.

VANDEPUTTE, O. M., KIENDREBEOGO, M., RAJAONSON, S., DIALLO, B., MOL, A., EL JAZIRI, M. & BAUCHER, M. 2010. Identification of catechin as one of the flavonoids from *Combretum albiflorum* bark extract that reduces the production of quorum-sensing-controlled virulence factors in *Pseudomonas aeruginosa* PAO1. *Applied and Environmental Microbiology,* 76, 243-253.

VANETTEN, H. D. & WU, Q. D. 2004. Introduction of plant and fungal genes into pea (*Pisum sativum* L.) hairy roots reduces their ability to produce pisatin and affects their response to a fungal pathogen. *Molecular Plant-Microbe Interactions,* 17, 798-804.

VERNIÉ, T., MOREAU, S., DE BILLY, F., PLET, J., COMBIER, J.-P., ROGERS, C., OLDROYD, G., FRUGIER, F., NIEBEL, A. & GAMAS, P. 2008. EFD is an ERF transcription factor involved in the control of nodule number and differentiation in *Medicago truncatula*. *Plant Cell,* 20, 2696-2713.

VERNOUX, T., WILSON, R. C., SEELEY, K. A., REICHHELD, J.-P., MUROY, S., BROWN, S., MAUGHAN, S. C., COBBETT, C. S., VAN MONTAGU, M. & INZÉ, D. 2000. The ROOT MERISTEMLESS1/CADMIUM SENSITIVE2 gene defines a glutathione-dependent pathway involved in initiation and maintenance of cell division during postembryonic root development. *Plant Cell,* 12, 97-109.

VITHA, S., BENEŠ, K., PHILLIPS, J. P. & GARTLAND, K. M. 1995. Histochemical GUS analysis. *Agrobacterium Protocols.* Springer.

VON BODMAN, S. B., BAUER, W. D. & COPLIN, D. L. 2003. Quorum sensing in plant-pathogenic bacteria. *Annual Review of Phytopathology,* 41, 455-482.

WALKER, T. S., BAIS, H. P., GROTEWOLD, E. & VIVANCO, J. M. 2003. Root exudation and rhizosphere biology. *Plant Physiology,* 132, 44-51.

WANG, K. L., LI, H. & ECKER, J. R. 2002. Ethylene biosynthesis and signaling networks. *Plant Cell,* 14 Suppl, S131-51.

WANG, Y. C., CHEN, S. & YU, O. 2011. Metabolic engineering of flavonoids in plants and microorganisms. *Applied Microbiology and Biotechnology,* 91, 949-956.

WASSON, A. P., PELLERONE, F. I. & MATHESIUS, U. 2006. Silencing the flavonoid pathway in *Medicago truncatula* inhibits root nodule formation and prevents auxin transport regulation by rhizobia. *Plant Cell,* 18, 1617-1629.

WASSON, A. P., RAMSAY, K., JONES, M. G. K. & MATHESIUS, U. 2009. Differing requirements for flavonoids during the formation of lateral roots, nodules and root knot nematode galls in *Medicago truncatula*. *New Phytologist,* 183, 167-179.

WATERHOUSE, P. M., GRAHAM, H. W. & WANG, M. B. 1998. Virus resistance and gene silencing in plants can be induced by simultaneous expression of sense and antisense RNA. *Proceedings of the National Academy of Sciences of the United States of America,* 95, 13959-13964.

WATERHOUSE, P. M. & HELLIWELL, C. A. 2003. Exploring plant genomes by RNA-induced gene silencing. *Nature Reviews Genetics,* 4, 29-38.

WATERS, M. T., BREWER, P. B., BUSSELL, J. D., SMITH, S. M. & BEVERIDGE, C. A. 2012. The Arabidopsis ortholog of rice DWARF27 acts upstream of MAX1 in the control of plant development by strigolactones. *Plant Physiology,* 159, 1073-85.

WEIDENHAMER, J. D., BOES, P. D. & WILCOX, D. S. 2009. Solid-phase root zone extraction (SPRE): a new methodology for measurement of allelochemical dynamics in soil. *Plant and Soil,* 322, 177-186.

WEIGEL, D. & GLAZEBROOK, J. 2005. Transformation of agrobacterium using the freeze-thaw method. *CSH protocols,* 2006, 1031-1036.

WEINSTEIN, L. I. & ALBERSHEIM, P. 1983. Host-Pathogen Interactions XXIII. The mechanism of the antibacterial action of glycinol, a pterocarpan phytoalexin synthesized by soybeans. *Plant Physiology,* 72, 557-563.

WEIR, T. L., BAIS, H. P. & VIVANCO, J. M. 2003. Intraspecific and interspecific interactions mediated by a phytotoxin, (-)-catechin, secreted by the roots of *Centaurea maculosa* (spotted knapweed). *Journal of Chemical Ecology,* 29, 2397-2412.

WEISSHAAR, B. & JENKINS, G. I. 1998. Phenylpropanoid biosynthesis and its regulation. *Current Opinion in Plant Biology,* 1, 251-257.

WEISSKOPF, L., ABOU-MANSOUR, E., FROMIN, N., TOMASI, N., SANTELIA, D., EDELKOTT, I., NEUMANN, G., ARAGNO, M., TABACCHI, R. & MARTINOIA, E. 2006. White lupin has developed a complex strategy to limit microbial degradation of secreted citrate required for phosphate acquisition. *Plant Cell and Environment,* 29, 919-927.

WERNER, T. & SCHMULLING, T. 2009. Cytokinin action in plant development. *Current Opinion in Plant Biology,* 12, 527-538.

WHIPPS, J. M. 2004. Prospects and limitations for mycorrhizas in biocontrol of root pathogens. *Canadian Journal of Botany,* 82, 1198-1227.

WHITE, L. J., JOTHIBASU, K., REESE, R. N., BROZEL, V. S. & SUBRAMANIAN, S. 2014. Spatio temporal influence of isoflavonoids on bacterial diversity in the soybean rhizosphere. *Molecular Plant-Microbe Interactions.*

WINKEL-SHIRLEY, B. 2001. Flavonoid biosynthesis. A colorful model for genetics, biochemistry, cell biology, and biotechnology. *Plant Physiology,* 126, 485-493.

WINKEL, B. S. J. 2004. Metabolic channeling in plants. *Annual Review of Plant Biology,* 55, 85-107.

WOODWARD, A. W. & BARTEL, B. 2005. Auxin: regulation, action, and interaction. *Annals of Botany,* 95, 707-35.

WUYTS, N., LOGNAY, G., SWENNEN, R. & DE WAELE, D. 2006a. Nematode infection and reproduction in transgenic and mutant *Arabidopsis* and tobacco with an altered phenylpropanoid metabolism. *Journal of Experimental Botany,* 57, 2825-2835.

WUYTS, N., SWENNEN, R. & DE WAELE, D. 2006b. Effects of plant phenylpropanoid pathway products and selected terpenoids and alkaloids on the behaviour of the plant-parasitic nematodes *Radopholus similis, Pratylenchus penetrans* and *Meloidogyne incognita*. *Nematology,* 8, 89-101.

XIE, D. Y., JACKSON, L. A., COOPER, J. D., FERREIRA, D. & PAIVA, N. L. 2004. Molecular and biochemical analysis of two cDNA clones encoding dihydroflavonol-4-reductase from *Medicago truncatula*. *Plant Physiology,* 134, 979-94.

XIE, X. N., YONEYAMA, K. & YONEYAMA, K. 2010. The Strigolactone Story. *Annual Review of Phytopathology,* 48, 93-117.

YAMAGUCHI, S. 2008. Gibberellin metabolism and its regulation. *Annual Review of Plant Biology,* 59, 225-251.

YANO, K., SHIBATA, S., CHEN, W. L., SATO, S., KANEKO, T., JURKIEWICZ, A., SANDAL, N., BANBA, M., IMAIZUMI-ANRAKU, H. & KOJIMA, T. 2009. CERBERUS, a novel U-box protein containing WD-40 repeats, is required for formation of the infection thread and nodule development in the legume–*Rhizobium* symbiosis. *The Plant Journal,* 60, 168-180.

YIN, C., HULBERT, S. H., SCHROEDER, K. L., MAVRODI, O., MAVRODI, D., DHINGRA, A., SCHILLINGER, W. F. & PAULITZ, T. C. 2013a. Role of bacterial communities in the natural suppression of *Rhizoctonia solani* bare patch disease of wheat (*Triticum aestivum* L.). *Applied and Environmental Microbiology,* 79, 7428-38.

YIN, R., HAN, K., HELLER, W., ALBERT, A., DOBREV, P. I., ZAZIMALOVA, E. & SCHAFFNER, A. R. 2013b. Kaempferol 3-O-rhamnoside-7-O-rhamnoside is an endogenous flavonol inhibitor of polar auxin transport in *Arabidopsis* shoots. *New Phytologist,* 201, 466-475.

YOKOSAWA, R., KUNNIGA, S. & SEKIZAKI, H. 1986. *Aphanomyces euteiches* zoospore attractant isolated from pea root prunetin. *Annals of the Phytopathological Society of Japan,* 52, 809-816.

YU, O., SHI, J., HESSION, A. O., MAXWELL, C. A., MCGONIGLE, B. & ODELL, J. T. 2003. Metabolic engineering to increase isoflavone biosynthesis in soybean seed. *Phytochemistry,* 63, 753-763.

ZAMIOUDIS, C. & PIETERSE, C. M. 2012. Modulation of host immunity by beneficial microbes. *Molecular Plant-Microbe Interactions,* 25, 139-150.

ZAŽÍMALOVÁ, E., MURPHY, A. S., YANG, H., HOYEROVA, K. & HOŠEK, P. 2010. Auxin transporters--why so many? *Cold Spring Harbor Perspectives in Biology,* 2, a001552.

ZHANG, C., BOUSQUET, A. & HARRIS, J. M. 2014. Abscisic acid and LATERAL ROOT ORGAN DEFECTIVE/NUMEROUS INFECTIONS AND POLYPHENOLICS modulate root elongation via reactive oxygen species in *Medicago truncatula*. *Plant Physiology,* 166, 644-58.

ZHANG, J., SUBRAMANIAN, S., STACEY, G. & YU, O. 2009. Flavones and flavonols play distinct critical roles during nodulation of *Medicago truncatula* by *Sinorhizobium meliloti*. *The Plant Journal,* 57, 171-183.

ZHANG, J., SUBRAMANIAN, S., ZHANG, Y. & YU, O. 2007. Flavone synthases from *Medicago truncatula* are flavanone-2-hydroxylases and are important for nodulation. *Plant Physiology,* 144, 741-751.

ZHANG, J. Z. 2003. Overexpression analysis of plant transcription factors. *Current Opinion in Plant Biology,* 6, 430-440.

ZHAO, J. & DIXON, R. A. 2009. MATE transporters facilitate vacuolar uptake of epicatechin 3'-O-glucoside for proanthocyanidin biosynthesis in *Medicago truncatula* and *Arabidopsis*. *Plant Cell,* 21, 2323-40.

ZHAO, J., HUHMAN, D., SHADLE, G., HE, X. Z., SUMNER, L. W., TANG, Y. & DIXON, R. A. 2011. MATE2 mediates vacuolar sequestration of flavonoid glycosides and glycoside malonates in *Medicago truncatula*. *Plant Cell,* 23, 1536-55.

ZHAO, Y. 2010. Auxin biosynthesis and its role in plant development. *Annual Review of Plant Biology,* 61, 49.

ZHU, H., CHEN, T., ZHU, M. S., FANG, Q., KANG, H., HONG, Z. L. & ZHANG, Z. M. 2008. A novel ARID DNA-Binding protein interacts with SymRK and is expressed during early nodule development in *Lotus japonicus*. *Plant Physiology,* 148, 337-347.

ZUANAZZI, J. A. S., CLERGEOT, P. H., QUIRION, J. C., HUSSON, H. P., KONDOROSI, A. & RATET, P. 1998. Production of *Sinorhizobium meliloti nod* gene activator and repressor flavonoids from *Medicago sativa* roots. *Molecular Plant-Microbe Interactions,* 11, 784-794.